Characterisation of Three Novel Genes and Their Role in Neural Induction

ANNA GIBSON

PhD. DEVELOPMENTAL BIOLOGY

UNIVERSITY COLLEGE LONDON

September 2006

ProQuest LLC
789 East Eisenhower Parkway
P.O. Box 1346
Ann Arbor, MI 48106-1346

ABSTRACT

In 1924, Spemann and Mangold (Spemann and Mangold, 1924) demonstrated the instructive effect of the vertebrate organiser, located in the dorsal lip of the blastopore in amphibia, in the acquisition of neural character during early development. This discovery led to much interest in the process of neural induction. More recently, a "default model" was proposed to account for neural induction, which postulates that ectoderm cells acquire a neural fate autonomously, if they receive no signal. However, this neural fate is inhibited by BMPs, which induce epidermis. The organiser in turn secretes BMP antagonists, which release neighbouring cells from inhibition. However, other results suggested that neural induction is more complex, comprising several sequential and/or parallel signals, which cooperate to induce neural fates.

One such finding was that chick epiblast cells do not respond to BMP antagonists unless they are first exposed to an organiser for at least 5 hours, suggesting that other signals are required upstream of BMP inhibition. To identify the differences between cells that have or have not received such signals, a differential screen was performed. Among 15 genes isolated, only 3 correspond to previously known genes: Defender Against Cell Death (*Dad1*), Polyubiquitin II (*UbII*) and Heavy chain ferritin (*hcf*). All 3 of these had been implicated in Programmed Cell Death (PCD). This project was designed to investigate whether PCD is important in neural induction and to study the role of these three proteins in both processes. First, the distribution of apoptotic cells was examined at different stages of development using TUNEL staining. It was found that PCD is random at first, but by the time the neural plate starts to be established PCD becomes concentrated at its lateral and anterior border. The expression patterns of the three genes were studied: all three are expressed in the neural plate around the time of neural induction, however they are not exclusive markers of the neural plate. The ability of the organiser (Hensen's node) to induce their expression within 5 hours was confirmed, and the ability of FGF signals to mimic this was also tested. The effects of the overexpression of the genes outside their normal expression domain were then examined, scoring both for changes in the distribution of PCD and for the expression of markers for neural, epidermal and border (prospective neural crest) territories. This revealed that overexpression of *hcf* leads to an increase in the number of cells undergoing PCD, but this effect is not cell autonomous. Finally, the expression patterns of the pro-apoptotic gene *Cas9* and of

the death effector *Cas3* were tested and compared to the apoptotic patterns. An increase in PCD was observed in the region where expression of *Cas3* and *Cas9* overlaps and which is free from *Dad1*, consistent with the notion of an amplification loop between Caspase 3 and Caspase9, and with a possible involvement of DAD1 in the regulation of this process.

To my mum

ACKNOWLEDGEMENTS

First and foremost, I would like to thank Professor Claudio Stern - the most impressive chick man on the planet - and wonderful human being; thank you for welcoming me to your lab, for teaching me the importance of hypothesis, trying to implant in me an idea of logical thinking and for not giving up on me.

I like to thank Professor Steve Wilson for giving me the opportunity to work in his Zebrafish lab and allowing me to discover and fall in love with science. This would not have been possible without my friends in his lab Jacquie Hoyle, Tetsu Kudoh and Diz Bailey.

I would also like to thank Anukampa Barth, my first supervisor and friend who not only taught me everything I know about bench work but also tried to keep me fit and sane with her yoga classes.

My thanks also go to Carol Bartell, Marg Glover, Ian Blaney and Steve Townsend for all the help they gave me throughout my PhD years and during my degree in Neuroscience.

Thank you to every single member of our lab, but especially to: Irene de Almeida for being Irene and for teaching me in ovo electroporation, Federica Bertocchini and Claudia Linker for moral support; Octavian Voiculescu for providing me with pCAβ construct containing *lacZ* and introducing us to the history and culture of Romania, Ricardo Correa for NFkappaB idea, Ferran Lloret Vilaspasa for his great dry humour and for introducing me to Catalonian wine, Costis Papanayotou for understanding my struggle in obtaining any meaningful results and being a good friend, Ali Ghanem for reminding me that I should always follow my dreams, Pamela Simonsson for her smile and friendliness, Sharon Boast not only for her technical support and her friendship but also for being such a special person and of course Guojun "Godrung" Sheng for his scientific and spiritual guidance.

Amanda Albazerchi a true friend - the only person able to share and fully appreciate my sense of humour, without her, my time in the lab would not be the same.

I would also like to thank Stephen Price for his advice and help and Professor Takeharu Nishimoto for anti-DAD1 antibody.

The work in this thesis was sponsored by BBSRC studentship.

I have to thank my family and friends without whom my life and work would be meaningless especially, the late Peter Luff, my brother Chris and my sister Anja, Caron Bottali, Gina Gortatowicz, Monika Krause, Anita Szerszen, Guy and Jo Eaton, Marcus Smithwick, Galazka and Marian Kos, Professor Tadeusz Kowalak, Andos Pasznik, Pani Nogi and Rafal Deja, Malgosia Maszycka, Professor Wiesiu Grochowski, Neil Gibson, Leigh Bernard, Lisa Sewell and her wonderful family, especially: Teresa Anne and Hugh Henry "Charles" and Laura Jones. Pawel Sitarz for giving me a push when I needed it.

Muhamed Hawadle for restoring my belief in me, my molecular biology abilities and reminding me what is important in life - molecular biology and sense of humour. My two late cats Clarrence and Knobie for all their love and moral support - I could not have done it without them.

CONTENTS

CHAPTER 1:

General Introduction

1.1. Introduction to chick embryology

1.1.1. Strengths of the chick as an experimental system

The embryo of the domestic fowl, *Gallus gallus domesticus* is probably the oldest model used to study embryonic development (Stern, 2004c) and still remains a popular choice today. In some respects (such as having a flat blastoderm rather than a cylinder, as well as some surprisingly close similarities in the genome), chick embryos resemble human embryos at early stages of development more closely than rodents (mouse and rat). Particularly attractive features of chick embryos for modern developmental biology include their large size, easy access and and manipulation. They can also be grown in culture in such a way that they lend themselves to fate mapping and lineage analysis using localised injections of fluorescent and other vital dyes, that it has a very compact genome with few repetitive sequences (Boardman et al., 2002; Wallis et al., 2004) and that DNA constructs and morpholino oligonucleotides are easy to introduce in specific places and stages by electroporation.

For studies on induction, where it is especially important to distinguish cells derived from the grafted inducing tissue from the responding cells of the host, the use of quail-chick chimaeras has been especially useful. This technique was first introduced by Le Douarin (Le Douarin, 1969; Le Douarin and Teillet, 1973) who took advantage of the characteristic accumulation of heterochromatin in quail nucleoli, detected by Feulgen-Rossenbeck staining. Since then, detection of quail cells has been made easier and more reliable by the availability of an antibody (QCPN) that recognises a perinuclear antigen in all quail cells (see Chapter 2).

The earliest stages of chick embryo development, from fertilisation to the equivalent of the early blastula stage, occur while the egg is still *in utero*. The egg is laid when the embryo already has some 10,000-20,000 cells and the central area pellucida has separated from the peripheral area opaca, the precursor cells that will give rise to the hypoblast have already segregated to the ventral side of the embryo, and other regional structures have appeared such as the presence of a marginal zone and special regions posteriorly posterior marginal zone (PMZ) and a Koller's sickle (Stern, 2004a). This makes it difficult to study pre-blastula stages of development in the chick, but the system excels for studies of processes occurring from this stage onwards.

New techniques still continue to be developed, promising even more exciting times for chick embryology in the future. This includes the newly available chicken embryonic stem cells (Horiuchi et al., 2006; Pain et al., 1996; Petitte et al., 2004; van de Lavoir et al., 2006), and a newly-described method for producing transgenic birds

(Sang, 2004; Stern, 2005b). And although mutants affecting development of domestic fowl started to be identified long ago, even the most interesting ones have still not been studied; a notable exception is the *talpid-3* mutant (Buxton et al., 2004), which displays defects in limb development, for which the gene responsible has recently been identified by positional cloning and shown to encode a novel member of the Hedgehog signalling pathway (Davey et al., 2006). The recent completion (May 2004) of the chicken genome sequencing project (ICGS Consortium) to a resolution of 6.6x, along with a large number of expressed sequence tags (ESTs) and a growing number of single nucleotide polymorphisms (SNPs) (Stern, 2005b) will simplify all of these tasks even further in the near future.

1.1.2. Brief description of early chick development

1.1.2.1. From blastula to early gastrula: formation of the primitive streak.

At the time of laying, the chick embryo comprises a disc shaped, single cell thick blastoderm of up to 20,000 cells (Stern, 2004a). It is already possible to distinguish two clear regions: an outer area opaca "opaque area" and an inner area pellucida "translucent area", despite the fact that the epiblast (dorsal most layer) is continuous across the entire blastoderm and its cells have almost identical shapes in both regions (Bancroft and Bellairs, 1974). Ventral (towards the yolk) to this continuous epiblast layer, the area opaca is made up of multiple layers of very large, yolky cells. This is called the germ wall and constitutes an extra-embryonic endodermal layer. The germ wall cells closest to the epiblast adhere very tightly to the latter in the most peripheral area (area opaca proper) but much less in a rim immediately outside the area pellucida. This generates a "flap" of yolky cells, called the germ wall margin (Stern, 1990), some of which will later give rise to the endoblast (see below). The deepest cells of the area opaca are tightly linked to the underlying yolk, while the central area pellucida stretches over a sub-germinal cavity containing "white yolk" originating from the nucleus of Pander and located in the middle of the yolk latebra (Callebaut, 2005). The epiblast above the germ wall margin, which defines a narrow ring separating the inner area pellucida from the outer area opaca, is called the Marginal Zone (Eyal-Giladi, 1984; Eyal-Giladi et al., 1992; Eyal-Giladi and Kochav, 1976; Stern, 2004a), whose fate is also entirely extra-embryonic (Bachvarova et al., 1998).

Underlying the area pellucida epiblast at around the time of laying are scattered "islands" of yolky cells (but which are smaller than those of the area opaca). The density of these islands is higher towards the future caudal (posterior) end of the embryo and decreases rostrally (anteriorly). These islands have been proposed to form

by polyinvagination, or cell shedding, from the area pellucida, starting from the prospective posterior region of the embryo (Eyal-Giladi, 1984; Fabian and Eyal-Giladi, 1981; Kochav et al., 1980; Peter, 1938) although the shedding process has never been demonstrated directly by cell labelling or direct observation.

Separating the area pellucida from the Marginal Zone, at the posterior edge of the former, is a ridge of small cells, tightly adherent to the epiblast, which forms a sickle shaped region describing a 60° arc. This is called Koller's sickle (Callebaut and Van Nueten, 1994; Eyal-Giladi et al., 1992; Vakaet, 1984), and its cells are destined to contribute largely to the early primitive streak (Bachvarova et al., 1998). However the bulk of the primitive streak also contains cells derived from elsewhere in the epiblast (see below).

With incubation after laying, the islands gradually merge together, in a posterior to anterior direction, to form a loose, single-cell thick layer, the hypoblast, whose fate is to contribute to the yolk sac stalk and is therefore also extraembryonic (Stern, 2004a). The entire embryo is derived from the epiblast layer present in the area pellucida at this stage (which also contributes some cells to extraembryonic lineages, especially mesoderm). Just before the beginning of gastrulation (marked by the appearance of a primitive streak), the hypoblast is displaced by a new ventral layer, also extraembryonic in fate: the endoblast (also called "secondary hypoblast" and "junctional endoblast"). These cells arise from a subset of posterior germ wall margin progenitors and gradually migrate centripetally, causing the hypoblast to become confined to an anterior domain (the germinal crescent) (Stern, 2004a). This domain is thought to contain the future primordial germ cells that will give rise to the male and female gametes.

Remarkably, even at this stage, the embryo is highly regulative. It is possible to fragment the blastoderm by cutting it into up to 8 pie-shaped slices, each of which is capable of developing independently into a smaller but apparently normal embryo (Spratt and Haas, 1960). Despite this, even finer regional differences can be detected in both the area pellucid and in peripheral, extraembryonic regions at this stage. Several genes are expressed in various regions and structures. For example, the Posterior Marginal Zone (the posterior portion of the Marginal Zone, just outside Koller's sickle) (Bachvarova et al., 1998; Eyal-Giladi et al., 1992; Skromne and Stern, 2002; Stern, 1990) is characterised by its expression of Vg1 (Seleiro et al., 1996; Shah et al., 1997; Skromne and Stern, 2002). The cells of Koller's sickle express *gooscoid* (Izpisua-Belmonte et al., 1993; Shah et al., 1997), FGF8 and Chordin (Streit et al., 1998; Streit and Stern, 1999a). And the anterior area pellucida epiblast, perhaps equivalent to the "anti-sickle" region of the rabbit embryo (Viebahn, 2004), expresses the transcription factors Gata2 and Gata3 (Sheng and Stern, 1999).

Likewise in the ventral layers, various tissues can be distinguished. The (primary) hypoblast (Stern, 1990; Vakaet, 1970) expresses, for example: *Hex* (Yatskievych et al., 1999); *Cerberus/Caronte* (Bertocchini and Stern, 2002), *Otx2* (Foley et al., 2000) and *Crescent* (Pfeffer et al., 1997). This tissue is therefore comparable in its movements, fate and genetic markers, to the anterior visceral endoderm (AVE) of the mouse (Bertocchini and Stern, 2002; Foley et al., 2000). The endoblast cells do not express any of the above markers (Bachvarova et al., 1998; Bertocchini and Stern, 2002; Foley et al., 2000) or indeed any other known markers (Bertocchini and Stern, 2002).

As mentioned above, neither the hypoblast, nor the endoblast, nor the PMZ contribute to the embryo proper (Rosenquist, 1966; Rosenquist, 1972). However all three of them separately or in combinations (along with Koller's sickle) have been implicated in the process of induction of the primitive streak (Bachvarova et al., 1998; Bertocchini and Stern, 2002; Callebaut et al., 2003; Callebaut et al., 1998; Shah et al., 1997). Despite controversy over some time about the precise mechanisms and sources of signals responsible for inducing the primitive streak as the site of gastrulation in the avian embryo (Bellairs, 1986), the events, signals and tissues involved are finally becoming clear (Stern, 2004a). Briefly, the Posterior Marginal Zone (PMZ) has been proposed to be the functional equivalent of the amphibian Nieuwkoop centre (Bachvarova et al., 1998) in that it is able to induce an axis including the "organizer" (see below) without making a direct cellular contribution to the latter structure. The main signal responsible for initiating this is the TGF_ factor Vg1, which requires Wnt activity in order to induce downstream events (Skromne and Stern, 2001; Skromne and Stern, 2002). A key target of Vg1+Wnt activity emanating from the PMZ is Nodal, whose expression is induced as a patch in the area pellucida epiblast just inside Koller's sickle. Together with FGF8 (emanating from Koller's sickle), Nodal induces mesoderm formation and the nascent primitive streak (Bertocchini et al., 2004; Stern, 2004a).

Given that the whole embryo periphery can initiate formation of a complete embryonic axis when isolated from the rest of the embryo, there must be mechanisms to prevent the formation of ectopic axes elsewhere than at the normal posterior site. One such mechanism has been shown to involve the Nodal antagonist Cerberus, which is expressed in the hypoblast. The displacement of the hypoblast away from the posterior edge of the area pellucida by the incoming endoblast (which does not express Cerberus) appears to be a key event in initiating primitive streak formation (Bertocchini and Stern, 2002).

Morphologically, the primitive streak emerges as a conical thickening in the

posterior region of the area pellucida that extends and elongates toward the centre of the embryo to become a straight longitudinal structure with tightly packed cells between epiblast and endoblast (Bellairs, 1986; Eyal-Giladi et al., 1992; Vakaet, 1984). The cells contributing to this early streak originate from Koller's sickle (Bachvarova et al., 1998; Izpisua-Belmonte et al., 1993; Wei and Mikawa, 2000), with the addition of some cells of epiblast origin which appear to poly-ingress and become incorporated into the early streak primordium (Canning et al., 2000; Canning and Stern, 1988; Mogi et al., 2000; Stern and Canning, 1988; Stern and Canning, 1990). As the primitive streak elongates, it incorporates progressively more cells of central epiblast origin (Hatada and Stern, 1994; Izpisua-Belmonte et al., 1993; Joubin and Stern, 1999; Streit et al., 2000). At the tip of the primitive streak when fully elongated (stages 3^{+} to 4), the "organizer", Hensen's node, will form as a thickened bulb involving all 3 layers (Streit et al., 2000). Hensen's node is derived from "posterior" (originating from Koller's sickle) and "central" cells (epiblast cells from the middle of the blastoderm) (Hatada and Stern, 1994; Izpisua-Belmonte et al., 1993; Selleck and Stern, 1991; Selleck and Stern, 1992; Streit et al., 2000).

The cellular events responsible for elongation of the primitive streak are still controversial. One group has claimed that this is largely due to highly oriented cell divisions (Wei and Mikawa, 2000). However this mechanism has been considered unlikely to be sufficient by mathematical models of cell behaviour (Bodenstein and Stern, 2005), and another group has invoked positive and negative chemotaxis of cells towards centres of attraction and repulsion (Chuai et al., 2006; Cui et al., 2005). Although the latter group has dismissed cell intercalation and the Wnt planar cell polarity pathway (PCP) that has been implicated in similar movements in amphibian and fish embryos, these mechanisms have not yet been formally excluded as playing a role.

Extensive morphogenetic movements of the epiblast also precede the formation of the primitive streak. These take the form of "Polonaise" movements by which cells converge to the posterior edge of the area pellucida and then move anteriorly along the midline. These movements were first revealed by pioneering time-lapse filming studies (Gräper, 1929; Vakaet, 1970; Wetzel, 1929) and can also be demonstrated by comparing fate maps of the epiblast at different stages (Hatada and Stern, 1994).

During primitive streak elongation, the streak changes from a triangle (stage 2) to a solid, parallel-sided rod (stage 3). This is quickly followed (stage 3+) by the formation of a groove running along the midline of the primitive streak. At this stage the epiblast lateral to the streak migrates more coherently towards the midline and cells ingress through and adjacent to the groove to colonise the deeper layers of the

embryo. This process is gastrulation proper and generates the 3 germ layers of the embryo: epiblast, mesoblast (mesendoderm) and definitive endoderm. The cells of the latter insert among the endoblast cells that formed the early deep layer of the embryo and displace them to the periphery of the blastoderm (Kimura et al., 2006; Stern, 2004a).

1.1.2.2. Formation of the definitive germ layers: ectoderm, mesoderm and endoderm

The formation of the endoderm (the lower/inner layer) has been a challenge to scientists and it took some considerable time to appreciate that the early lower layer (hypoblast/endoblast) does not contribute to the definitive (gut lining and associated organs) endoderm, as originally thought. The first studies to demonstrate that the endoderm is of epiblast origin, via the primitive streak, were the pioneering fate mapping experiments of Bellairs (Bellairs, 1953a; Bellairs, 1953b; Bellairs, 1955; Bellairs, 1957). Since then it has been confirmed that in all vertebrate Classes the definitive (gut) endoderm is derived during gastrulation by ingression through the blastopore/primitive streak (Fukuda and Kikuchi, 2005; Grapin and Constam, 2004; Stainier, 2002). The ingression of cells into this endodermal layer occurs at the anterior tip of the primitive streak, including Hensen's node (Selleck and Stern, 1991) and the routes by which they migrate to colonise the deep layer have recently been elucidated by careful fate mapping (Kimura et al., 2006). This study revealed, somewhat unexpectedly, that cells ingressing at the anterior primitive streak colonise the endoderm not directly, but only after migrating laterally some distance within the middle layer, which at these early stages contains both mesoderm and endoderm precursors ("mesendoderm"). By stage 4, no endoderm precursor cells can be found in the epiblast even at the midline of the embryo (Selleck and Stern, 1991), but ingression into the deep layers continues until stages 5-6, via the middle layer.

There is a correlation between the time of incorporation of cells into the lower layer with their ultimate fate. The earliest endoderm formed from stage 2-3 gives rise to the mid- and hindgut region (Kimura et al., 2006). The foregut and especially its ventral part do not emerge from the streak until stage 4 (Kimura et al., 2006).

At the time of formation of the endoderm, the hypoblast becomes confined to the anterior germinal crescent (containing future germ cells) in the most anterior-lateral region underlying the border of the area pellucida. The migrating endoderm replaces the hypoblast and the endoblast, and becomes the most ventral layer of the embryo proper. It has been suggested that the formation of the endoderm is regulated by the TGF-β family of signalling molecules, and specifically *Nodal* as it has been reported in

vertebrates (Mizoguchi et al., 2006; Poulain and Lepage, 2002). However other signalling pathways, such as *Bmp* and *Wnt* have also been implicated (Grapin and Constam, 2004; Stainier, 2002).

Formation of the mesoderm begins with the appearance of a middle layer, which condenses at the primitive streak but this appears to contain a mixture of cells destined for both endoderm and mesoderm (see above). However during gastrulation prospective endoderm cells become quickly confined to the most anterior regions of the primitive streak, and ingression of cells elsewhere through the streak contributes exclusively to mesoderm (both embryonic and extra-embryonic).

Within the forming mesodermal layer, cells migrate anteriorly to form the prechordal mesoderm and notochord. Cells migrating a little more laterally (on either side of the notochord at the midline) contribute to somites and to the paraxial mesoderm of the head, and those that migrate yet more laterally give rise to the intermediate mesoderm, heart and lateral plate (Brand-Saberi et al., 1996; Christ and Ordahl, 1995; Psychoyos and Stern, 1996; Rosenquist, 1966; Schoenwolf, 1992; Selleck and Stern, 1991). The intermediate mesoderm extends longitudinally between somites (medially) and lateral plate mesoderm, and eventually gives rise to the mesonephric duct and all kidney tissue and part of the gonads (James et al., 2006; Schultheiss et al., 1995; Yoshioka et al., 2005).

The lateral plate mesoderm becomes split into a superficial, somatic layer and a deep, splanchnic mesoderm – the former attaches firmly to the epiblast (to form the somatopleure) while the latter becomes fused with the underlying endoderm (splanchnopleure). The cavity formed between them is the coelom (Linask et al., 1997), which defines the Coelomata and distinguishes these animals from lower Acoelomata. The somatic mesoderm will contribute to the formation of the pleural, pericardial, and peritoneal cavities, while splanchnic mesoderm from both sides of the embryo contributes to the formation of the heart in the medial region of the embryo. In addition to these embryonic structures, the lateral plate mesoderm also contributes to blood vessels and haematopoietic blood islands in the embryo and outside it, as well as to other extraembryonic components.

The cardiogenic mesoderm that contributed to the splanchnic mesoderm is present in the primitive streak as early as stage 4/4^{+}. Some of these cells contribute to the endocardium and some differentiate into heart muscle (Andree et al., 1998; Lints et al., 1993; Schultheiss et al., 1995; Zaffran and Frasch, 2002). It has been recently reported that cranial paraxial mesoderm, as well as lateral plate mesoderm also contribute to myocardium and endocardium (Tirosh-Finkel et al., 2006).

The order of ingression and migration of the mesoderm through Hensen's node

and the primitive streak is directly correlated with the medio-lateral (axial/lateral, also called dorsoventral patterning) patterning of the mesoderm: the more anterior the site of ingression, the more medial/axial/dorsal the mesodermal contribution (Freitas et al., 2001; Lopez-Sanchez et al., 2001; Psychoyos and Stern, 1996; Sawada and Aoyama, 1999; Schoenwolf et al., 1992). The BMP signalling pathway is one critical factor in determining these fates, as high levels of BMP specify lateral mesoderm, while low levels specify paraxial and possibly axial mesoderm (James and Schultheiss, 2005; Streit and Stern, 1999b; Tonegawa et al., 1997).

The ingression of cells that contribute to mesoderm and endoderm ceases through the anterior part of the primitive streak at stage 4 (Gallera and Nicolet, 1969; Garcia-Martinez et al., 1997; Hatada and Stern, 1994; Joubin and Stern, 1999; Nicolet, 1965; Nicolet, 1970; Psychoyos and Stern, 1996). The transcription factor *Churchill*, acting via Sip1 (*Smad interacting protein 1*) has been recently identified as key regulators of this ingression, and specifically as being responsible for stopping the ingression of cells at the end of gastrulation (Sheng et al., 2003). This phase of early development (stage 4) thus demarcates the end of gastrulation proper and the beginning of the "neurula" stage. However it should be remembered that cell ingression in a process analogous to early gastrulation continues to take place through the tail bud and the remnants of the primitive streak as it regresses, primarily to generate lateral mesoderm (Knezevic et al., 1998).

1.1.2.3. Hensen's node

Hensen's node is the amniote equivalent of the amphibian organiser in that it can induce a complete central nervous system when transplanted into a competent region at an appropriate stage of development (see below). Despite its heterogeneous cell origin (see above), it can be defined by the expression of many genes including *Goosecoid*, *Chordin*, *HNF3β* and *Not1*. Since cells enter and leave Hensen's node continuously during gastrulation, yet these genes remain expressed in this particular region, there must be mechanisms responsible for ensuring such regional expression independent from cell lineage. Indeed, complex interactions between BMP, Vg1, Wnt and ADMP signalling as well as possibly Nodal have been implicated in this dynamic regulation of gene expression (Joubin and Stern, 1999).

In addition to the transient cell populations that make up Hensen's node, there also appear to be some permanent resident cells. Single cell lineage analysis of the superficial (epiblast) layer of the node revealed that descendants of some single cells can populate very large regions of the axis (contributing to notochord and/or somites) while one descendant of the originally labelled cell remains in place in the node

(Selleck and Stern, 1991; Selleck and Stern, 1992), These observations are consistent with the idea that the node contains a resident population of stem-cell-like cells which act as founders for cells that will gradually (in a head-to-tail direction) colonise the entire length of the embryonic axis in these mesodermal structures.

At stage 5, the node becomes morphologically asymmetric, with a visible tilt to the left (the position of the primitive pit, corresponding to the tip of the groove of the primitive streak, does not occupy a perfectly central position within the node). This morphological asymmetry is accompanied by left and right differences in gene expression, independent of the morphology. Thus *HNF3β*, *Sonic hedgehog* and *Nodal* are expressed on the left whilst *ActRIIa* is expressed on the right (Levin et al., 1995). Importantly, the asymmetric expression of some of these genes (all of the above except *Nodal*) precede the appearance of morphological asymmetry, indicating that the processes setting up left-right asymmetry are already underway by the time of Hensen's node formation.

1.1.2.4. Patterning of the ectoderm: neurulation

After the end of gastrulation proper (following stage 4), the next developmental stage is called "primary neurulation" and is characterised by the emergence of the notochord and head process from the node (in the middle layer), at the same time as the ectoderm (epiblast) thickens in the central region and elevates to form the neural plate. This subsequently folds to generate the neural tube. "Secondary neurulation" is said to take place at the later stages of the development (stage 16-35) in the caudal mass in the posterior regions of the embryo. The mechanisms of neural tube formation appear to differ in this region, where a medullary cord (continuous with the neural tube arising from primary neurulation) progressively hollows as the secondary neural tube is formed (Uehara and Ueshima, 1988; Yang et al., 2003). However the term neurulation is usually used exclusively to refer to the embryonic stages at which primary neurulation occurs, rather than the entire process of neural tube formation (just as "gastrulation" also refers to a stage of development rather than the process of cell ingression through the primitive streak, which continues at much later stages).

Neurulation first becomes apparent with morphological and molecular changes taking place in the ectoderm, starting just after stage 4. The molecular aspects of early neurulation are discussed in detail below (section 1.2 Neural Induction). Formation of the neural plate is characterised by changes in cell shape; epiblast cells destined to form the neural plate become columnar, a process that is accompanied by the onset of expression of the "definitive" neural marker *Sox2* (Rex et al., 1997). Formation of the neural tube is preceded by elevation of the lateral borders of the neural plate (with a

medial hinge in the midline and dorsal hinges at the top of emerging neural folds). This is followed by convergence of neural folds that eventually fuse in a rostral to caudal direction. Closure of the neural tube gives rise to the roof plate and the ectoderm overlying it (Schoenwolf, 1982) and also defines the site of neural crest formation (Di Virgilio et al., 1967; Steffek et al., 1979).

1.1.3. Summary of the stages used to classify early chick development

A particularly important advantage of the chick embryo over other species is the availability of an extremely fine and accurate staging system. For stages from the initial appearance of the primitive streak (stage 2) to hatching (stage 46), the system of Hamburger and Hamilton (Hamburger and Hamilton, 1951) is used. For pre-primitive streak stages there are 14 (I-XIV) additional stages (Eyal-Giladi and Kochav, 1976).

The stages of development relevant to this study are briefly introduced below:

Eyal-Giladi and Kochav (1976) stages:

X (20 hours after fertilisation - freshly laid egg): clear area pellucida and area opaca, islands of hypoblast visible on the ventral side. Koller's sickle distinguishable posteriorly.

XI: Islands of hypoblast begin to fuse, making a layer that covers 1/4-1/3 of the area pellucida (posteriorly)

XII: Hypoblast now covers 1/2 of the surface of the area pellucida.

XIII: Hypoblast covers entire lower surface of the area pellucida, with a well-defined posterior edge at Koller's sickle.

XIV (this appears to be a very short stage) formation of a "posterior bridge", just posterior to Koller's sickle but which may incorporate part of the sickle itself – this may be the very early primordium of the primitive streak.

Hamburger and Hamilton (1951) stages (intermediate stages denoted by + or -)

2. (6-7 hours after laying approximately) primitive streak clearly visible as a triangular thickening at the posterior edge of the area pellucida;

3. (12-13 hours approximately) the primitive streak is a parallel-sided solid rod, with no groove in the epiblast above it.

3+. (14-17 hours approximately) a groove develops in the epiblast overlying the midline of the primitive streak. Mesendoderm cells start to emerge laterally forming the lateral plates. No distinct node is yet visible at the anterior tip of the streak.

4. (18-19 hours) a distinct bulbous thickening becomes apparent at the tip of the primitive streak (Hensen's node). No mesoderm visible in front of the node. In some embryos the area pellucida changes shape into an inverted pear-shape (thinnest posteriorly) but this is not seen in all cases.

4+. a triangular condensation of mesendodermal cells is visible just anterior to the node, with its apex in contact with the node and its base extending anteriorly from it. This is the primordium of the prechordal mesendoderm.

5. (19-22 hours) a rod of mesoderm (the head process, or cephalic notochord) extends forwards from the node, with the triangular prechordal mesendoderm at its anterior tip. No head fold yet apparent.

6. (23-25 hours) the head fold begins to form anterior to the head process and prechordal mesendoderm.

7. (23-26 hours) appearance of the first pair of somites; beginning of the formation of blood islands.

8. (26-29 hours) 4 pairs of somites, blood islands clearly present posteriorly in the proximal area opaca; neural folds elevating and starting to fuse at the level of the hindbrain; the process of neural tube formation extends from this region posteriorly and to a lesser extent anteriorly.

9. (29-33 hours) 7 pairs of somites, the cephalic neural tube starts to subdivide into: prosencephalon, mesencephalon and rhombencephalon; primary optic vesicle can be detected; ventrally: fusion of the heart primordia, omphalomesenteric (vitelline) vein and margin of the anterior intestinal portal visible.

10. (33-38 hours), 10 pairs of somites, the first pair starts to disperse, clear division of cranial part into 3 brain vesicles; optic vesicle clearly visible in the prosencephalon; first signs of cranial flexure; rhombomeres become apparent; heart bends to the right.

11. (40-45 hours) 13 pairs of somites; cranial flexure more apparent; optic vesicle starts to converge at the base; prosencephalon divides into telencephalon and diencephalon, rhombencephalon divides into metencephalon and myelencephalon, 5 rhombomeres clearly visible; heart bent to the right

12. (45-49 hours) 16 pairs of somites; cranial flexure to the left; telencephalon covered with fold of amnion; primary optic vesicle has a stalk, auditory pit is visible; heart takes a S shape form.

13. (48-52 hours) 18 pairs of somites; head turning to the right, fold of amnion extends posteriorly; telencephalon is enlarged;

14. (50-53 hours) 22 pairs of somites; telencephalon positions itself at a right angle to the diencephalon; first and second branchial arch visible; invagination of the primary optic vesicle and formation of the lens placode; constriction of the auditory pit opening; amnion covers anterior part of the embryo to the level of 7th pair of somites.

1.2. Neural induction

"Induction" has been defined as "*an interaction between one (inducing) tissue and another (responding) tissue, as a result of which the responding tissue undergoes a change in its direction of differentiation*" (Gurdon, 1987). The idea of embryonic induction as a main player in determining the territories occupied by cells with different ultimate fates was first proposed over a century ago. Herbst suggested that normal development requires "*formative stimuli (...) exerted from one part of the embryo to another*", he even believed in "*the possibility of a complete resolution of the entire ontogenesis into a sequence of such inductions*" (Herbst, 1901) - translation from online companion to (Gilbert, 2006: http://8e.devbio.com/article.php?ch=10&id=110). The first evidence supporting this idea came from the lab of Hans Spemann working on the formation of the lens in amphibians, who found that the lens failed to develop when the optic stalk was removed and that grafts of the optic stalk to certain positions resulted in the formation of ectopic lenses (Spemann, 1901). However these experiments could not distinguish graft- from host-derived cells and therefore the contribution of the former to the new structure remained unclear. Some years later (Spemann, 1921), Spemann gave his PhD student Hilde Mangold the task of repeating earlier experiments by Warren Lewis (Lewis, 1907) in which Lewis had obtained supernumerary axes after implanting the dorsal lip of the blastopore in frog (*Rana*). In the absence of markers to distinguish donor and host cells, Lewis concluded that the nervous system arose from the grafted dorsal lip. Spemann and Mangold used a different approach: they combined differently pigmented species of newts (*Triturus taeniatus*, *T. cristatus* and *T. alpestris*) to distinguish between donor and host tissue. The results of these experiments allowed them to conclude that the donor graft can induce in the host a secondary axis containing a complete nervous system composed almost entirely of host cells, rather than being due to the differentiation/contribution of the donor cells (Spemann and Mangold, 1924). Spemann and Mangold (1924) proposed the name "organiser" for the dorsal lip of the blastopore, because of its ability to induce a fully patterned axis in the host. This was the first formal demonstration of the phenomenon of embryonic induction, which attracted considerable attention for many decades thereafter. This demonstration became one of the most pivotal experiments in the history of developmental biology. However, well over half a century had to elapse before any clue to the molecular mechanisms underlying it started to emerge. Indeed during Spemann's time, it was still being debated whether the "formative stimulus" from the organiser was chemical at all; Spemann himself favoured

a vitalistic explanation, a more holistic, or non-material notion of induction (Oppenheim, 2001; Oppenheimer, 1936; Stern, 2004b).

Soon after the landmark experiment of Spemann and Mangold (1924), regions with a similar activity were discovered in other vertebrate Classes: the embryonic shield in teleosts (Luther 1935, Oppenheimer 1936), the distal tip of the primitive streak (Hensen's node) in birds (Waddington, 1932; Waddington, 1933; Waddington, 1937) and mammals (Beddington, 1994; Blum et al., 1992; Waddington, 1936; Waddington, 1937). It was also established not only that all vertebrate Classes possess equivalent regions, but also that grafts of the organizer from one Class could induce an ectopic nervous system in another Class: fish to newt (Oppenheimer, 1936), chick to rabbit (Waddington, 1934), *Xenopus* to chick (Kintner and Dodd, 1991), chick to zebrafish (Hatta and Takahashi, 1996), rabbit to chick or duck (Waddington, 1937), chick to *Xenopus* (Kintner and Dodd, 1991), mouse to frog (Blum et al., 1992) and rabbit and mouse to chick (Knoetgen et al., 2000; Zhu et al., 1999). These findings imply that ectodermal cells are responsive to organiser-derived signals from other species/Classes, strongly suggesting a common mechanism for neural induction conserved across the Vertebrates.

Since Spemann's day, a huge literature has accumulated on neural induction mainly concerned with the identification of the putative inducing signals. It is not until the mid-1990s however that the first clues started to emerge, mainly from experiments performed in *Xenopus*.

1.2.1 The default model

The first plausible model for the molecular basis of neural induction was based on research in *Xenopus* rather than newts, because it turned out that the latter were very easy to neuralise with a number of non-specific stimuli (Stern, 2005). The first new insights arose from the observation that when the animal cap of the *Xenopus* blastula is dissociated into single cells, and after a few minutes the cells are reassociated and allowed to develop, the explant differentiates into neural tissue (Born et al., 1989; Godsave and Slack, 1989; Grunz and Tacke, 1989; Saint-Jeannet et al., 1990; Sato and Sargent, 1989). This surprising finding was initially interpreted to mean that some factor present between the cells may be removed by dissociation, and that such a factor might act as an antagonist of neural differentiation. The next important observation was made by Hemmati-Brivanlou and Melton, who reported that a great increase in the size of the neural plate is produced when embryos are injected with a dominant negative receptor for a factor then thought to be activin (this was later shown to inhibit many members of TGFβ family, including BMPs) (Hemmati-Brivanlou and

Melton, 1994). The same treatment also prevented formation of mesoderm (Hemmati-Brivanlou and Melton, 1992). The authors interpreted these results as implying that activin or related factors were required for mesoderm formation, but also normally inhibit neural plate formation.

However the model started to take shape only through several more or less simultaneous discoveries. In Richard Harland's laboratory, a screen for new dorsalising factors led to the identification of a novel protein, Noggin, capable when injected into an early embryo of dorsalising the embryo and of generating a large excess of tissue expressing neural markers (Lamb et al., 1993; Smith and Harland, 1992; Smith et al., 1993). These authors found that Noggin binds BMPs and to inhibit their activity and that it is expressed in the organizer, implicating BMP in the inhibition of neural fates predicted by the dissociation and dominant-negative "activin" receptor experiments mentioned above. Meanwhile, the laboratory of De Robertis discovered another protein, Chordin (homologous to *Drosophila short gastrulation*, or *sog*), which is also able to dorsalise the embryo when overexpressed, to bind to and inactivate BMPs (just like Sog binds to and inhibits the BMP homologue, Dpp) and which is expressed in the organiser (De Robertis and Sasai, 1996; Fainsod et al., 1997; Hawley et al., 1995; Piccolo et al., 1996; Sasai et al., 1995; Sasai et al., 1994; Zimmerman et al., 1996). At the same time, the Hemmati-Brivanlou laboratory uncovered a third protein expressed in the organiser and with the ability to inhibit various TGF_ molecules including both activin and BMPs: Follistatin (Hemmati-Brivanlou et al., 1994). Finally, Hemmati-Brivanlou demonstrated that addition of BMP4 protein to freshly dissociated animal cap cells prevented the neuralising effects of dissociation, and induced epidermal markers instead (Wilson and Hemmati-Brivanlou, 1995). Together, this collection of observations converged on the influential "default model" (Hemmati-Brivanlou and Melton, 1997), which proposes that ectodermal cells in the animal cap have an endogenous tendency to become neural, but BMPs (especially BMP4, which is present ubiquitously in the animal cap at the blastula stage of *Xenopus*) normally inhibit this fate and instead induces them to become epidermal. The organiser produces a variety of BMP antagonists which are proposed to diffuse into the animal cap such that cells close to this region (at the dorsal side of the embryo) receive little BMP and can express their "default" neural fate, while cells remote from the organiser (ventral) are exposed to high amounts of BMP and become epidermal.

This model was received very favourably almost immediately because of its great simplicity and because it appeared at first sight to provide a definitive and compelling explanation for the whole phenomenon of neural induction by the organiser as well as explaining how the neural plate forms in normal development. Further

support quickly followed, including observations that animal caps from embryos not able to convey the BMP signal (after injection of a dominant negative receptor for BMP, or of non-cleavable forms of both BMP4 and BMP7, or injected with morpholinos against BMP4) undergo neural differentiation (Hawley et al., 1995; Hemmati-Brivanlou and Melton, 1994; Sasai et al., 1995; Xu et al., 1995). These observations are also consistent with earlier findings that xBMP (DVR4) signalling has a potent ventralising effect (Dale et al., 1992; Jones et al., 1992). The expression patterns of *BMP4* transcripts also suggest that the lifting of the BMP inhibition could be a step in "releasing" neural character: *BMP4* is ubiquitously expressed in the ectoderm of the *Xenopus* blastula but disappears from the region of the forming neural plate at early gastrula stage (Fainsod et al., 1994). Furthermore, as the transcription of *BMP* is regulated by the activity of BMP protein in *Drosophila* (Biehs et al., 1996) and zebrafish (Schulte-Merker et al., 1997), these patterns of *BMP* expression are likely to reflect changes in BMP activity in different regions. Similar results are obtained when the patterns of expression of other downstream targets of BMP signalling are analysed: *Smad5* (Suzuki et al., 1997a), *msx1* (Suzuki et al., 1997b), *Smad1* (Wilson et al., 1997). It was also reported recently that removal of all three BMP inhibitors (noggin, chordin and follistatin) causes a great expansion of the ventral structures and almost complete failure of dorsal structures - including neural plate - to form (Khokha et al., 2005) and more dramatically, that removal of three BMPs (-2, -4 and –7) along with a related TGF_ factor expressed dorsally, ADMP, causes almost the entire animal cap to become neuralised (Reversade and De Robertis, 2005)

Since the initial proposal of the default model, other secreted molecules, some of which are expressed either in the organiser or in some of its derivatives have been identified as BMP antagonists: Cerberus (Bouwmeester et al., 1996; Belo et al., 1997), - Gremlin (Hsu et al., 1998; Khokha et al., 2003), Dan (Eimon and Harland, 2001), Drm (Dionne et al., 2001; Pearce et al., 1999) and Ogon/Sizzled (Wagner and Mullins, 2002; Yabe et al., 2003).

Thus, the default model is supported by an overwhelming number of experimental results and is still regarded by many as the best model to explain the processes taking place during neural induction. However many observations are not entirely consistent with the model in its simplest form, and suggest considerably more complexity than the proposals of the default model.

1.2.2 Some evidence against the default model

Soon after the default model was proposed in *Xenopus* based on the experiments described above, data mainly from chick embryos started to suggest that the default model could not be a sufficient explanation for neural induction, at least in this species. First, most of the molecular players implicated in this model in *Xenopus* (especially BMPs -2, -4 and -7, Noggin, Chordin and Follistatin) are not expressed in the chick as might be expected from the *Xenopus* findings. The BMPs are not expressed ubiquitously to start with, and although transcripts are absent from the later neural plate, they are especially high at the border of the neural plate, corresponding to the future neural crest and placode territory (Streit et al., 1998). This territory has been proposed to be defined by intermediate levels of BMP signalling in *Xenopus* (Marchant et al., 1998), which is inconsistent with the endogenous expression patterns of these genes in both *Xenopus* and chick at the stages when neural crest induction is presumed to take place. Likewise BMP antagonists are not expressed appropriately: neither Follistatin nor Noggin is expressed in the chick node at all, at any stage. Follistatin does not appear to be expressed until much later stages of development, while Noggin appears at stage 5 in the head process but excluding the node (Streit et al., 1998; Streit and Stern, 1999a; Streit and Stern, 1999b). This timing is especially significant since careful time-course experiments with node grafts (Fig. 1.1) from differently aged donors and hosts revealed that the competence of the host to respond to neural induction disappears rapidly between stages 4 and 4+, while the inducing ability of the node declines to about half at precisely the same stage, strongly suggesting that neural induction by the organiser is normally finished by stage 4+ (Dias and Schoenwolf, 1990; Storey et al., 1992). Perhaps more compellingly, misexpression of BMP4 in the prospective neural plate of the chick does not completely block the expression of the early neural marker Sox3 (Linker and Stern, 2004; Streit et al., 1998) although it does block expression of the later neural marker Sox2; (Linker and Stern, 2004) and misexpression of Chordin or Noggin (Streit et al., 1998; Streit and Stern, 1999b), or of powerful intracellular antagonists of BMP signalling like Smad6 and/or dominant-negative BMP receptor in competent epiblast does not induce expression of any neural marker, either alone or in combination with the secreted inhibitors (Linker and Stern, 2004).

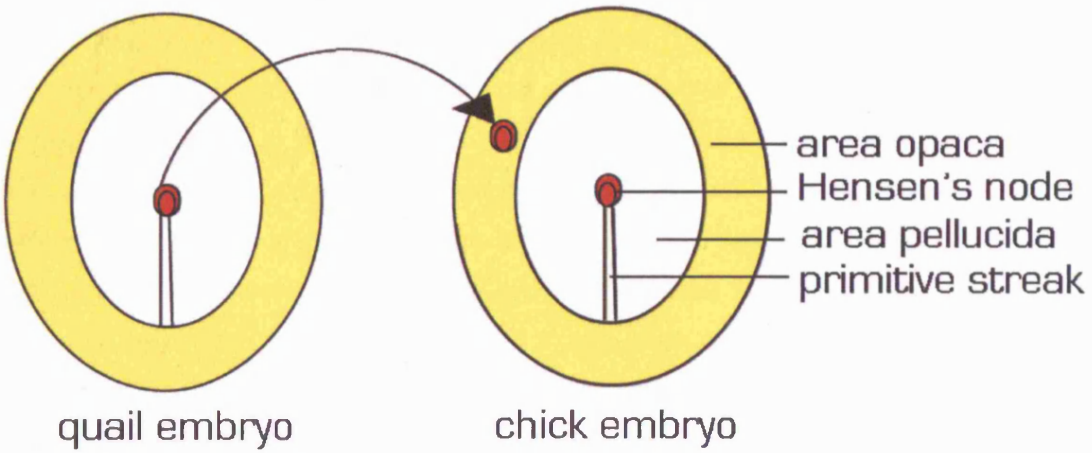

Fig. 1.1

Node graft. A quail node is transplanted to the inner 1/3 of the anterior part of the area opaca. This region of the embryo, despite its extraembryonic fate (Gallera, 1970) is able to respond to inducing signals from the node at stages 3^{+} to 4 (Dias and Schoenwolf, 1990; Storey et al., 1992; Streit et al., 1997).

Notably, neural induction requires a long period of contact between the organiser and the responding tissue. Timed node removal experiments revealed that as long as 13 hours of contact are required before the responding tissue is committed to a neural plate fate i.e. forms a neural plate after removal of the graft (Gallera and Nicolet, 1969). Moreover, molecular markers for the neural plate are expressed in the responding epiblast at different time points after the graft – thus Sox3 is induced after 3 hours, while Sox2 is induced only after 9 hours of contact (Streit et al., 2000; Streit et al., 1998; Streit and Stern, 1999a). These observations make it unlikely that neural induction could consist of a single step.

The ability to perform carefully timed grafts in the chick embryo enabled an investigation of whether signals other than BMP antagonists might be required upstream of BMP inhibition. Since BMP antagonists have no detectable effect when misexpressed in the area opaca, a node was grafted into this region and removed at various times before replacing it with a graft of Chordin-secreting cells. After 3 hours, Sox3 was induced but if the node was removed Sox3 expression was lost and no neural plate developed. However if the node was removed after 5 hours and cells secreting Chordin placed in its place, Sox3 expression was maintained, although no mature neural plate developed (Streit et al., 1998). This result strongly suggested that factors other than BMP antagonists, secreted by the organiser, are required before cells can respond to BMP antagonists (Streit et al., 1998; Streit et al., 2000).

To characterise the molecular differences between cells that have or have not been exposed to an organiser for 5 hours (and thus identify steps required upstream of

BMP inhibition during neural induction), a differential screen was designed (Streit et al 2000) using a method devised by Dulac and Axel (Dulac and Axel 1995). A stage 3+ quail node was grafted into the area opaca on one side of a single chick host embryo at stage 3+ (Fig.1.2 a). After 5 hours (Fig.1.2 b) the node was removed and discarded (Fig.1.2 c). Host epiblast cells that had been in contact with the node were excised and control cells from an identical position on the opposite side (which had not received a graft) similarly excised. Each explant was dissociated into single cells, and 5 small groups of cells from each were selected to generate cDNA libraries from the induced and control sides (Fig.1.2 d). Radioactive probes made from both libraries were used to perform a differential screen, in which both upregulated and downregulated genes were selected for analysis. In all, 15 genes with differential expression were identified.

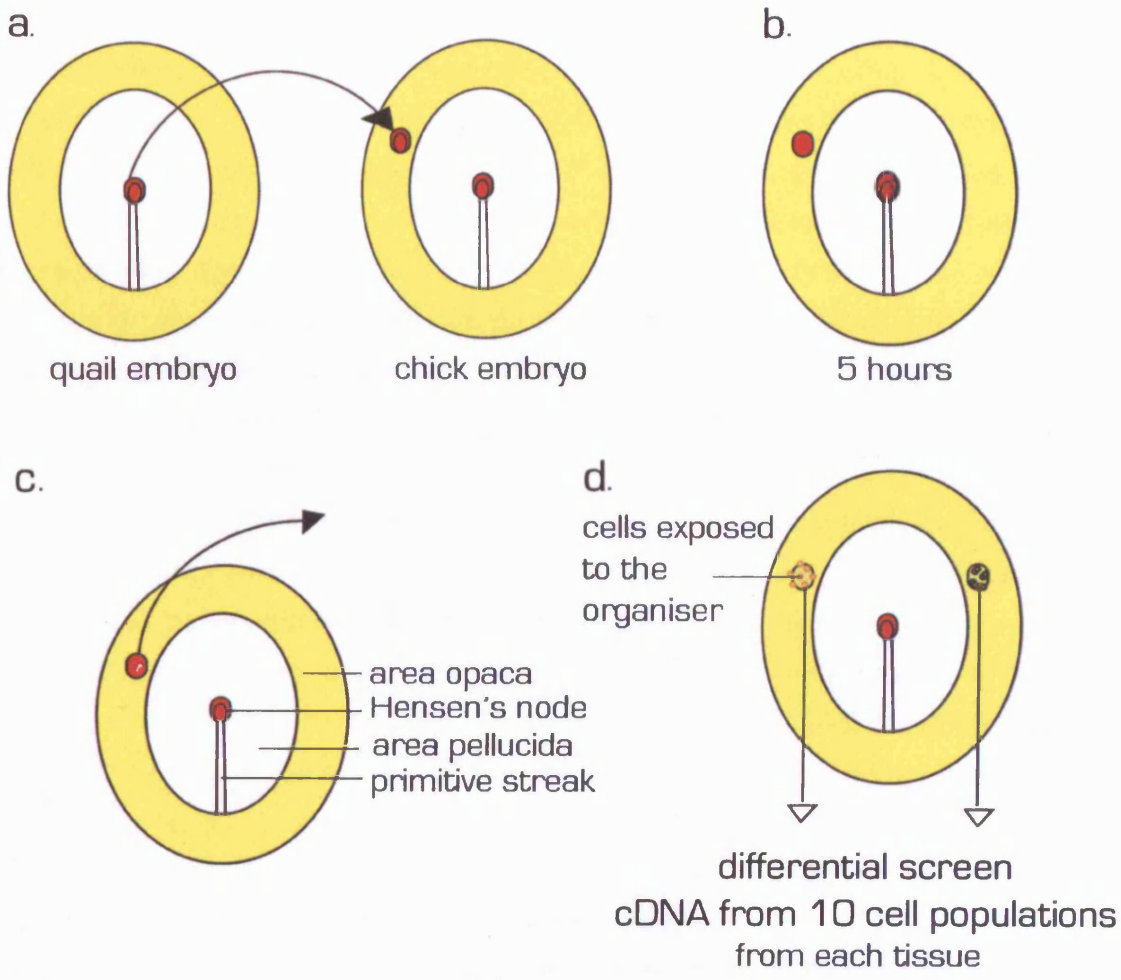

Fig. 1.2

A screen for early responses to signals from the organiser.

Of these 15 genes, two have so far been studied and the results published: *Churchill* turned out to encode a novel zinc finger transcriptional activator whose target is *Sip1* (Smad-interacting protein 1; see above). *Churchill* is induced after 4-5 hours' contact with the node and is involved in preventing continued cell ingression through the primitive streak at the end of gastrulation (see above), ensuring that some cells can remain on the surface and become part of the neural plate (Sheng et al., 2003). The second gene is induced much more quickly by the node (in just 1-2 hours) and was therefore named *ERNI* (Early Response to Neural Induction). *ERNI* expression is first detected in normal embryos long before gastrulation begins, at stages XII-XIII. It was shown that *ERNI* cannot be induced by BMP antagonists but can be induced by FGF8 independently of induction of *Brachyury* (Streit et al., 2000). Prior to primitive streak formation, *FGF8* is expressed both in the hypoblast and in Koller's sickle, and both of these structures can induce *ERNI* expression when grafted into the area opaca, with the same time course as a grafted node (Streit et al., 2000; Albazerchi and Stern, 2006). Moreover, induction of *ERNI* (as well as of *Sox3* and *Churchill*, and even the later neural plate marker *Sox2*) requires FGF signalling as node grafts in the presence of the FGF inhibitor SU5402 or with cells secreting a competitive antagonist (isolated ligand-binding domain of the FGF receptor) completely abolish induction of these genes and properties by a grafted node (Streit et al., 2000). These findings, together with explant experiments from early embryos (Wilson et al., 2000) suggested that the earliest steps of neural induction begin very early, even before gastrulation, and are mediated by FGF signalling.

Apart from these two genes, a further 13 isolated from the screen remain to be studied. Among them, 3 clones upregulated by the node (with initial denominations A4, C4 and F5) turned out to encode previously described genes: data base searches revealed that they represent chicken homologues of Heavy chain Ferritin (*hcf*), Defender against Apoptotic Death 1 (*Dad1*) and Polyubiquitin 2 (*Ubl*). There is evidence (reviewed elsewhere in this thesis) that all three genes have roles in controlling cell death in other systems. Since all three are expressed in the early developing neural plate, this raised the possibility that these genes, and perhaps the regulation of apoptosis, may play an important role in the early stages of neural induction. For these reason they were chosen for further study and constitute the subject matter of this thesis.

Here we establish the exact expression patterns of those genes and investigate their possible roles in the process of neural induction. We also investigated the distribution of apoptotic cells at early stages of chick development with special emphasis on the correspondence of apoptotic death and neural induction. We also

investigate the expression and functional activities of Cas3 and Cas9 and compare these to the patterns of PCD. Overall although this study did not uncover essential roles for any of these genes in neural induction, it does provide evidence that tight regulation of programmed cell death may accompany the early stages of neural induction, and results suggesting that the early neural plate is protected against apoptosis (probably partly by *Dad1*) and that cell death thus becomes concentrated at the edges of the neural plate, where the neural crest will later form.

CHAPTER 2:

Materials and Methods

2.1. Eggs and embryos

Fertilized Brown Bovan Gold hens' eggs were obtained from Henry Stewart & Co. Fertilized quails' eggs were obtained from B.C. Potter - Rosedean farm. Eggs were incubated at 38°C to the desired stages, which were determined according to Eyal-Giladi and Kochav for pre-streak stages (Roman numerals, X-XIV) (Eyal-Giladi and Kochav, 1976) and to Hamburger and Hamilton in Arabic numerals for later stages (Hamburger and Hamilton, 1951).

2.2. Embryo culture and transplantation experiments

For embryo culture, a modified version of the New (New, 1955) technique was used (Stern and Ireland, 1981). Embryos were explanted from the eggs in Pannett-Compton saline (Pannett and Compton, 1924) and cultured on glass rings over a pool of egg albumen in 35mm plastic dishes as previously described (Stern and Ireland, 1981).

Transplantation of Hensen's node was performed as described previously (Stern, 1999; Storey et al., 1992). The quail donor embryos were explanted and placed in a dish of Pannett-Compton saline (Pannett and Compton, 1924). Hensen's nodes were obtained from stage 3+/4 embryos by cutting the extreme tip of the primitive streak using fine mounted insect pins or G21 hypodermic needles. The most posterior part of the primitive streak of the same embryo was dissected to act as negative control in some experiments. Following excision, the graft was transferred to the host embryo in modified New culture and transplanted under a flap of yolky extraembryonic endoderm in the area opaca so as to be in contact with the ectoderm of this region. All such grafts were placed into the inner 1/3 of the area opaca at or above the level of the host node. Following transplantation, cultured embryos were incubated at 38°C in a humid chamber to the required stage (usually between 1.5-5 hours, or overnight).

2.3. Application of FGF or its inhibitor SU5402 and other secreted factors

When purified protein factors were available, these were delivered using plastic beads as vehicle. This was the case for FGFs. FGF4 or FGF8b (Streit and Stern, 1999a) were adsorbed onto heparin-coated acrylic beads (Sigma) as described (Streit et al., 2000). These were soaked at 4°C for 1-2 hours with murine FGF8b (R&D Systems, Sigma) at 25µg/ml or 50µg/ml in PBS, rinsed in PBS and transferred to the host embryo for grafting as described for Hensen's node grafts. PBS coated heparin-acrylic beads were used as controls.

FGF8b from (R&D Systems) and (Sigma) were tested and the results compared. It was

found that different batches of FGF8b had different activities in terms of its ability to induce *Sox3* and *Bra* in area opaca epiblast. At 25μg/ml, FGF8b from either Sigma or R&D did not induce *brachyury* (10/10) (except perhaps extremely weakly – see Fig. 2.1 a and b). At 50μg/ml, FGF8b from R&D usually did not induce *brachyury* whereas Sigma FGF8b did, although in some cases the opposite was found (Fig. 2.1 a and b). However, FGF8b from both sources induced *Sox3* (20/20) (Fig. 2.1 c and d).

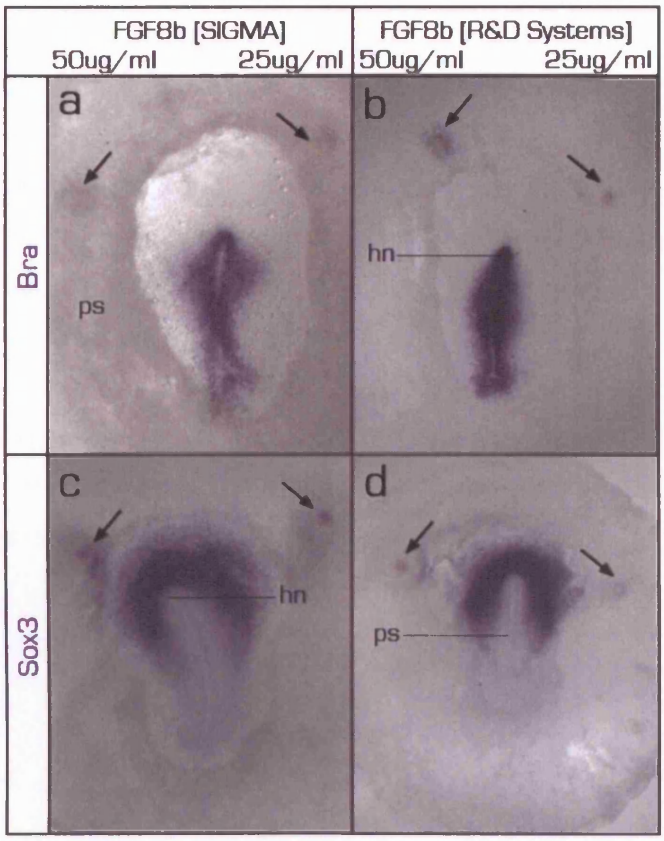

Fig. 2.1

Expression of *Sox3* and *brachyury* following application of different batches and concentrations of FGF. Arrows indicate the position of the grafted beads; **hn** - Hensen's node and **ps** - primitive streak.

To test whether FGF signalling is required for induction of different markers, the FGF-receptor inhibitor SU5402 (Mohammadi et al., 1997) (Calbiochem) was used. A stock at 1mM in Dimethylsulphoxide (DMSO) was diluted in PBS to a concentration of 25μM and this incubated with AG1X2 (BioRad) ion exchange beads for 1-2 hours at 4°C. Beads were kept on ice during loading and rinsed in PBS prior to transplantation. As a control for possible toxic effects of DMSO, pure DMSO-incubated AG1X2 beads were used, after rinsing in PBS. Beads were grafted as described for FGF and the embryos cultured in the same manner.

2.4. Electroporation

When purified factors were not available, when a non-secreted protein was to be tested, or for morpholino loss-of-function experiments, *in vivo* electroporation (Muramatsu et al., 1997; Sheng et al., 2003; Tur-Kaspa et al., 1986) was used to introduce an expression construct or fluorescein-labelled morpholinos into selected cells in living whole embryos. Chick embryos at stage 3+/4 were explanted in Pannett-Compton saline and placed in a plastic chamber containing a platinum cathode embedded in the bottom but exposed to the saline through a 1.5 mm diameter window. The embryo was positioned over the window, dorsal side up. For expression plasmids, DNA at a concentration of 1μg/μl in water containing 0.04% Fast Green and 6% sucrose was applied using a pulled micro-capillary pipette just above the dorsal side of the embryo. A movable anode electrode (sharpened Platinum wire insulated except for the tip) was lowered over the region to be electroporated (Fig.2.2). Three or four 50 millisecond pulses (500 milliseconds apart) of 5.5-6 Volts were given with a TSS10 pulse generator (Intracel). Following electroporation embryos were placed onto a vitelline membrane as for New culture (New, 1955; Stern and Ireland, 1981) and grown to the desired stage at 38°C.

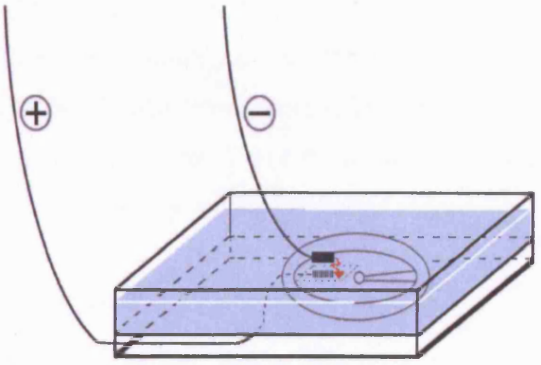

Fig 2.2

Schematic representation of the electroporation chamber.

2.5. In situ RNA hybridisation

To detect cells expressing various genes, whole-mount in situ hybridisation with digoxigenin- (DIG) or fluorescein-labelled riboprobes was used, following the protocols described (Stern, 1998; Streit and Stern, 2001). Embryos were fixed in 4% paraformaldehyde (PFA) containing 2mM EGTA in Ca^{++}/Mg^{++}-free PBS, pH 7.5 for 1 hour at room temperature or 4°C overnight. Labelled antisense riboprobes were

transcribed from each DNA construct after digestion with the appropriate restriction enzyme to generate a linear template as follows: cGata2 and cGata3 (Sheng and Stern, 1999) cloned in pGEM T easy were linearised with NdeI and transcribed with T7 polymerase. cMsx1 (Suzuki et al., 1991) (kind gift of Karel Liem, Jessell lab) cloned in pBlueScript was linearised with Bgl-II and transcribed with T3. cDlx5 (Pera et al., 1999) cloned in pBlueScript was linearised with NcoI and transcribed with T7. cCaspase3 (Johnson and Bridgham, 2000) cloned in pBlueScript was linearised with Nco I and transcribed with SP6. cSox2 (Uwanogho et al., 1995) (kind gift of Paul Scotting) - in pBlueScript was linearised with XbaI and transcribed with T7. cSox3 (Uwanogho et al., 1995) (kind gift of Paul Scotting) in pBlueScript was linearised with PstI and transcribed with T7. cERNI (Streit et al., 2000) cloned in pBlueScript was linearised with KpnI and transcribed with T3.

For in situ hybridization with two probes, one probe was detected using Nitro Blue Tetrazolium (NBT) and Bromo-Chloro-Indole-Phosphate (BCIP) as alkaline-phosphatase substrates to yield a deep purple colour. The other probe was detected using BCIP alone to give a light blue colour. In some cases Iodophenyl-Nitrophenyl-Phenyl-Tetrazolium Chloride (INT)-BCIP was used as an alternative to the latter to give a brick-red colour. The chromogens (all obtained from Roche) were diluted in 100mM Tris-Buffered saline (pH 9.5) containing 50mM Mg^{++} and 1% Tween-20 (NTMT): 4.5µl NBT stock (75µg/ml in 70% dimethylformamide, DMF), 3.5µl BCIP stock (50mg/ml in 100% DMF) per 1.5 ml for dark purple, 7.5µl BCIP stock: (50mg/ml in 100% DMF) per ml for light blue or 7.5µl INT-BCIP per ml for brick-red colour.

2.6. Whole mount immunohistochemistry

To detect quail cells after grafting into chick embryos, or to detect Green Fluorescent Protein (GFP) from an expression plasmid, embryos were subjected to whole-mount immunohistochemistry based on previously described protocols (Streit et al., 1998). For GFP detection, a rabbit anti-GFP (Molecular Probes) antibody diluted 1:2,500 in blocking buffer was used, followed by horseradish peroxidase (HRP) coupled goat anti-rabbit (Santa Cruz) secondary antibody diluted 1:2,500 in blocking buffer. Quail cells were detected with mouse (IgG) monoclonal antibody QCPN (anti-quail perinuclear antigen) (developed by Dr B.M. Carlson and obtained from the Developmental Studies Hybridoma Bank, maintained by the Department of Pharmacology and Molecular Sciences, The John Hopkins University School of Medicine, Baltimore, MD 21205, under contract N01-HD-2-3144 from NICHD) following published protocols (Streit et al., 1997). Anti-mouse IgG antibody conjugated to HRP (Jackson) was used as secondary

antibody, diluted 1:2,500 in blocking buffer. All HRP-labelled antibodies were detected using diaminobenzidine (DAB) in the presence of H_2O_2 as previously described (Stern, 1998).

2.7. Wax embedding and sectioning

Following in situ hybridisation, TUNEL staining and/or immunochemistry, embryos were rinsed in PBS and dehydrated with alcohol washes (5 minutes in 100% methanol and 10 minutes in 100% propan-2-ol). They were then cleared in absolute tetrahydronaphthalene for 30 minutes at room temperature. Paraffin wax was added at 1:1 ratio and embryos were placed at 60-65 °C for 30 minutes. Three changes of 30 minutes each in paraffin wax followed, after which embryos were placed into moulds and allowed to set at room temperature. 8μm thick sections were cut on a microtome (Zeiss Microm) and mounted on gelatin-albumen-coated glass slides. After drying overnight, they were de-waxed using Histoclear and mounted in Canada Balsam under a glass coverslip.

2.8. Photography

Photographs were taken using a SMZ-2 dissection microscope or a Vanox-T Olympus compound microscope fitted with an AxioCam (Zeiss) camera and Zeiss AxioVision 3.1 software. Composite images were prepared using Adobe Photoshop CS.

2.9. Polymerase Chain Reaction (PCR) and sequencing

To amplify various plasmids for cloning, the Polymerase Chain Reaction (PCR) (Saiki et al., 1988) was used. A hot start of 5 minutes was carried out at 95°C when a library was used as a template. After this, an initial incubation for 5 minutes was carried out at 95°C in a PCR mix containing 1μM of appropriate reverse and forward primers, 0.2mM of each dNTPs, 1x magnesium-free buffer, 1.5mM $MgCl_2$ and of 2.5 units/50μl Taq Polymerase. Unless otherwise specified, all PCR reactions involved 32 cycles of: 3 minutes at 95°C, 1.5 minutes at 49°C and 1.5 minutes at 72°C using a DNA Thermal Cycler 480 (Perkin Elmer). After the last cycle the samples were kept at 72°C for 10 minutes and then cooled down to 4°C.

When sequencing of DNAs was required, this was performed by the Advanced Biotechnology Centre at Imperial College London from PCR products.

2.10. Plasmid transfection into competent bacteria

DH5α competent cells (40-50 μl) were transformed with 50ng cDNA by standard techniques (Sambrook et al., 1989). Colonies were picked, cultured overnight at 37°C in LB broth containing ampicillin (50μg/ml). Plasmids were extracted using Mini or Maxi Prep kits (Qiagen), following the manufacturer's instructions.

CHAPTER 3:

Defender Against Cell Death (*Dad1*)

3.1. Introduction

Defender Against Cell Death (*Dad1*) (Fig. 3.1) was first identified as a gene responsible for apoptotic cell death in temperature-sensitive mutants (*tsBN7*) of the hamster BHK21 cell line (Nakashima et al., 1993). In tsBN7 mutants, *Dad1* has a point mutation, where a G>A substitution results in the conversion of glycine-38 into arginine (Nakashima et al., 1993). It has been suggested that DAD1 could be involved directly in mechanisms regulating programmed cell death (PCD) (Hauptmann et al., 2006; Makishima et al., 1997; Nakashima et al., 1993; Sugimoto et al., 1995). Since then, homologues of *Dad1* have been identified in other species, and the orthologues from human (Nakashima et al., 1993; Sugimoto et al., 1995), mouse (Makishima et al., 1997), *Xenopus* (Sugimoto et al., 1995) and nematode (Sugimoto et al., 1995) can all rescue the phenotype of the *tsBN7* mutation in the hamster cells. *Dad1* is not even restricted to animals; strikingly, even the *Arabidopsis* (Gallois et al., 1997) and rice (Makishima et al., 1997) genes can complement the *tsBN7* mutation.

Ectopic expression of human or nematode DAD1 prevents over 20% of PCD that would otherwise take place during normal embryogenesis in *C. elegans* (Sugimoto et al., 1995). The only known *Dad1* homologue not able to complement the *tsBN7* mutation is from the yeast *Saccharomyces cerevisiae* (Makishima et al., 2000). In all species, *Dad1* codes for the ξ-subunit (called *Ost2* in yeast) of the oligosaccharyltransferase complex OST (Kelleher and Gilmore, 1997; Makishima et al., 1997; Silberstein et al., 1995). There is evidence that DAD1 is required for the function - including catalytic activity (Makishima et al., 1997; Sanjay et al., 1998; Silberstein and Gilmore, 1996) and structural integrity of OST (Makishima et al., 1997; Sanjay et al., 1998; Silberstein et al., 1995). This complex is involved in the initial step of N-linked glycosylation (Kaplan et al., 1987; Silberstein and Gilmore, 1996; Tanner and Lehle, 1987), a highly conserved post-translational modification required for the effective transport of proteins through the secretory pathway and many other activities (Guan et al., 1985; Herscovics and Orlean, 1993; Kornfeld and Kornfeld, 1985; Riederer and Hinnen, 1991; Winther et al., 1991). During this process the oligosaccharyl core, rich in mannose, (Gly3Man9GlcNAc2) is transferred from the lipid carrier dolichol pyrophosphate to asparagine residues within a consensus site (Asn-X-Ser/Thr) in polypeptide chains (Gavel and von Heijne, 1990). Certain mutations in *Dad1* or other components of the OST complex can cause under-glycosylation of membrane bound and soluble glycoproteins (Makishima et al., 1997; Sanjay et al., 1998; Silberstein and Gilmore, 1996).

Disruption of the *Ost2* locus is lethal in yeast (Silberstein et al., 1995) and in homozygous mutant mice (Brewster et al., 2000; Hong et al., 1997; Hong et al., 2000; Nishii et al., 1999). However the phenotypes of different mutations in the *Dad1* gene differ significantly. Mutants with a disrupted open reading frame (at the site of the first membrane-spanning domain) have more severe abnormalities and do not survive beyond E7.5 (Nishii et al., 1999). Another mutation was made by replacing Exon 1 of *Dad1* with a Neo^R cassette. Homozygous mice carrying this mutation die at the blastocyst stage, before implantation (Brewster et al., 2000). Heterozygotes do not show visible defects but have a tendency towards increased apoptosis when cultured in vitro, compared to the wild type (Brewster et al., 2000). In a third mutation, $N_{\Delta}26$, homozygous animals carrying a deletion of Exon 3 (which is not translated) of *Dad1* start to deteriorate by E10.5 (Hong et al., 1997). $N_{\Delta}26$ embryos are characterised by a slower rate of development and shortened, underdeveloped posterior axes by E8.5, but do have a head fold, a beating heart and somites (Hong et al., 2000). All three mutants die from excess apoptosis (Brewster et al., 2000; Hong et al., 2000; Nishii et al., 1999) confirming an important requirement for DAD1 as an anti-apoptotic protein. Interestingly in $N_{\Delta}26$ mutants, apoptosis takes place mainly in the mesoderm and ectoderm and especially at the distal tip of the primitive streak (Hong et al., 2000), suggesting a requirement for inhibition of cell death in the organizer. Heterozygous mice are also mildly affected, having a partially penetrant phenotype including soft tissue syndactyly and mild thymic hypoplasia (Nishii et al., 1999).

Only two of these mutations were tested for the presence of N-glycans to assess for possible changes in the activity of the OST complex. Surprisingly, homozygous mice with a mutation in the open reading frame of *Dad1* seem to retain some N-linked glycosylation function (Nishii et al., 1999). The opposite is true for $N_{\Delta}26$ embryos, where membrane and secreted proteins are significantly underglycosylated (Hong et al., 2000).

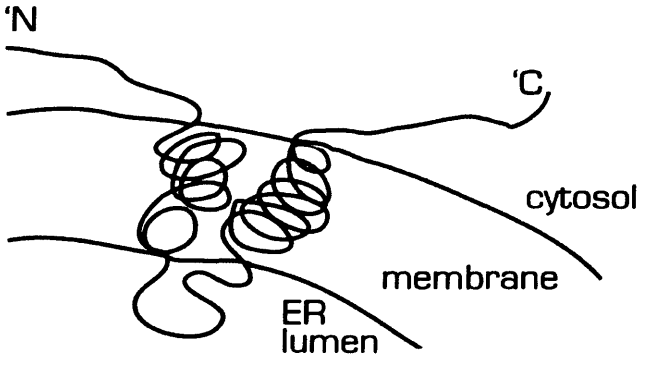

Fig 3.1

Schematic representation of cellular topography of DAD1; (based on Makishima et al., 1997).

The exact mechanisms by which DAD1 is involved in the process of apoptosis are still not known. Proposed interactions with a known anti-apoptotic protein myeloid cell leukemia-1 (MCL-1) cannot explain this process (Makishima et al., 2000). DAD1 binds to the anti-apoptotic protein MCL-1 in vitro; however a mutant version still able to interact in this way, but lacking the last 4 amino acids from the C-terminus, disrupts N-linked glycosylation and prevents the rescue of the *tsBN7* mutation in BHK21 hamster cells (Makishima et al., 2000). However, some controversy remains concerning the requirement for N-linked glycosylation for preventing apoptosis: on one hand, the above study (Makishima et al., 2000) reports that tunicamycin treatment (to disrupt N-linked glycosylation) does not mimic the phenotype. On the other hand, another group showed that the same treatment does cause apoptosis in this cell line (Yoshimi et al., 2000), in agreement with observations in yeast and other mammalian cell lines (Hauptmann et al., 2006; Lin et al., 1999; Miyake et al., 2000; Perez-Sala and Mollinedo, 1995; Walker et al., 1998). Additionally, the use of different GFP-fusion constructs of DAD1 also suggested that the C terminus is important for the correct functioning of the protein, since fusions at the C-terminus disrupt DAD1 function (Nikonov et al., 2002). These data support the hypothesis that a function in glycosylation by DAD1 is responsible for its anti-apoptotic activity. It has also been suggested that N-linked glycosylation plays an additional role in protein quality control, where accumulated misfolded proteins can be detected by endoplasmic reticulum chaperones and targeted for degradation (Helenius, 1994). In addition, DAD1 may have yet another role, because its overexpression in mouse transgenics causes proliferation in the peripheral immune system and overexpression in the thymus does not prevent naturally occurring apoptosis (Hong et al., 1999).

The exact role of DAD1 during normal development has not been studied so far. The finding from the screen presented in the Introduction (Chapter 1) that this gene is induced within 5 hours' exposure of epiblast to signals from Hensen's node suggests a role of this protein, and perhaps of apoptosis, in neural induction. This chapter explores these functions using a variety of embryological and molecular approaches.

3.2. Materials and methods

3.2.1. Bioinformatic analysis

Three main databases containing chick genome information were accessed: www.ensembl.org, www.ncbi.nlm.nih.gov and www.genome.ucsc.edu. To analyse and align sequences, ClustalW (www.ebi.ac.uk/clustalw) was used and the results visualised using Jalview 2.08.1 (Clamp et al., 2004). The degree of amino acid identity

was calculated using MUSCLE – a multiple sequence alignment with high accuracy and high throughput (Edgar, 2004). The results were calculated using the Kyte and Doolittle hydrophobicity scale (Kyte and Doolittle, 1982) and also visualised using Jalview 2.08.1. Further analysis of the protein structure and intracellular localisation was performed in the ExPASy (www.expasy.org) database. The promoter searches were performed using Gene2Promoter program, and putative transcription factor binding sites identified using MatInspector (both in www.genomatix.de).

3.2.2. Riboprobe transcription

The *Dad1* cDNA was cloned into the pBlueScript vector. To generate antisense riboprobes for in situ hybridisation, the plasmid containing *Dad1* was linearised by digestion with XhoI and transcribed with T3 RNA Polymerase. In situ hybridisation was performed as described in Chapter 2.

3.2.3. Constructs for electroporation

To investigate the possible function of *Dad1 in vivo*, *Dad1* was over- or misexpressed using *in vivo* electroporation. The pCAβ vector, containing the ubiquitously expressed chick β-actin promoter, a CMV enhancer followed by the cloning site and then by an Internal Ribosome Entry Site (IRES) to direct translation of Green Fluorescent Protein (GFP) was digested with BsmBI and ClaI and gel-purified using a Gel Extraction Kit (Qiagen). The reading frame of chick *Dad1* was amplified by PCR from two chick cDNA libraries (stage 2-4 and 18-20, respectively). Primers (Forward: GATCAGCGGCCGC ATGTCGGGCACGGCGGG; Reverse: TGCTCATCGATTCAGCCAACAAAATTGATA) were designed to incorporate recognition sites for digestion by NotI and ClaI (underlined, respectively, in the two sequences above). This made the PCR product compatible for ligation into the product of the BsmBI / ClaI digestion of pCAβ. The insert was ligated with purified vector using T4 DNA ligase (Promega).

The ligation products were transformed into DH5α competent cells. Plasmids were harvested from different colonies and sequenced. Despite numerous attempts, each plasmid containing a full length *Dad1* cDNA in pCAβ had some mutations. Two plasmids, designated 11 and 8 with complementary error free regions were selected and digested with NotI / BamHI and BamHI / ClaI respectively. These were cloned into pGEM T-Easy (Promega, according to the manufacturer's instructions) and again cut with NotI / BamHI and BamHI / ClaI respectively. A three way ligation between purified fragments 11, 8 and the BsmBI / ClaI digested fragment of pCAβ allowed the creation of a mutation free vector for electroporation. The sequence was verified against the chick genome sequence contained in Ensembl.

To test whether any potential role of DAD1 in early development requires N-linked glycosylation (which requires the C-terminus of the protein), a mutated version of *Dad1* lacking the C-terminal 6 amino acids (VINFVG) was constructed by the same method using the same forward primer as above and a new reverse primer (TGC TCATCGATTCAGACGAGATGCAGGATGGT), again containing a ClaI recognition site (underlined). Plasmids were sequenced with: pCAβ forward primer (GCC TCTGCTAACCATGTT) and IRES reverse primer (CTTATTCCAAGCGGCTTC). The resulting sequences were analysed using NCBI Blast.

The pCA_ vectors described above were introduced by electroporation into stage 3+/4 embryos as described in Chapter 2. The electroporated embryos were grown for 6 hours (to study short term effects) or to stages 8-12 (for longer-term consequences). At the end of this period embryos were fixed as described for in situ hybridisation (Chapter 2) and processed for in situ with various markers including *Sox3* (Rex et al., 1997), *Sox2* (Rex et al., 1997), *Dlx5* (McLarren et al., 2003; Streit and Stern, 1999a; Yang et al., 1998), *Pax7* (McLarren et al., 2003; Otto et al., 2006) and *Gata2* (Sheng and Stern, 1999). After in situ hybridisation, antibody staining against GFP was used to reveal the cells that had been electroporated using the procedures described in Chapter 2.

3.2.4. Design of morpholinos

To test whether *Dad1* is required for normal development of the early nervous system, morpholino-mediated knock-down experiments were performed. Electroporation of fluorescein-labelled morpholino antisense oligonucleotides (GeneTools; www.gene-tools.com) was chosen as a method for preventing DAD1 translation *in vivo*.

The chick *Dad1* sequence (Ensembl and GenBank; accession numbers AAC60276.1 and U83627 respectively) was confirmed by sequencing a fragment of genomic DNA containing the *Dad1* gene.

Extraction of genomic DNA: one embryo at stage 20 was collected and washed 3 times in PBS. The PBS was replaced with 500 μl of lysis buffer (50mM Tris pH8.0, 100mM NaCl, 100m EDTA, 1% SDS with 25 μl 10mg/ml Proteinase K) and incubated overnight at 56°C. The following day the lysed embryo solution was mixed for 5 minutes or more on the shaker. 170 μl of 5M NaCl solution was added. Following a further 5 minutes on the shaker the solution was spun for 5-10 min at 14,000rpm in an Eppendorf benchtop Microfuge at room temperature. The supernatant was removed to a new tube and 500 μl of propan-2-ol was added. The solution was mixed by inversion and centrifuged for 10 min at 14,000rpm at room temperature. The pellet was washed twice with 70% ethanol and centrifuged for 5 min and the supernatant discarded. The dried pellet was

resuspended in 200μl of 1XTE and placed for at least 2 hrs at 37 °C with occasional shaking to allow the DNA to dissolve.

A fluorescein-tagged morpholino (CACCCGAACCCGCCGTGCCCGACAT) targeting the first 25 bases of the coding sequence was designed by Dr. Paul Morcos (Gene Tools) and purchased from Gene Tools. A fluorescein-labelled standard control morpholino (sequence CCTCTTACCTCAgTTACAATTTATA) (Gene Tools) was used as a negative control. Each morpholino was used at 2mM in water containing 0.01% Fast Green and 6% sucrose, mixed with empty pCAβ at a final dilution of 1μg/μl (used as a carrier and as an additional marker for the electroporated cells) was introduced into cells by electroporation as described above (Kos et al., 2003; Sheng et al., 2003).

3.2.5. DAD1 antibody staining

To detect DAD1 protein, a rabbit anti-DAD1 antibody (Nakashima et al., 1993) (kind gift of Professor Takeharu Nishimoto; raised against the peptide sequence: NPQNKADFQGISPER was used - for comparison, the corresponding sequence of chick DAD1 is: NPQNKGEFQGISPER). The antibody was diluted in blocking buffer (see Chapter 2) at 1:300 dilution, and goat anti-rabbit HRP (Santa Cruz) as secondary antibody was used.

3.3. Results

3.3.1. Identification of *Dad1*

A cDNA clone, originally designated C4, containing an insert of 734 bp was obtained from the screen (see Chapter 1). Database searches were conducted to identify this clone and found that a 510 bp region of this insert contained a putative complete open reading frame (372 bp), highly homologous to chicken *Dad1*. Subsequent screening of a stage 3-4 chick embryo cDNA library resulted in the isolation of a full-length clone containing, in addition to the entire open reading (ORF) frame, 9 bp putative 5' UTR and 215 bp of 3' UTR, adding up to 734 bp, suggesting that no untranslated sequences exist either up- or downstream of those contained in the clone originally isolated. This sequence is almost identical to the cDNA deposited under EMBL accession number U83627, with 9 separate single base pair differences in ORF.

The genomic locus of chicken *Dad1* is found on chromosome 27 at location 74,837–77,599 (Ensembl gene id: ENSGALG00000000196). The only variation identified to date (July 2006) in Dad1 genomic sequence is a single non-synonymous SNP (Single Nucleotide Polymorphism) affecting V^9 > Y. The gene contains three

exons (250 bp, 149bp and 198bp) separated by 2 introns. There appears to be 9 bp 5' UTR and a longer (225 bp) 3' UTR (contained at the end of exon 2 and the whole of exon 3, nt 372-597). The transcript is predicted to encode a 123 amino acid protein.

As previously discussed (see Introduction above), the protein sequence of DAD1 is conserved through evolution (Table 3.1, Fig. 3.1). There is over 80% conservation between vertebrates. The vertebrate proteins also share over 40% amino acid identity with plant species, over 50% with nematode and over 60 % with fly. The lowest homology is with yeast, which is less than 40% identical to all except the fly.

	Chicken	Nematode	Hamster	Mouse	Human	Cress	Fly	Rice	Dog
Yeast	31.45	37.72	36.21	36.21	36.52	34.43	40.7	32.2	37.82
Dog	81.42	61.06	99.12	99.12	99.11	48.67	68.7	47.8	
Fly	60.71	62.50	68.75	68.75	68.75	45.54			
Cress	46.55	48.67	47.79	47.79	48.21				
Human	82.14	61.61	100.00	100.00					
Mouse	81.42	61.95	100.00						
Hamster	81.42	61.95							
Nematode	59.29								

Table 3.1

Relative identity between the amino acid sequences of DAD1 from different organisms.

A Neighbour Joining tree (Fig. 3.2) was constructed using PID (the percentage identity between two sequences at each aligned position) from MUSCLE also illustrates the predicted phylogenetic relationships between DAD1 sequences in these species. Given that the degree of amino acid identity between the different species is in some cases not particularly high, the sequences were aligned and the amino acids assigned different colours according to their hydrophobicity (Fig. 3.3). This shows very strong conservation among all the species compared including yeast. Notably the C-terminal-most amino acid is N in yeast (hydrophilic), whereas this position is occupied by G in other homologues, which is neutral.

3.3.2. Expression of *Dad1* during early development

To determine the spatial and temporal pattern of expression of *Dad1* during early development in normal embryos, and especially to find out whether its expression is consistent with the finding that *Dad1* may be induced as an early response to signals

from Hensen's node, whole mount in situ hybridisation was used. Virtually no expression could be detected in any region before stage 4 (Fig. 3.4 a-c). At stage 4 (Fig. 3.4 d), *Dad1* is upregulated in the epiblast especially around Hensen's node (Fig. 3.4 d, arrow). Higher levels of expression are detected in the lips of the entire primitive streak except in Hensen's node (Fig. 3.4 d). Expression is also seen in the epiblast in a region corresponding to the area already colonised by mesoderm (Fig. 3.4 d, k). The most anterior-lateral epiblast does not reveal expression and the mesoderm and endoderm show barely detectable expression (Fig. 3.4 k).

During neurulation and early somite stages, *Dad1* is expressed weakly, predominantly in Hensen's node (Fig. 3.4 e, arrow), the forming neural plate (Fig. 3.4 e-g) and in somites (Fig. 3.4 f-j). Some expression is also seen in the lateral mesoderm (Fig. 3.4 l, arrows) and in the primitive streak (Fig. 3.4 e-h).

At stages 12 – 14 *Dad1* is still expressed in the neuroepithelium, especially dorsally (Fig. 3.4 i, j, m and n, arrow). In the notochord, expression varies along the axis. The most rostral regions do not display expression (not shown), which is followed by strong expression in the hindbrain and upper trunk (Fig. 3.4 s, r and q) and finally the most caudal regions do not express *Dad1* (Fig. 3.4 o). There is also marked expression in the forming mesonephric rudiments (Fig. 3.4 j, q and r).

In conclusion, *Dad1* is expressed in early nervous system for a brief period (around stage 4), but it is not exclusive to this region and transcripts are also found elsewhere and at later stages.

3.3.3. Time-course of induction of *Dad1* by Hensen's node

The original screen that led to the isolation of *Dad1* was conducted after 5 hours' contact between the Hensen's node graft and the responding epiblast. To confirm that *Dad1* is indeed induced by the node and to determine the timing of induction more precisely, Hensen's node grafts were performed in time-course and the expression of *Dad1* analysed. The previous section showed that *Dad1* is expressed very weakly indeed during early stages of normal development, therefore it was not surprising that its induction by the node was also barely detectable (Fig. 3.5). No expression at all is seen after 1.5 hours following a Hensen's node graft (0/9; Fig. 3.5 a and e). Very weak expression is first seen after 3 hours (9/13; Fig. 3.5 b and f) which only barely intensifies at 4 (9/11) and 5 hours (11/13) Fig. 3.5 c-d, g-h). Control grafts (posterior primitive streak) did not induce *Dad1* at any time point: 1.5 (0/5), 3 (0/10), 4 (0/4) or 5 (0/9) hours following grafting. Identification of quail donor cell by QCPN antibody staining confirmed that node-derived cells do not contribute to the induced ectodermal cells expressing *Dad1*.

In conclusion, these results suggest that if the node can induce *Dad1* in the epiblast, this induction is extremely weak.

3.3.4. *Dad1* does not affect neural, neural crest or epidermal fates

To establish whether expression of *Dad1* might influence cell fate choices at early stages of neural development, it was misexpressed using *in vivo* electroporation. Ectopic expression of DAD1 does not induce the neural markers *Sox3* (21/21; Fig. 3.6 a, f) or *Sox2* (19/19; Fig. 3.6 d, i), the neural crest and neural plate border markers *Dlx5* (15/15; Fig. 3.7 b, g) or *Pax7* (9/9; Fig. 3.7 e, j) or the epidermal marker *Gata2* (8/8; Fig. 3.7 b, e). In addition, the effects of *Dad1* misexpression on the other two genes (*UbII* and *hcf*) that are the subject of this thesis were tested. Neither gene was induced or repressed by ectopic *Dad1* (*UbII*: 8/8; Fig. 3.9 b, f; *hcf*: 13/13; Fig. 3.9 c, g). Finally, the effects of misexpression of a putative inhibitory construct (*Dad1* lacking the extreme 3' end which encodes the C-terminal 6 amino acids) were studied. Again there were no effects on the expression of *Sox3*, *Sox2*, *Dlx5*, *Gata2* or *hcf* (Fig. 3.6 e, j; Fig. 3.6 e, j; Fig. 3.7 c, h; Fig 3.8 c, f; Fig. 3.9 d, h). Control electroporation (empty pCAβ vector) does not alter patterns of expression of any genes tested (some shown Fig.3.6 c, h; Fig.3.7 a, f, d, i; Fig.3.8 a, d; 3.9 a, e)

In conclusion neither overexpression, nor ectopic expression nor expression of a putative dominant-negative form of DAD1 could be demonstrated to change cell fates (in terms of a decision between epidermis, neural crest / neural plate border and neural plate) during early chick development.

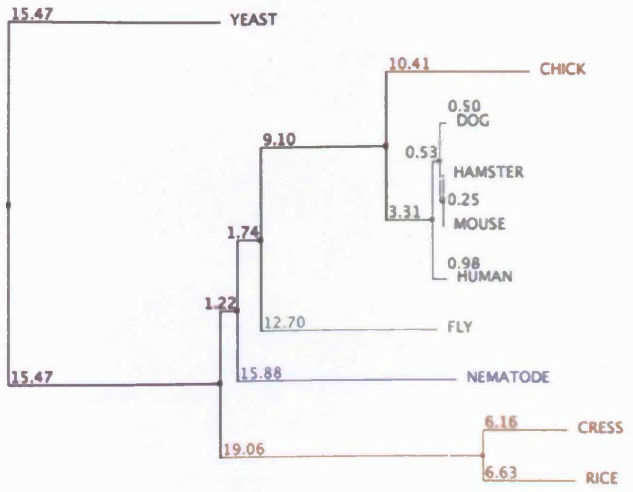

Fig. 3.2
Neighbour Joining Tree (Saitou and Nei, 1987) of DAD1 protein.
Amino acid sequences from different organisms: yeast (NP_014746), chick (AAC60276), dog (XP_537361), hamster (PB1806), mouse (NP_034145), human (NP_001335), fly (NP_609222), nematode (AAB96727) and yeast (NP_014746).

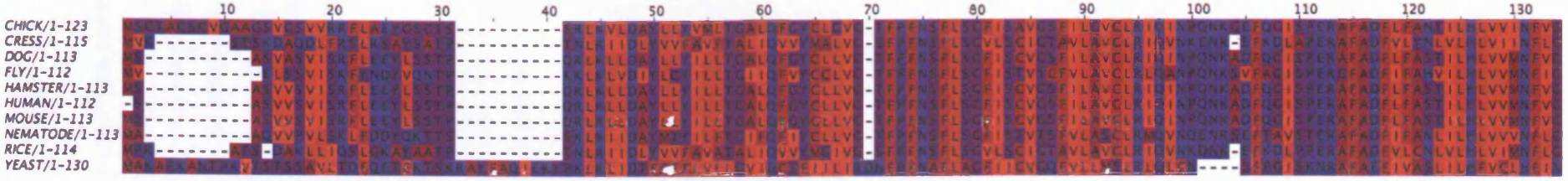

Fig. 3.3
Alignment of DAD1 amino acid sequences from different organisms,
showing the degree of hydrophobicity of each residue (Kyte and Doolittle, 1982).
The most hydrophobic and hydrophilic residues are coloured red and blue, respectively.
Neutral amino acids are shown in purple.
Accession numbers: chick (AAC60276), cress (CAA64837), dog (XP_537361), fly (NP_609222), hamster (P61806), human (NP_001335), mouse (NP_034145), rice XP_472334) and yeast (NP_014746).

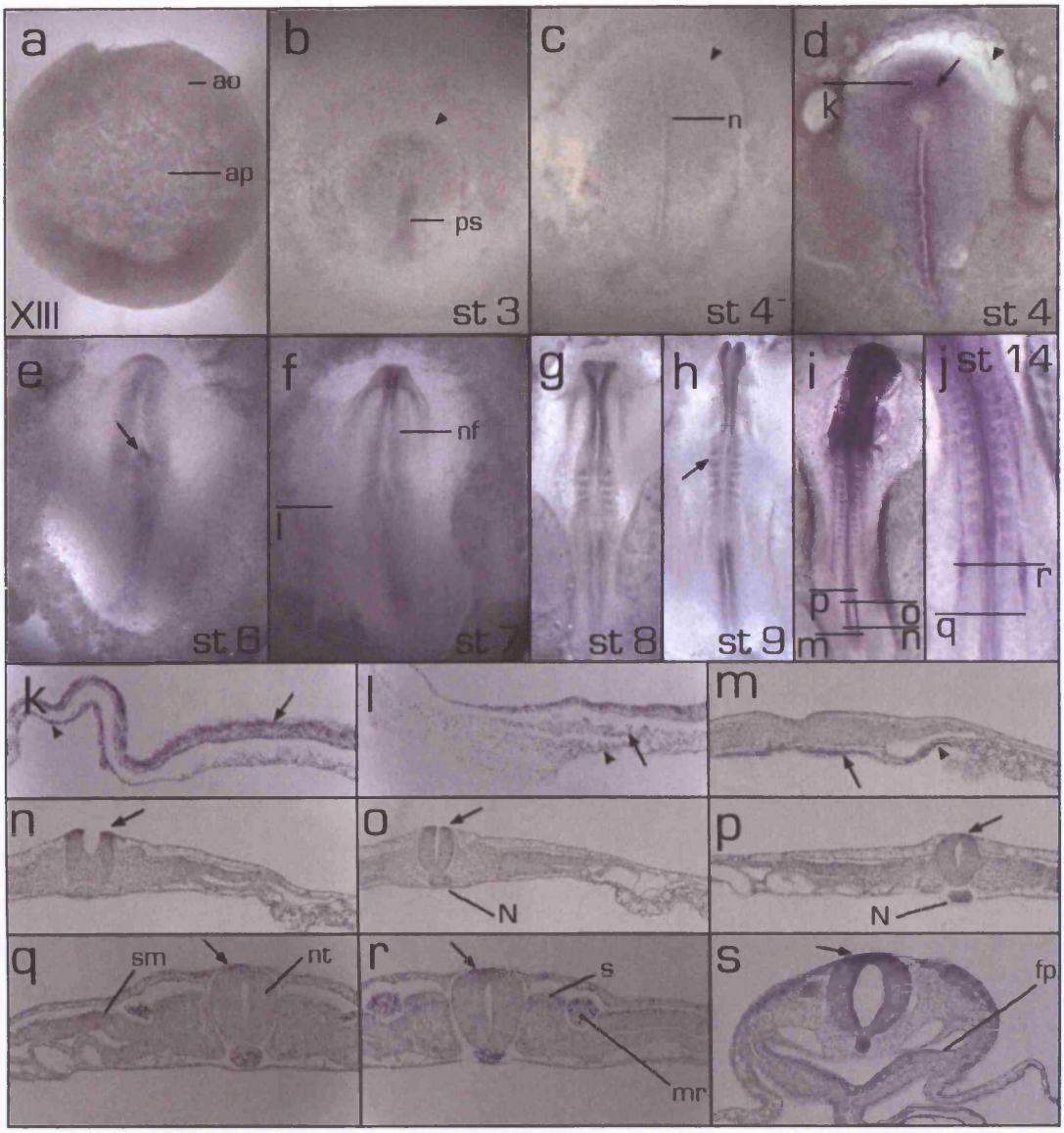

Fig. 3.4

Expression patterns of ***Dad1*** in a pre-primitive streak stage embryo (**a**) and at stages 3 (**b**), 4⁻ (**c**), 4 (**d**), 6 (**e**), 7 (**f**), 8 (**g**), 12 (**i**) and 14 (**j**), **k**: section through the embryo shown in **d**; **l**: section through the embryo in **f**; **m**, **n**, **o**, **p**: sections through the trunk of a stage 12 embryo; **q**, **r**: sections through the trunk of the embryo at stage 14; **s**: section through the hindbrain of a stage 14 embryo. Arrowheads in **b**, **c** and **d** point to the anterior region of the epiblast not expressing *Dad1*; the area with higher levels of *Dad1* in the neural ectoderm is shown in **k** and by an arrow in **d**. Node at stage 6 is indicated by an arrow in **e**; somatic mesoderm (**p** - **r**) and somites (**q**, **r**, **f** - **j**) also express *Dad1* indicated by arrow in **h**. arrow in **l**, most later endoderm arrowheads in **k** - **m** and the posterior endoderm (arrow in **m**). There is a strong expression in the tips of the neural folds (arrow in **n**) and the most dorsal region of the neural tube (arrows **o** - **s**).

ap - area pellucida; **ao** - area opaca; **ps** - primitive streak; **n** - Hensen's node; **nf** - neural folds; **nt** - closing neural tube; **s** - somites; **mr**- mesonephric rudiment; **sm** - somatic mesoderm; **fp** - floor of the pharynx and **N** - notochord.

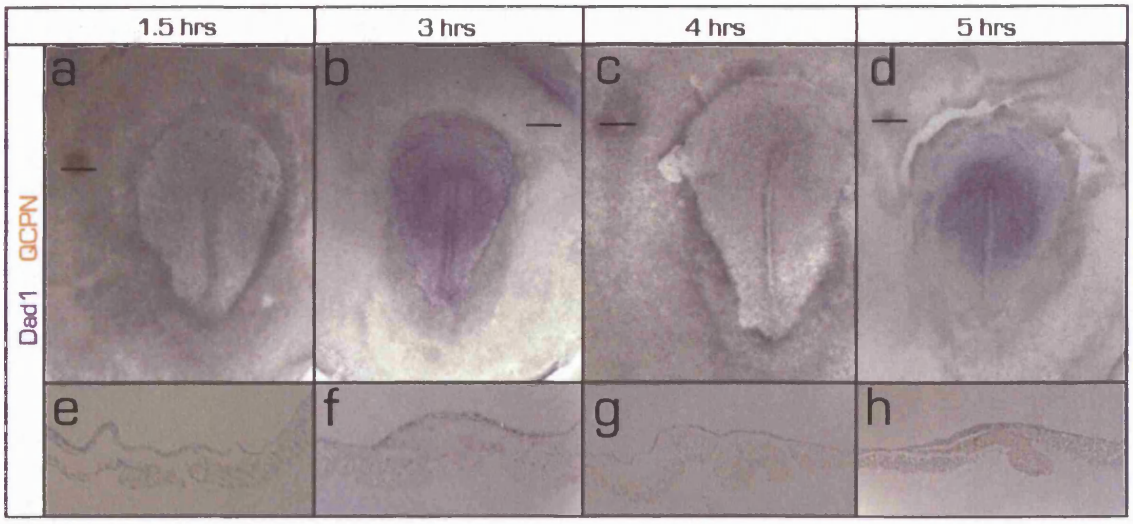

Fig. 3.5

Induction of ***Dad1*** in the area opaca by a graft of **Hensen's node**: no induction is seen sfter 1.5 hours (**a**), and only extremely weak induction after 3 hours (**b**). Induction is still weak after 4 hours (**c**) and 5 (**d**) hours; **e**-**h**: sections at the level of the graft, showing graft-derived quail cells stained brown by QCPN antibody after 1.5 hours (**e**), 3 hours (**f**), 4 hours (**g**) and 5 hours (**h**) incubation following the graft.

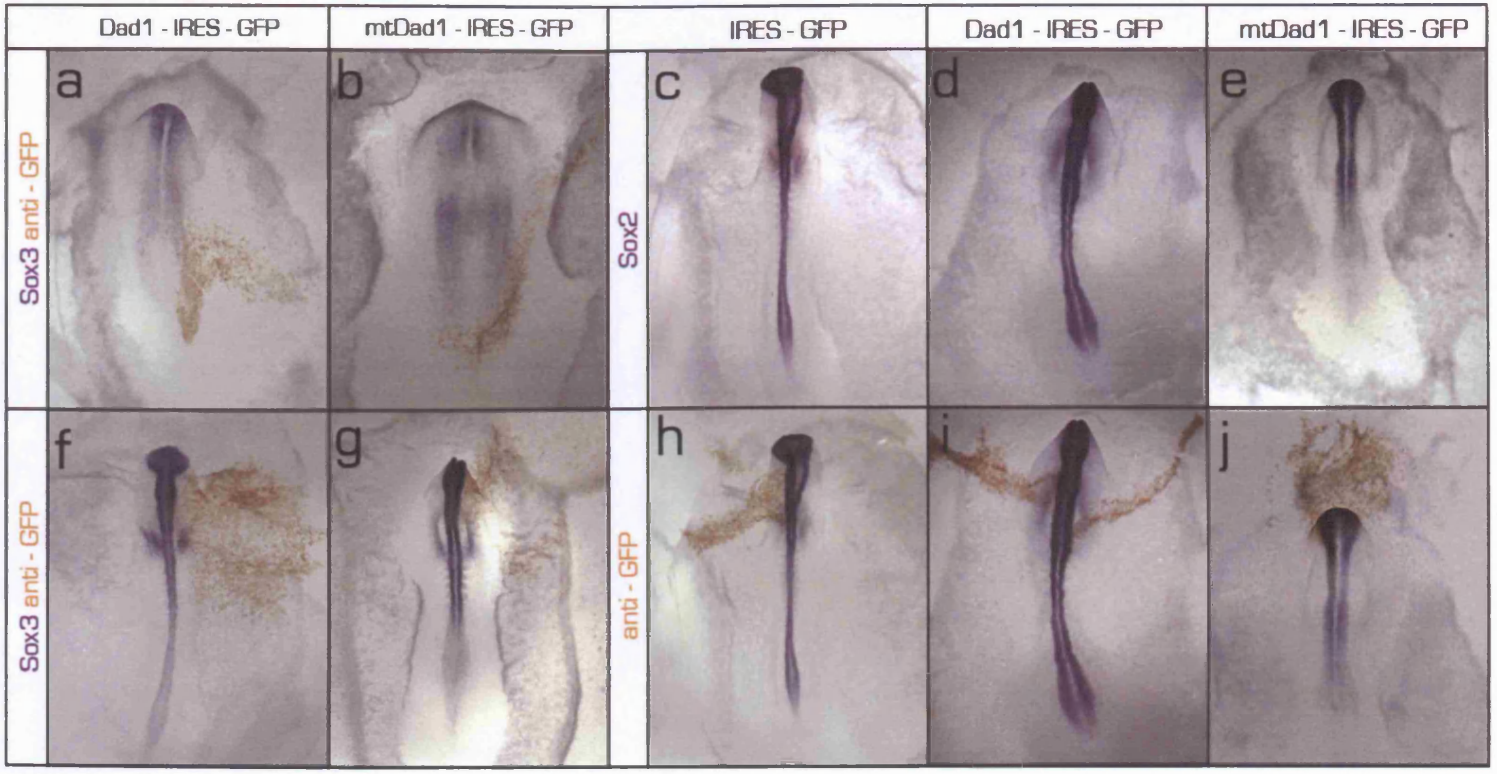

Fig. 3.6
Effects of **DAD1** electroporation on ***Sox3*** and ***Sox2*** expression.
Sox3 expression (blue) following electroporation of **DAD1** is shown after 6 hours (**a**) and overnight (**f**) incubation.
The effects of electroporation of **truncated DAD1** on ***Sox3*** expression are shown after 6-7 hours (**b**) and overnight (**g**).
Sox2 expression (blue) is own following electroporation of a control, empty **pCAB vector** (**c**, **h**), of **DAD1** (**d**, **i**)
and of **truncated DAD1** (**e**, **j**), before (**c-e**) and after (**h-j**) staining with anti-GFP antibody (brown).

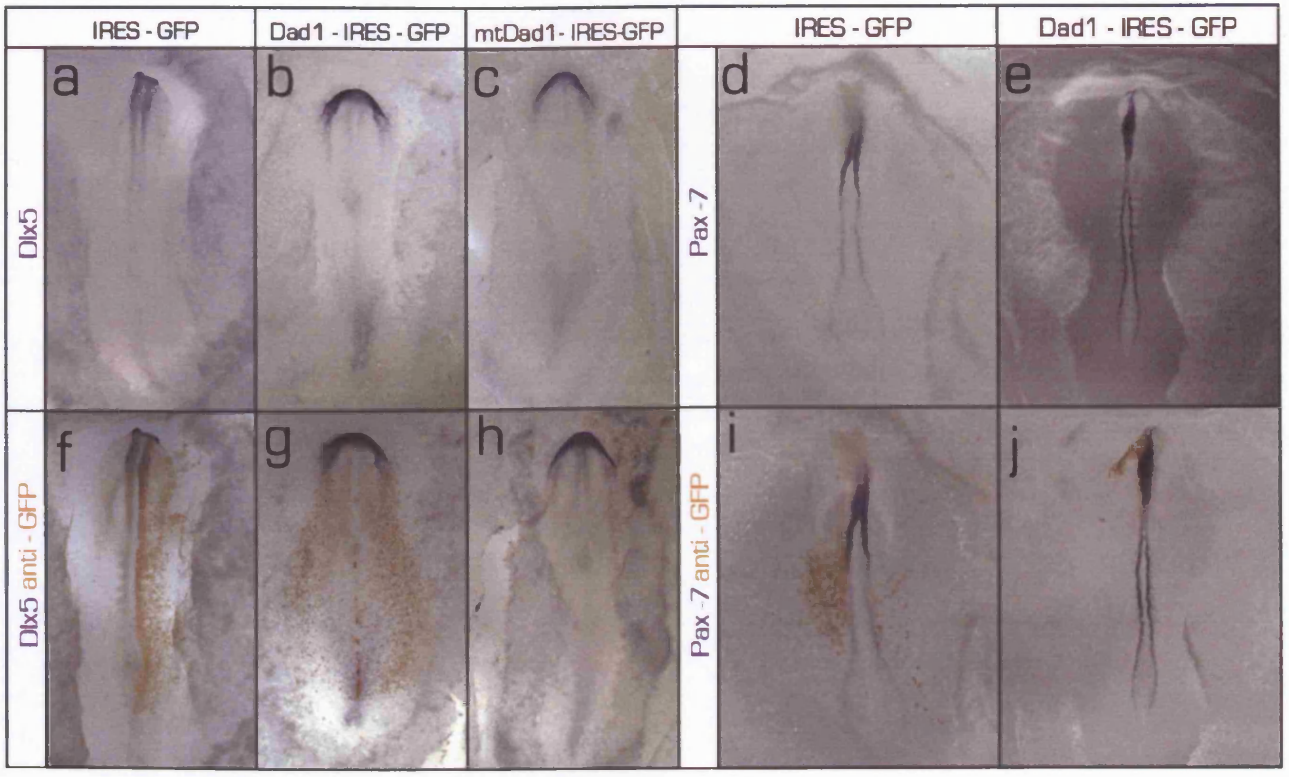

Fig. 3.7
Effects of **DAD1** electroporation on ***Dlx5*** and **Pax7** expression.
Dlx5 expression (blue) following electroporation of a control, empty **pCAB vector** (**a**, **f**), of **DAD1** (**b**, **g**) and **truncated DAD1** (**c**, **h**) before (**a-c**) and after (**f-h**) staining with anti- Gfp antibody (brown).
Pax7 expression (blue) is shown following electroporation of a control, empty pCAB vector (**d**, **i**) and **DAD1** (**e**, **j**) before (**d-e**) ad after (**i-j**) staining with anti-GFP antibody (brown).

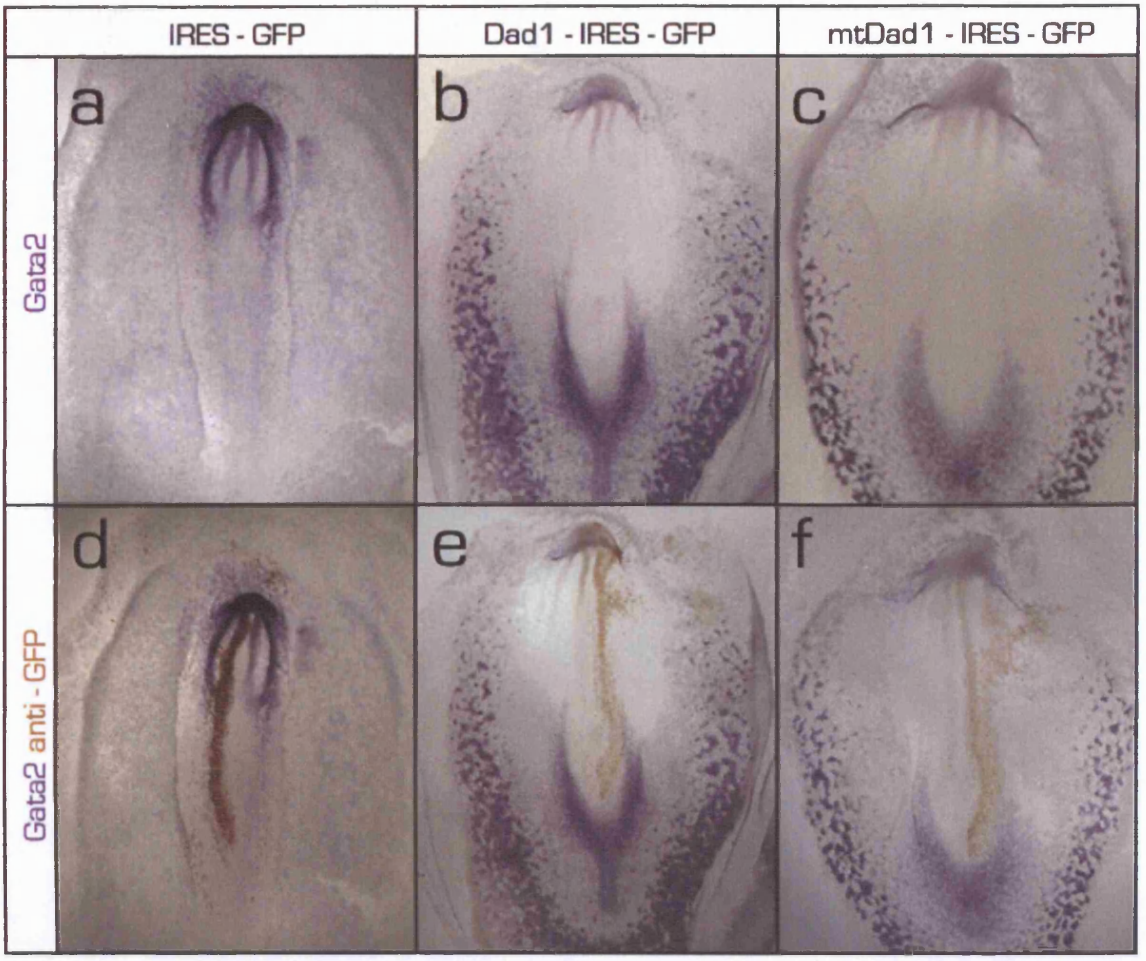

Fig. 3.8

Effects of **DAD1** electroporation on ***Gata2*** expression. ***Gata2*** expression (blue) following electroporation of a control, empty **pCAβ vector** (**a**, **d**), of **DAD1** (**b**, **e**) and **DAD1** (**c**, **f**) before (**a-c**) and after (**d-f**) staining with anti- GFP antibody (brown).

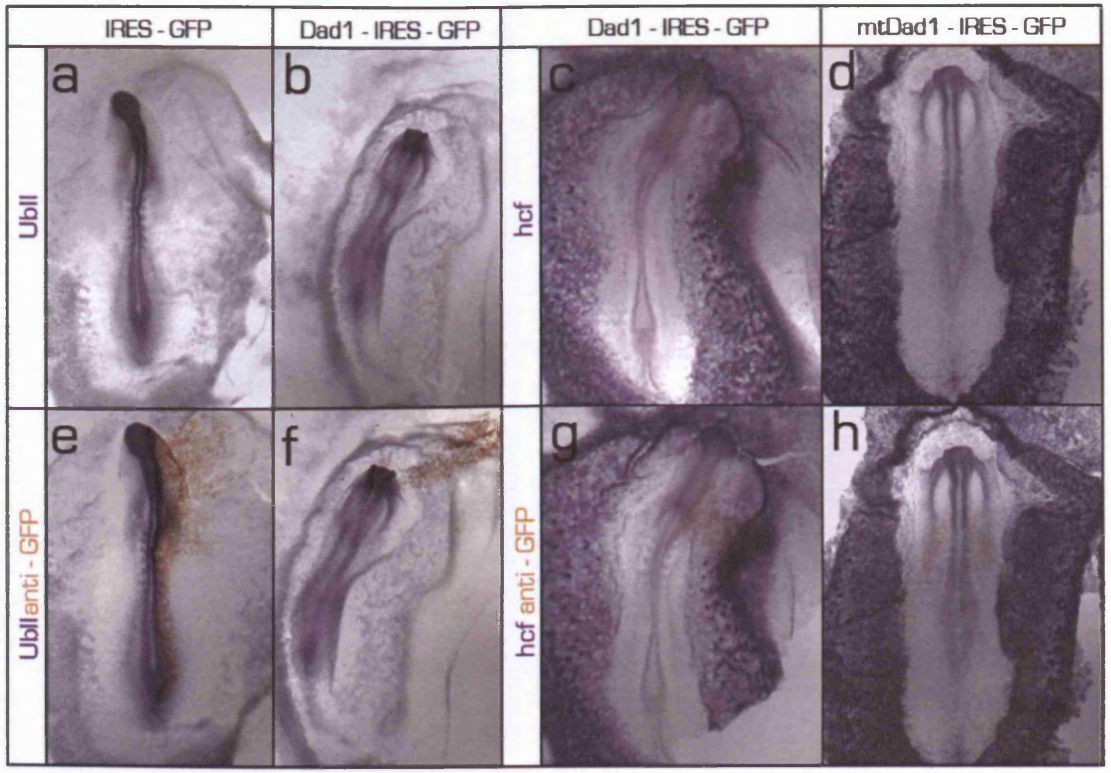

Fig. 3.9
Effects of **DAD1** electroporation on ***UbII*** and ***hcf*** expression.
UbII expression (blue) following electroporation of a control, empty **pCAB vector** (**a**, **e**)
and of **DAD1** (**b**, **f**) before (**a-b**) and after (**e-f**) staining with anti- GFP antibody (brown).
hcf expression (blue) following electroporation of **DAD1** (**c**, **g**) and **truncated DAD1** (**d**, **h**);
shown after overnight incubation before (**c-d**) and after (**g-h**) staining with anti- GFP antibody (brown).

3.4. Discussion

To qualify as an "early response to neural induction" as defined by the screen, a gene must (a) be induced by a grafted Hensen's node within 5 hours, and (b) be expressed within the future neural plate of the normal embryo. The findings presented in this chapter reveal that the normal expression of *Dad1* before stage 4 (when neural induction is thought to take place (Stern, 2005a; Streit et al., 2000) is only extremely weak, not entirely confined to the future neural plate and also does not cover the entire prospective neural plate. For example, the most anterior part of the prospective neuroectoderm (future forebrain) does not express *Dad1* at stage 4 (Fig. 3.3 d). Concerning the time-course of induction by the node, the low levels of normal expression were mirrored by a similarly low levels induction and made this analysis very difficult. Nevertheless the earliest change detected was at 3 hours following the graft, with maximal induction (still very weak) seen at 4-5 hours. This is comparable to the time required for a node to induce Churchill (Sheng et al., 2003) but longer than 1 hour required for ERNI induction (Streit et al., 2000).

Even if its expression is weak and only feebly induced, it is still possible that it plays a role in early neural development. To assess this *Dad1* was misexpressed outside the neural plate, overexpressed in various regions and a putative inhibitory form misexpressed prior to examining the effects on early neural, epidermal and border markers. None of these treatments revealed any changes in the expression of any of 5 markers for these cell fates, nor any effect on the expression of the other two genes studied in this thesis (*Ubll* and *hcf*). Since DAD1 is a subunit of an enzyme complex and therefore requires other proteins for its activity (Makishima et al., 1997; Sanjay et al., 1998; Silberstein and Gilmore, 1996), it is conceivable that ectopic expression of this single component is not sufficient to exert any effect. In the case of the truncated form of DAD1 (predicted to lack activity; Makishima et al., 2000) it is likewise possible that there is sufficient wild-type, functional DAD1 within these cells to fulfil this function without interference by the mutated form.

As a further test for a possible requirement for DAD1 in the process of neural induction, knock-down experiments using *Dad1* morpholino were attempted. To determine whether the DAD1 protein is successfully down-regulated by this treatment, an antibody against DAD1 was used. Unfortunately, these experiments failed for two reasons: first, antibody staining did not produce a clear enough pattern to assess the efficiency of down-regulation by the *Dad1* morpholino. This might have been expected given its low level of expression at the mRNA level. In addition, the antibody used had been raised against a specific peptide within human DAD1 (NPQNKADFQGISPER),

whose sequence contains 2 amino acid differences with the chick counterpart and it may therefore not recognise the chick protein. Second, in these experiments, electroporation of the standard control morpholino gave false-positive results: induction of *Sox2*. For these various reasons it was not possible to use this approach to assess the requirement for DAD1 function in early neural development.

Had these approaches worked, it might have been interesting to test whether the reported polymorphism (SNP) of D*ad1* might affect its function. Tyrosine is an unusual amino acid in that it contains a protruding carbon ring (the only other amino acid like this is phenylalanine), a property not shared by valine; whilst Y>F changes usually do not affect protein function, it would be surprising if V>Y did not.

In Chapter 6, further studies of DAD1 function will be presented in the context of its possible roles in regulating apoptosis during early neural development.

CHAPTER 4:

Polyubiquitin II (*UbII*)

4.1. Introduction

Ubiquitin, the most conserved protein known (Ozkaynak et al., 1984; Sharp and Li, 1987) was identified as a 74 amino acid polypeptide (first called Ubiquitous Immunopoietic Polypeptide (UBIP)) involved in lymphocyte differentiation (Goldstein et al., 1975). Homologues were almost immediately identified in mammals, chick, fish (Goldstein et al., 1975), yeast (Goldstein et al., 1975; Ozkaynak et al., 1984), bacteria (Goldstein et al., 1975), higher plants (Goldstein et al., 1975), insects (Gavilanes et al., 1982) and *Xenopus* (Dworkin-Rastl et al., 1984). For example, yeast ubiquitin differs from that of animal ubiquitin by only 3 amino acids (Ozkaynak et al., 1984). This high degree of conservation suggests the existence of strong evolutionary pressures preventing changes in this protein (Lazar et al., 1997; Sharp and Li, 1987; Wilkinson et al., 1986). Mita and colleagues proposed that numerous ubiquitin genes existed before speciation occurred; at certain genomic locations, fusions are proposed to have occurred with neighbouring genes to generate different proteins (Mita et al., 1991). However, the previously reported existence of monoubiquitin genes at multiple locations in the genome (Wiborg et al., 1985) was later shown to be incorrect (Lund et al., 1985; Salvesen et al., 1987) perhaps with the exception of potato, which does contain a single monoubiquitin gene (Accession number: 031C02). In humans (Wiborg et al., 1985), proposed monoubiquitin loci were later shown to encode a fusion protein including ubiquitin and an additional 80 amino acid peptide at the C-terminus (Lund et al., 1985; Salvesen et al., 1987). In yeast (Bond and Schlesinger, 1986), UBI3 encodes ubiquitin fused to a 76 residue protein, while UBI1 and UBI2 have identical 52 amino acid tails (Ozkaynak et al., 1987). In human (Lund et al., 1985; Mori et al., 1987; Salvesen et al., 1987) and chick (Mezquita et al., 1988; Rocamora and Agell, 1990), their homologues Ub-t52 and Ub-t80 are fused, respectively, to 52 and 80 amino acids to generate proteins involved in ribosomal assembly (Finley et al., 1989; Mezquita et al., 1997). Other proteins which appear to have originated from ancestral fusions of ubiquitin and other genes have also been identified; these are grouped together as a subclass of Ubiquitin-like (UBL) proteins (Glickman and Ciechanover, 2002). Despite similarity to ubiquitin in their structure and involvement in the regulation of the same processes, including the proteasome proteolytic pathway, most UBLs appear to lack the characteristic Gly-Gly sequence at the Carboxy-terminus that is critical for ubiquitination, nor are they processed by de-ubiquitinating enzymes (DUB- like proteases) (Glickman and Ciechanover, 2002). The Small Ubiquitin-related Modifiers (SUMOs), which are among the members of the UBL family, have recently been the subject of considerable attention due to their role in the regulation of protein functions

(Bossis and Melchior, 2006; Kerscher et al., 2006; Kroetz, 2005).

Typically, however, ubiquitins are found in the genome as polyubiquitins (Hunt and Dayhoff, 1977; Ozkaynak et al., 1984), which encode tandem repeats of the 76 amino acid Ubiquitin sequence monomer. They are thought to be a result of duplications of an ancestral gene (Mita et al., 1991). The number of ubiquitins in each can vary; for example, there are forms with 3 (Bond and Schlesinger, 1986; Mezquita et al., 1987); or 4 (Bond and Schlesinger, 1985) in chicken, 5 in yeast (Ozkaynak et al., 1984), 9 in humans (Wiborg et al., 1985), 8 in *Xenopus* (NCBI: NM_001006687) and 10 or 14 in *Drosophila* (NCBI: CG11624 and AT20865p). The genome may also contain several polyubiquitin loci, whose number also differs between species. While only one has been described in yeast (Finley et al., 1987) and *Plasmodium falciparum* (Horrocks and Newbold, 2000), there are two in chicken (Bond and Schlesinger, 1986; Mezquita et al., 1987) and human (UBB, and UBC) (Baker and Board, 1987; Wiborg et al., 1985), and 4 in the multicellular green algae *Volvox carteri* (Schiedlmeier and Schmitt, 1994). In addition, there also appear to be a number of pseudogenes with related sequences: in human, 4 pseudogenes related to of UBB have been described (Cowland et al., 1988).

The last amino acid in the C-terminal ubiquitin of Polyubiquitin differs between species and even between different Polyubiquitin proteins within a species. For example, cysteine occupies this position in Human UBB (Baker and Board, 1987), while asparagine is found in chick UbII and tyrosine in chick UbI (Bond and Schlesinger, 1986; Mezquita et al., 1987).

Ubiquitins can be added to other proteins in a process called "ubiquitination" (or "ubiquitinylation"). Recently, the former (ubiquitination) has been used to designate processes leading to selective targeting and degradation by the ubiquitin-proteasome system while the latter (ubiquitinylation) is used to refer to the now expanding field of non-turnover-related post-translational modifications by ubiquitin (Abriel and Staub, 2005; Emre and Berger, 2004; Haglund and Dikic, 2005; Huang and D'Andrea, 2006; Liu et al., 2005; Staub and Rotin, 2006). Although conjugation of ubiquitin to target proteins may occur at a variety of positions, it usually involves Gly76 of ubiquitin and a Lys residue in the substrate. For example, IκBα is ubiquitinated at Lys-21 or Lys-22, while p53 is modified at Lys-372, Lys-373 or Lys-381, and histone H2A at Lys-119 or -120 (Busch and Goldknopf, 1981; Goldknopf and Busch, 1977; Thorne et al., 1987) according to the species, while Histone H2B is ubiquitinated at Lys-123 in yeast (Robzyk et al., 2000). There are also other variations involving the polybiquitin chain itself. For example, polyubiquitin chains with Lys48-linkages act as signals for degradation, while Lys63-linkages are implicated in the DNA damage response

(Glickman and Ciechanover, 2002; Pickart, 2001; Sun and Chen, 2004; Ulrich, 2003).

An additional role of ubiquitinylation in chromatin modification was observed long ago (Andersen et al., 1981; Cary et al., 1980; Goldknopf and Busch, 1975; Matsui et al., 1979). Ubiquitin is either covalently conjugated to the C–terminus of ε-amino-group of histone H2A (Andersen et al., 1981; Cary et al., 1980; Goldknopf and Busch, 1975; Levinger and Varshavsky, 1982; Watson et al., 1978) or found in the free form in association with chromatin (Hunt and Dayhoff, 1977; Mezquita et al., 1982). Since then, great progress has been made in understanding the mechanisms regulating ubiquitinylation of core histones (H2B and H3), the linker H1 and the variant H2A.Z (Osley, 2004). Additionally other proteins involved in DNA replication and/or transcription, and especially in DNA repair processes that require ubiquitinylation have been identified. For example, proliferating cell nuclear antigen (PCNA), plays different role in protecting genomic stability depending on whether it is mono- or polyubiquitinylated (Chiu et al., 2006; Haglund and Dikic, 2005). Monoubiquitination of other substrates, like FANCD2 or Translation DNA Synthesis (TLS) polymerase η is required for homologous recombination and TLS (Huang and D'Andrea, 2006). Polyubiquitinylation of DNA-damage-binding protein 2 (DDB2) or RNA polymerase II is necessary for nucleotide-excision repair (Huang and D'Andrea, 2006; Ribar et al., 2006). Polyubiquitination is also required for the action of transcription factors, which are activated or inactivated directly or indirectly by the destruction of specific co-factors (Chen et al., 2006; Pickart, 2001; Salghetti et al., 2001).

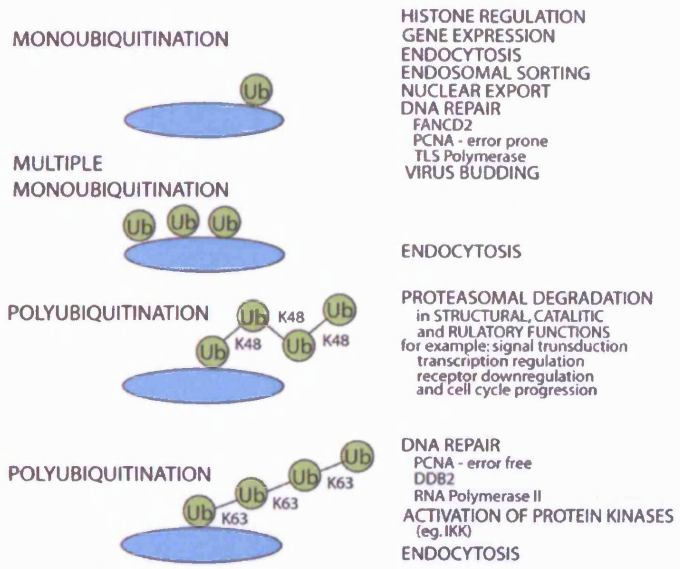

Fig. 4.1

Ubiquitin modification and their cellular functions; (modified from Haglund and Dikic, 2005 and Pickart, 2001).

The ubiquitin pathway mediates selective degradation (Fig .4.1) and is therefore extremely important for the continuous turnover of proteins necessary for structural, catalytic and regulatory functions, signal transduction, transcriptional regulation, receptor down-regulation, cell cycle progression (Nakayama and Nakayama, 2006) and endocytosis (reviewed in Glickman and Ciechanover, 2002; Hershko and Ciechanover, 1998; Pickart, 2001). Ubiquitinylation by addition of a single ubiquitin plays a role in many crucial cell functions (Fig. 4.1), including intracellular membrane events such as nuclear trafficking (Deroo et al., 2002; Hochstrasser, 2000) and targeting proteins for release from the endoplasmic reticulum (ER) (Hitchcock et al., 2003; Staub and Rotin, 2006). ER-associated protein degradation (ERAD) involves re-translocation of misfolded proteins back to the ER and selection for the cytosolic proteasome by polyubiquitination (Bays et al., 2001; Hitchcock et al., 2003). Monoubiquitin modification also plays a role in endocytosis, both for protein sorting (Urbe, 2005) and for the internalisation of integral plasma membrane proteins (Hicke, 2001; Staub and Rotin, 2006). Ubiquitin conjugation is also crucial for cell cycle progression (Nakayama and Nakayama, 2006).

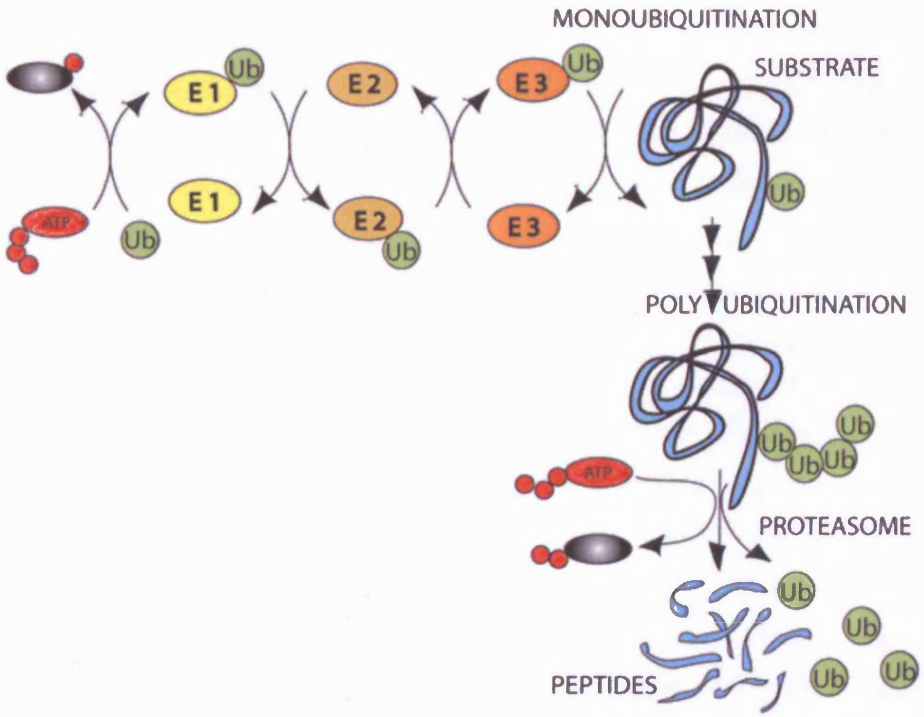

Fig. 4.2

The ubiquitin-proteasome pathway; (modified from Cooper, 2000 and Pickart, 2001).

Protein ubiquitination for non-lysosomal degradation is an ATP-dependent (Ciechanover et al., 1984; Hershko, 1983; Wilkinson et al., 1980) multi-step process (Fig.4.2) involving the catalytic action of three classes of enzymes: E1, E2 and E3. The first step is called activation and involves adenylation of glycine (Hershko et al., 1981) at the C-terminus of ubiquitin and the formation of a thiol ester linkage with E1. This is the ATP-dependent step and involves E1 (Ciechanover et al., 1982; Ciechanover et al., 1981; Haas et al., 1982). Activated ubiquitin is transferred to the conjugating enzyme E2 (to form a thiol bond) and is then transacylated to the cysteine residue of E3 (a ligase), which is bound to the target protein directly or via ancillary proteins (Hershko et al., 1983; for review see Glickman and Ciechanover, 2002). E3 catalyses the transfer of ubiquitin to the ε-NH_2 group at an internal lysine or to the terminal α-NH_2 group of the target (reviewed in Glickman and Ciechanover, 2002). E3 also recognises a "degron" (a substrate degradation signal) on the target protein (An et al., 2006; Bachmair et al., 1986; Finley et al., 1989; Varshavsky, 1996).

Recently a novel group of enzymes, designated E4, was proposed to be involved in the elongation of the ubiquitin chain together with E1, E2, E3 or other ubiquitin-conjugating factors (Hoppe, 2005; Kuhlbrodt et al., 2005). Yeast UFD2 (ubiquitin fusion degradation protein-2), was the first E4 protein to be described (Conforti et al., 2000), which has since also been identified in other species (Caren et al., 2006; Hatakeyama et al., 2001), including plants (Azevedo et al., 2001). Elongation of the ubiquitin chain involves formation of an isopeptide bond between the side chain at Lys48 and the carboxyl Gly76 group of the C-terminus of ubiquitin (Cook et al., 1994; for review see Glickman and Ciechanover, 2002). Proteins modified by more that 3 ubiquitins are transferred to large 26S proteasome complexes for degradation, while the released ubiquitin units themselves are recycled by ubiquitin C-terminal hydrolases or isopeptidases (Hershko and Ciechanover, 1998). In general there is a single copy of E1 in the genome, with very few exceptions, for example wheat (Hatfield and Vierstra, 1992). The specificity of the process, i.e. the target protein or the type of linkage chain used is ensured by the specific combination from among various E2- and E3-group enzymes (Glickman and Ciechanover, 2002; Hicke, 2001; Pickart, 2001).

Ubiquitins also provide protection from environmental stress. They are involved in the Heat Shock Response of cells exposed to extreme conditions (Bond and Schlesinger, 1987; Ritossa, 1962; Schlesinger et al., 1982). Their high degree of stability towards pH and temperature changes (Lenkinski et al., 1977) make them ideally suited for this function, comparable to chaperones such as the Heat Shock Proteins (HSPs) (Diller, 2006; Lindquist and Craig, 1988; Neidhardt et al., 1984; Yost and Lindquist, 1991). At first, proteolytic degradation was proposed to be the main

mode of action of ubiquitin during the responses to heat shock and stress (Ciechanover et al., 1984; Finley et al., 1984). However, later studies (Bond et al., 1988) suggested that protein degradation does not take place until after the stress conditions have ceased. One reason why ubiquitins are such abundant proteins is that several proteins expressed at high levels need to be degraded very rapidly in certain conditions; among them, histone H2A is quickly degraded in response to heat shock (Bond et al., 1988). The existence of heat shock-specific transcription factors has also been proposed, which are themselves ubiquitinated during normal conditions and de-ubiquitinated during the heat shock response (Munro and Pelham, 1985). Through the targeted mutation experiments it has been established that the position of the ubiquitin linkage determines the exact type of stress protection (Fujimuro et al., 2005). For example Lys-48 and Lys-63 linked chains play role in the stress response to ethanol, H_2O_2 and methyl methanesulfonate (MMS) treatment, but only Lys48-linked polyubiquitin is required for HSR triggered by heat shock (Fujimuro et al., 2005).

Polyubiquitins have been found to be expressed in a tissue specific way or upregulated depending on the states of the cell. In yeast, for example, UBI4 (consisting of 5 repeats) is critical for the stress response and survival during starvation (Finley et al., 1987), while in chick, Ubl and UbII and their fusion products differ in their expression during chick testis maturation (Agell and Mezquita, 1988; Mezquita et al., 1987; Mezquita et al., 1997; Rocamora and Agell, 1990). It has been proposed that birds, where spermatogenesis occurs at the internal body temperature (38-39°C), need to protect these cells against the higher temperature as compared to mammals whose external testes allow spermatogenesis to proceed at lower temperatures (Mezquita et al., 1993). Chick UbII has been implicated in this protective function.

Some tissue specific expression can be accounted for by differential splicing and/or alternative translation initiation sites, which allows production of stage- and tissue-specific mRNAs and proteins (Mezquita et al., 1993). For example, it has been reported that the translation initiation site of UbII is different in chick embryos at day 4 and in adult kidney than in the mature chicken testis (Mezquita et al., 1993). In addition to different translation start sites, there is also differential splicing. During spermatogenesis there is mainly intronless transcription of UbII, while in kidneys and embryos at day 4 a 448bp intron is included in the transcript. In some cases mRNAs with longer 5' UTR were found, initiated upstream of the TATA box (Mezquita et al., 1993).

Some attempts have been made to characterise the regulatory regions controlling different aspects of the expression of ubiquitins. In chick, a heat-responsive element directing expression of Ubl has been located to a position -369 to -359

upstream of the transcription start site (Bond and Schlesinger, 1986). Regulatory regions directing UbII expression have also been identified (Mezquita et al., 1993). Both UbI and UbII have proximally located unmethylated CpG islands in their 5' UTR. In the distal regions methylation differs for UbI (hypermethylated in mature testis) and UbII (where 3' CCGG is only 50% methylated) (Rocamora and Agell, 1990).

Given the importance of ubiquitins in a large number of normal cell functions, as well as pathological changes, and the huge amount of information available about the control of their expression and relationships with other proteins, it is very surprising that there is almost no information about the expression or functions of ubiquitins and polyubiquitins in early development in normal embryos.

4.2. Materials and Methods

4.2.1. Bioinformatics

Translation of the sequence was performed by the ExPASy (www.expasy.org) database. To align and analyse sequences, ClustalW (www.ebi.ac.uk/clustalw) was used and the results visualised using Jalview 2.08.1 (Clamp et al., 2004). The degree of amino acid identity was calculated using MUSCLE (Edgar, 2004). Translation of the sequence was performed in the ExPASy (www.expasy.org) database. Comparisons with other sequences in the public domain were made through standard sites (Ensembl, Genbank, UCSC genome server).

4.2.2. Riboprobe transcription

To distinguish between almost identical sequences of UbI and UbII, antisense riboprobes were designed to incorporate 3' UTR sequence, which differs between for these genes. The fragments were isolated by PCR from a mixture of two cDNA libraries (stage 2-4 and stages 18-20). The following primers were used: *UbI*: Forward: ACTACAACATCCAGAAG; Reverse: ATGTGCAACAGAAAAACT. *UbII*: Forward: CCTGTCTGACTACAACATC; reverse: GGATGCAAGAACTTTATTG. PCR fragments were extracted, cloned into pGEM T-easy and transformed into competent bacteria (Promega) according to the manufacturer's protocol. After sequencing to validate the clones and to determine the orientation of the insert, they were digested with NcoI and transcribed with SP6 RNA Polymerase to generate antisense riboprobes.

4.2.3. Constructs for electroporation

To investigate the possible functions of *UbII in vivo*, *UbII* was misexpressed by electroporation. The pCAβ vector, containing the ubiquitously expressed chick β-actin promoter, a CMV enhancer followed by the cloning site and then by an Internal Ribosome Entry Site (IRES) to direct translation of Green Fluorescent Protein (GFP), was digested with BsmBI and ClaI and gel-purified using a Gel Extraction Kit (Qiagen). The open reading frame of chick *UbII* was amplified by PCR from two chick cDNA libraries (stage 2-4 and 18-20). The following primers were used:

Forward: GATCAGCGGCCGCGACCAACATGCAGATCTTC;

Reverse: TGCTAATCGATTCTTCAGTTACCACCCCTG

These were designed to incorporate recognition sites for digestion by NotI and ClaI (underlined, respectively, in the two sequences above). This made the PCR product compatible for ligation with the product of BsmBI/ClaI digestion of pCAβ. The insert was ligated with purified vector using T4 DNA ligase (Promega). The ligation products were transformed into DH5α competent cells. Plasmids were harvested and sequenced.

The pCA_ vectors described above were introduced by electroporation into stage 3+/4 embryos as described in Chapter 2. The electroporated embryos were grown for 6 hours (to study short term effects) or to stages 8-12 (for longer-term consequences). At the end of this period embryos were fixed as described for in situ hybridisation (Chapter 2) and processed for in situ hybridisation with various markers including *Sox3* (Rex et al., 1997), *Sox2* (Rex et al., 1997), *ERNI* (Streit et al., 2000) and *Pax7* (McLarren et al., 2003; Otto et al., 2006). After in situ hybridisation, antibody staining against GFP was used to reveal the cells that had been electroporated as described in Chapter 2.

4.3. Results

4.3.1. Identification of *UbII*

The original "early response screen" (see Chapter 1) identified clone F5 as one such early response gene. It contains an insert of 843 bp, found by NCBI BLAST analysis to match a 329 bp (except for 11 separate differences, corresponding to 96% nucleotide identity) sequence corresponding to *UbII* (X58195), located on chromosome 15 (UCSC 4,480,251-4,481,721; Ensembl 4,480,852-4,481,364).

No SNPs have been reported in this sequence by the Beijing Genomics Institute. The *UbII* sequence in Ensembl (ENSGALG00000002977) does not contain the whole sequence of the open reading frame. However the Ensembl database does

report a number of SNPs (synonymous SNPs in positions L^{69}>K and V^{70}>S of the first ubiquitin of *UbII* and non-synonymous SNPs at T^{12}>N and K^{48}>R in the last ubiquitin repeat).

During database searching it became apparent that F5 is also related, but more distantly so, to another chick ubiquitin gene. NCBI BLAST reveals 88% identity (283 bp; 33 differences in sequence) with *UbI* (M14693), found on chromosome 19 (6157729 to 6158054).

As discussed above (Section 4.1), there is extreme conservation of the amino acid sequence of Ubiquitins but a variable number of repeats in polyubiquitin genes. In chick, seven ubiquitin monomers contribute to two polyubiquitin genes (4 in UbI and 3 in UbII). These were compared to each other (Fig 4.3), excluding the extreme 3' terminal codon and stop codon in each gene. Within UbI, monomers UbI1 and UbI3 are the most similar at the nucleotide level. In some regions conservation is shared by all four UbI monomers, for example in the region 78-114. An Average Distance Tree (Fig 4.4) generated by ClustalW Multiple Sequence Alignment (Thompson et al., 1994) illustrates these relationships. Perhaps surprisingly, according to this level of analysis, the divergence in nucleotide sequence appears to occur before the division into two polyubiquitin genes, suggesting that the last two ubiquitins in UbII are more closely related to all four monomers in UbI than to the fist ubiquitin of UbII.

For analysis between species and among related genes within a genome, only the last ubiquitin (including the unique terminal amino acids and stop codon) was selected for analysis of conservation. Alignment of the nucleotide (Fig. 4.5) and amino acids (Fig. 4.6) sequences show strong conservation. The only amino acid substitutions are at position 19, where a "small" Proline is replaced by a "tiny" Serine (these terms used as described by (Livingstone and Barton, 1993) in all plant species. Amoeba has a "tiny" hydrophobic Glycine at position 20 instead of Serine; at position 28 a "tiny" hydrophobic Alanine is substituted by a polar Glutamine in tobacco and Amoeba, while spurge has a Serine instead of a negatively charged Asparate at position 39 and in all plant species there is an Alanine instead of a Serine at position 57. The last amino acid following the characteristic Gly-Gly sequence also differs between species: some have more than one amino acid (parsley and potato have Aspartate followed by an aromatic Phenylalanine, Amoeba has positively charged Histidine and Cysteine, while fly polyubiquitin terminates with three amino acids: an aliphatic Isoleucine, a charged Glutamine and Alanine). The average distance tree using % identity based on MUSCLE alignment (Fig. 4.7) illustrates the corresponding phylogenetic relationships. Chick UbI is more closely related to the UbB polyubiquitin of rat, while chick UbII has more in common with the equivalent sequence in mosquito. It

is worth mentioning that different trees are obtained by comparing nucleotide sequences from comparisons of amino acid sequences; comparison of nucleotide sequences yield a tree that more closely resembles the phylogenetic relationships between the species, with possible exception of tobacco and beetle (Fig. 4.8).

In conclusion, sequence analysis strongly suggests that the F5 clone encodes part of the open reading frame of the *UbII* gene, whose sequence is represented in part by several incomplete entries in the databases (X58195, Z14958, ENSGALG00000002977 and X06580). Subsequent screening of a stage 3-4 chick embryo cDNA library resulted in the isolation of a single, full-length clone containing the entire open reading frame (ORF) of *UbII*, representing three tandem repeats of 76 long-long ubiquitin sequences with an additional N residue just before the end of the ORF.

4.3.2. Expression of *UbII* and *UbI* in normal development

To begin to assess whether *UbII* could play a role in the early stages of neural development, its expression was analysed by whole mount in situ hybridization. No expression was found in pre-primitive streak stage embryos (Fig. 4.9 a). Expression is first detected at stage 3+/4- (Fig. 4.9 b). Initially, *UbII* is almost exclusively transcribed in the epiblast of the area pellucida especially in the anterior half of the embryo, in a region roughly corresponding to the future neural plate but extending a little laterally, especially at the posterior boundary of this domain (Fig. 4.9 c, h, i). A striking apical localisation of the mRNA is seen in neural plate show increased expression in many embryos (Fig. 4.9 d).

At stage 5 (Fig. 4.9 e) *UbII* becomes stronger and more restricted to the neural plate. Outside the epiblast, some expression is also seen in the mesoderm and endoderm, although this is somewhat variable from one embryo to another. In most cases the lateral plate and lateral endodermal layer appear to have increased expression compared to more medial regions (Fig. 4.9 l). At this time the mRNA appears to lose its apical localisation and is instead distributed throughout the cytoplasm (Fig. 4.9 m-n). At stages 6-7 (Fig. 4.9 f), expression is still seen throughout the neural plate and more weakly in the lateral mesoderm. In addition there is expression in the forming head fold and in the middle section of the primitive streak as well as in the forming somite (stage 7).

At stage 11-12 (Fig. 4.9 g), expression is still seen in the neural tube especially in the hindbrain, midbrain and forebrain. A stream of cells at the level of rhombomere 2, probably corresponding to neural crest cells, also show expression. Weaker levels of transcript can be seen in the mesoderm. At this stage, sections reveal that the

mRNA localisation in the neural tube has shifted to become stronger at the basal aspect of the neuroepithelial cells (Fig. 4.10 a, arrow b). Additional expression is seen in the floor of the pharynx (Fig. 4.10 a and b) and weakly in the somites and notochord (Fig. 4.10 c-e).

For comparison, the normal expression of *Ubl* was also studied. To ensure lack of cross-reaction between the two probes, riboprobes were made against the 3' untranslated regions of the two cDNAs, which is not conserved. At least at early stages, the expression of *Ubl* is very similar or identical to that of *Ubll* (Fig. 4.11).

In conclusion, *Ubll* transcripts are predominantly seen in the epiblast from the late primitive streak stage, becoming concentrated in the neural plate and its derivatives. Lower levels of expression are seen in other layers.

4.3.3. Time-course of induction of *Ubll* by Hensen's node and induction by FGF8b

To confirm the results of the screen (discussed in the Introduction) and in order to establish the exact timing of the *Ubll* induction by Hensen's node, a quail node was grafted to the area opaca of a chick host and the induction of *Ubll* examined at different times following the graft (for details see Chapter 2). No induction is detected either after 1.5 hours following a node graft (0/8; Fig. 4.12 a) or with a control graft (posterior primitive streak) and any time tested (0/18). Weak induction of *Ubll* is first apparent after 3 hours (13/13; Fig. 4.12 b), which becomes stronger at 4 hours (9/9; Fig. 4.12 c) and 5 hours (10/10; Fig. 4.12 d) following a node graft.

Since several genes isolated in the early response screen turned out to be inducible by FGF8b (Sheng et al., 2003; Streit et al., 2000) the ability of this factor to induce *Ubll* expression was also tested in time-course. Again, there is no induction of *Ubll* at 1.5 hours (right arrow Fig. 4.12 e), or with control bead grafts at any time point (right arrows Fig. 4.12 e-f). Weak induction by FGF8b in the area opaca is first seen after 3 hours (11/11; left arrow Fig. 4.12 f), and the response increases after 4 hours (8/8; Fig. 4.12 g) and 5 hours (12/12; Fig. 4.12 h). Under these conditions, and with the same batches of FGF8b, there is no induction of the mesendodermal marker *Brachyury* (Fig. 2.1), suggesting that the induction of *Ubll* by FGF8b is not due to prior induction of mesendoderm.

In conclusion, *Ubll* is induced in the epiblast of the early chick embryo after 3-4 hours of exposure to either a node graft or to FGF8b-soaked beads.

4.3.4. *Ubll* does not affect neural or neural crest fate

To explore a possible role of *Ubll* in neural induction, *Ubll* was misexpressed *in vivo*.

Since electroporation even of an empty pCAβ vector can induce expression of *ERNI* (Fig. 4.13 a and g), almost as strongly as electroporation of *UbII* (5/5; Fig. 4.13 b and h), the later and more reliable early neural markers *Sox3* and *Sox2* were analysed. *UbII* electroporation does not induce either *Sox3* (9/9; data not shown) or *Sox2* (16/16; Fig. 4.13 d-f and j-l), either after 6 hours or after overnight incubation of the embryos (Fig. 4.13 d-f and j-l). To investigate whether *UbII* could affect the fate of cells at the border between the neural plate and epidermis (prospective neural crest), *Pax7* expression was analysed. Again this is not induced by ectopic expression of *UbII* (7/7; Fig. 4.14 d and h). Electroporation with a control empty pCAβ vector did not induce *Sox3*, *Sox2*, or *Pax7* (Fig. 4.13 a, c, g and i and Fig. 4.14 a, c, e and g) at the same time points. As an additional control, a mutated version of *UbII* lacking the last two ubiquitin monomers was electroporated; no changes in *Sox2* expression were detected (Fig. 4.14 b and f).

In conclusion, ectopic expression of *UbII* is not sufficient to induce early neural or neural crest markers.

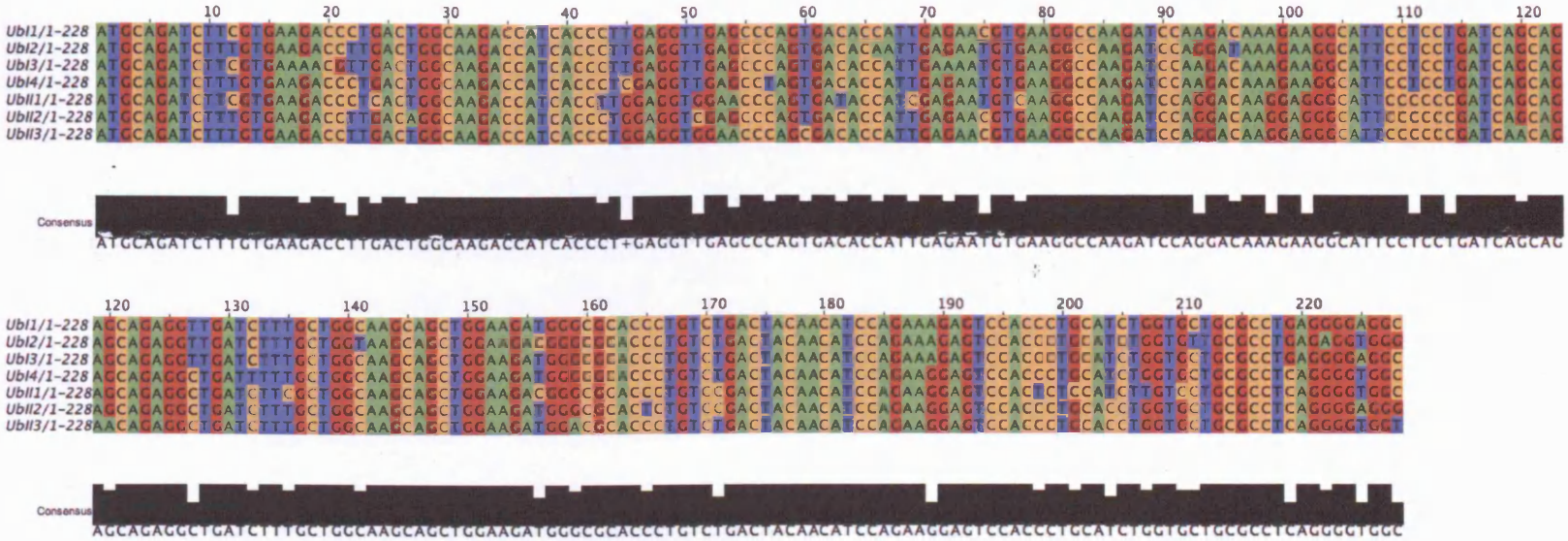

Fig. 4.3
Alignment of nucleotide sequences of ubiquitin monomers contributing to chick UbI and UbII. Accession number UbI (M14693) and UbII (X58195).

Fig. 4.4
Average Distance Tree of nucleotide sequences of ubiquitin monomers contributing to chick UbI and UbII.
Accession numbers: UbI (M14693) and UbII (X58195).

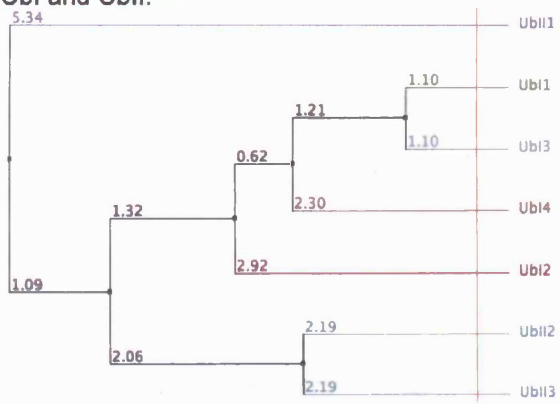

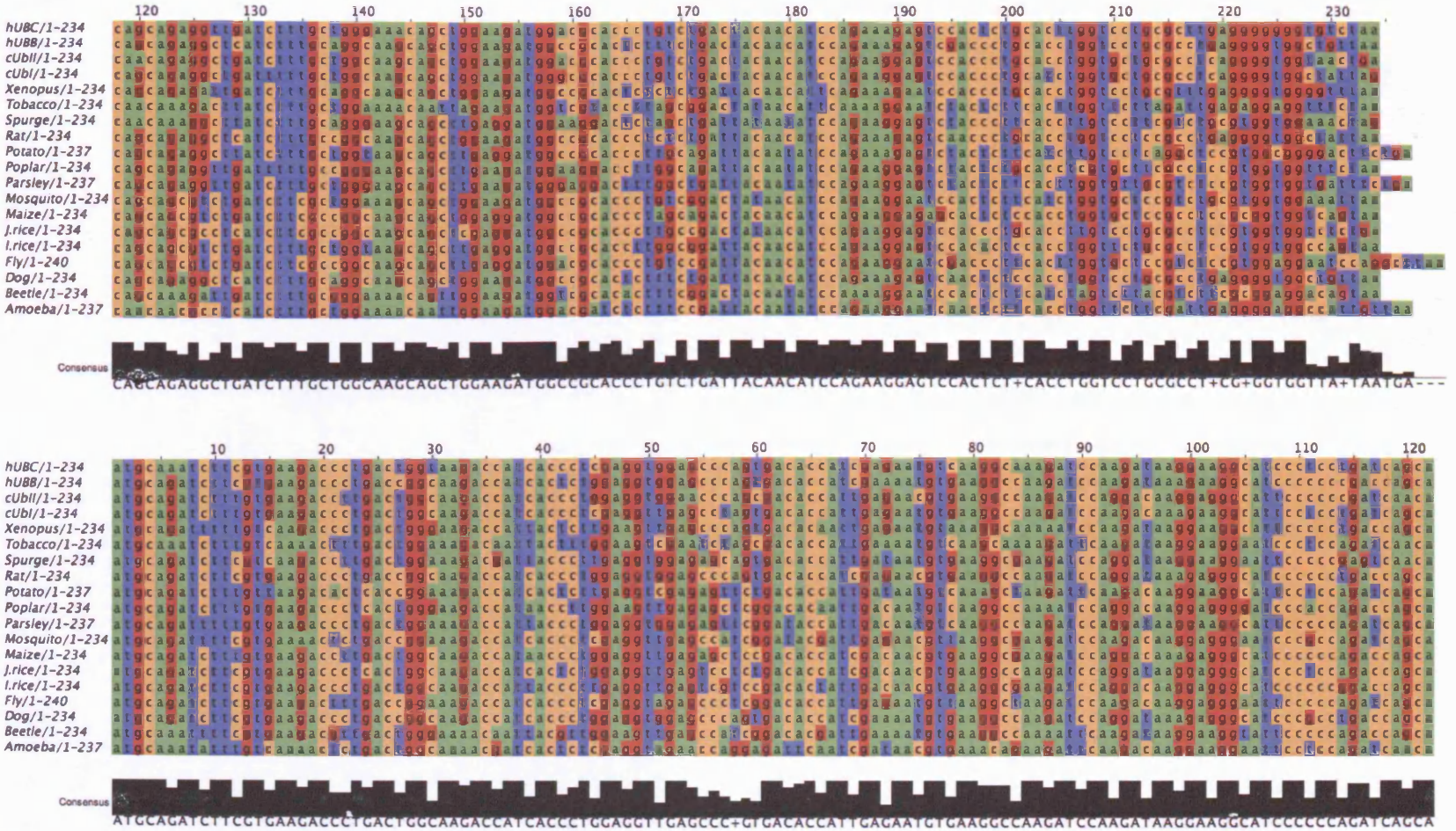

Fig. 4.5
Alignment of nucleotide sequences of the last monomer of Ubs from different organisms or related Ubs within the genome.
Accession numbers: hUBC (NM_021009), hUBB (NM_018955), cUbII (X58195), cUbI (M14693), Xenopus (NM_001006687), tobacco (AJ223330), spurge (DQ011576), rat (NM_138895), potato (DQ252482), poplar (AB182939), parsley (X64345), mosquito (L36067), maze (S94466), Japanese rice (AY954394), Indian rice (X76064), fly (AY118702), dog (XM_536651), beetle (NM_001039417) and Amoeba (AF034789).

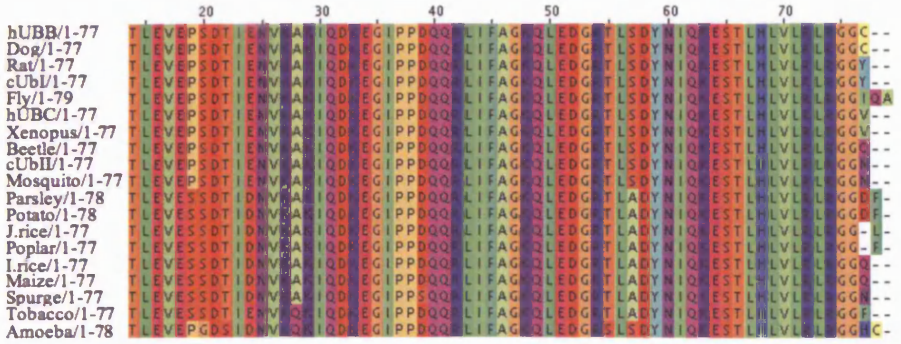

Fig. 4.6
Alignment of amino acid sequences of last monomers of Ubs from different organisms or related Ubs within a genome. Accession numbers: hUBB (NP_061828), dog-UbB(XP_536651), rat-ubB (NP_620250), cUbI (AAA49128), fly (AAM50562), hUBC (NP_066289), Xenopus (NP_001006688), beetle (NP_001034506), cUbII, mosquito (AAA29362), parsley (CAA45622), potato (ABB55360), Japanese rice (AAX40652), poplar (BAD26592), Indian rice (CAA53665), maze (AAB21994), spurge (AAY33920), tobacco (CAA11269) and Amoeba (AAB87694).

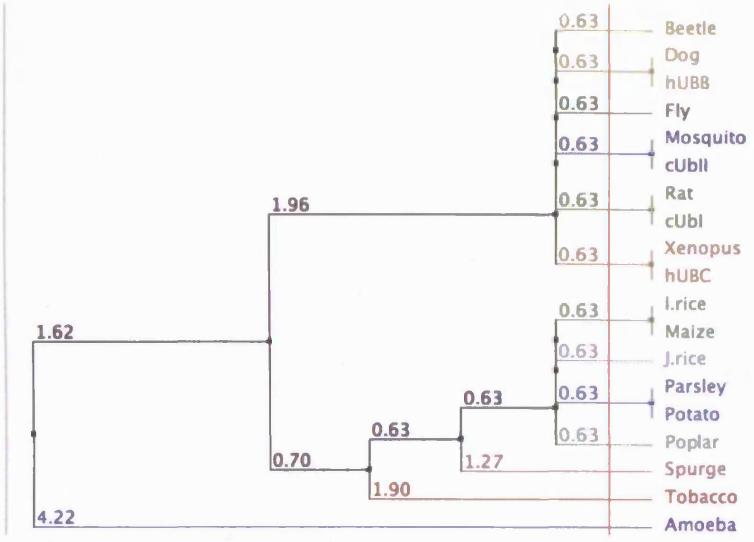

Fig. 4.7
Average Distance Tree using % identity based on amino acid sequences alignment of last monomers of Ubs from different organisms or related Ubs within a genome. Accession numbers: beetle (NP_001034506), dog-UbB(XP_536651), hUBB (NP_061828), fly (AAM50562), mosquito (AAA29362), cUbII, rat-ubB (NP_620250), cUbI (AAA49128), hUBC (NP_066289), Xenopus (NP_001006688), Indian rice (CAA53665), maze (AAB21994), Japanese rice (AAX40652), parsley (CAA45622), potato (ABB55360), poplar (BAD26592), spurge (AAY33920), tobacco (CAA11269) and Amoeba (AAB87694).

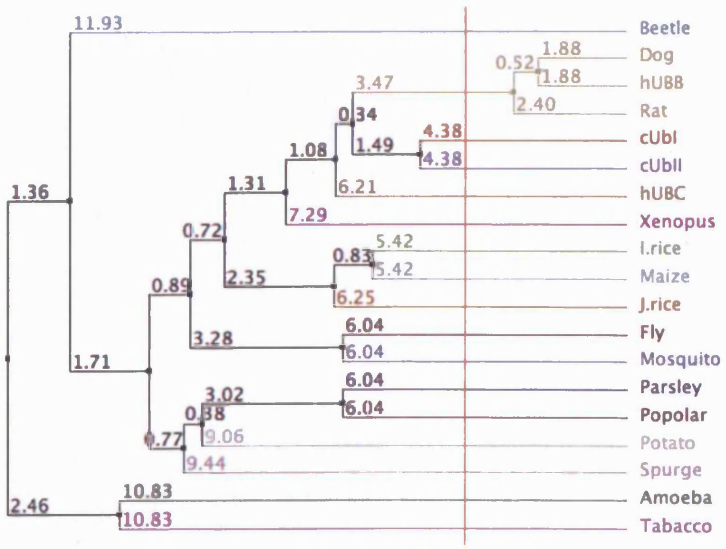

Fig. 4.8
Average Distance Tree using % identity based on nucleotide sequences alignment of last monomers of Ubs from different organisms or related Ubs within a genome.
Accession numbers: beetle (NM_001039417), dog (XM_536651), hUBB (NM_018955), rat (NM_138895), cUbI (M14693), cUbII (X58195), hUBC (NM_021009), Xenopus (NM_001006687), Indian rice (X76064), maze (S94466), Japanese rice (AY954394), fly (AY118702), mosquito (L36067), parsley (X64345), poplar (AB182939), potato (DQ252482), spurge (DQ011576), Amoeba (AF034789) and tobacco (AJ223330).

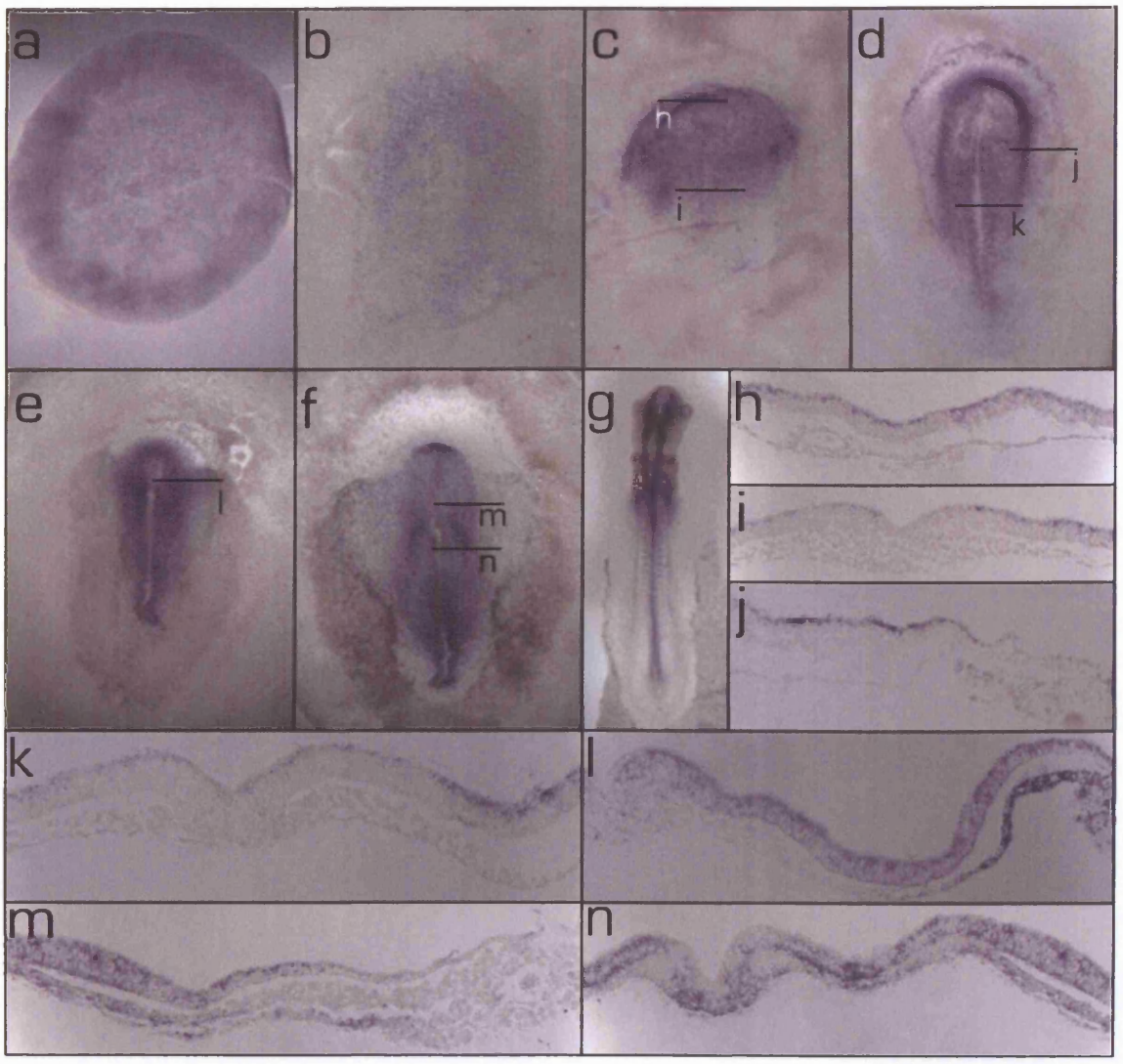

Fig. 4.9

Normal **expression patterns** of ***Ubll*** in the pre-primitive streak stage embryo (**a**) and at stages 3(**b**), 4(**c**), 5(**d**), 5(**e**), 7(**f**), 12(**g**), section through the anterior (**h**) and the posterior region (**i**) of embryo shown in **c**; section through the lateral region (j) and the primitive streak (**k**) of embryo shown in **d**; **l** section of embryo shown in **e**; **m**-**n** sections through stage 7 embryo shown in **f**.

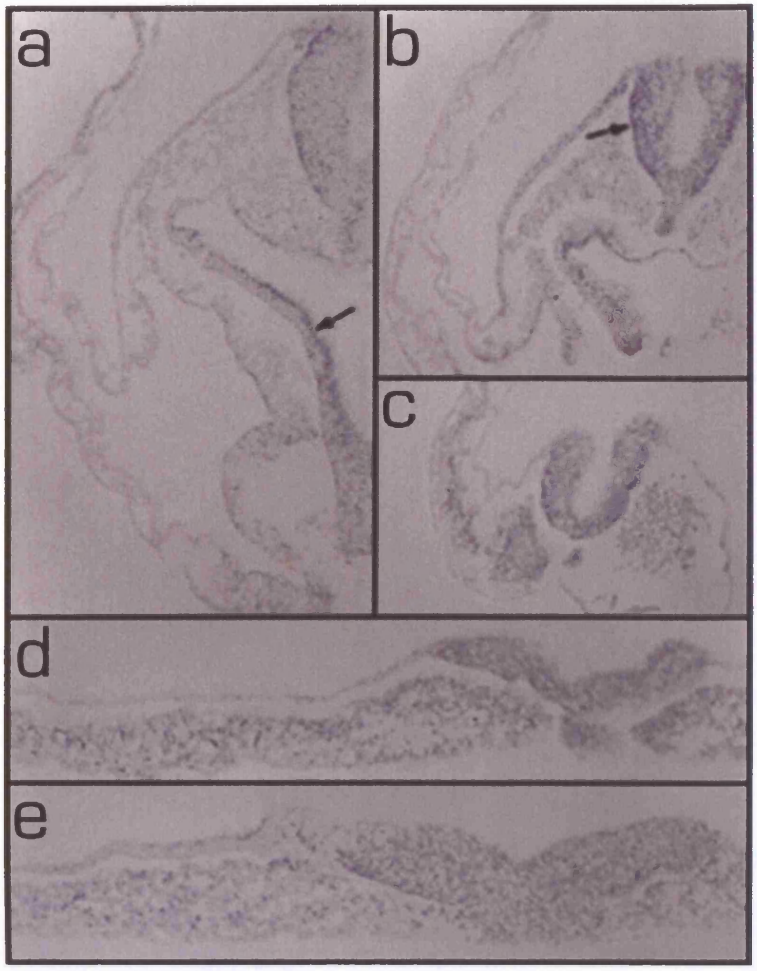

Fig. 4.10

Normal **expression patterns** of ***Ubll***. Sections through stage 12 embryo at the stage of hindbrain (**a**-**b**), somite (**c**) and posterior regions of the trunk (**d**-**e**).

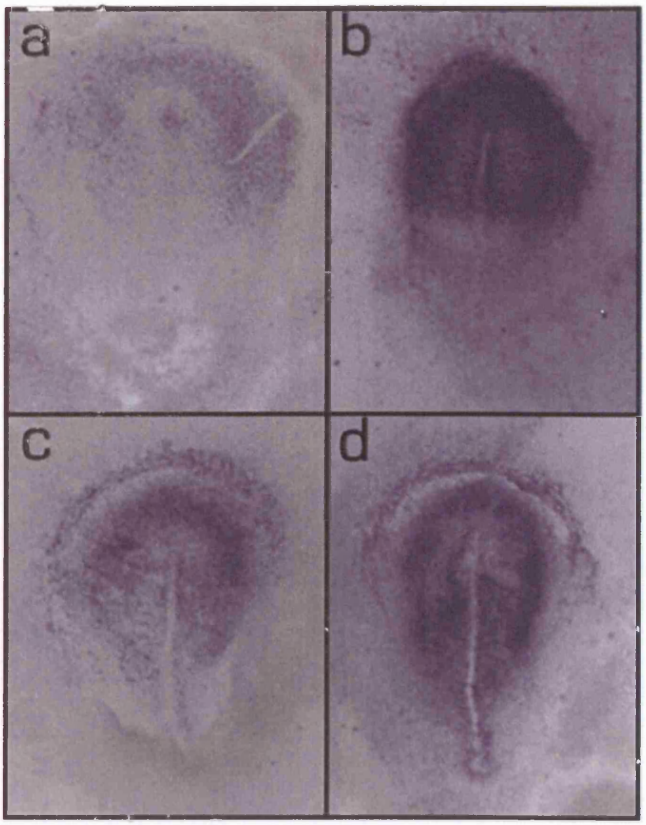

Fig. 4.11

Normal **expression patterns** of ***Ubl*** in a pre-primitive streak stage embryo at stages 3(**a**), 3^{+}(**b**), 4^{-}(**c**) and 4(**d**).

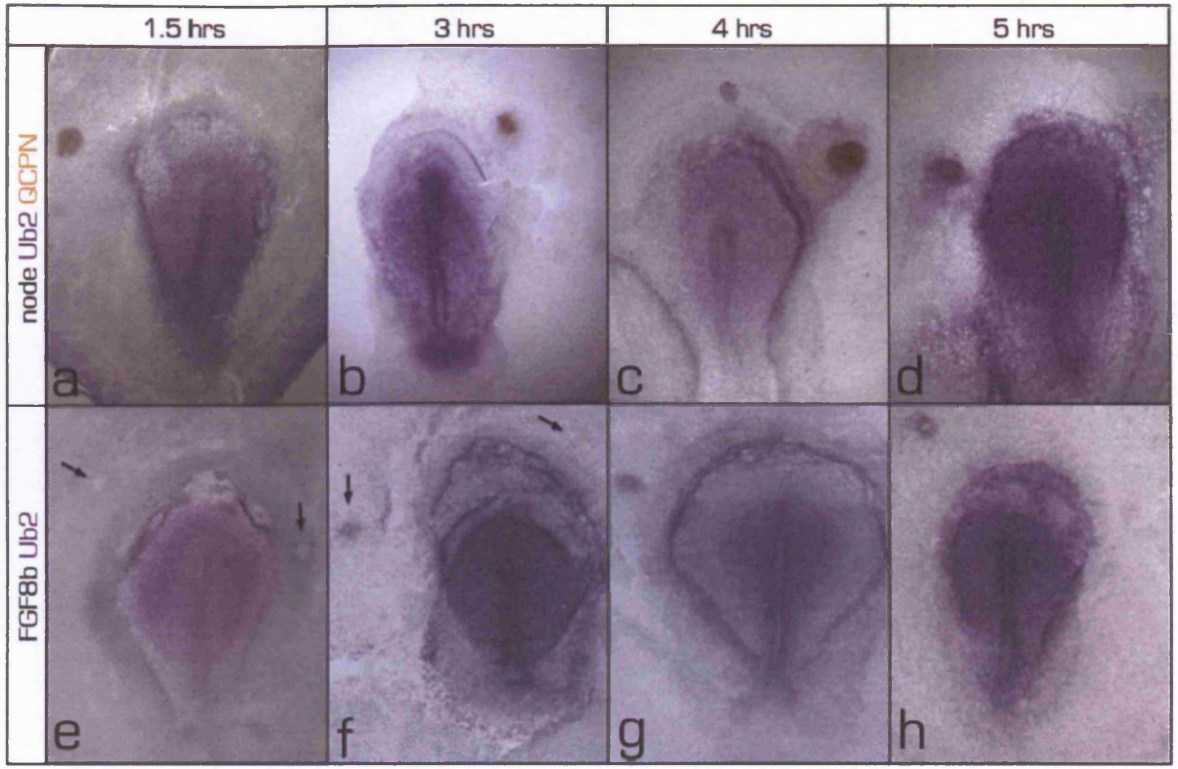

Fig. 4.12
Induction of ***UbII*** in the area opaca by a graft of **Hensen's node**:
no induction is seen after 1.5 hours (**a**) weak induction after 3 hours (**b**),
induction of ***UbII*** after 4 hours (**c**) and 5 (**d**) hours.
Induction of ***UbII*** expression in the area opaca by **FGF8b secreting beads**;
weak induction (left arrow) after 3 (**f**), 4 (**g**) and 5 (**h**) hours;
e: no induction is detected after 1.5 hours of exposure to FGF8b (left arrow),
no induction by negative control (right arrow),

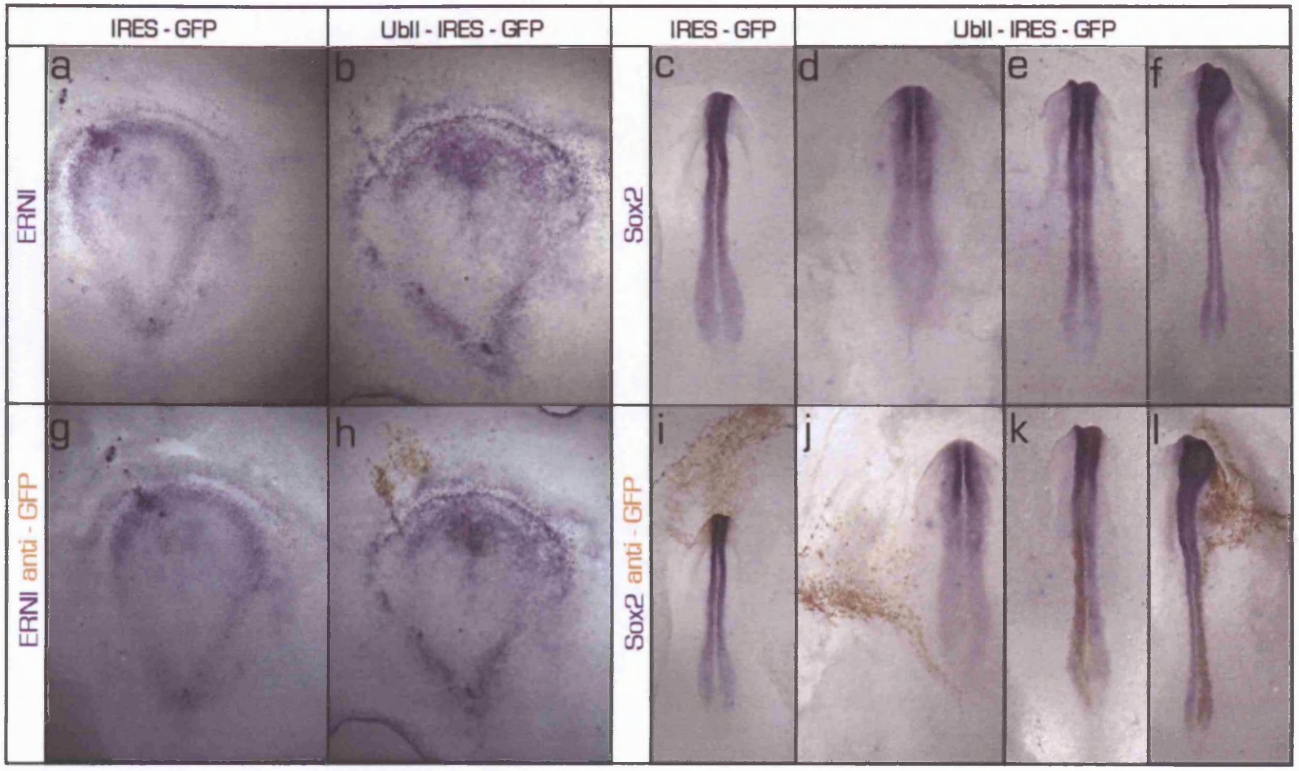

Fig. 4.13
Effects of **UBII** electroporation on ***ERNI*** and ***Sox2*** expression.
ERNI expression (blue) is shown following electroporation of a control, empty **pCAB vector** (**a**, **g**) and of **UBII** (**b**, **h**) before (**a-b**) and after (**g-h**) staining with anti- GFP antibody (brown).
Sox2 expression (blue) following electroporation of UBII is shown after 9 hours (**d**, **j**) and overnight (**e**, **f**, **k**, **l**) incubation. The effects of electroporation of a control, empty pCAB vector on ***Sox2*** expression are shown after overnight incubation (**c**, **i**) before (c-f) and after (**i-l**) staining with anti-GFP antibody (brown).

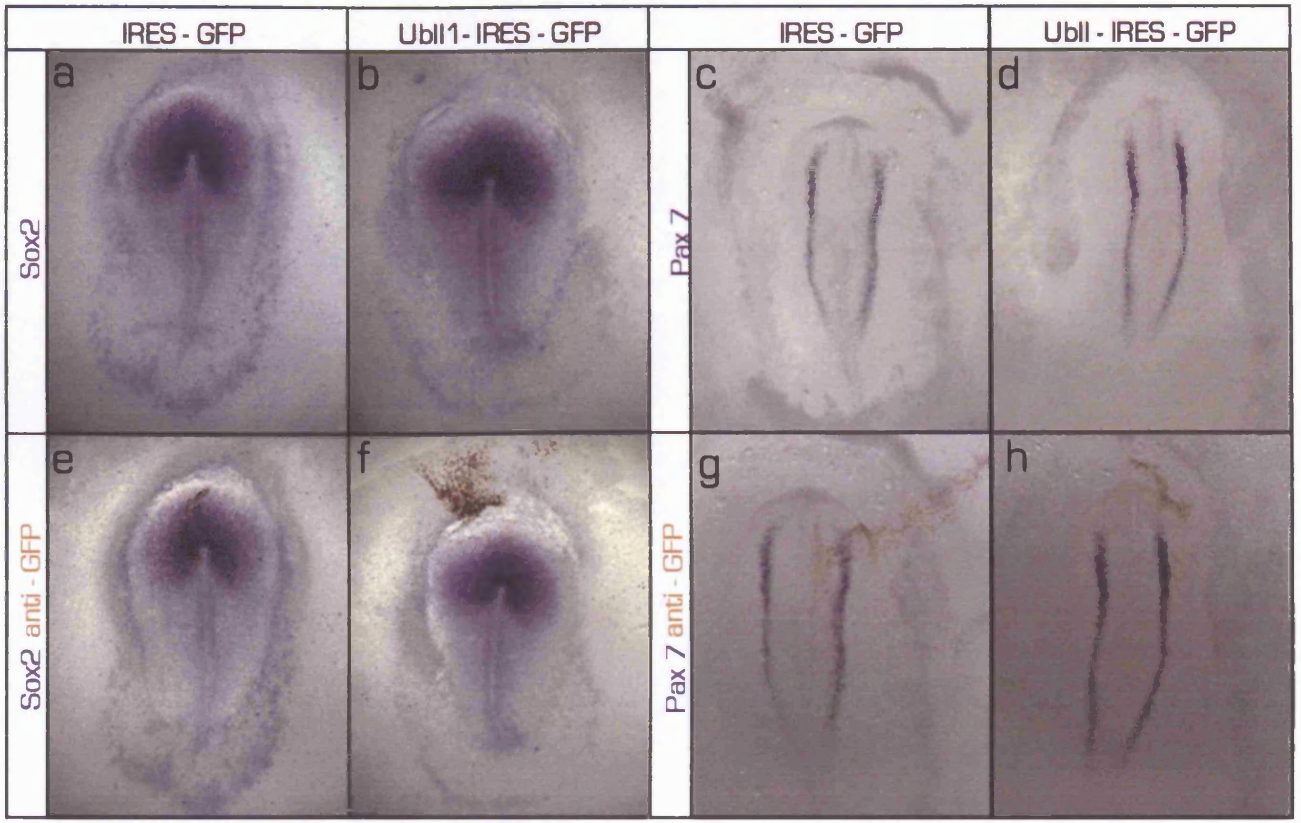

Fig. 4.14
Effects of electroporation of the **first ubiquitin of UBII** (**UBII1**) on ***Sox2*** expression and **UBII** on ***Pax7*** expression. ***Sox2*** expression (blue) is shown following electroporation of a control, empty **pCAB vector** (**a**, **e**) and of the **first ubiquitin of UBII** (**UBII1**) (**b**, **f**) before (**a-b**) and after (**e-f**) staining with anti-GFP antibody (brown). ***Pax7*** expression (blue) is shown after 9 hours incubation following electroporation of a control, empty **pCAB vector** (**c**, **g**) and of **UBII** (**d**, **h**) before (**c-d**) and after (**g-h**) staining with anti-GFP antibody (brown).

4.3. Discussion

The experimental data presented in this chapter demonstrate that Polyubiquitin II *(UbII)* fulfils the requirements of an early response to neural induction by a grafted node. It is expressed in the neural plate of the normal embryo at around the time of neural induction, and is induced in the epiblast of the area opaca after 3-4 hours' contact with a grafted Hensen's node. Additionally, this process can be mimicked by FGF8b with the same time course as a node graft. However, to test whether FGF signalling is required for the node to induce *UbII* expression, a node should be grafted together with beads soaked in SU5402, an inhibitor of the FGF-receptors (Mohammadi et al., 1997), as previously done for *ERNI* (Streit et al., 2000) and *ChurchillI* (Sheng et al., 2003). Unfortunately in the case of *UbII*, the low level of ubiquitous expression would make such an experiment difficult to interpret.

The results in this Chapter are compatible with the idea that some aspect involving ubiquitination and/or de-ubiquitination may be involved in the early stages of neural induction, since polyubiquitin II expression is rapidly upregulated under the influence of signals from Hensen's node. Since almost all proteins in the cell are likely to be regulated by a ubiquitin-dependent mechanism, it is impossible a priori to determine which are the most likely targets. However, one interesting possibility worthy of future investigation is raised by the presence of several SUMOylation sites revealed by ELM analysis in the protein encoded by the *ERNI* gene (unpublished observations). *ERNI* is currently the earliest gene to be up-regulated by signals from Hensen's node, being induced in just 1-2 hours following the graft, and its expression is quickly downregulated again just before expression of the stable neural plate marker, *Sox2* at stage 4+ (Stern, 2005a; Streit et al., 2000). Other unpublished observations in the lab implicate ERNI as an antagonist of neural plate development through its inhibition of *Sox2* expression, and further suggest that the level of *ERNI* transcripts are regulated by ERNI activity (Papanayotou et al., submitted). An interesting possibility therefore is that very early signals from Hensen's node first induce *ERNI* expression, followed more slowly (3-4 hours) by *UbII*, which in turn contributes to downregulate the expression of *ERNI* after this initial time point.

Moreover, two HMG proteins related to Sox2 (*Drosophila* SoxN and human Sox3) are also modified by SUMOylation (Savare et al., 2005). There is some evidence that several transcription factors can be alternatively regulated by SUMOylation and by ubiquitinylation. The absence of good working antibodies against ERNI, Sox2 or Sox3 prevented direct investigation of the effects of *UbII* misexpression or loss of function on the levels of these proteins. However since it is possible that transcript levels of

particular genes are regulated by the activity (and thus the level) of the protein encoded by them (as appears to be the case for both ERNI, see above, and for BMPs), the effects of *UbII* misexpression on the levels of transcripts of *Sox2*, *Sox3* and *ERNI* (as well as *Pax7* as a marker of cells situated between neural plate and epidermis) were analysed. No effects were found. Although this does not allow any conclusions to be drawn concerning the roles of UBII in regulating the levels of the proteins encoded by these genes, they do suggest that UBII overexpression is not sufficient to affect the levels of their mRNAs.

An interesting feature of the expression of *UbII* at the early stages of development is the localisation of the mRNA within the cells at different stages of neural plate development: message is found concentrated at the apical surface of future neural plate cells at stages 3+/4, while at later stages (9-11) the mRNA appears to move to a predominantly basal position in the neuroepithelium, passing through a stage (stage 5-7) when the mRNA does not appear to be localised. This raises the possibility that sub-cellular compartmentalisation of ubiquitination processes may be involved in some aspect of neural plate induction or of its later development, in particular the transition from a flat neural plate to a neural tube, which is the period at which the localisation of the message appears to change most dramatically. Interestingly, ferritin (another candidate early response gene isolated from this screen and discussed in Chapter 5) is also localised apically at the earliest stages (stages 3+/4), as is another candidate gene isolated from the same screen, *Obelix* (Pinho, in preparation).

Together, although it was impossible to pin-point a precise role for UbII in the early stages of neural plate development, the present results do raise the possibility that localised ubiquitin-dependent processes, restricted both in space and time in the embryo and even within the cells, may be an important and hitherto unexplored mechanism in these early events of neural development.

CHAPTER 5:

Heavy Chain Ferritin (*hcf*)

5.1 Introduction

Iron is a crucial as well as potentially extremely toxic element in cell biology. It takes part in a number of enzymatic reactions important for critical cell functions such as the cell cycle, the conversion of ribonucleotides to deoxyribonucleotides, electron transfer and oxygen metabolism (Quintana et al., 2004; Torti and Torti, 2002) In mammals there are no mechanisms for iron excretion other than through bleeding or loss of the mucosal/skin cells; therefore the absorption, transport, storage and metabolism of iron are very tightly regulated (Le Gall et al., 2005; Mladenka et al., 2005). Ferritins play a critical role in iron sequestration in cells (Torti and Torti, 2002) and are responsible for storage of 90% of non-haeme iron (Quintana et al., 2004). The crucial, general importance of ferritin is demonstrated by the phenotype of ferritin mutants in mouse. For example, $Fth^{(-/-)}$ (HCF in mice) mutants die between E3.5 and E9.5 (heterozygous embryos develop normally) (Ferreira et al., 2000).

There are two main types of ferritins in animals: heavy (HCF) and light chain (LCF) encoded by different genes of common origin (Harrison and Adams, 2002; Harrison et al., 1998). An additional M subunit has been identified only in amphibians (Bou-Abdallah et al., 2005; Dickey et al., 1987; Ha et al., 1997)

HCF is a highly conserved protein found in the plastids (chloroplast) of plants (van der Mark et al., 1983a; van der Mark et al., 1983b), in the hemolymph and vascular system of most insects (Dunkov et al., 2002; Dunkov et al., 1995; Kim et al., 2004a) and mainly in the cytoplasm of chordates (Hasan et al., 2006; Kim et al., 2004b; Surguladze et al., 2005). HCF has also been reported to be present in the cell nucleus in some tissues, for example, in corneal epithelium in chick (Cai et al., 1997; Linsenmayer et al., 2005). In insects, ferritins appear to exist in a secretable form, with both H and L types containing special modifications such as unique disulfide bonds that generate a more spherical configuration (Hamburger et al., 2005).

In the chicken genome, there is only a single *hcf* gene and no pseudogenes have been reported to date (NCBI) (see also Stevens et al., 1987). Despite earlier reports (Stevens et al., 1987) of the existence of numerous copies in other genomes, for example in human, most of them were found to be pseudogenes (Cragg et al., 1985; Percy et al., 1995; Quaresima et al., 1994; Zheng et al., 1997; Zheng et al., 1995) and only the H-ferritin gene (BC000857.1), located on chromosome 11, encodes a functional protein. One of the genes originally thought to be a human pseudogene was later identified as a mitochondrial ferritin (Drysdale et al., 2002; Levi et al., 2001) and later found in other species, for example mouse (Levi and Arosio, 2004; Nie et al., 2006), *Drosophila* (Missirlis et al., 2006) and plants (Zancani et al., 2004). The ratio of

HCF and LCF expression varies between different tissues (Cairo et al., 1991) and often depends on the physiological state of the cell. HCF and LCF form a spherical, apoferritin shell, consisting of 24 small subunits (held together by hydrogen and ionic bonds), with a total mass of 480 kDa and a diameter of 12 nm surrounding an internal cavity of 256 nm^3 (Ford et al., 1984; Harrison and Arosio, 1996; Theil, 2003). In plants and bacteria the 24 unit core is formed from the single type of ferritin expressed in these organisms (Bou-Abdallah et al., 2005). HCF plays an important role in the regulation of iron homeostasis and is vital in coping with states that could otherwise be disastrous for cell iron/oxygen chemistry (Theil, 2003). In vertebrates, the heavy chain is responsible for accelerated oxidation of toxic Fe (II) to Fe(III), which is less toxic to cells (Fig. 5.1) (Levi et al., 1989a; Levi et al., 1989b; Quintana et al., 2004). LCF enables formation of the apoferritin shell and possibly contains sites for nucleation and aids stabilisation of the protein complex (Bou-Abdallah et al., 2005; Harrison and Arosio, 1996; Levi et al., 1989b). An iron inorganic core capable of storing large quantities of iron (around 4500 atoms) is found inside the apoferritin shell (Ford et al., 1984; Harrison and Arosio, 1996; Levi et al., 1992; Torti and Torti, 2002). Each shell contains either the very labile ferrihydrite (Ft), or the more stable haematite (ht), or a hybrid magnetite/maghemite phase (with both ferrous and ferric ions) (Quintana et al., 2004). Ferrihydrate is the main type of apoferritin core seen under normal physiological conditions, while nanocrystals with cubic magnetite/maghemite phase and face-centered-cubic (fcc) structure predominate in the pathology of Alzheimer and other neurodegenerative diseases (Quintana et al., 2004). Other characteristics of the apoferritin shell are 8 entry and exit channels and 12 mineral attachment sites (Theil, 2003). Prior to the deposition in the core, the sequestered iron undergoes a number of chemical modifications. Each HCF subunit forms 4 α-helices surrounding the ferroxidase centre (Lawson et al., 1991; Lawson et al., 1989) - it is the site of formation of oxo-bridged Fe(III) dimers that represent an intermediate in the formation of the ferrihydrite core (Bauminger et al., 1991; Levi et al., 1992).

Human heavy chain ferritin (HuHF) can oxidise up to 48 Fe(II), two per each ferroxidase centre, to Fe(III) (Bou-Abdallah et al., 2005; Zhao et al., 2003). The ferroxidase activity of each site is regenerated during the process of iron oxidation in HuHF (Bou-Abdallah et al., 2005).

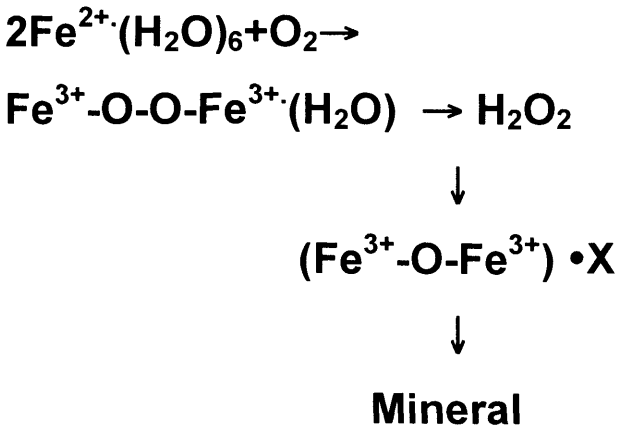

Fig. 5.1
Ferroxidase site reaction in HCF (from Theil, 2003).

The main mode of *hcf* regulation is post-transcriptional and the same levels of mRNA can result in a 10-fold difference in protein level (Stevens et al., 1987; Zahringer et al., 1975). This regulation involves interaction between a conserved 28 bp Iron Regulatory Element (IRE) sequence, located within the 5' untranslated region (UTR) of the mRNA, which forms a hairpin loop, and the Iron Regulatory Proteins (IRPs) 1 and 2 (Fig. 5.2) (Eisenstein, 2000; Harrell et al., 1991; Kim et al., 1995; Theil, 1990; Thomson et al., 1999). Both IRPs repress HCF translation when the level of iron is low. However their regulation differs: IRP1 acts as a cytosolic aconitase responsible for the enzymatic conversion of citrate into isocitrate with an iron sulphate cluster [4Fe-4S] that completely dissociates when the level of iron is low, in order to bind to the IRE (Clarke et al., 2006; Pantopoulos, 2004; Philpott et al., 1994). IRP2 is also regulated by iron; high levels catalyse the oxidation of IRP2, which is the signal for its ubiquitination for proteasome degradation (Iwai et al., 1998; Pantopoulos, 2004). IRPs are also responsible for the coordination between HCF activity (responsible for iron sequestration) and transferrin receptor TR stability (involved in the internalisation of transferrin and the intracellular release of iron) (Fig. 5.2) (Ponka et al., 1998). The mechanisms regulating TR stability are also mainly iron dependent and involve the interaction between IRPs and an IRE located in the 3' UTR of TR (Hentze and Kuhn, 1996; Klausner et al., 1993; Thomson et al., 1999). Depletion or targeted deletion of IRP2 causes an imbalance in iron metabolism and leads to neurodegenerative disease (LaVaute et al., 2001; Smith et al., 2004), while *IRP1*$^{(-/-)}$;*IRP2*$^{(-/-)}$ double-mutant mice do not survive beyond the blastocyst stage (Smith et al., 2006).

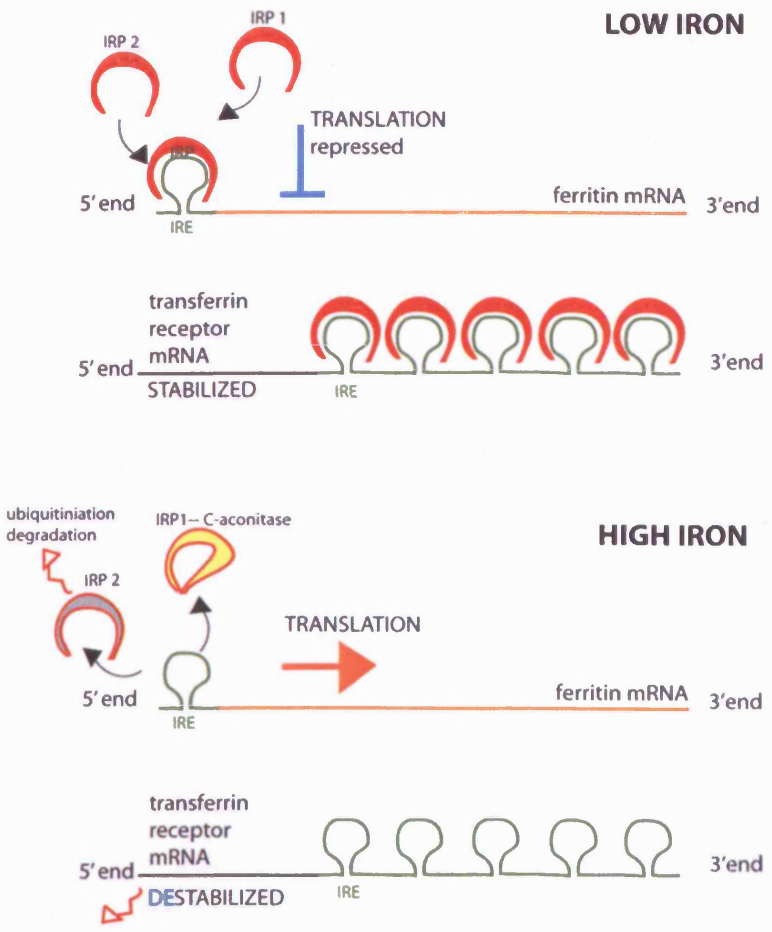

Fig. 5.2

Post-transcriptional regulation of HCF and TR by IRP1 and IRP; (modified from Torti and Torti, 2002).

There is evidence that HCF production is also regulated at the transcriptional level (for example, as a result of TNF, cAMP, *c-myc* and oxidative stress), as well as post-transcriptionally in an IRP-independently manner (in this case it is regulated by haemin, phorbol ester or IL-1β) (Santamaria et al., 2006; Torti and Torti, 2002). Some aspects of these modes of regulation as well as a more detailed look into the roles of ferritin in the protection against oxidative stress will be presented in Chapter 6.

5.2. Materials and Methods

5.2.1. Bioinformatic analysis

Comparisons with other sequences in the public domain were made through standard sites (Ensembl, Genbank, UCSC genome server). To align and analyse sequences, ClustalW (www.ebi.ac.uk/clustalw) (Thompson et al., 1994) was used and the results visualised using Jalview 2.08.1 (Clamp et al., 2004). The degree of amino acid identity was calculated using MUSCLE (Edgar, 2004).

5.2.2. Riboprobe transcription

The *hcf* cDNA was cloned into the pBlueScript vector. To generate antisense riboprobes for in situ hybridisation, the plasmid containing *hcf* were linearised by digestion with XhoI and transcribed with T3 RNA Polymerase. In situ hybridisation was performed as described in Chapter 2.

5.2.3. Constructs for electroporation

To study the possible functions of *hcf* in early chick development, *hcf* was misexpressed by electroporation. The pCAβ vector, containing the ubiquitously expressed chick β-actin promoter, a CMV enhancer followed by the cloning site and then an Internal Ribosome Entry Site (IRES) to direct translation of Green Fluorescent Protein (GFP), was digested with BsmBI and ClaI and gel-purified using a Gel Extraction Kit (Qiagen). A cDNA containing the entire open reading frame of chick *hcf* and the iron regulatory element (IRE) present in the 5' UTR was amplified by PCR from two chick cDNA libraries (stage 2-4 and 18-20). The following primers were used:

Forward: GATCAGCGGCCGCGATTGGGACGGAACCGGC

Reverse: TGCTCATCGATGCCTTCAGCTGTCACTTTCCCCG

These were designed to incorporate recognition sites for digestion by NotI and ClaI (underlined, respectively, in the two sequences above). This made the PCR product compatible for ligation with the product of BsmBI/ClaI digestion of pCAβ. The insert was ligated with purified vector using T4 DNA ligase (Promega). The ligation products were transformed into DH5α competent cells. Plasmids were harvested and sequenced.

To avoid possible effects of the IRE on translation of *hcf*, the ORF of *hcf* lacking 5' UTR sequences was amplified using primers:

Forward: GATCAGCGGCCGCGCCATGGCTACGCCTCC

Reverse: TGCTCATCGATGCCTTCAGCTGTCACTTTCCCCG

5.2.4. Electroporation

The pCA_ vectors described above were introduced by electroporation into stage 3+/4 embryos as described in Chapter 2. The electroporated embryos were grown for 6 hours (to study short term effects) or to stages 8-12 (for longer-term consequences). At the end of this period embryos were fixed and processed for in situ hybridisation (Chapter 2) with various markers including *Sox3* (Rex et al., 1997), *Sox2* (Rex et al., 1997), *Dlx5* (McLarren et al., 2003; Streit and Stern, 1999a; Yang et al., 1998) and *UbII* as described in Chapter 4. After in situ hybridisation, antibody staining against GFP or fluorescence microscopy was used to reveal the cells that had been electroporated as described in Chapter 2.

5.2.5. HCF antibody staining

To detect HCF proteins *in vivo* in chick embryos were subjected to whole-mount immunohistochemistry based on previously described protocols (Stern, 1998). An affinity-purified, rabbit anti-human HCF antibody (FERH13-A, Alpha Diagnostic) was used, which had been raised against a 15aa peptide near the amino-terminus of HCF, which is 100% conserved in mouse, rat, human, bovine monkey and chicken HCF. This antibody was diluted 1:250 in blocking buffer and was detected using HRP-coupled goat anti-rabbit (Santa Cruz) antibody diluted 1:2,500 in blocking buffer. HRP activity was revealed using diaminobenzidine (DAB) in the presence of H_2O_2 as previously described (Stern, 1998); see Chapter 2.

5.3. Results

5.3.1. Cloning and identification of *hcf*

The "early response screen" identified one clone (A4) with a 551 bp insert. BLAST analysis of this sequence revealed strong homology with accession number Y14698 (heavy chain ferritin, HCF), with only 6 separate nucleotide differences in 547 bp. The A4 clone contains the entire 5' UTR (150bp) and the product of the first two exons and 17 bp of exon 3 (401 bp) of the 539 bp open reading frame (ORF) of Heavy chain ferritin (NCBI: Y14698). To obtain a full-length clone, a stage 3-4 chick embryo cDNA library was screened and full-length clone was isolated. It contained 150 5' UTR and the entire ORF (539 bp). This sequence is identical to the cDNA deposited under accession number NCBI: Y14698.

In the chicken genome, *Hcf* (ENSGALG00000007220) is found on chromosome 5 at location 14,161,743-14,167,779. There are no SNPs reported (Ensembl, UCSC). A

CpG-rich region is located in the 5'UTR (UCSC) in accordance with published data (Stevens et al., 1987).

To compare chick HCF with the corresponding sequences in other species, an Average Distance tree was constructed using PID (the percentage identity between two sequences at each aligned position) in MUSCLE (Fig. 5.3). The relationships between the genes compared closely resemble the phylogenetic relationships between the species, with the surprising exception of the pig sequence, which has substitutions (Fig. 5.4) in the Glu-61 and Glu-62, two of the four residues that act as ligands in the intermediate step of formation of the iron core (Lawson et al., 1991; Levi et al., 1992).

5.3.2. Expression of *hcf* during early development

To establish the spatial and temporal pattern of expression of *hcf* in early embryos and to validate the results of the screen, whole mount in situ hybridisation was used. In early embryos (prior to about stage 5), expression seems fairly ubiquitous and weak, with some variability in staining between embryos. This was also seen by whole-mount immunostaining (data not shown). In pre-primitive streak embryos, *hcf* transcripts are found at very low levels throughout the epiblast (Fig. 5.5 a, j). At stage 3, the level of expression appears to decrease, with transcripts concentrated mainly in the epiblast of the primitive streak (Fig. 5.5 b, k) and in more anterior epiblast (Fig. 5.3 b, l). Within the epiblast, *hcf* transcripts are found predominantly in the apical region (Fig. 5.5 k, l). At stages 3^{+}/-4 considerable variability is seen, including embryos that show fairly uniform staining throughout the area pellucida (e.g. Fig. 5.5 c, d, m, n) and others in which the central portions of the area pellucida show low expression while the anterior-lateral borders show higher levels (Fig. 5.5 e). By stage 5, the pattern becomes more consistent. While *hcf* expression is still relatively ubiquitous (long periods of staining resulting in uniformly stained embryos), shorter staining reveals strong localisation of mRNA in the lateral plate mesoderm at the border between area pellucida and area opaca (Fig. 5.5 e-g), which quickly resolves to the forming blood islands of this region (Fig. 5.5 g, h, r, s). Within the embryo proper, relatively weak expression in the prospective neural plate is seen at stage 5 (Fig. 5.5 f), and this quickly becomes confined first to the future midbrain and hindbrain territories (Fig. 5.5 g, h) and then to a specific rhombomere within the hindbrain, possibly r3 or r4 at stage 10 (Fig. 5.5 i). In sections, closure of the neural tube is accompanied by an apparent shift of the mRNA from an initial apical to a basal localisation within the neuroepithelium (c.f. Fig. 5.5 k, l, o with 5.5 q, s).

In conclusion, although *hcf* is expressed in the future nervous system, it is not a good marker for prospective neural plate cells. Its expression throughout the neural

plate is very transient, being broader at earlier stages and much more restricted at later stages. Furthermore, the strongest expression observed is in blood islands at almost all stages tested.

5.3.3. Induction of *hcf* by Hensen's node

For the other genes studied in this thesis, a time-course of the induction of transcripts by a graft of Hensen's node and/or FGF was conducted. In the case of *hcf*, however, expression in the neural plate is so transient and weak (see above) that these experiments would be meaningless. This is especially problematic since short time-courses (less than about 6 hours) following a node graft at stage 3+ would only allow the host to develop to stage 4-4+, at which stage *hcf* expression is too variable. For these reasons, the induction of *hcf* by grafted nodes was not studied.

5.3.4. *hcf* does not affect neural, neural crest or affects the *Ubll* expression

To establish whether *hcf* might influence cell fate choices at early stages of neural development, it was introduced into the embryo *in vivo* by electroporation. Two different constructs were tested for activity: a cDNA containing the entire ORF as well as the 5' untranslated sequence that encodes the iron regulatory sequence (IRE), and the ORF alone, without 5' UTR sequences. Successful electroporation and expression of HCF was assessed by immunohistochemistry with an antibody against HCF (data not shown) as well as by fluorescence of the GFP in the pCA_ vector. Neither construct induced the neural markers *Sox3* (15/15; Fig. 5.6 c, h, e, j and 14/14; Fig. 5.6 b, g, d, I) or *Sox2* (9/9; Fig. 5.7 c, f and 11/11; Fig. 5.7 b, e) nor the neural crest and neural plate border marker *Dlx5* (9/9; Fig. 5.8 d, I and 7/7; Fig 5.8 e, j) after 6 hours (for *Sox3*), 9 hours (for *Sox2)* or overnight (for *Sox3* and *Dlx5*) culture.

It has been reported (LaVaute et al., 2001) that the iron regulatory protein IRP2 is a main regulator of HCF synthesis in the nervous system, and that IRP2 levels are regulated by ubiquitin-mediated degradation. To assess the possibility of a feedback loop by which HCF and ubiquitin-related genes might regulate each other's expression, the effects of overexpression of *hcf* on the expression patterns of *Ubll* were tested. No changes were found in the normal expression pattern of *Ubll* after missexpression of *hcf*, with or without the IRE sequence (Fig. 5.8 c, h and b, g). Control electroporation (empty pCAβ vector) does not alter patterns of expression of any genes tested (Fig. 5.6 a, f, fig 5.7 a, d and Fig. 5.8 a, f). In conclusion, these experiments do not reveal an effect of hcf misexpression on the expression of early neural markers or on *Ubll*.

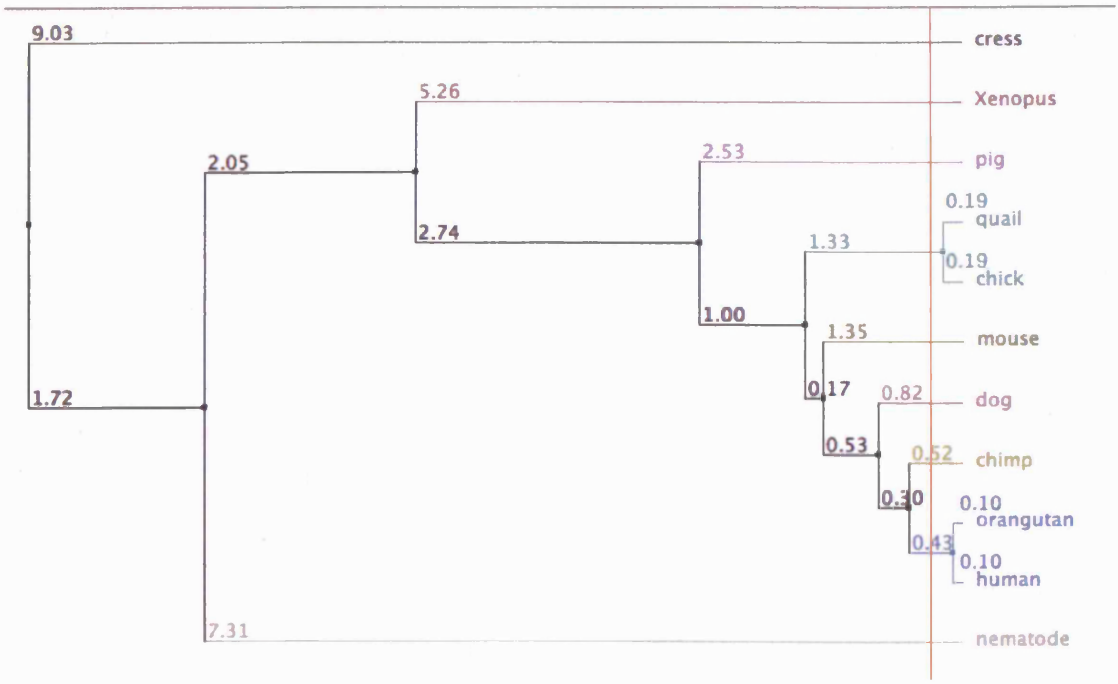

Fig. 5.3

Average Distance Tree of HCF protein sequences from different organisms.

cress (BAE98576), *Xenopus* (AAH77674), pig (NP_999140), quail (AAT01287), chicken (CAA75004), mouse (NP_034369), dog (NP_001003080), chimp (XM_522030), orangutan (CAH91913), human (AAH00857) and nematode (AAG24016).

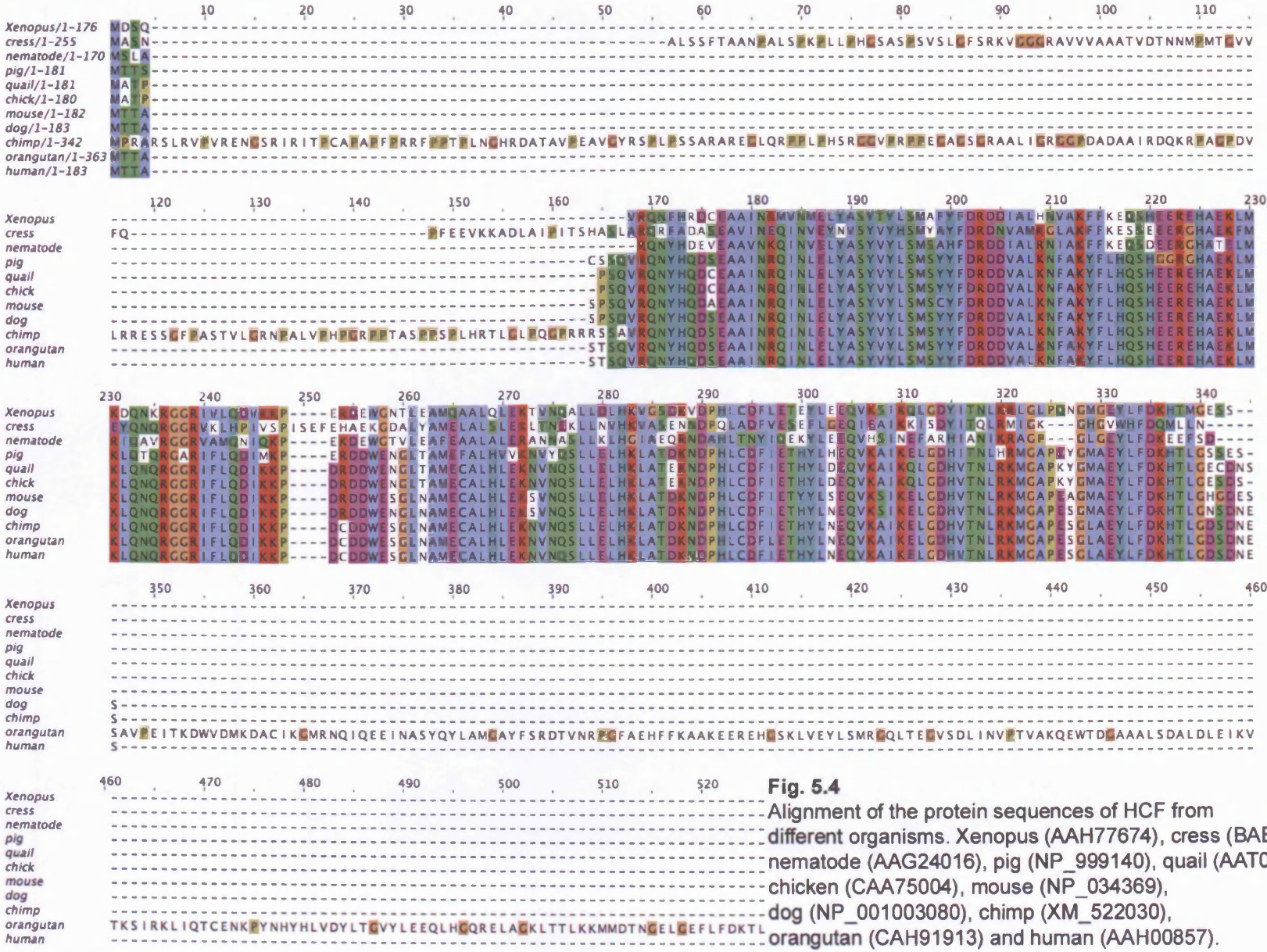

Fig. 5.4
Alignment of the protein sequences of HCF from different organisms. Xenopus (AAH77674), cress (BAE98576), nematode (AAG24016), pig (NP_999140), quail (AAT01287), chicken (CAA75004), mouse (NP_034369), dog (NP_001003080), chimp (XM_522030), orangutan (CAH91913) and human (AAH00857).

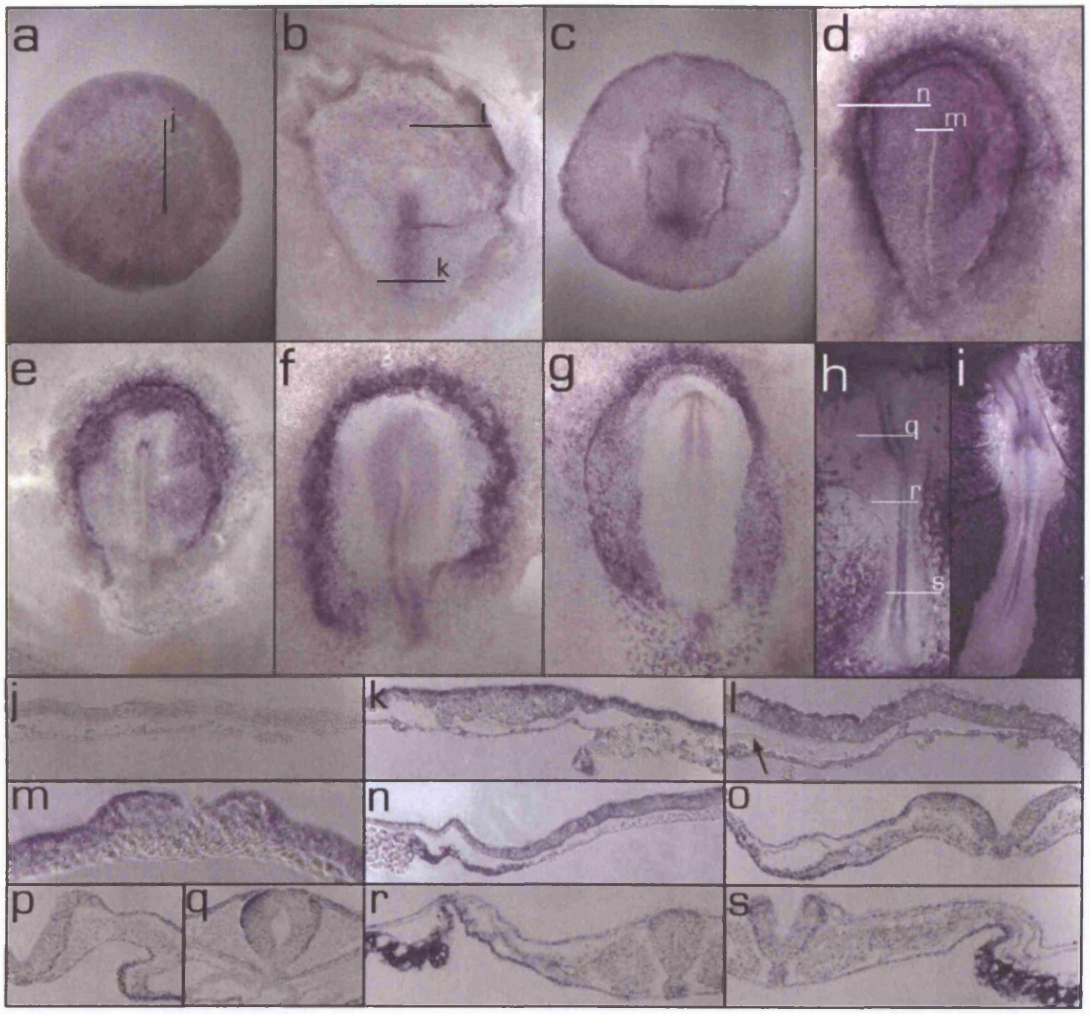

Fig. 5.5

Normal **expression patterns** of chick ***hcf*** in the pre-primitive streak stage embryo (**a**) and at stages 3(**b**), 4(**c-e**), 5(**f**), 6(**g**), 9(**h**), 12(**i**); **j**: longitudinal section through pre-streak embryo shown in **a**; section through the posterior primitive streak (**k**) and the anterior region (**l**) of embryo shown in **b**; section through the node (**m**) and anterior- lateral region (**n**) of embryo shown in **d**; **o**: section through trunk at stage 7; **p**: section through the anterior region of stage 8; section through the hindbrain (**q**) and through trunk (**r-s**) of the stage 9 embryo shown in **h**.

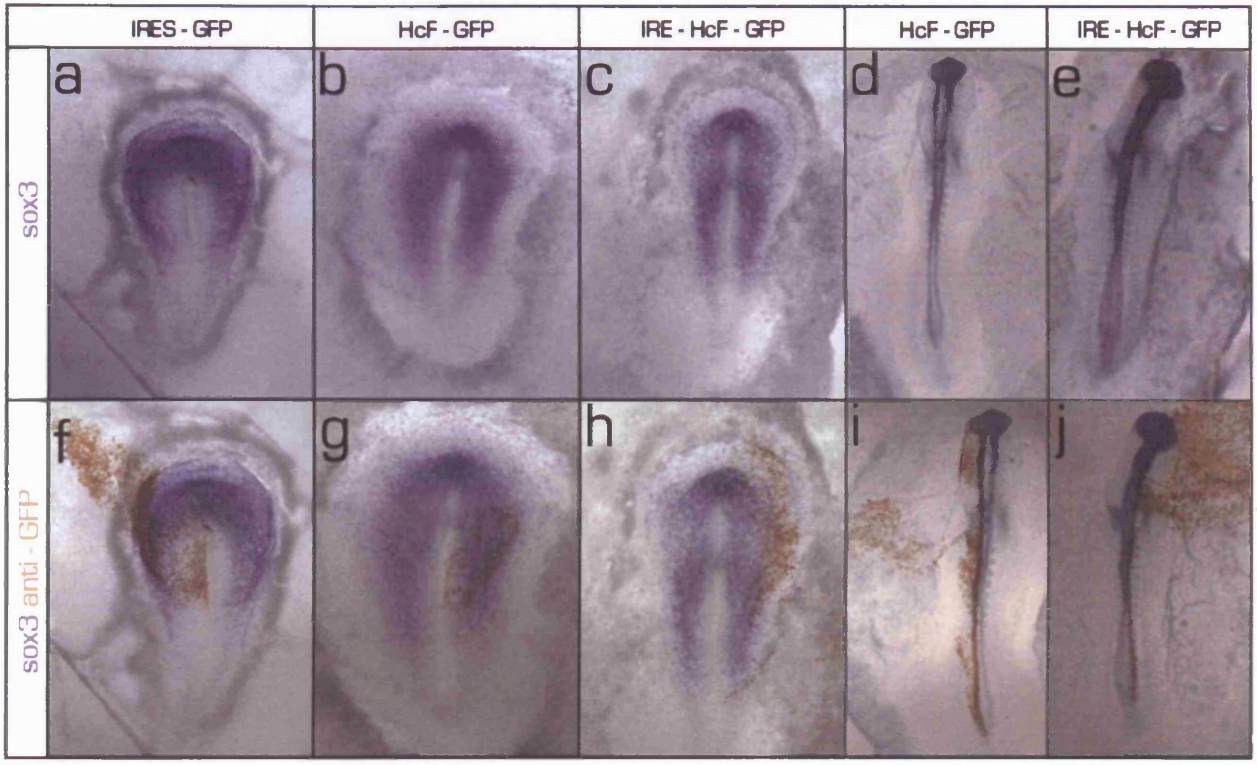

Fig. 5.6
Effects of **HCF** electroporation on ***Sox3*** expression (blue) following electroporation of a control, empty **pCAB vector** (**a**, **f**) and **HCF** is shown after 6 hours (**b**, **g**) and overnight (**d**, **i**) incubation. The effects of elecroporation of **HCF** construct **containing IRE** on ***Sox3*** expression are shown after 6 hours (**c**, **h**) and overnight (**e**, **j**) before (**a-e**) and after (**f-j**) staining with anti-GFP antibody (brown).

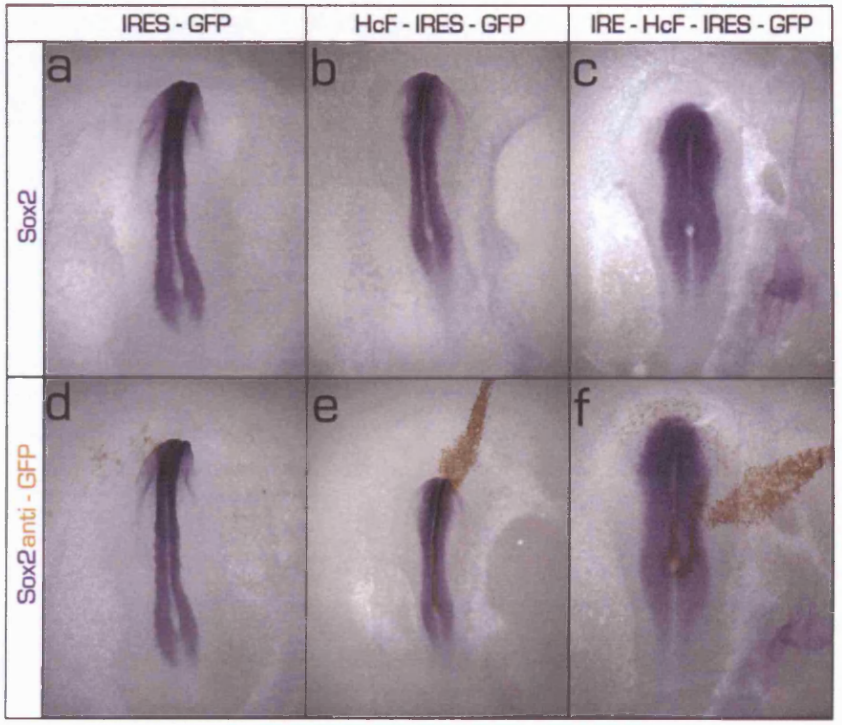

Fig. 5.7
Effects of **HCF** electroporation on ***Sox2*** expression (blue) following electroporation of a control, empty **pCAB vector** (**a**, **d**) and **HCF** is shown after 9 hours (**b**, **e**) and overnight (**d**, **i**) incubation. The effects of elecroporation of **HCF** construct **containing IRE** on ***Sox3*** expression are shown after 6 hours (**c**, **f**) before (**a-c**) and after (**d-f**) staining with anti-GFP antibody (brown).

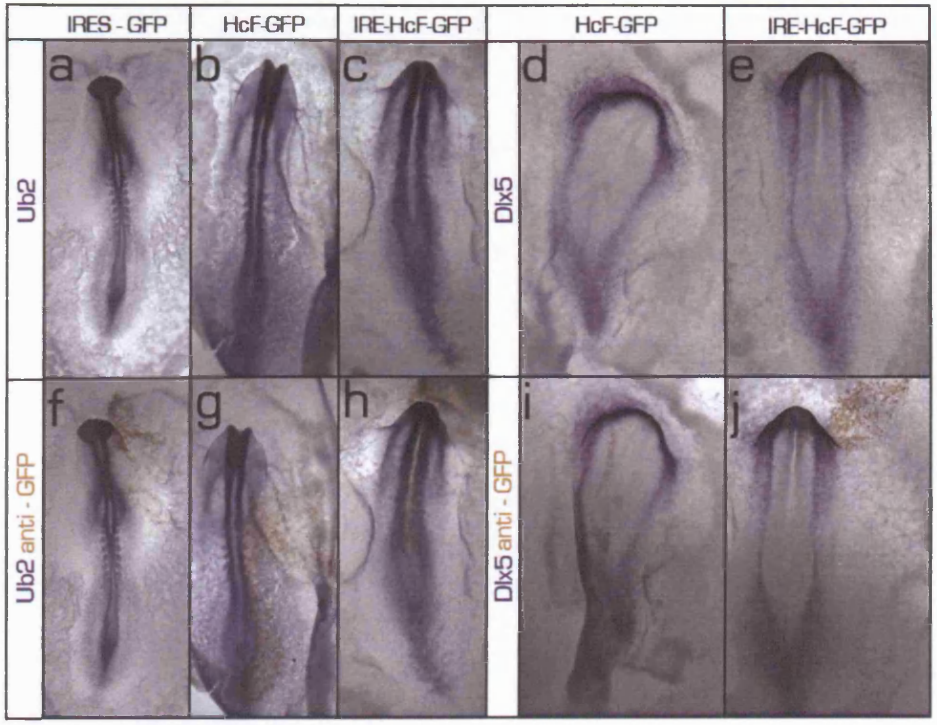

Fig. 5.8
Effects of **HCF** electroporation on ***UbII*** expression (blue) following electroporation of a control, empty **pCAB vector** (**a**, **f**), **HCF** (**b**, **g**) and of **HCF** construct containing **IRE** (**c**, **h**) are shown after 12 hours incubation. The effects of elecroporation on ***Dlx5*** expression are shown after 9 hours: **HCF** (**c**, **h**) and **HCF** construct **containing IRE** (**e**, **j**) after 9 hours incubation. The expression is shown before (**a-e**) and after (**f-j**) staining with anti-GFP antibody (brown).

5.4. Discussion

Hcf was isolated from the screen conducted to identify genes whose expression is an early response to neural induction by a grafted node. As explained in Chapters 1, 3 and 4, two criteria are expected to be satisfied for any such gene to be considered as an "early response to neural induction": if the expression of the gene is upregulated by the node graft, this should be verifiable by in situ hybridisation within a 5 hour window following the node graft into the area opaca, and the gene should normally be expressed at higher levels in the prospective neural plate at early stages of neural induction. In this case, weak ubiquitous expression of *hcf* at early stages made it impractical to assess whether it can be induced or upregulated by a grafted node or by FGF8. Furthermore, its normal expression prior to stage 4+ (when neural induction is thought to end, Dias and Schoenwolf, 1990; Storey et al., 1992) is weak as well as variable from embryo to embryo.

Although it is not possible to test whether *hcf* fulfils these criteria to be an early response gene, it is expressed at higher levels in the neural plate from stage 5 and remains upregulated in the developing nervous system (and especially within the hindbrain), consistent with some role in early development of the neural plate. The possibility that iron metabolism or intracellular regulation of iron levels could be important in very early stages of neural plate development has not been considered before, and the present results, although purely descriptive at this stage, do raise this interesting possibility even though they did not provide information to help identify what these roles might be.

It has been reported that in vitro and *in vivo* overexpression of *hcf* without or mutated the 5' IRE sequence results, in a sustained upregulation of HCF (Cozzi et al., 2000; Picard et al., 1996; Wilkinson Iv et al., 2006). In experiments conducted for this project there was an upregulation of the synthesised HCF measured by immunochemistry for both electroporated constructs: *hcf* and *hcf* and IRE, however there was no effect on the expression patterns of the neural or crest markers tested. These results suggest that HCF alone is not sufficient to affect the expression of these markers. However, it is possible that other elements involved in iron homeostasis are required along with HCF for it to exert its functions. One way to test whether the intracellular levels of ferric iron (oxidised Fe(III) often found bound to ferritin) are affected by electroporation would have been to use Prussian Blue staining (LaVaute et al., 2001), but this method is quite crude and insensitive as compared with more quantitative methods using radioactive Fe isotopes (Cozzi et al., 2000). It might also have been interesting to test whether the levels of transferrin receptor (another main

player in iron regulation) are affected. Likewise, it has been shown that overexpression of *hcf* in vitro causes an increase in the activity of IRP, which binds to the IRE sequence in *hcf*. However this mechanism is not dependent solely on HCF but rather a consequence of decreasing levels of the LIP (Labile Iron Pool) in cells following sequestering of iron by excess ferritin (Cozzi et al., 2000; Picard et al., 1996). Other experiments in which HCF was overexpressed without its ferroxidase activity (E^{62}>K and H^{65}>G) (Bauminger et al., 1991; Cozzi et al., 2000) in HeLa cells has been reported to have almost no effect on the cells (Cozzi et al., 2000). This makes it unlikely that such mutated forms of HCF could function as dominant-negative versions that might otherwise have been used to abrogate HCF function *in vivo*.

In conclusion, the lack of obvious effects of overexpression of HCF on the early neural markers studied could either indicate that iron metabolism plays no role in the regulation of expression of these markers, or that overexpression of this component alone is not sufficient to alter the levels of intracellular iron sufficiently to cause a detectable effect.

CHAPTER 6:

Apoptosis and neural induction

6.1. Introduction

The term "apoptosis" (from the Greek words *apo* = from and *ptosis* = falling) was introduced in 1972, initially to distinguish this form of naturally occurring, predictable cell death from necrosis (Kerr et al., 1972) (for details of morphological descriptions of these processes see Table.6.1). Apoptosis is the most common form of Programmed Cell Death (PCD) (Kroemer et al., 2005) and in this thesis the two terms are used interchangeably.

APOPTOSIS	NECROSIS
• Chromatin condensation • DNA fragmentation • Cell Shrinkage and Pyknosis • Preservation of Organelles and Cell membranes • Blebbing and Budding • Engulfment by neighbouring cells preventing inflammation	• Cell swelling • Disruption of Organelles • Increase of permeability, rupture of cells and release of the cellular content • Coagulation, shrinkage • Inflammatory response

Table 6.1

Apoptosis versus necrosis comparison of morphological events.

Caspases (cysteinyl aspartate-specific proteases) belong to the family of cysteine proteases capable of specific cleavage of proteins at the C-terminal of the peptide bond next to an aspartate residue (Earnshaw et al., 1999; Riedl and Shi, 2004; Zhivotovsky, 2003). All caspases are synthesised as an inactive precursor, a pro-caspase also called zymogen. It consists of a prodomain at the N-terminus of the caspase chain (short or long) and two subunits (Fig. 6.1). The long chain prodomain is required for the activation of initiator caspases and contains interaction domains: DEDs (death effector domains) in pro-caspases -8 and -10 and CARDs (caspase-recruitment domains) found in pro-caspases -2, -9 and in initiator caspases involved in inflammation -1, -4, -5 (Budihardjo et al., 1999; Riedl and Shi, 2004; Zhivotovsky, 2003). The active site of Caspases consists of a Cysteine (underlined) located in the conserved pentapeptide sequence: QACXG (Zhivotovsky, 2003). Caspases also have high substrate specificity cleavage sites summarised in the Fig. 6.1 (Thornberry et al., 1997).

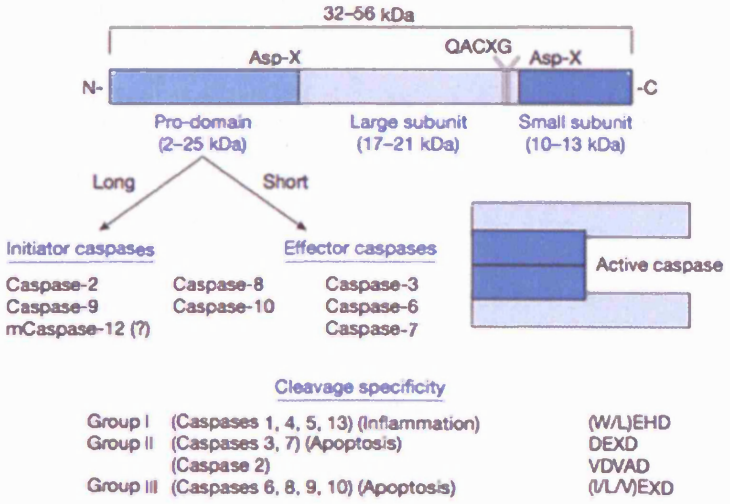

Fig. 6.1

Mammalian procaspases, their structure, activation and substrate specificity - from (Thornberry et al., 1997).

Cleavage of proteins by Caspases can result in activation or inactivation of the protein. The substrate proteins can be divided into: cytoplasmic (mainly cytoskeletal and intermediate fusion proteins), nuclear (structural, RNA-binding, chromosome scaffolding), and/or may be involved in DNA metabolism and repair, in the regulation of the cell cycle, of proliferation and differentiation, in signal transduction, mainly via protein kinases and in the cleavage of proteins directly involved in apoptosis (including some pro-caspases, Bcl-2, Bcl-X L, Bid and Bax to name a few) (Earnshaw et al., 1999; Fischer et al., 2003; Zhivotovsky, 2003).

A wide range of regulators of caspase activity exist, which can be classified as belonging to two pathways: extrinsic (death receptor activation) and intrinsic (for example: transcriptional regulation, post-transcriptional modifications, including nitric oxide (NO) and possibly phosphorylation, cytochrome c release, MAC - second mitochondria-derived activator of caspases, Smac/DIABLO - direct inhibitor of apoptosis, IAPs inhibitor-of-apoptosis proteins, IAP-binding protein with low pI, AIF apoptosis-inducing factor, EndoG endonuclease G and OMI/HTRA2 high-temperature-requirement protein). The intrinsic pathway is also activated in the response to the DNA damage, activity of oncogenes and heat stress (Earnshaw et al., 1999; Riedl and Shi, 2004; Zhivotovsky, 2003).

The first caspase to be identified was interleukin1-converting enzyme (ICE - later recognised as Caspase1), which has been studied for its role in inflammation - (Bensi et al., 1987; Gray et al., 1986; Telford et al., 1986). ICE was found to be homologous to a protein later identified in *C. elegans*, CED3 (cell-death abnormality 3) (Henkart, 1996; Yuan et al., 1993) suggesting that process of PCD is conserved throughout evolution. Work from Horvitz's group that led to discovery and subsequent studies of PCD in *C. elegans* (Hengartner et al., 1992; Xue and Horvitz, 1997; Yuan et al., 1993; Yuan and Horvitz, 1990) were of great importance in the process of understanding programmed cell death in vertebrates (Hengartner and Horvitz, 1994; Metzstein et al., 1998). Recently homologues of caspases have also been identified in insects: *Drosophila melanogaster* (Fraser et al., 1997; Song et al., 1997), *Spodoptera frugiperda* (Ahmad et al., 1997; Forsyth et al., 2004) and yeast (Madeo et al., 2002). There are also suggestions that caspases may exist in plants (Hatsugai et al., 2004; Rojo et al., 2004; Woltering et al., 2002).

Among the homologs of CED3, Caspase9 (Apaf3/Mch6/ICE-LAP6 - the main initiator of the intrinsic pathway) and Caspase3 (CPP32/Yama/apopain - the main converging effector of intrinsic and extrinsic pathways leading to PCD) have attracted a great deal of attention over the last decade. It has been demonstrated that Caspase9 is the most upstream caspase that triggers apoptosis in the response to the release of cytochrome c from mitochondria (Li et al., 1997). Following the release of cytochrome c Caspase9 binds to Apaf1 via an NH2 domain in presence of dATP (Li et al., 1997). The activation of Caspase9 takes place in the presence of the ternary complex the "apoptosome" (Chinnaiyan, 1999) and involves autoprocessing (Fig. 6.1) that results in the formation of an active oligodimer (Bratton et al., 2001; Chao et al., 2005; Donepudi and Grutter, 2002; Pop et al., 2006; Rodriguez and Lazebnik, 1999; Shi, 2002; Zhivotovsky, 2003). Different models of apoptosome involvement in this process have been reviewed (Bao and Shi, 2006; Shi, 2004). Recently, another, apoptosome-independent pathway for Caspase9 activation and for the execution of PCD has been reported (Aleo et al., 2006).

Caspase9 (Table.6.1) is responsible for the intra-chain cleavage of pro-caspases Caspase3 and other effector caspases (-6 and -7) resulting in their activation (Fujita et al., 2001; Kuida, 2000; Li et al., 1997; Pan et al., 1998). Effector caspases exist in homodimer form even before full activation and therefore are capable of performing their functions. However the conformational changes following cleavage increase Caspase 3 activity by several fold (Riedl and Shi, 2004). It has also been demonstrated

that Caspase3 directly or indirectly regulates processing of Caspases2, -6, -8 and 10 as well as to some degree Caspase 9 (Slee et al., 1999), revealing the amplification loop later demonstrated *in vivo* by (Fujita et al., 2001). Recent data from mice fibroblast cells lacking both Caspase3 and Caspase7 function $Cas3^{(-/-)}$ /$Cas7^{(-/-)}$ suggest that these caspases can play an important role in the amplification of the mitochondrial death signal (Lakhani et al., 2006).

Caspase 3 is required for chromatin condensation and DNA fragmentation, two of the main morphological hallmarks of apoptosis (Janicke et al., 1998b; Woo et al., 1998). However, Caspase3 activity is dispensable for cleavage of a number of death substrates (with the exception of alpha-fodrin and topoisomerase I) and for PCD in certain cell types (Janicke et al., 1998a; Samejima et al., 1999; Woo et al., 1998).

The interactions between caspases, their activators and inhibitors are complex. The actions of individual caspases depend on many factors, including tissue specificity, developmental stage and the kind of apoptotic signals, often limiting the relevance of the data available to certain types of cell or to the specific apoptotic trigger used. The fact that many caspases play redundant functions in the cell death machinery makes understanding the exact functions of individual caspases even more difficult. In addition, even "death" caspases often play functions not related to this process (Fadeel et al., 2000; Riedl and Shi, 2004; Zhivotovsky, 2003). PCD can also be triggered and/or executed in caspase-independent way (Broker et al., 2005). Our present understanding of the action of Caspases 3 and 9 in living animals is limited. In vivo results often give surprising results, for example $Cas3^{(-/-)}$ mutant mice (Kuida et al., 1996) have defects mainly affecting the nervous system but are born viable and die in the 1-3 week of their life, while $Cas9^{(-/-)}$ mutant mice have similar but much more severe defects that result in embryonic lethality for the majority of embryos (Kuida et al., 1998). In this study we investigate the expression of Caspase3 and Caspase9 and their possible role in the process of PCD and neural induction in early chick development. Our data suggest a possible link between Caspase3 and neural development and implicate Caspase9 and/or interaction between both of them in PCD at the early stages of neural development in chick.

PCD has been considered an important and necessary part of normal development (Jacobson et al., 1997; Vaux and Korsmeyer, 1999), and was originally envisaged as a process of elimination of embryonic cells for "phylogenetic, histogenetic and morphogenetic" purposes (Glucksmann, 1951). There have been extensive

studies investigating the role of apoptosis in the formation of various structures and organs, for example, the limb bud (Garcia-Martinez et al., 1993; Hurle et al., 1995; Zuzarte-Luis and Hurle, 2005), heart (Pexieder, 1975; Poelmann and Gittenberger-de Groot, 2005); tail bud (Miller and Briglin, 1996; Sanders et al., 1986; Schoenwolf, 1981); eye (Linden et al., 2005; Silver and Hughes, 1973; Vecino et al., 2004; Yan et al., 2006; Young, 1984) and neural crest (Ellies et al., 2002; Graham et al., 1993; Graham et al., 1996; Homma et al., 1994; Jeffs et al., 1992; Jeffs and Osmond, 1992; Lawson et al., 1999; Lumsden et al., 1991; Wakamatsu et al., 1998). In mammalian embryos; apoptosis is thought to play a role during pre-implantation development, as the ratio of apoptotic to non-apoptotic cells seems to be related to successful implantation (Betts and King, 2001; Hardy, 1999; Jurisicova and Acton, 2004; Levy et al., 2001).

In the chick embryo, cells with all the hallmarks of apoptosis during early chick embryogenesis were described as early as 1961, based on electron microscopical observations (Bellairs, 1961). Subsequently, apoptosis has been investigated during the early stages of chick development (from pre-primitive streak stages) (Hirata and Hall, 2000); however this study largely ignores gastrulation and early neurulation, and then concentrates on later stages. More detailed comparative studies of PCD patterns during gastrulation in chick and mouse are also available (Sanders et al., 1997). However the published data did not investigate how the domains of increased apoptosis correlate with neural patterning events taking place in early embryonic development, or especially whether apoptosis could play any important role in neural induction or the subsequent patterning of the neural plate. These relationships have been analysed in more detail in *Xenopus* (Hensey and Gautier, 1998; Yeo and Gautier, 2003; Yeo and Gautier, 2004). In particular, these authors proposed that apoptosis could play a role in adjusting the size of the neural plate and in regulating neuronal differentiation.

Of the 15 genes identified by the "early response screen" performed in our laboratory, four encoded previously studied proteins: Dad1, ferritin, polyubiquitin and a metallothionein. We were interested in that all four of these have been implicated in the regulation or execution of cell death in a variety of systems (see previous chapters), either as pro- or anti-apoptotic factors, raising the possibility that an early response to neural induction involves tight regulation of cell death in the responding tissue. In Chapters 3-5, the possible involvement of three of these proteins in neural induction was investigated. This chapter explores their roles in the control of cell death, and the possible relationships between apoptosis and neural induction.

6.2. Materials and Methods

6.2.1. Bioinformatic analysis

Genome information about chick caspases and those from other species were accessed from the three main databases (www.ensembl.org, www.ncbi.nlm.nih.gov and www.genome.ucsc.edu). To analyse and align sequences, ClustalW (www.ebi.ac.uk/clustalw) was used and the results visualised using Jalview 2.08.1 (Clamp et al., 2004). The degree of amino acid identity was calculated using MUSCLE – a multiple sequence alignment with high accuracy and high throughput (Edgar, 2004).

6.2.2. Riboprobe transcription

To establish the expression patterns of caspase 3 (*Cas3*) and caspase (*Cas9*) during normal early development, *Cas3* and *Cas9* cDNA (both in pGEMTeasy) were linearised by digestion with NcoI and transcribed with SP6 RNA Polymerase to generate antisense riboprobes. In situ hybridisation was performed as described in Chapter 2.

6.2.3 Terminal deoxynucleotidyl transferase mediated nick-end labelling (TUNEL)

To detect cells dying by apoptosis in the embryo, the TUNEL method was used, modified from published protocols (Gavrieli et al., 1992; Wijsman et al., 1993). Embryos were fixed in 4% PFA in PBT (0.1% Tween-20 in PBS, pH 7.5) as for in situ hybridisation, and stored overnight in 100% methanol at -20°C. They were then rehydrated gradually back to PBT and washed in this for 1 hour. Embryos were placed in TdT buffer (30 mM Tris pH 7.4,100 mM Na cacodylate, 1 mM $CoCl_2$) for 30 min and rocked gently. The TdT buffer was replaced with 400_l of TdT reaction mix (TdT buffer, 0.5 _l DIG-dUTP, 2_l terminal transferase; all from Roche) for 4 hours at room temperature. To stop terminal transferase activity embryos were rinsed several times and then washed 3 times for 1 hour in TBST at 65 °C and four times for 1 hr at room temperature. They were then placed in blocking buffer (Tris-buffered saline, pH 7.5, containing 5% heat-inactivated goat serum and 1mg/ml bovine serum albumin) for 3-6 hours. Anti-DIG-Alkaline Phosphatase (Roche) antibody (1:5000) was added and embryos incubated overnight at 4°C. Post-antibody washes and the subsequent staining procedure were identical to those described in Chapter 2 for in situ hybridisation (Stern, 1998; Streit and Stern, 2001).

6.2.4 Caspase inhibition

The Caspase inhibitors Z-DEVD-FMK (specific for Caspase-3) (R&D Systems, BD PharMingen), Z-VAD(OMe)-FMK (general Caspase inhibitor) (R&D Systems) and a negative control for Caspase inhibitors (Z-FA-FMK) (R&D Systems, Calbiochem) were dissolved in dimethylsulphoxide (DMSO) at 10mM or 20mM according to the manufacturers' instructions, and aliquots stored at –20 °C. These stocks were diluted in PBS to final concentrations between 2μM-10μM. The embryos were soaked in 1 ml inhibitor solution in a small Petri dish before rinsing in PBS. In some instances the reagent was added to the albumen pool of the New culture for 1-2 hrs and the embryos incubated at room temperature before transferring the cultures to 38°C. The embryo was then grown for 6 hours or overnight. TUNEL staining and/or in situ hybridisation were performed as described above.

6.2.5. Constructs for electroporation

These were described in Chapter 2 (empty pCA_; negative control), Chapter 3 (*Dad1* and truncated *Dad1*), Chapter 4 (*UBII*) and Chapter 5 (*HCF* with or without its Iron regulatory Element, IRE). A construct containing *lacZ* in pCAβ with a CMV immediate-early enhancer (kind gift of Dr. Voiculescu) was also used as an additional negative control. To visualise _-galactosidase activity, embryos were fixed for 20-30 minutes in 4% PFA and incubated in PBS containing: 4 mM $K_4[Fe(CN)_6]$, 4 mM $K_3[Fe(CN)_6]$, 4 mM $MgCl_2$ and 200 mg/ml of X-gal (5-bromo-4-chloro-3-indolyl-beta-D-galactopyranoside) until the colour reaction was fully developed.

6.4 Results

6.3.1. Bioinformatic analysis

Caspase9 is located on chromosome 21 (UCSC) of the chick genome, whilst Caspase 3 is located on chromosome 4 (Ensembl; gene id: ENSGALG00000010638). The latter consists of 8 exons; there is one non-synonymous Single Nucleotide Polymorphism (SNP) but it does not result in any change to the amino acid sequence (position 160); there are 3 variations in the 3' untranslated region.

To compare chick Caspase3 and Caspase9 to the homonymous sequences in other species, an Average Distance tree was constructed using PID (the percentage identity between two sequences at each aligned position) in MUSCLE (Fig. 6.2 and Fig. 6.3).

For both alignments, nematode CED3 was used, as it is the only *C. elegans* homologue of the numerous vertebrate caspases. The results show that the CED3 sequence is also more similar to Caspase3 than Caspase9, as reported for nematode CED3 in comparison with mammalian Caspases (Xue and Horvitz, 1997). It has also been demonstrated that CED3 is a functional ortholog of Caspase 9 (Riedl and Shi, 2004).

6.3.2. Localisation of cells undergoing apoptosis during normal development

TUNEL staining is a method for identifying cells dying by programmed cell death (PCD) based on one of its most important characteristics: DNA fragmentation, which accompanies PCD but not necrosis (Gavrieli et al., 1992; Wijsman et al., 1993). The distribution of TUNEL positive cells until stage 4 seems to be random (Fig.6.4 **a-h**), although there are no major differences between embryos in the overall number of cells undergoing apoptotic death at these stages. As development proceeds, the number of cells undergoing PCD appears to increase. Very few TUNEL-positive cells are seen at pre-primitive streak stages (Fig. 6.4 **a**); by stage 3 the number increases substantially but the distribution remains random (Fig. 6.4 **c-d**). TUNEL positive cells are found in all three germ layers at these stages (Fig.6.4 **g-h**). A reproducible pattern begins to become apparent from stage 4^+-5 in the epiblast (Fig.6.4 **i-j**), when apoptotic cells start to become concentrated as an arc surrounding the forming anterior neural plate and extending latero-caudally (Fig.6.4 **j-k**). This is also occasionally seen in embryos as young as stage 3^+ (Fig.6.4 **g**, **h**). Other locations also contain apoptotic cells patterns at these stages, but there is considerable randomness in the patterns observed.

As the embryo elongates antero-posteriorly and narrows medio-laterally (stages 5-14), the apoptotic arc expands caudally and almost converges posteriorly at the primitive streak (Fig.6.4 **k-l**), reminiscent of the patterns of expression of BMP4 and BMP7 (see Streit et al., 1998; Streit and Stern, 1999a). In some embryos at stages 6-8, the anterior arc is missing and this is replaced by an arc with its centre at the caudal tip of the embryonic axis (Fig.6.4 **l**). More frequently, from stage 9, TUNEL-positive cells are seen in the remnants of the primitive streak at the caudal tip of the axis (Fig.6.4 **m-n**). The dorsal midline of the neural tube shows an increase in the number of TUNEL positive cells in regions where the neural folds are fusing (Fig.6.4 l-**p**). In addition, there are two regions of concentrated apoptosis, one in the rhombencephalon (Fig.6.4 **o**) which later becomes restricted to rhombomeres 3 and 5 (Fig.6.4 **n-p;** see (Graham et al., 1993) and another in the olfactory region at stages 9 -14 (Fig.6.4 **n-q**) (see also (Yang et al., 1998)). Finally, at stage 13, a line of dying cells is seen at the edge of the

anterior intestinal portal at the level of the future sinus venosus (Fig.6.4 **q**). The arc of TUNEL staining is retained in the anteriormost epidermis and extraembryonic ectoderm in front of the head (Fig.6.4 **p, q**).

Hensey and Gautier (Hensey and Gautier, 1998) observed a similar arc of dying cells in *Xenopus* embryos at neurula stages, and interpreted it as being within the neural plate. To investigate the precise position of the arc in chick embryos, TUNEL staining was combined with in situ hybridisation for neural plate markers *Sox3* and *Sox2* (Fig.6.5), with the neural/epidermal border markers *Dlx5* and *Msx1* (prospective neural crest and pre-placodal regions; (McLarren et al., 2003) and with the early epidermal markers *GATA2* and *GATA3* (Fig.6.6). Comparison with neural plate markers reveals that there are indeed some apoptotic cells within the neural plate in some embryos, but the strongest and most consistent patterns do localise at the neural-epidermal border (Fig. 6.6 **c**, **d**). Compared with expression of border markers, apoptotic cells can clearly be seen both outside and inside of the border, but again the pattern is more concentrated in a region overlapping with the border as defined by *Msx1* and *Dlx5* expression (Fig.6.6 **a**, **d**, **h-i**, **k-l**). The correspondence between these regions becomes particularly evident during closure of the neural plate (stages 8-10), when PCD is particularly concentrated in the *Msx1/Dlx5*-expressing neural folds (Fig.6.4 **l** and Fig. 6.6 **i**, **l**) and prospective olfactory region (Fig.6.4 **n-q**). Finally, comparison with epidermal markers shows some overlap with the restricted epidermal region expressing *GATA2* and *GATA3*, but also some apoptosis both inside and outside this domain (Fig.6.6 **g-j**, **b-c**, **e-f**). In conclusion, the arc seems to be mainly centered at the neural-epidermal border but does extend both centrally and peripherally to overlap with the neural plate and the epidermal domains.

6.3.3. Expression of *Cas3* during early development

Apoptotic death is believed to be controlled by the activity of specific Caspases. To determine whether the localisation of TUNEL staining corresponds to areas of high caspase expression, we first examined the expression of *Caspase 3* (*Cas3*) (the most downstream caspase in the cascade; Assefa et al., 2004; Faleiro et al., 1997; Li et al., 1997) by whole mount in situ hybridisation. Virtually no expression could be detected in any region before stage 4 (Fig.6.7 **a**). At stage 4 (Fig.6.7 **b**), *Cas3* starts to be concentrated especially in the future neural plate, a pattern that becomes clearer as development proceeds. Higher levels of expression are detected in the lips of the primitive streak and especially in Hensen's node (Fig.6.7 **b-e**). However, as described for TUNEL staining, there is considerable variation among embryos of the same stage especially for the earliest stages. Unlike TUNEL staining, which is concentrated at the

neural/epidermal border, *Cas3* expression appears to be concentrated progressively to the neural plate itself, becoming strongest in the elevating neural folds at around stage 8 (Fig.6.7 **g**). This is especially evident after double-staining for TUNEL and *Cas3* (Fig. 6.7 **i-k**, compare 6.7 c and j), which reveal that TUNEL staining is elevated at the very edge of the *Cas3*-expressing domain.

6.3.4. Expression of *Cas9* during early development

A more upstream caspase was also examined, *Cas9* (Srinivasula et al., 1998). Its expression is weak and fairly ubiquitous, but from stage 5 a region of slightly upregulated expression is seen surrounding the neural plate, not unlike the domain revealed by TUNEL staining (Fig.6.8 **a-c**). Therefore the expression of *Cas9* appears to correlate more closely with TUNEL staining patterns than does *Cas3*.

6.3.5. Neural induction is accompanied by downregulation of PCD

Is the localisation of *Cas3* in the neural plate a result of neural induction? To test this, a graft of Hensen's node was placed into the area opaca and the resulting ectopic axis tested by in situ hybridisation for *Cas3*. *Cas3* expression in the secondary axis mirrors that in the normal neural plate Fig. 6.8 **d-e**). To test whether this can be induced by FGF, FGF8b beads were placed in the same location – weak induction of *Cas3* was seen in the vicinity of the beads after 5 hours (Fig.6.8 **f**). In cases when the induced axis falls close to or overlaps with the arc of TUNEL staining of the normal embryo, apoptosis sharply decreases in the induced region – in some cases the TUNEL staining region is displaced away from the induced neural plate, and becomes confined to a sharp border between the induced region and the host embryo (Fig. 6.8 **g**). Despite considerable variation from embryo to embryo both in normal development and after a node graft (Fig.6.4 and Fig.6.8 **g-i**), the absence of apoptosis from the area surrounding the grafted node within a few hours of the operation is a consistent feature of neural induction, and resembles the relatively lower levels of TUNEL staining within the normal neural plate than in surrounding regions.

6.3.6. Inhibitors

To test whether caspase activity is required for PCD and/or neural plate development, embryos were exposed to pharmacological inhibitors of caspases and the effects analysed by TUNEL staining. No decrease in the number of TUNEL positive cells was found (Fig.6.9 **a-f**). Surprisingly, inhibition of CAS3 activity seems to increase PCD rather than the reverse. In addition, in most cases the incidence of PCD was clearly higher in control embryos treated with the control inhibitor Z-FA-FMK (Fig.6.9 **b**, **e**).

Therefore, these results do not allow any firm conclusions to be reached about whether or not Caspase activity is required for either PCD or for the formation of the neural plate (based on in-situ hybridisation for *Sox2* - data not shown).

6.3.7. Can DAD1 rescue cells from PCD?

DAD1 was initially isolated (and named) as an antagonist of cell death (see Chapter 3). The present experiments suggested that *Dad1* is expressed in the newly-induced neural plate where it overlaps with caspase expression, perhaps preventing caspase-mediated cell death in this region. PCD is concentrated at the edge of the Cas3 domain, where *Dad1* expression may be lower than in the neural plate itself. To test the possibility that Dad1 is responsible for preventing cell death in the early stages of neural plate formation, we first investigated the relationship between *Dad1* expression and apoptosis. As more direct tests for the requirement of Dad1 function, we introduced a truncated inhibitory form of DAD1 (Fig. 6.11 **c**, f and i, l) (Makishima et al., 2000) as well as attempted to use morpholinos against *Dad1* (data not shown) and examined the effects by TUNEL staining.

Dad1 is only very weakly expressed at early stages; in addition the patterns of PCD vary considerably at stages 4-4^{+}. However, at stage 5-6 there seems to be a higher concentration of TUNEL positive cells in the neural/non neural border, areas of lower expression of *Dad1* (Fig.6.10). This correlation supports the notion that DAD1 may contribute to inhibit cell death within the young neural plate.

However, electroporation experiments did not succeed in demonstrating a clear role for DAD1 in apoptosis at these stages (Fig.6.11 **a-i**). There were no obvious differences between the effects of electroporation of either a negative control (empty pCAβ), or of *Dad1*, or of truncated *Dad1*, or of morpholino against *Dad1* or of a standard control morpholino (data not shown). Although cell counts were attempted, the variation between embryos receiving any one treatment (or among controls) was so great as to swamp any possible effects due to the inhibitory treatments.

6.3.8. Do *hcf* or *Ubll* affect PCD?

To test whether *hcf* is able to alter apoptosis, the two constructs used in Chapter 5 were tested. Cells undergoing PCD were identified by TUNEL staining and the electroporated cells visualised by antibody staining against GFP. In some cases, a construct encoding _-galactosidase (*lacZ*), rather than GFP, was used for the control side, while the experimental vector contained GFP as a marker. This helped in cases where it would otherwise have been difficult to distinguish cells electroporated with control and experimental vectors in the same embryo.

No obvious changes were found in the patterns of TUNEL staining when electroporated embryos were incubated for 6 hours (data not shown), or in embryos electroporated with the control pCAβ vector (Fig.6.12 **a**, **d**). However, after overnight incubation following *hcf* electroporation, an increase in number of PCD cells is seen in the electroporated area (Fig.6.12 **b**, **e**). This effect does not seem to be cell-autonomous as some TUNEL-positive cells are not stained by anti-GFP antibody. Furthermore, not all cells electroporated with *hcf* (either with or without the 5' untranslated sequence containing the iron regulatory sequence, IRE) are TUNEL-positive (Fig.6.12 **b**, **c**, **e**, **f**). Strikingly this effect is only seen in the ectoderm of the embryo proper and especially the in the neuroectoderm (Fig.6.12, compare regions marked by an arrow to those indicated by an arrow-head) suggesting that HcF has differential effects on apoptosis in different domains of the epiblast.

To test whether overexpression of *UbII* affects PCD, a *UbII* vector was electroporated as described above. Unlike what was found with *hcf* (above), no significant differences were seen in the number of TUNEL positive cells between embryos electroporated with control constructs (Fig.6.13 **a**-**c**), or with *UbII*, either after 6 hours of incubation (Fig. 6.13 **b**) or after overnight incubation (Fig.6.13 **c**).

Taken together, these results presented in this Chapter suggest that the regulation of PCD may indeed be important in the early stages of neural induction. Not only is the anti-apoptotic gene *Dad1* induced as a very early response to neural induction, but the pro-apoptotic genes *Caspase3* and *Caspase9* are also expressed in partly overlapping domains, with a border in the region where PCD becomes concentrated (the edge of the neural plate). Moreover, *hcf* overexpression increases apoptosis preferentially in the neural plate of early embryos. We also show that induction of a secondary axis by a graft of Hensen's node is accompanied not only by induction of several genes with pro- and anti-apoptotic activity, but also with an overall inhibition of cell death in the forming neural plate. These effects are especially prominent when the induced region is close to the host's neural plate and its border. In this case, PCD becomes strongly concentrated to a sharp line separating the host and induced domains.

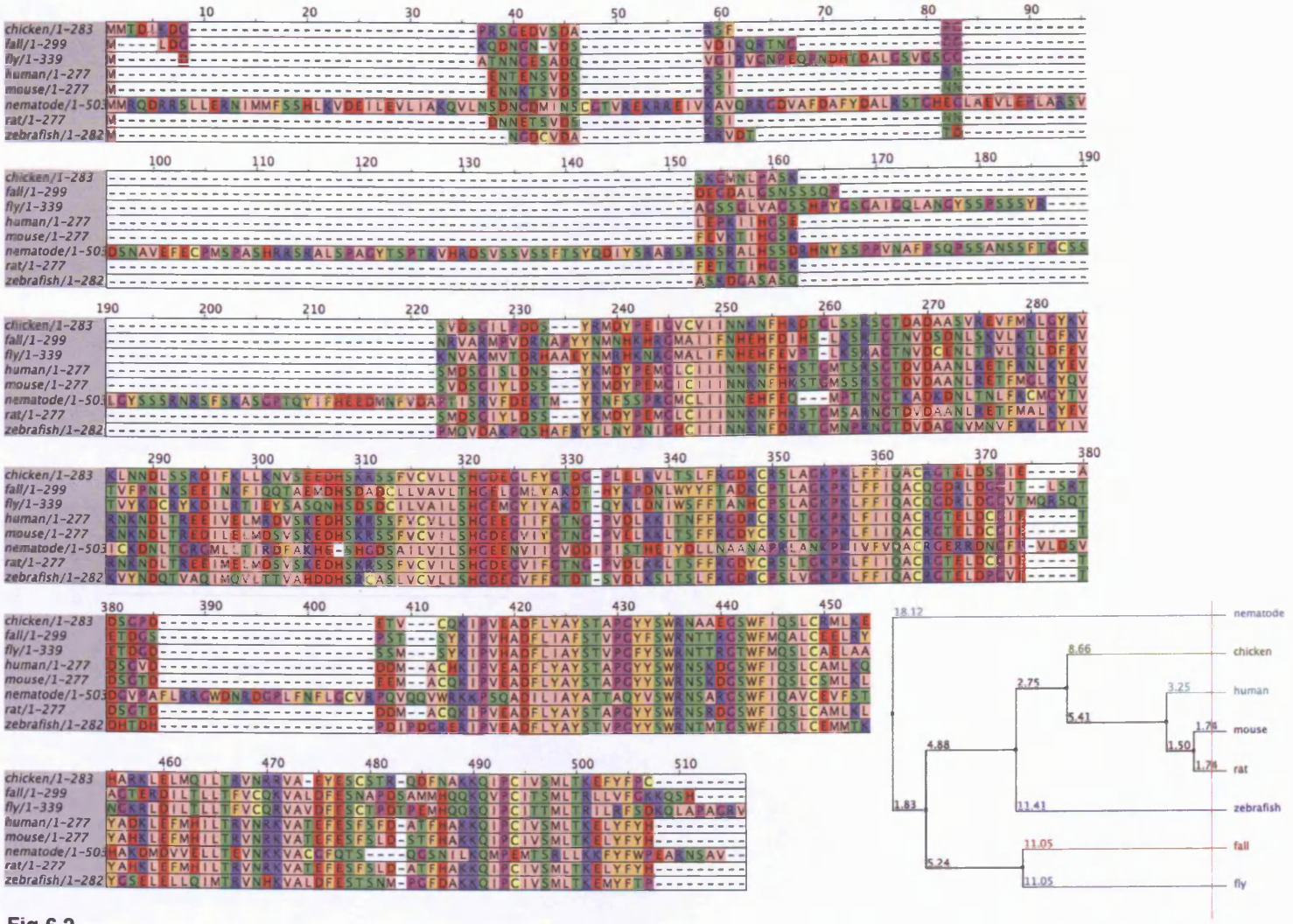

Fig.6.2

Alignment and Average Distance Tree of protein sequences of Caspase 3 from different organisms: chick (AAC32602), fall armyworm (AAE01643), fly (CAA72937), human (NP_004337), mouse (NP_033940), nematode (AAG42045), rat (NP_037054), zebrafish (NP_571952).

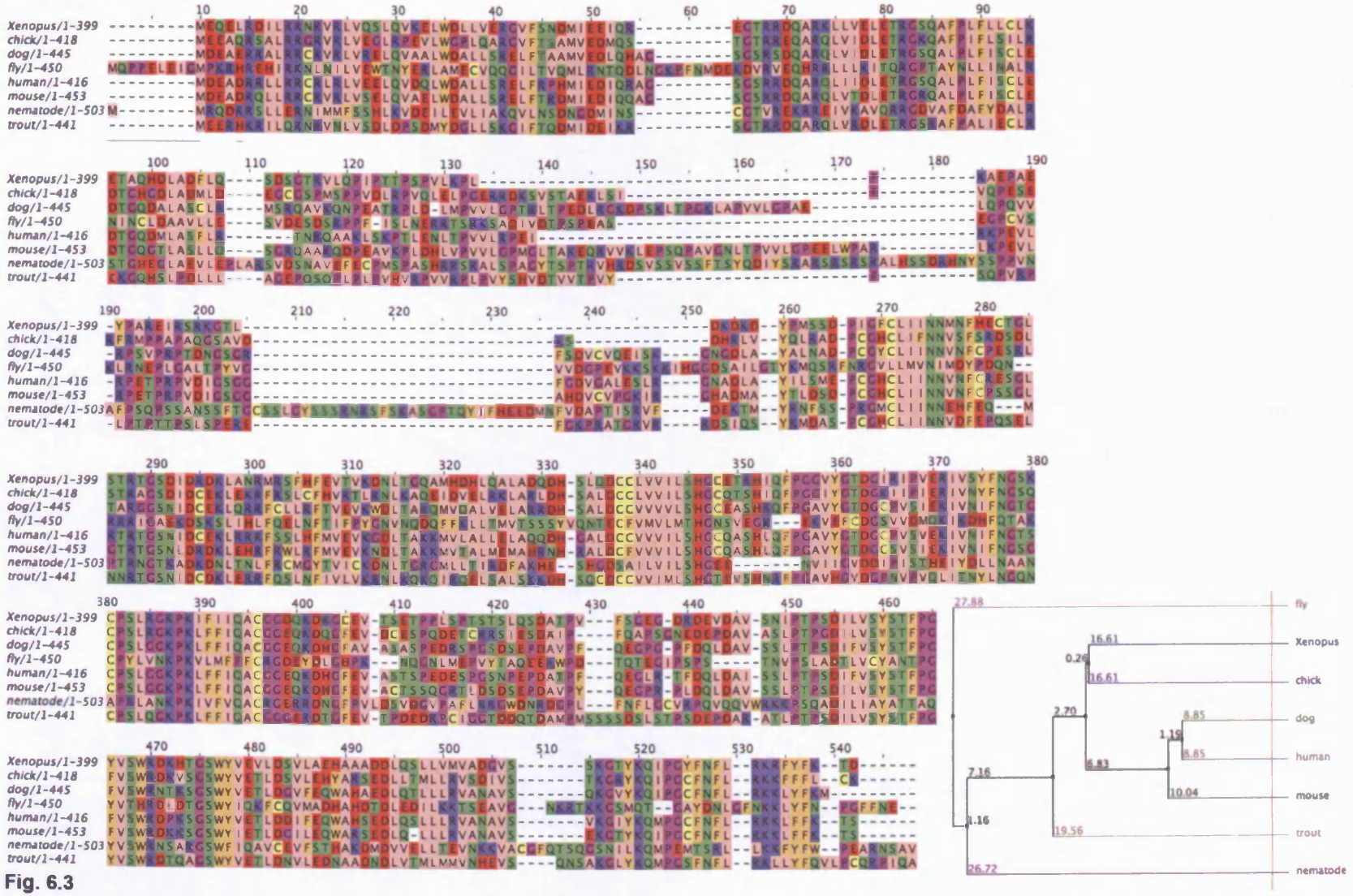

Fig. 6.3

Alignment and Average Distance Tree of protein sequences of Caspase 9 from different organisms: fly (CAB53565), Xenopus (BAA94750), chick (XP_424580), dog(NP_001026803), human (NP_004337), mouse (BAA86895), trout (AAY88917), nematode (AAG42045).

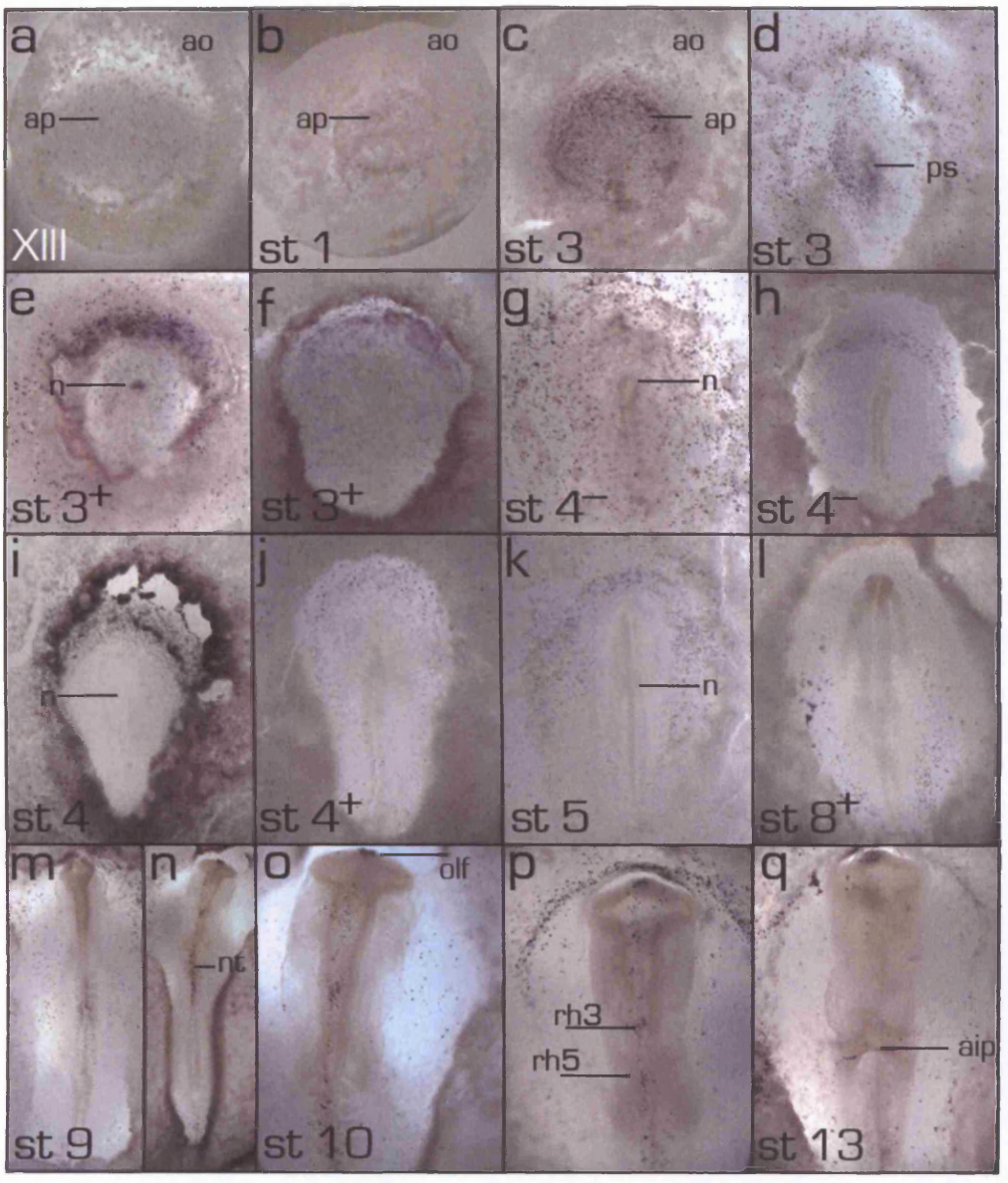

Fig. 6.4

TUNEL. The distribution of **TUNEL** positive cells during a normal early development in the pre-primitive streak (**a**) and at stages 1-12 (**b-q**).

The differences in the number and the position of T+ve cells between individual embryos at stages 3- 4^{+}; **h**: embryo shown in (**g**) after removal of the hypoblast; **o**: details: cephalic region, anterior somites and neural tube of the embryo shown in (**n**); **p**: the increased number of T+ve cells in the rhombomere 3 and 5 and olfactory region at stage 12 (dorsal view); **q**: ventral view at stage 13.

ap - area pellucida; **ao** - area opaca; **ps** - primitive streak; **n** - Hensen's node; **nt** - closing neural tube; **olf** - olfactory region; **rh3**, **rh5** - **rhombomere** 3, 5 and **aip** - anterior intestinal portal.

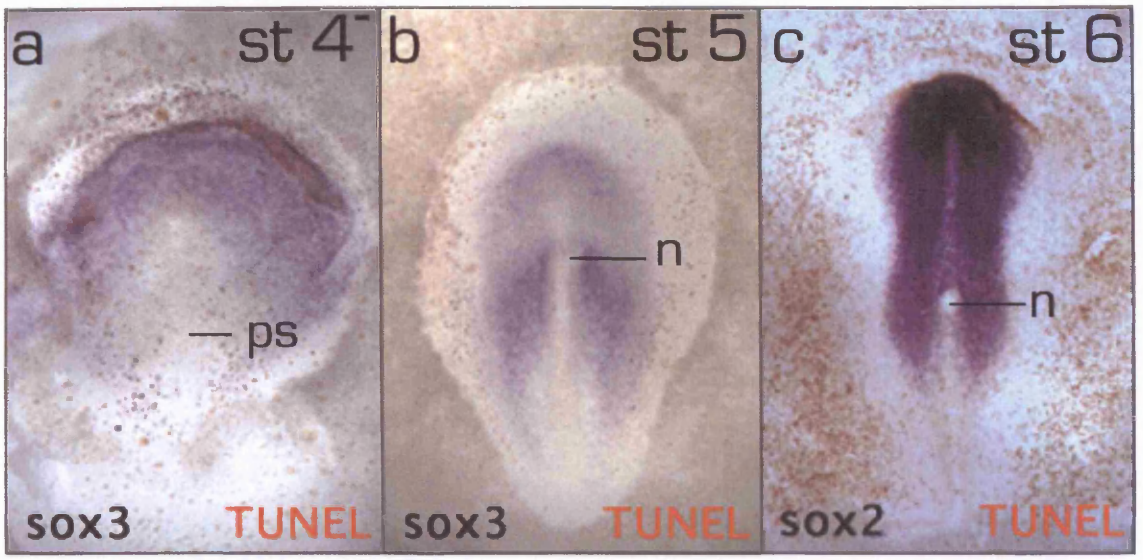

Fig. 6.5

Expression patterns of ***Sox3*** (**a-b**) and ***Sox2*** in dark purple (**c**) combined with **TUNEL** staining in brick-red at stages 4- (**a**), 5 (**b**) and 6 (**c**).

ps - primitive streak; **n** - Hensen's node.

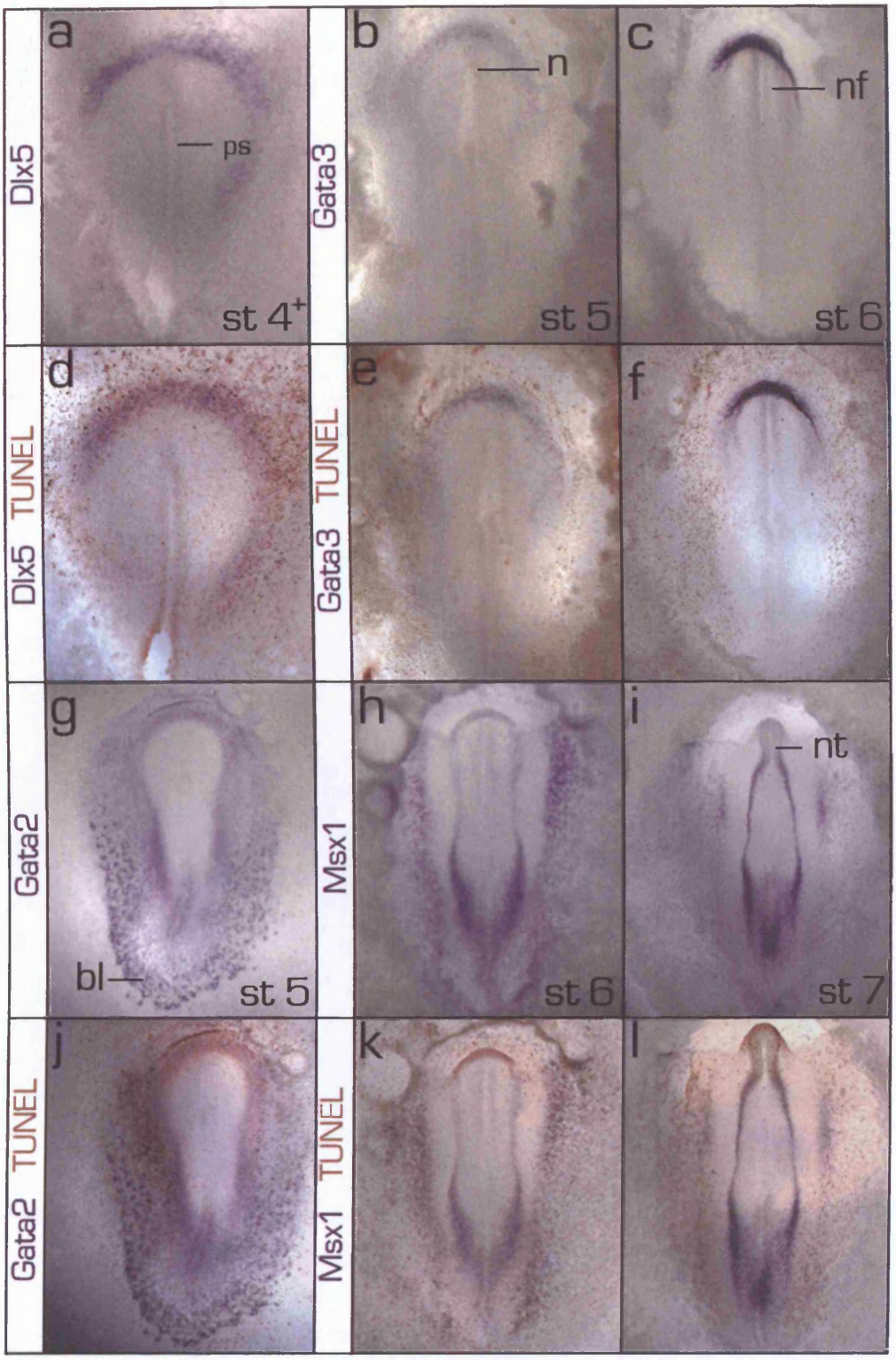

Fig. 6.6

Expression patterns of ***Dlx5*** (**a**, **d**), ***Gata3*** (**b-c**, **e-f**), ***Gata2*** (**g**, **f**) and ***Msx1*** (**b-c**, **e-f**) combined with TUNEL staining before (**a-c**, **g-i**) and anti-GFP antibody staining.

ps - primitive streak; **n** - Hensen's node; **nf** - elevated neural folds prior to the fusion to form the neural tube, **bl** - forming blood islands.

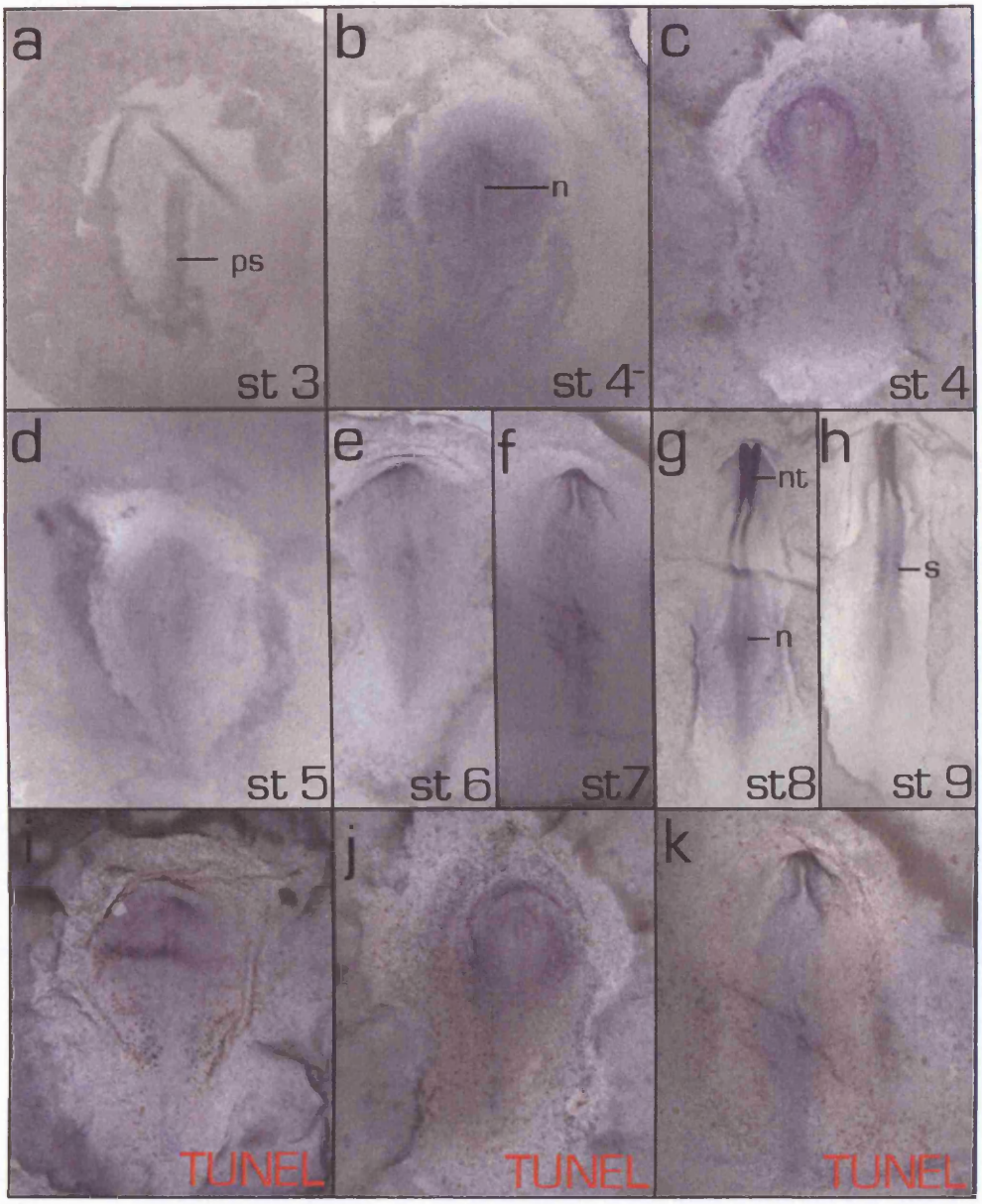

Fig. 6.7

Normal expression of chick ***Cas3*** during early development at stages 3 (**a**), 4- (**b**), 4(**c**), 5(**d**), 6(**e**), 7(**f**), 8(**g**) and 9(**h**). ***Cas3*** expression combined with **TUNEL** staining in dark brick-red at stags 4 (**I, j**) and 7(**k**) before (**c, f**) and after the anti-GFP antibody staining (**i-k**).

ps - primitive streak; **n** - Hensen's node; **nt** - closing neural tube; **s** - somites.

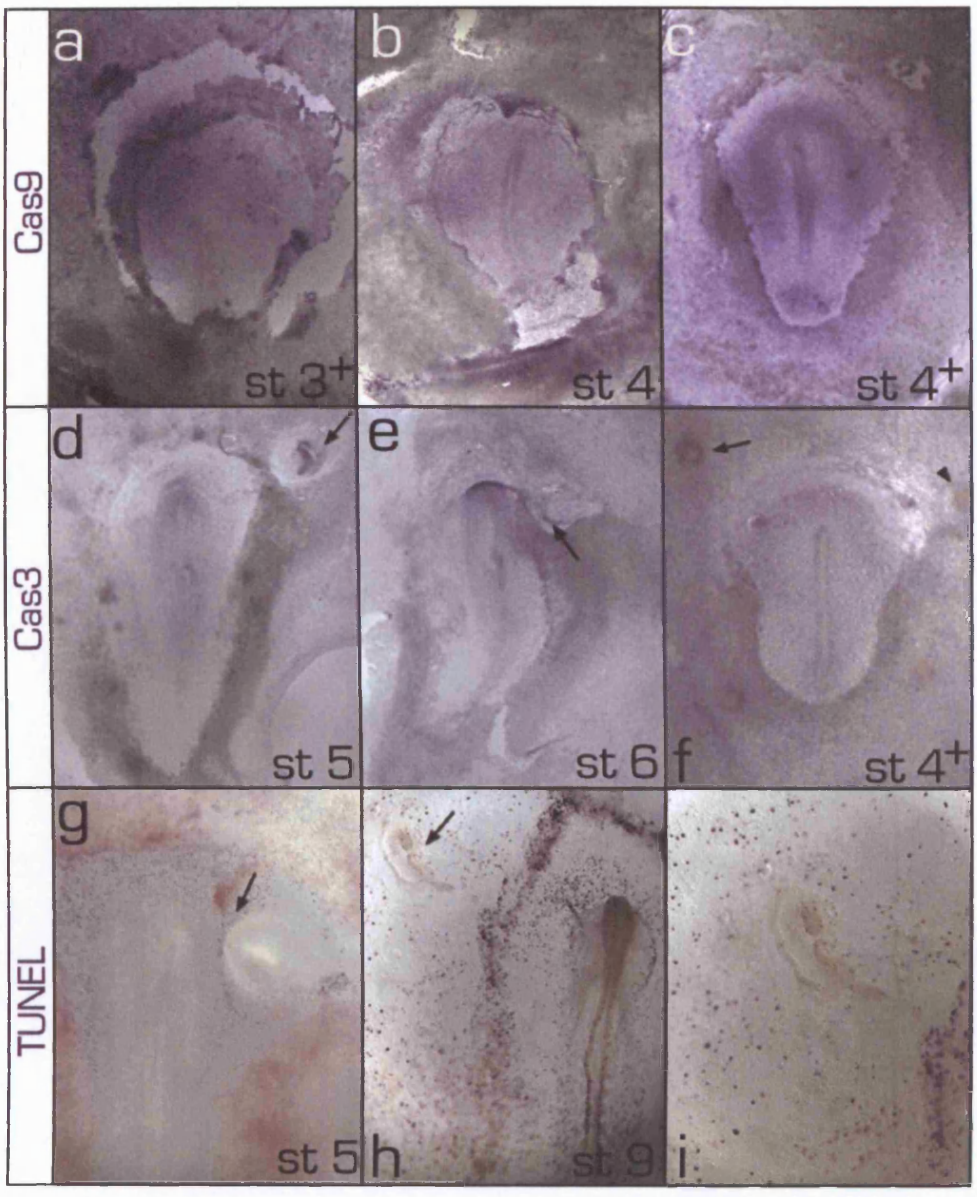

Fig. 6.8

Normal expression of chick ***Cas9*** during early development at stages 3^{+} (**a**), 4(**b**), 4(**c**). Expression patterns of ***Cas3*** in the induced secondary axis at stage 5 (**d**) and 6 (**e**); arrows indicate the similarities to the *Cas3* expression seen during normal development. **Induction** of ***Cas3*** expression in the area opaca **by FGF8b** secreting bead (indicated by arrow) after 5 hours; no induction by negative control (arrow head). TUNEL staining following graft of Hensen's node in the area opaca indicated by arrows, seen after 8 hours (**g**) and 18 hours (**h** and **i** - the detail of embryo seen in **h**).

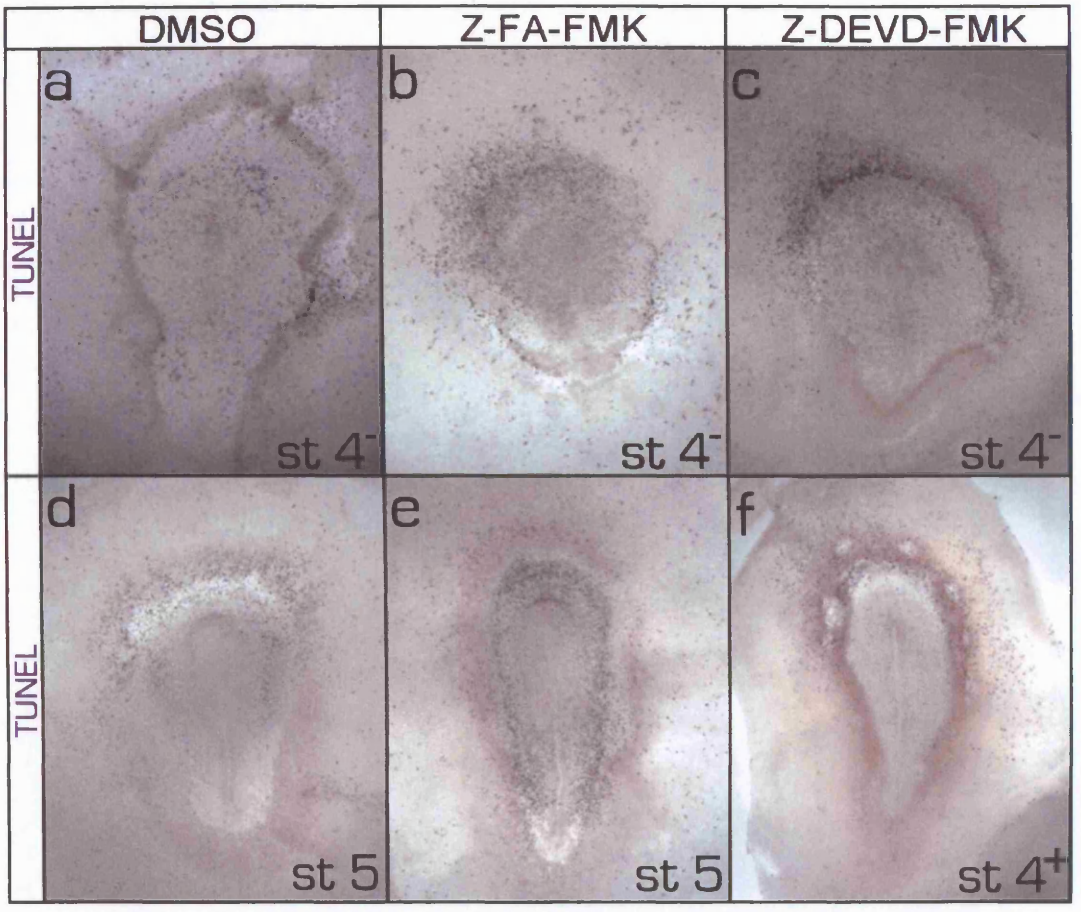

Fig. 6.9

TUNEL staining following 1 hour's exposure to 10μM solution of DMSO (a, d), negative control for caspase inhibition Z-FA-FMK (**b**, **e**) and **inhibitor of Caspase 3** Z-DEVD-FMK, following 5 hours (**a**-**c**) and 8 hours (**d**-**f**) incubation

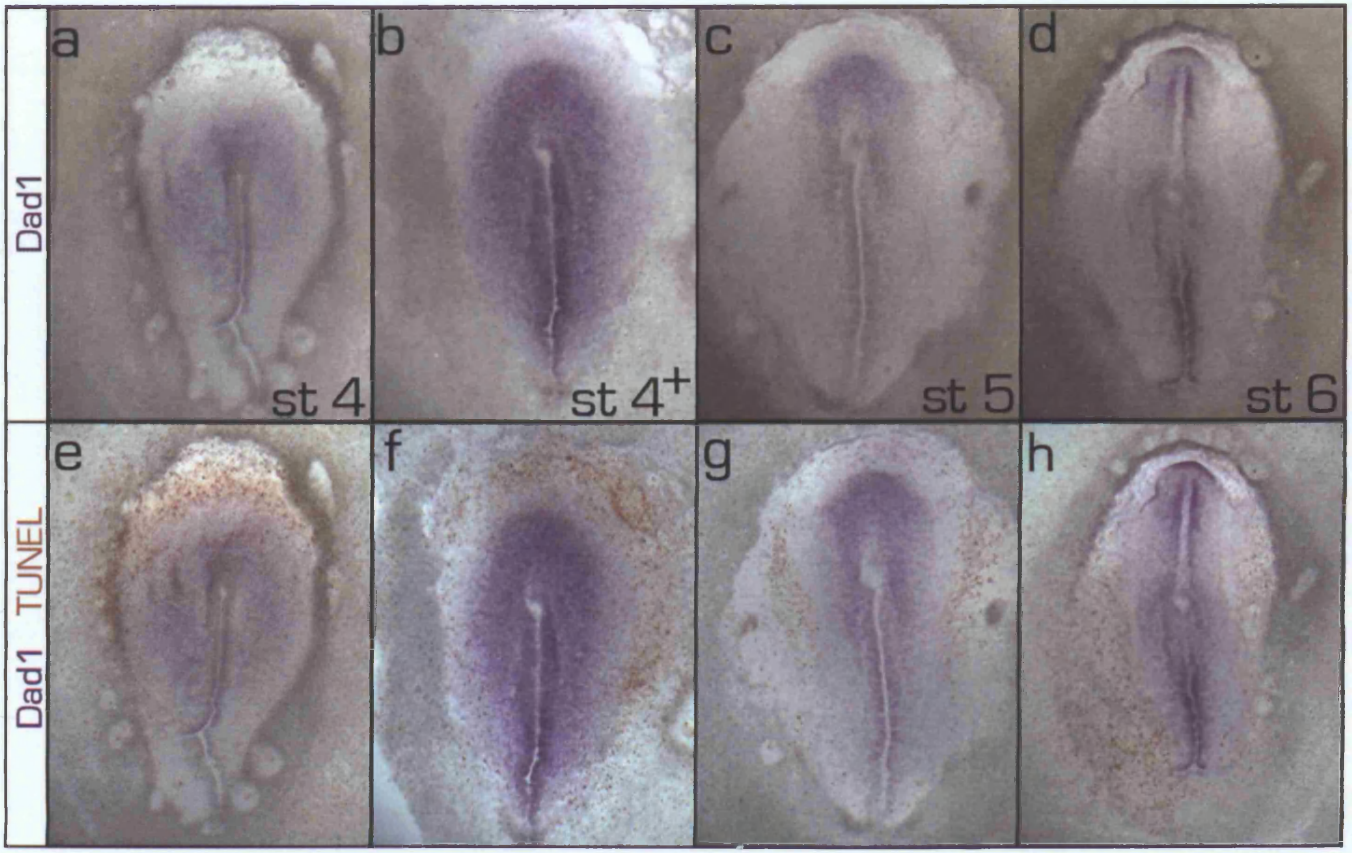

Fig. 6.10
Expression patterns of ***Dad1*** and **PCD** during early development.
Dad1 in dark purple before (**a-d**) and after **TUNEL** staining in brick-red (e-h).

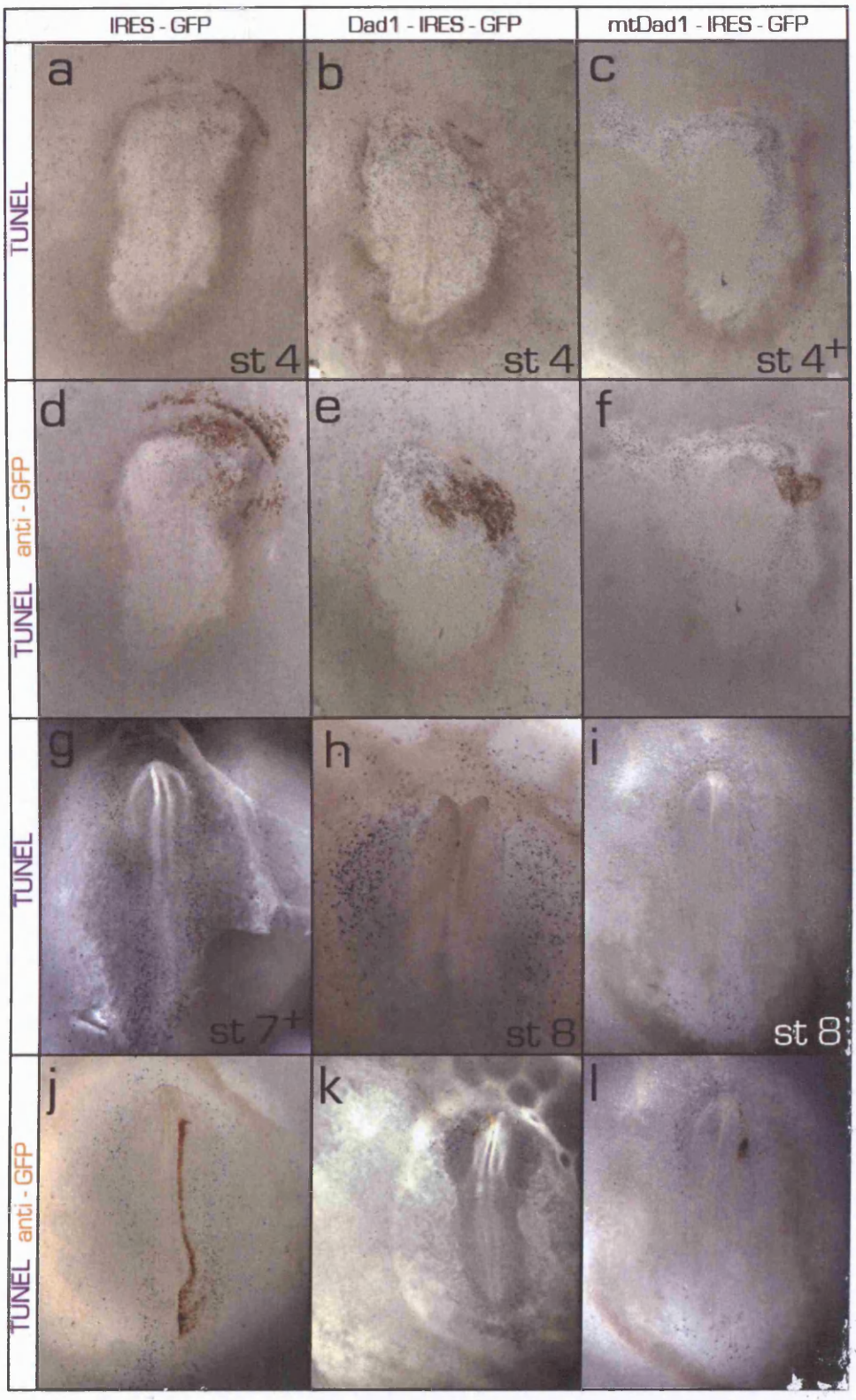

Fig. 6.11

Effects of **DAD1** electroporation on **PCD.**
The distribution of **TUNEL** positive cells (dark blue) following electroporation of a control, empty pCAβ vector (**a**, **d**, **g**, **j**), of **DAD1** (**b**, **e**, **h**, **k**) and of **DAD1 mutant** lacking the C-terminal 6 amino acids (c, f, i, l) is shown after 6 hours (**a-f**) or 12 hours incubation (**g-l**). **PCD** patterns are shown before (**a-c**, **g-i**) and after staining (brown) with the anti-GFP antibody (**d-f**, **j-l**).

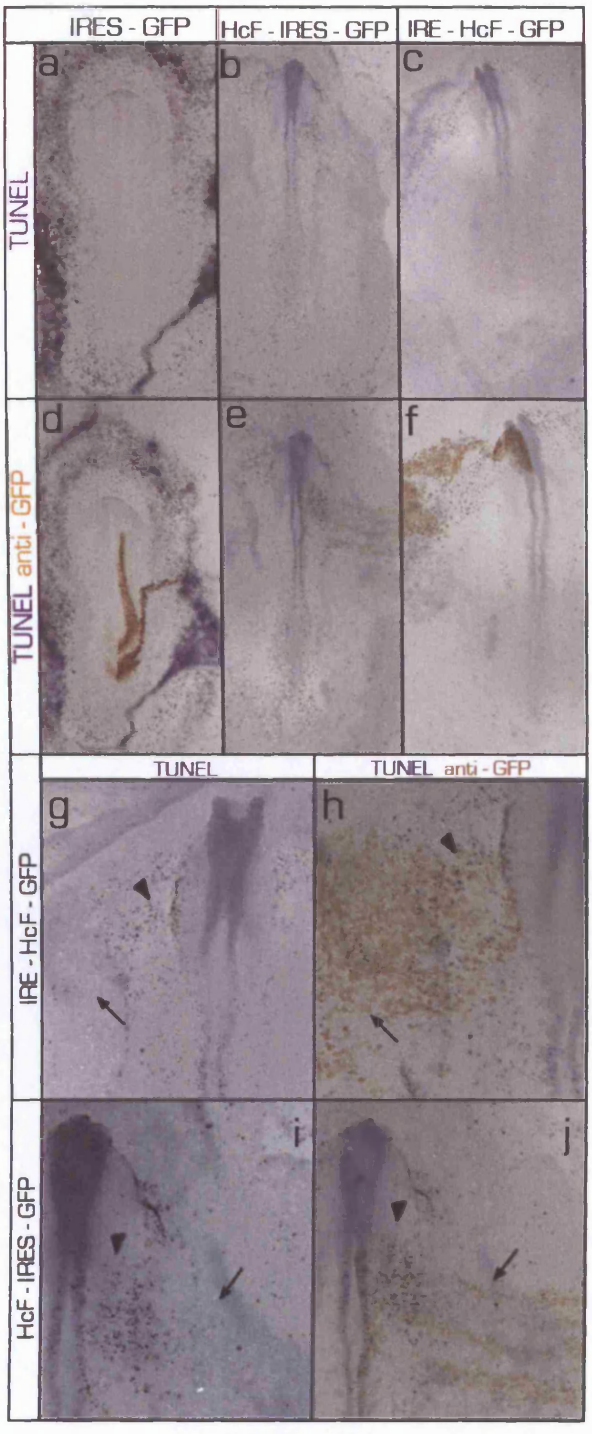

Fig. 6.12

Effects of **HCF** electroporation on **PCD.**

The distribution of **TUNEL** positive cells (dark blue) following electroporation of a control, empty pCAβ vector (a, d), of **HcF** (**b**, **e**, **i**, **j**) and of vector containing **HcF** with **IRE** (**c**, **f**, **g**, **h**) is shown before (**a-c**, **g**, **i**) and after (**d-f**, **h**, **j**) staining (brown) with the anti-GFP antibody; **g** and **h** are details of embryo shown in **b** and **e** panel. Arrow-heads indicate areas of increased PCD following electroporation of **HcF** with (g, h) or without IRE (I, j), while arrows point to not affected the regions.

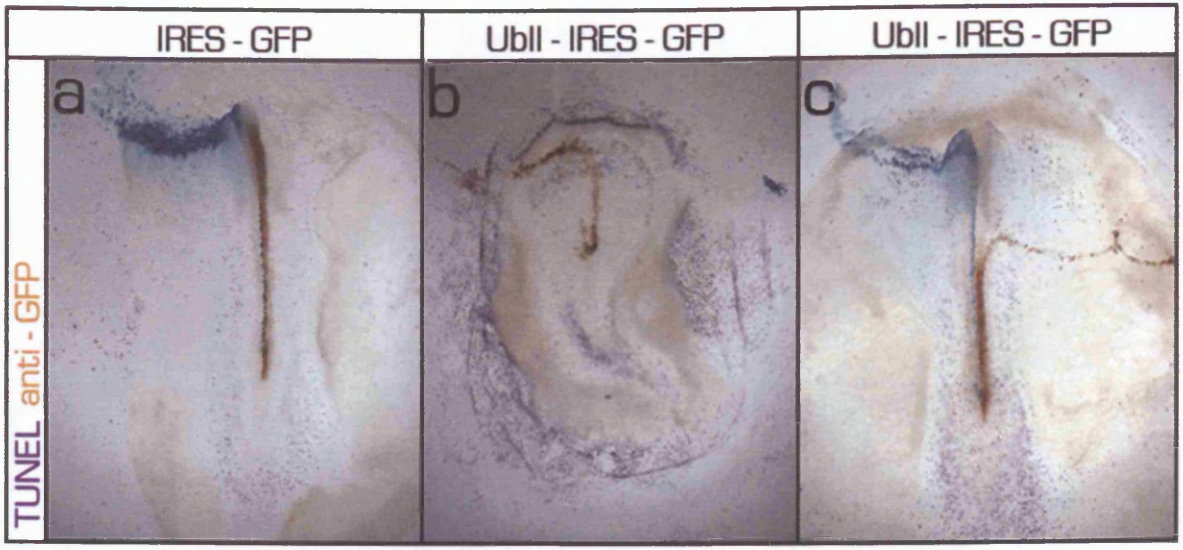

Fig. 6.13
Effects of **UbII** electroporation on **PCD**.
The distribution of **TUNEL** positive cells (dark blue) following electroporation of an empty **pCAB vector** expressing GFP (**a**) or **UbII** (**b-c**) with control empty **pCAB - lacZ vector** in the same embryo in order to allow quantification of experimental and control data after 6 (**b**) or 12 hours (**a**, **c**) following anti-GFP (brown) antibody staining and visualisation of Beta-galactosidase activity (turquoise)

6.4. Discussion

The patterns of apoptosis described in this study confirm some of the data for TUNEL staining previously described in the chick (Hirata and Hall, 2000; Sanders et al., 1997), and especially those from the group of Sanders. This group also reports some apparent randomness in the staining patterns, including observations such as increased PCD in the tip of the streak and left-right asymmetric patterns in a small number of embryos (Sanders et al., 1997) (see Fig.6.4 **d-e** in this thesis), suggesting that these patterns are a rare but nevertheless reproducible feature at early stages of chick development. Significant discrepancies are found when our data were compared to the other study on early embryos (Hirata and Hall, 2000); for example, the increased PCD in the posterior marginal zone and Koller's sickle ("embryonic shield", as described by Hirata) was not observed in any of more than 10 embryos stained at this stage (see Fig.6.4 **a**). Likewise, Hirata described the notochord as a site of increased PCD at stages 8-14 (Hirata and Hall, 2000), which was seen in only a few cases (6 out of more than 60 analyzed).

In *Xenopus,* although some of the figures of the studies of (Hensey and Gautier, 1998; Yeo and Gautier, 2003) look very similar to the results described in this thesis, the authors interpreted these as implying that the neuroectoderm is a region of elevated cell death, unlike the present study (and those of Sanders's laboratory; see above), which suggest that the neural plate is an area of decreased or even almost absent PCD (Sanders et al., 1997). At later stages of *Xenopus* development, increased PCD is seen in stripes of primary neurones, in the developing sensory placodes and then later in sensory organs and in the spinal cord (Hensey and Gautier, 1998). However, the patterns of PCD in *Xenopus* show even greater variability than in chick; for example only 67% of *Xenopus* embryos at neural plate stages (stage 13) and 52% of embryos at stage 37 contained more than 5 TUNEL cells per embryo (Hensey and Gautier, 1998). The same authors suggested that Pax6 might be an important regulator of PCD, as its expression overlaps with the patterns of PCD in *Xenopus* (Hensey and Gautier, 1998). However, this hypothesis was not tested experimentally. Blocking apoptosis by overexpression of human *Blc2* in *Xenopus* led to defects in neurogenesis; however, defects were also seen outside the neural plate, suggesting that a role of apoptosis is not exclusive to neural cells (Yeo and Gautier, 2004). It has been suggested (Hensey and Gautier, 1998; Merino et al., 1998) that one possible role for PCD in early neural plate development is to sharpen the boundaries between neural and non-neural territories. The present results, demonstrating progressively increasing numbers of dying cells primarily at the neural/non-neural border, support this suggestion.

Several secreted factors have been implicated in regulation of cell death in a non-cell-autonomous manner. They include BMPs and FGFs (Macias et al., 1996; Merino et al., 1998; Merino et al., 1999; Montero et al., 2001; Yokouchi et al., 1996) for the limb bud, and especially BMP4 as an effector for the localisation of apoptosis to rhombomeres 3 and 5, which has been suggested as an important mechanism to ensure that these rhombomeres do not produce neural crest cells (Graham et al., 1994; Jeffs et al., 1992).

Published data on PCD at early stages of development in other animal species is very incomplete. In mouse, TUNEL positive cells are scarce and randomly distributed (Sanders et al., 1997). In zebrafish, the only data on early PCD concern earlier (Negron and Lockshin, 2004; Yabu et al., 2001b) or later stages of development (Cole and Ross, 2001); however, for those stages at which it has been studied, the results correspond closely to the observations presented here for the chick at equivalent stages (from 5 somites) (Cole and Ross, 2001). It is also important to take into account that in lower vertebrates, which possess a clear mid-blastula transition (MBT), embryos appear to be incapable of undergoing apoptosis prior to this transition. This has been established in zebrafish (Ikegami et al., 1999; Negron and Lockshin, 2004), *Xenopus* (Hensey and Gautier, 1997) and sea urchin (Mizoguchi et al., 2000). However since MBT occurs at the mid-blastula stage (equivalent perhaps to stage XII-XIII in the chick), and since at these stages PCD is random as well as infrequent in the chick, this is not a particularly significant difference.

At gastrulation stages of the zebrafish, cells undergoing apoptosis have only very low levels of active caspase3 (Negron and Lockshin, 2004; Yabu et al., 2001a; Yabu et al., 2001b), despite *Cas3* being present in the pool of maternal factors as well as being expressed during gastrulation and later in development (Yabu et al., 2001a). The patterns of *Cas3* expression in zebrafish (Yabu et al., 2001a) are comparable to those seen in our study of early chick development, including the low levels of expression (Yabu et al., 2001a). Nether the less, the strong similarity of *Cas3* expression and of PCD distribution in zebrafish and chick strongly suggest that they are causally linked and that their functions have been conserved during vertebrate evolution.

It is unfortunately impossible to interpret the present results using Caspase antagonists because it was not possible to demonstrate that the antagonists actually blocked Caspase3 activity. Given more time, it would have been interesting to establish first whether caspase3 is active at gastrula and early neurula stages of normal chick development, for example using the fluorescent substrate Ac-DEVD-AFC for caspase3. Then, we could have determined the concentrations at which this activity can be

blocked by the inhibitors Z-DEVD-FMK (specific for Caspase 3), Z-VAD(OMe)-FMK (for all Caspases) in comparison with the negative control Z-FA-FMK. Finally the effects of caspase activity inhibition on the incidence of TUNEL staining and on expression of neural markers would have been tested. It might also have been interesting to test whether overexpression of *Cas3* is sufficient to cause PCD, as has been done in zebrafish (Yabu et al., 2001b).

The expression patterns of *Cas9* and *Cas3* overlap significantly; *Cas9* is expressed more ubiquitously but at low levels. However there is a region of increased *Cas9* expression that surrounds the prospective neural plate and which seems to correspond to the main sites of cells undergoing PCD. *Dad1* appears to be located within this domain, raising the interesting possibility that a Dad1 protects cells against apoptosis within the newly induced neural plate, while a narrow region expressing *Cas3* and *Cas9* but devoid of *Dad1* ensures that PCD becomes restricted to the edge of the neural plate (prospective neural crest and placode territory).

It has been reported that the "initiator" Caspase9 is auto-activated by Apaf1 mediated oligomerisation (Srinivasula et al., 1998) before it activates the "executor" Caspase3 (Hu et al., 1999; Saleh et al., 1999; Zou et al., 1999). In addition an amplification feedback loop between Caspase9 and Caspase3 has been suggested (Fujita et al., 2001; Slee et al., 1999). It has been proposed that Caspase3 is not required for autoactivation of Caspase9 but is necessary for its full activation via this amplification loop. The results presented in this study are consistent with a Caspase9-Caspase3 amplification loop around the time of neural induction The results of Caspase3 activity assay already suggested for inhibition experiments and data gathered from inhibition experiments themselves could provide further evidence for the existence of such co-operation between these two caspases in the initiation and execution of PCD in early chick development.

The partial overlap between the expression domains of *Dad1* and that of *Cas3* around the time of neural induction, leaving a border of *Cas3* expression free of *Dad1* (see above) would be worth investigating in the context of a possible link between DAD1, the activation of Caspase3 (possible amplification loop) and apoptosis. An attempt to investigate this was made using morpholino antisense oligonucleotides against *Dad1*, electroporated into the early neural plate (where *Dad1* is normally expressed). Unfortunately these experiments did not show the expected increase in PCD. However, it was not possible to confirm that the morpholino succeeded in

lowering the levels of DAD1 protein because the available antibody against DAD1 does not recognise the chick protein (see Chapter 3). In addition it has been reported that 6 hours are necessary for complete turnover of intracellular DAD1 protein when its synthesis is prevented (Makishima et al., 2000). This finding suggests that for complete downregulation of DAD1, it may be necessary to introduce the morpholino at an earlier stage (stage 3 or even earlier, rather than $3^{+}/4^{-}$ as done here).

Similarly, the lack of effect on PCD of experiments in which the truncated form of *Dad1* was electroporated does not help to address the question of whether the last 4 amino acids are crucial for the antiapoptotic action of DAD1, as previously suggested (Makishima et al., 2000). One reason may be that the mutated DAD1 is not truly dominant-negative, and/or that insufficient levels of the mutated version are expressed to interfere with endogenous, functional DAD1 protein in the electroporated cells. We also were not able to demonstrate clearly a decrease in the number of apoptotic cells following ectopic expression of *Dad1*. However in other studies, DAD1 was only able to rescue around 20% of cells undergoing apoptosis in *C. elegans* (Sugimoto et al., 1995), where the number of cells undergoing PCD is much more predictable than in the chick. The great variability in the number of TUNEL-positive cells in the chick would make it very difficult to detect such weak effects. Therefore it cannot be excluded that ectopic *Dad1* might have rescued a subset of cells from apoptosis.

Apart from the well-documented connection between Dad1 and programmed cell death, there are also some isolated reports suggesting involvement of polyubiquitin and ferritin in the regulation of apoptosis. For example, a link between PCD and increased expression of polyubiquitin has been made in the intersegmental muscles of the tobacco hawkmoth (Haas et al., 1995; Schwartz et al., 1990). However in vertebrates, although polybiquitin is upregulated during apoptosis in non-neural cell cultures (Cai et al., 2004; Delic et al., 1993; Kugawa and Aoki, 2004; Young et al., 1998) this was not the case for embryonic sympathetic neurons undergoing PCD as a result of NGF deprivation (D'Mello and Galli, 1993). These findings suggest, not unexpectedly, that although polyubiquitin may have some role in PCD, it is not the only regulator of apoptosis. In the present experiments, our results did not reveal changes in apoptotic patterns after either overexpression or ectopic expression of UbII, suggesting that upregulation of ubiquitin is not sufficient to induce PCD during early chick development.

As for polyubuiquitin, HCF can have both pro- and anti-apoptotic functions. It has been reported to protect nuclear proteins in the chick cornea from the effects of oxidative stress (Cai et al., 1997). Cytoplasmic HCF is also involved in protection against PCD in hepatocytes and endothelial cells in response to some apoptotic inducers (Theil, 1987 662, Cairo, 1995# 663). Up-regulation of heavy chain ferritin during B-lymphocyte differentiation reduces free iron levels and also increases their resistance to oxidative damage (Cozzi et al., 2000 648; Epsztejn et al., 1999 660), whilst down-regulation increases free iron, is associated with increased apoptosis (Yang et al., 2002) and is also critical for cell transformation by c-MYC in certain types of tumour cells (Wu et al., 1999). In all of these studies, altered levels of HCF resulted in changed intracellular free iron concentrations, and HCF was proposed to be responsible for the pro- or anti-apoptotic action of ferritin. Our experiments revealed an increase in the incidence of PCD (especially in the prospective neuroectoderm) following overexpression of *Hcf* (either with or without the 5' untranslated sequence containing the iron regulatory sequence, IRE). The results are especially apparent after prolonged incubation, consistent with a pro-apoptotic function of HCF in these cells. It is worth pointing out that the effects were not cell autonomous, as some cells that had apparently not been electroporated with the plasmid displayed TUNEL staining, suggesting that the link between HCF and apoptosis might be indirect, via secreted factors.

CHAPTER 7:

General discussion and conclusions

As outlined in Chapter 1, studies mainly performed in the chick embryo have cast some doubt on the "default model" as a sufficient explanation for neural induction. The default model predicts that inhibition of BMP signalling in ectodermal cells should be sufficient to assign neural fates to these cells. However, ectopic expression of BMP antagonists, even in combination with other factors, turned out to be unable to induce competent epiblast to acquire expression of neural markers in a variety of experiments (Linker and Stern, 2004; Streit et al., 2000). Hensen's node grafts followed by removal of the graft at various time points revealed that while 13 hours of contact with the graft are required for stable induction of a neural plate, some genes such as *Sox3* are induced after 3-5 hours, yet this induction is transient if the node is removed (Albazerchi and Stern, 2006; Streit et al., 2000). If epiblast is exposed to a node for 5 hours and the node then removed and replaced by a graft of cells secreting a BMP antagonist, then the latter is able to stabilise the otherwise transient expression of *Sox3* (Albazerchi and Stern, 2006; Streit et al., 2000), although even this combination is insufficient to induce later markers like *Sox2* or the formation of a morphological neural plate. These findings suggested that 5 hours of exposure to signals from the organiser are required before epiblast cells become sensitive to BMP signalling or its inhibition. To begin to identify these upstream signals, it was essential first to establish the molecular differences in cells that have been exposed to an organiser for 5 hours (which should now be sensitive to BMP antagonists) from those that have not. To this end, a differential screen was conducted between one small group of cells that had been in contact with a grafted node for exactly 5 hours and another, otherwise identical group of cells, which had not been adjacent to a grafted node (Sheng et al., 2003; Streit et al., 2000). Differential screening between the cDNA libraries made from these two cell populations uncovered 15 genes with differential expression. Of these, most encoded novel predicted proteins, including *ERNI* (Streit et al., 2000) and *Churchill* (Sheng et al., 2003), both of which revealed important and previously unappreciated aspects of the early stages of neural induction.

The early onset of expression of *ERNI* both in normal embryos and after a node graft, as well as correspondence between its expression and that of FGF8, suggested that FGF8 might represent at least one upstream factor required before cells become sensitive to BMP inhibition. Indeed, FGF8 is sufficient to induce both *ERNI* and *Sox3*, and it does so in a transient manner (Albazerchi and Stern, 2006; Streit et al., 2000). Moreover, inhibition of FGF signalling abolishes the induction of both of these genes as well as later steps of neural plate development, showing that FGF signalling is required for neural induction. Last, exposure of epiblast to FGF8 followed by a graft of Chordin-secreting cells is able to mimic the effects of exposure to a node for 5 hours followed by

Chordin: *Sox3* expression is induced and maintained (Albazerchi and Stern, 2006; Streit et al., 2000). As yet we know nothing about the possible roles of ERNI in neural induction, except that it is also expressed in chick embryonic stem cells (Acloque et al., 2001).

Churchill turned out to be just as informative on the early steps of neural induction. It is normally expressed in the prospective neural plate starting at stage 4/4+ (just before the onset of *Sox2* expression) and is also induced by a node graft and by FGF8, but more slowly than *ERNI* and *Sox3*: 4-5 hours' exposure to either stimulus are required to induce *Churchill*. Paradoxically, although *Churchill* expression is induced by FGF8, experiments in both chick and *Xenopus* revealed that its activity blocks "immediate-early" effects of FGF signalling in mesoderm induction, such as expression of the T-box genes *Brachyury* and *Tbx6L* (Sheng et al., 2003). The timing of this activity and the onset of expression of *Churchill* correlate very well with the time at which epiblast cells adjacent to the anterior end of the primitive streak cease to ingress through the streak to form the deep layers and instead remain on the outside to contribute to the neural plate. It was therefore proposed that an important role of Churchill is to ensure that some cells remain on the surface of the embryo, available to generate a neural plate. Importantly, this study revealed that neural induction involves not just a decision between neural and epidermal fates, but also between neural and mesendodermal fates (Sheng et al., 2003). Last, it was shown that *Churchill* acts by inducing the target *Sip1* (Smad-interacting Protein 1), originally isolated from a 2-hybrid screen for binding partners of the BMP effector Smad1, and which had been shown to inhibit *Brachyury* in *Xenopus* (Postigo et al., 2003). Moreover, Sip1 only binds to Smad1 when the latter is phosphorylated (Postigo et al., 2003), suggesting that Sip1 could act as a sensor for the BMP signalling status of the cell. This provides an attractive explanation for the original observation that epiblast cells become sensitive to BMP signalling after 5 hours' exposure to FGF or to a grafted node (Sheng et al., 2003).

Of the remaining genes isolated from the screen, only 3 turned out to encode known products: Heavy Chain Ferritin (*Hcf*), Polyubiquitin (*Ubil*) and Defender against Apoptotic cell Death (*Dad1*). Since all three of these genes had been implicated as either pro- or anti-apoptotic factors in other contexts, this raised the interesting possibility that the regulation of programmed cell death could play a role in the early stages of neural induction. This study was designed to answer the questions of whether apoptosis is connected with these stages of neural induction in the chick, as well as to study the possible involvement of these three genes in both processes.

The original design of the screen aimed to identify genes induced (or repressed) by a grafted node within 5 hours' exposure to the graft. In the case of induced genes, if

these play a role in the normal process of neural plate development, then they should normally be expressed in the prospective neural plate at some early stage in development corresponding to when cells are receiving the signals required upstream of BMP inhibition. Therefore an important criterion for the significance of any gene found to be upregulated by a node graft within 5 hours is that it should be expressed in the prospective neural plate of the early embryo.

In this study we demonstrate that *Dad1* and *UbII* are indeed induced within 5 hours in response to a node graft: *Dad1* and *UbII* are induced after 3-4 hours. The exact timing of *hcf* induction could not be determined, as the normal expression patterns obscured the results. Importantly, all three are expressed in the neural plate around the time of neural induction (stages 3-5). However, misexpression and preliminary loss-of-function experiments of different types were unable to demonstrate either an essential role of any of these three genes in the process of neural induction, or sufficiency of any of them to cause induction of other early neural markers such as *Sox3*, *Sox2* or other genes identified from the screen.

Programmed cell death (PCD), has been considered an important and necessary part of normal organism development (Jacobson et al., 1997). A number of mechanisms implicated in the regulation of PCD have been identified and some processes taking place during PCD are understood in great detail. These data came from whole spectrum of animal models (Riedl and Shi, 2004; Vaux, 1993). However, the majority of these published analyses cover later stages of embryogenesis.

Here we conducted a detailed study of apoptosis at very early stages of chick development and the results are correlated with neural induction and the early stages of neural plate development. An "arc" shape region where apoptotic cells become concentrated was discovered to overlap, or even coincide with the prospective border between neural and epidermal territories. Although PCD is not restricted to this domain, the incidence of apoptotic cells is especially low within the neural plate.

Using double in situ hybridisation we reveal an interesting correspondence between the area of increased PCD with a region where 3 genes already implicated in the execution of PCD show complementary expression: *Cas3*, *Cas9* and *Dad1.* The former two are involved in the execution of cell death while the latter has anti-apoptotic functions. Interestingly, it appears that Dad1 is expressed within the neural plate but in a slightly smaller domain than the Caspases, leaving a narrow border where the latter are expressed but the anti-apoptotic factor is absent. This appears to correspond to the position of increased cell death at the border of the neural plate. Our data are also consistent with previous proposals of a feedback amplification loop between Caspase3 and Caspase9 (Fujita et al., 2001; Slee et al., 1999), and *Dad1* could be involved in the

regulation of this process. However assays of Caspase3 activity will be required to test this directly as well as successful downreguation of *Dad1*. Alternatively overexpression of *Cas3* and/or *Cas9* could be conducted in the area presumed to be protected by *Dad1* and outside of its domain. It should also be possible to determine whether the N-linked glycosylating activity of Dad1 is required for its anti-apoptotic functions using a *Dad1* construct lacking the domain required for glycosylation, as has been done in other systems (*tsBN7* mutation in BHK21 hamster cells Makishima et al., 2000).

The expression pattern of Caspase3 in the early neural plate is consistent with the idea that it may play roles other than as an executor of apoptosis during early development of the nervous system. Interestingly, our results raise the possibility that *Caspase3* (perhaps also *Caspase9*) are themselves "early response genes to neural induction": the former is induced by FGF8b and most probably also by node within 5 hours, along with *Dad1* and *UbII*.

In this study we demonstrate that overexpression of *hcf* increases the incidence of PCD, especially in the neuroectoderm, while it has almost no effect in other regions. Based on published reports (Cozzi et al., 2000; Epsztejn et al., 1999; Wu et al., 1999; Yang et al., 2002) that *hcf* can alter the levels of intracellular free iron, our data suggest that iron imbalance (most likely depletion) can be detrimental for neuroectodermal cells. We also observed that this process is not cell autonomous and probably involves a secreted factor. Taken together, our findings suggest that the regulation of apoptosis may indeed be important for the early steps of neural induction in the chick.

REFERENCES

Abriel, H. and Staub, O. (2005). Ubiquitylation of ion channels. *Physiology (Bethesda).* **20**, 398-407.

Acloque, H., Risson, V., Birot, A. M., Kunita, R., Pain, B. and Samarut, J. (2001). Identification of a new gene family specifically expressed in chicken embryonic stem cells and early embryo. *Mech Dev.* **103**, 79-91.

Agell, N. and Mezquita, C. (1988). Cellular content of ubiquitin and formation of ubiquitin conjugates during chicken spermatogenesis. *Biochem J.* **250**, 883-9.

Ahmad, M., Srinivasula, S. M., Wang, L., Litwack, G., Fernandes-Alnemri, T. and Alnemri, E. S. (1997). Spodoptera frugiperda caspase-1, a novel insect death protease that cleaves the nuclear immunophilin FKBP46, is the target of the baculovirus antiapoptotic protein p35. *J Biol Chem.* **272**, 1421-4.

Albazerchi, A. and Stern, C. D. (2006). A role for the hypoblast (AVE) in the initiation of neural induction, independent of its ability to position the primitive streak. *Dev Biol* **in press**, available online 30 August 2006.

Aleo, E., Henderson, C. J., Fontanini, A., Solazzo, B. and Brancolini, C. (2006). Identification of new compounds that trigger apoptosome-independent caspase activation and apoptosis. *Cancer Res.* **66**, 9235-44.

An, J. Y., Seo, J. W., Tasaki, T., Lee, M. J., Varshavsky, A. and Kwon, Y. T. (2006). Impaired neurogenesis and cardiovascular development in mice lacking the E3 ubiquitin ligases UBR1 and UBR2 of the N-end rule pathway. *Proc Natl Acad Sci U S A.* **103**, 6212-7. Epub 2006 Apr 10.

Andersen, M. W., Ballal, N. R., Goldknopf, I. L. and Busch, H. (1981). Protein A24 lyase activity in nucleoli of thioacetamide-treated rat liver releases histone 2A and ubiquitin from conjugated protein A24. *Biochemistry.* **20**, 1100-4.

Andree, B., Duprez, D., Vorbusch, B., Arnold, H. H. and Brand, T. (1998). BMP-2 induces ectopic expression of cardiac lineage markers and interferes with somite formation in chicken embryos. *Mech Dev.* **70**, 119-31.

Assefa, Z., Bultynck, G., Szlufcik, K., Nadif Kasri, N., Vermassen, E., Goris, J., Missiaen, L., Callewaert, G., Parys, J. B. and De Smedt, H. (2004). Caspase-3-induced truncation of type 1 inositol trisphosphate receptor accelerates apoptotic cell death and induces inositol trisphosphate-independent calcium release during apoptosis. *J Biol Chem.* **279**, 43227-36. Epub 2004 Jul 28.

Azevedo, C., Santos-Rosa, M. J. and Shirasu, K. (2001). The U-box protein family in plants. *Trends Plant Sci.* **6**, 354-8.

Bachmair, A., Finley, D. and Varshavsky, A. (1986). In vivo half-life of a protein is a function of its amino-terminal residue. *Science.* **234**, 179-86.

Bachvarova, R. F., Skromne, I. and Stern, C. D. (1998). Induction of primitive streak and Hensen's node by the posterior marginal zone in the early chick embryo. *Development.* **125**, 3521-34.

Baker, R. T. and Board, P. G. (1987). The human ubiquitin gene family: structure of a gene and pseudogenes from the Ub B subfamily. *Nucleic Acids Res.* **15**, 443-63.

Bancroft, M. and Bellairs, R. (1974). The onset of differentiation in the epiblast of the chick blastoderm (SEM and TEM). *Cell Tissue Res.* **155**, 399-418.

Bao, Q. and Shi, Y. (2006). Apoptosome: a platform for the activation of initiator caspases. *Cell Death Differ* **15**, 15.
Bauminger, E. R., Harrison, P. M., Hechel, D., Nowik, I. and Treffry, A. (1991). Mossbauer spectroscopic investigation of structure-function relations in ferritins. *Biochim Biophys Acta.* **1118**, 48-58.
Bays, N. W., Wilhovsky, S. K., Goradia, A., Hodgkiss-Harlow, K. and Hampton, R. Y. (2001). HRD4/NPL4 is required for the proteasomal processing of ubiquitinated ER proteins. *Mol Biol Cell.* **12**, 4114-28.
Beddington, R. S. (1994). Induction of a second neural axis by the mouse node. *Development.* **120**, 613-20.
Bellairs, R. (1953a). Studies on the development of the foregut in the chick blastoderm. 1. The presumptive foregut area. *J. Embryol. exp. Morph.* **1**, 115-124.
Bellairs, R. (1953b). Studies on the development of the foregut in the chick blastoderm. 2. The morphogenetic movements. *J. Embryol. exp. Morph.* **1**, 115-124.
Bellairs, R. (1955). Studies on the development of the foregut in the chick embryo. 3. The role of mitosis. *J. Embryol. exp. Morph.* **3**, 242-250.
Bellairs, R. (1957). Studies on the development of the foregut in the chick embryo. 4. Mesodermal induction and mitosis. *J. Embryol. exp. Morph.* **5**, 340-350.
Bellairs, R. (1961). Cell death in chick embryos as studied by electron microscopy. *Journal of Anatomy* **95**, 54-60.
Bellairs, R. (1986). The primitive streak. *Anat Embryol (Berl).* **174**, 1-14.
Belo, J. A., Bouwmeester, T., Leyns, L., Kertesz, N., Gallo, M., Follettie, M. and De Robertis, E. M. (1997). Cerberus-like is a secreted factor with neutralizing activity expressed in the anterior primitive endoderm of the mouse gastrula. *Mech Dev.* **68**, 45-57.
Bensi, G., Raugei, G., Palla, E., Carinci, V., Tornese Buonamassa, D. and Melli, M. (1987). Human interleukin-1 beta gene. *Gene.* **52**, 95-101.
Bertocchini, F., Skromne, I., Wolpert, L. and Stern, C. D. (2004). Determination of embryonic polarity in a regulative system: evidence for endogenous inhibitors acting sequentially during primitive streak formation in the chick embryo. *Development.* **131**, 3381-90.
Bertocchini, F. and Stern, C. D. (2002). The hypoblast of the chick embryo positions the primitive streak by antagonizing nodal signaling. *Dev Cell.* **3**, 735-44.
Betts, D. H. and King, W. A. (2001). Genetic regulation of embryo death and senescence. *Theriogenology.* **55**, 171-91.
Biehs, B., Francois, V. and Bier, E. (1996). The Drosophila short gastrulation gene prevents Dpp from autoactivating and suppressing neurogenesis in the neuroectoderm. *Genes Dev.* **10**, 2922-34.
Blum, M., Gaunt, S. J., Cho, K. W., Steinbeisser, H., Blumberg, B., Bittner, D. and De Robertis, E. M. (1992). Gastrulation in the mouse: the role of the homeobox gene goosecoid. *Cell.* **69**, 1097-106.
Boardman, P. E., Sanz-Ezquerro, J., Overton, I. M., Burt, D. W., Bosch, E., Fong, W. T., Tickle, C., Brown, W. R., Wilson, S. A. and Hubbard, S. J. (2002). A comprehensive collection of chicken cDNAs. *Curr Biol.* **12**, 1965-9.
Bodenstein, L. and Stern, C. D. (2005). Formation of the chick primitive streak as studied in computer simulations. *J Theor Biol.* **233**, 253-69.
Bond, U., Agell, N., Haas, A. L., Redman, K. and Schlesinger, M. J. (1988). Ubiquitin in stressed chicken embryo fibroblasts. *J Biol Chem.* **263**, 2384-8.
Bond, U. and Schlesinger, M. J. (1985). Ubiquitin is a heat shock protein in chicken embryo fibroblasts. *Mol Cell Biol.* **5**, 949-56.

Bond, U. and Schlesinger, M. J. (1986). The chicken ubiquitin gene contains a heat shock promoter and expresses an unstable mRNA in heat-shocked cells. *Mol Cell Biol.* **6**, 4602-10.
Bond, U. and Schlesinger, M. J. (1987). Heat-shock proteins and development. *Adv Genet.* **24**, 1-29.
Born, J., Janeczek, J., Schwarz, W., Tiedemann, H. and Tiedemann, H. (1989). Activation of masked neural determinants in amphibian eggs and embryos and their release from the inducing tissue. *Cell Differ Dev.* **27**, 1-7.
Bossis, G. and Melchior, F. (2006). SUMO: regulating the regulator. *Cell Div.* **1**, 13.
Bou-Abdallah, F., Zhao, G., Mayne, H. R., Arosio, P. and Chasteen, N. D. (2005). Origin of the unusual kinetics of iron deposition in human h-chain ferritin. *J Am Chem Soc* **127**, 3885-93.
Bouwmeester, T., Kim, S., Sasai, Y., Lu, B. and De Robertis, E. M. (1996). Cerberus is a head-inducing secreted factor expressed in the anterior endoderm of Spemann's organizer. *Nature.* **382**, 595-601.
Brand-Saberi, B., Wilting, J., Ebensperger, C. and Christ, B. (1996). The formation of somite compartments in the avian embryo. *Int J Dev Biol.* **40**, 411-20.
Bratton, S. B., Walker, G., Srinivasula, S. M., Sun, X. M., Butterworth, M., Alnemri, E. S. and Cohen, G. M. (2001). Recruitment, activation and retention of caspases-9 and -3 by Apaf-1 apoptosome and associated XIAP complexes. *Embo J.* **20**, 998-1009.
Brewster, J. L., Martin, S. L., Toms, J., Goss, D., Wang, K., Zachrone, K., Davis, A., Carlson, G., Hood, L. and Coffin, J. D. (2000). Deletion of Dad1 in mice induces an apoptosis-associated embryonic death. *Genesis.* **26**, 271-8.
Broker, L. E., Kruyt, F. A. and Giaccone, G. (2005). Cell death independent of caspases: a review. *Clin Cancer Res.* **11**, 3155-62.
Budihardjo, I., Oliver, H., Lutter, M., Luo, X. and Wang, X. (1999). Biochemical pathways of caspase activation during apoptosis. *Annu Rev Cell Dev Biol.* **15**, 269-90.
Busch, H. and Goldknopf, I. L. (1981). Ubiquitin - protein conjugates. *Mol Cell Biochem.* **40**, 173-87.
Buxton, P., Davey, M. G., Paton, I. R., Morrice, D. R., Francis-West, P. H., Burt, D. W. and Tickle, C. (2004). Craniofacial development in the talpid3 chicken mutant. *Differentiation.* **72**, 348-62.
Cai, C. X., Birk, D. E. and Linsenmayer, T. F. (1997). Ferritin is a developmentally regulated nuclear protein of avian corneal epithelial cells. *J Biol Chem.* **272**, 12831-9.
Cai, D., Lee, K. K., Li, M., Tang, M. K. and Chan, K. M. (2004). Ubiquitin expression is up-regulated in human and rat skeletal muscles during aging. *Arch Biochem Biophys.* **425**, 42-50.
Cairo, G., Rappocciolo, E., Tacchini, L. and Schiaffonati, L. (1991). Expression of the genes for the ferritin H and L subunits in rat liver and heart. Evidence for tissue-specific regulations at pre- and post-translational levels. *Biochem J.* **275**, 813-6.
Callebaut, M. (2005). Origin, fate, and function of the components of the avian germ disc region and early blastoderm: role of ooplasmic determinants. *Dev Dyn.* **233**, 1194-216.
Callebaut, M. and Van Nueten, E. (1994). Rauber's (Koller's) sickle: the early gastrulation organizer of the avian blastoderm. *Eur J Morphol.* **32**, 35-48.
Callebaut, M., Van Nueten, E., Bortier, H. and Harrisson, F. (2003). Positional information by Rauber's sickle and a new look at the mechanisms of primitive streak initiation in avian blastoderms. *J Morphol.* **255**, 315-27.

Callebaut, M., Van Nueten, E., Van Nassauw, L., Bortier, H. and Harrisson, F. (1998). Only the endophyll-Rauber's sickle complex and not cells derived from the caudal marginal zone induce a primitive streak in the upper layer of avian blastoderms. *Reprod Nutr Dev.* **38**, 449-63.

Canning, D. R., Amin, T. and Richard, E. (2000). Regulation of epiblast cell movements by chondroitin sulfate during gastrulation in the chick. *Dev Dyn.* **219**, 545-59.

Canning, D. R. and Stern, C. D. (1988). Changes in the expression of the carbohydrate epitope HNK-1 associated with mesoderm induction in the chick embryo. *Development.* **104**, 643-55.

Caren, H., Holmstrand, A., Sjoberg, R. M. and Martinsson, T. (2006). The two human homologues of yeast UFD2 ubiquitination factor, UBE4A and UBE4B, are located in common neuroblastoma deletion regions and are subject to mutations in tumours. *Eur J Cancer.* **42**, 381-7. Epub 2006 Jan 4.

Cary, P. D., King, D. S., Crane-Robinson, C., Bradbury, E. M., Rabbani, A., Goodwin, G. H. and Johns, E. W. (1980). Structural studies on two high-mobility-group proteins from calf thymus, HMG-14 and HMG-20 (ubiquitin), and their interaction with DNA. *Eur J Biochem.* **112**, 577-80.

Chao, Y., Shiozaki, E. N., Srinivasula, S. M., Rigotti, D. J., Fairman, R. and Shi, Y. (2005). Engineering a dimeric caspase-9: a re-evaluation of the induced proximity model for caspase activation. *PLoS Biol.* **3**, e183. Epub 2005 May 10.

Chen, H., Zheng, C., Zhang, Y., Chang, Y. Z., Qian, Z. M. and Shen, X. (2006). Heat shock protein 27 downregulates the transferrin receptor 1-mediated iron uptake. *Int J Biochem Cell Biol* **7**, 7.

Chinnaiyan, A. M. (1999). The apoptosome: heart and soul of the cell death machine. *Neoplasia.* **1**, 5-15.

Chiu, R. K., Brun, J., Ramaekers, C., Theys, J., Weng, L., Lambin, P., Gray, D. A. and Wouters, B. G. (2006). Lysine 63-polyubiquitination guards against translesion synthesis-induced mutations. *PLoS Genet.* **2**, e116. Epub 2006 Jun 12.

Christ, B. and Ordahl, C. P. (1995). Early stages of chick somite development. *Anat Embryol (Berl).* **191**, 381-96.

Chuai, M., Zeng, W., Yang, X., Boychenko, V., Glazier, J. A. and Weijer, C. J. (2006). Cell movement during chick primitive streak formation. *Dev Biol.* **296**, 137-49. Epub 2006 Apr 26.

Ciechanover, A., Elias, S., Heller, H. and Hershko, A. (1982). "Covalent affinity" purification of ubiquitin-activating enzyme. *J Biol Chem.* **257**, 2537-42.

Ciechanover, A., Finley, D. and Varshavsky, A. (1984). The ubiquitin-mediated proteolytic pathway and mechanisms of energy-dependent intracellular protein degradation. *J Cell Biochem.* **24**, 27-53.

Ciechanover, A., Heller, H., Katz-Etzion, R. and Hershko, A. (1981). Activation of the heat-stable polypeptide of the ATP-dependent proteolytic system. *Proc Natl Acad Sci U S A.* **78**, 761-5.

Clamp, M., Cuff, J., Searle, S. M. and Barton, G. J. (2004). The Jalview Java alignment editor. *Bioinformatics.* **20**, 426-7. Epub 2004 Jan 22.

Clarke, S. L., Vasanthakumar, A., Anderson, S. A., Pondarre, C., Koh, C. M., Deck, K. M., Pitula, J. S., Epstein, C. J., Fleming, M. D. and Eisenstein, R. S. (2006). Iron-responsive degradation of iron-regulatory protein 1 does not require the Fe-S cluster. *Embo J* **19**, 19.

Cole, L. K. and Ross, L. S. (2001). Apoptosis in the developing zebrafish embryo. *Dev Biol.* **240**, 123-42.

Conforti, L., Tarlton, A., Mack, T. G., Mi, W., Buckmaster, E. A., Wagner, D., Perry, V. H. and Coleman, M. P. (2000). A Ufd2/D4Cole1e chimeric protein and overexpression of Rbp7 in the slow Wallerian degeneration (WldS) mouse. *Proc Natl Acad Sci U S A.* **97**, 11377-82.
Consortium., I. C. G. S. (2004). Sequence and comparative analysis of the chicken genome provide unique perspectives on vertebrate evolution. *Nature.* **432**, 695-716.
Cook, W. J., Jeffrey, L. C., Kasperek, E. and Pickart, C. M. (1994). Structure of tetraubiquitin shows how multiubiquitin chains can be formed. *J Mol Biol.* **236**, 601-9.
Cooper, G. M. (2000). The Cell: A Molecular Approach: Sinauer Associates, Inc.
Cowland, J. B., Wiborg, O. and Vuust, J. (1988). Human ubiquitin genes: one member of the UbB gene subfamily is a tetrameric non-processed pseudogene. *FEBS Lett.* **231**, 187-91.
Cozzi, A., Corsi, B., Levi, S., Santambrogio, P., Albertini, A. and Arosio, P. (2000). Overexpression of wild type and mutated human ferritin H-chain in HeLa cells: in vivo role of ferritin ferroxidase activity. *J Biol Chem.* **275**, 25122-9.
Cragg, S. J., Drysdale, J. and Worwood, M. (1985). Genes for the 'H' subunit of human ferritin are present on a number of human chromosomes. *Hum Genet.* **71**, 108-12.
Cui, C., Yang, X., Chuai, M., Glazier, J. A. and Weijer, C. J. (2005). Analysis of tissue flow patterns during primitive streak formation in the chick embryo. *Dev Biol.* **284**, 37-47.
D'Mello, S. R. and Galli, C. (1993). SGP2, ubiquitin, 14K lectin and RP8 mRNAs are not induced in neuronal apoptosis. *Neuroreport.* **4**, 355-8.
Dale, L., Howes, G., Price, B. M. and Smith, J. C. (1992). Bone morphogenetic protein 4: a ventralizing factor in early Xenopus development. *Development.* **115**, 573-85.
Davey, M. G., Paton, I. R., Yin, Y., Schmidt, M., Bangs, F. K., Morrice, D. R., Smith, T. G., Buxton, P., Stamataki, D., Tanaka, M. et al. (2006). The chicken talpid3 gene encodes a novel protein essential for Hedgehog signaling. *Genes Dev.* **20**, 1365-77.
De Robertis, E. M. and Sasai, Y. (1996). A common plan for dorsoventral patterning in Bilateria. *Nature.* **380**, 37-40.
Delic, J., Morange, M. and Magdelenat, H. (1993). Ubiquitin pathway involvement in human lymphocyte gamma-irradiation-induced apoptosis. *Mol Cell Biol* **13**, 4875-83.
Deroo, B. J., Rentsch, C., Sampath, S., Young, J., DeFranco, D. B. and Archer, T. K. (2002). Proteasomal inhibition enhances glucocorticoid receptor transactivation and alters its subnuclear trafficking. *Mol Cell Biol.* **22**, 4113-23.
Di Virgilio, G., Lavenda, N. and Worden, J. L. (1967). Sequence of events in neural tube closure and the formation of neural crest in the chick embryo. *Acta Anat (Basel).* **68**, 127-46.
Dias, M. S. and Schoenwolf, G. C. (1990). Formation of ectopic neurepithelium in chick blastoderms: age-related capacities for induction and self-differentiation following transplantation of quail Hensen's nodes. *Anat Rec* **228**, 437-48.
Dickey, L. F., Sreedharan, S., Theil, E. C., Didsbury, J. R., Wang, Y. H. and Kaufman, R. E. (1987). Differences in the regulation of messenger RNA for housekeeping and specialized-cell ferritin. A comparison of three distinct ferritin complementary DNAs, the corresponding subunits, and identification of the first processed in amphibia. *J Biol Chem.* **262**, 7901-7.
Diller, K. R. (2006). Stress Protein Expression Kinetics. *Annu Rev Biomed Eng* **13**, 13.

Dionne, M. S., Skarnes, W. C. and Harland, R. M. (2001). Mutation and analysis of Dan, the founding member of the Dan family of transforming growth factor beta antagonists. *Mol Cell Biol.* **21**, 636-43.
Donepudi, M. and Grutter, M. G. (2002). Structure and zymogen activation of caspases. *Biophys Chem.* **101-102**, 145-53.
Drysdale, J., Arosio, P., Invernizzi, R., Cazzola, M., Volz, A., Corsi, B., Biasiotto, G. and Levi, S. (2002). Mitochondrial ferritin: a new player in iron metabolism. *Blood Cells Mol Dis.* **29**, 376-83.
Dunkov, B. C., Georgieva, T., Yoshiga, T., Hall, M. and Law, J. H. (2002). Aedes aegypti ferritin heavy chain homologue: feeding of iron or blood influences message levels, lengths and subunit abundance. *J Insect Sci.* **2**, 7. Epub 2002 Apr 22.
Dunkov, B. C., Zhang, D., Choumarov, K., Winzerling, J. J. and Law, J. H. (1995). Isolation and characterization of mosquito ferritin and cloning of a cDNA that encodes one subunit. *Arch Insect Biochem Physiol.* **29**, 293-307.
Dworkin-Rastl, E., Shrutkowski, A. and Dworkin, M. B. (1984). Multiple ubiquitin mRNAs during Xenopus laevis development contain tandem repeats of the 76 amino acid coding sequence. *Cell.* **39**, 321-5.
Earnshaw, W. C., Martins, L. M. and Kaufmann, S. H. (1999). Mammalian caspases: structure, activation, substrates, and functions during apoptosis. *Annu Rev Biochem.* **68**, 383-424.
Edgar, R. C. (2004). MUSCLE: multiple sequence alignment with high accuracy and high throughput. *Nucleic Acids Res.* **32**, 1792-7. Print 2004.
Eimon, P. M. and Harland, R. M. (2001). Xenopus Dan, a member of the Dan gene family of BMP antagonists, is expressed in derivatives of the cranial and trunk neural crest. *Mech Dev.* **107**, 187-9.
Eisenstein, R. S. (2000). Iron regulatory proteins and the molecular control of mammalian iron metabolism. *Annu Rev Nutr* **20**, 627-62.
Ellies, D. L., Tucker, A. S. and Lumsden, A. (2002). Apoptosis of premigratory neural crest cells in rhombomeres 3 and 5: consequences for patterning of the branchial region. *Dev Biol.* **251**, 118-28.
Emre, N. C. and Berger, S. L. (2004). Histone H2B ubiquitylation and deubiquitylation in genomic regulation. *Cold Spring Harb Symp Quant Biol.* **69**, 289-99.
Epsztejn, S., Glickstein, H., Picard, V., Slotki, I. N., Breuer, W., Beaumont, C. and Cabantchik, Z. I. (1999). H-ferritin subunit overexpression in erythroid cells reduces the oxidative stress response and induces multidrug resistance properties. *Blood.* **94**, 3593-603.
Eyal-Giladi, H. (1984). The gradual establishment of cell commitments during the early stages of chick development. *Cell Differ.* **14**, 245-55.
Eyal-Giladi, H., Debby, A. and Harel, N. (1992). The posterior section of the chick's area pellucida and its involvement in hypoblast and primitive streak formation. *Development* **116**.
Eyal-Giladi, H. and Kochav, S. (1976). From cleavage to primitive streak formation: a complementary normal table and a new look at the first stages of the development of the chick. I. General morphology. *Dev Biol.* **49**, 321-37.
Fabian, B. and Eyal-Giladi, H. (1981). A SEM study of cell shedding during the formation of the area pellucida in the chick embryo. *J Embryol Exp Morphol.* **64**, 11-22.
Fadeel, B., Orrenius, S. and Zhivotovsky, B. (2000). The most unkindest cut of all: on the multiple roles of mammalian caspases. *Leukemia.* **14**, 1514-25.

Fainsod, A., Deissler, K., Yelin, R., Marom, K., Epstein, M., Pillemer, G., Steinbeisser, H. and Blum, M. (1997). The dorsalizing and neural inducing gene follistatin is an antagonist of BMP-4. *Mech Dev.* **63**, 39-50.

Fainsod, A., Steinbeisser, H. and De Robertis, E. M. (1994). On the function of BMP-4 in patterning the marginal zone of the Xenopus embryo. *Embo J.* **13**, 5015-25.

Faleiro, L., Kobayashi, R., Fearnhead, H. and Lazebnik, Y. (1997). Multiple species of CPP32 and Mch2 are the major active caspases present in apoptotic cells. *Embo J.* **16**, 2271-81.

Ferreira, C., Bucchini, D., Martin, M. E., Levi, S., Arosio, P., Grandchamp, B. and Beaumont, C. (2000). Early embryonic lethality of H ferritin gene deletion in mice. *J Biol Chem* **275**, 3021-4.

Finley, D., Bartel, B. and Varshavsky, A. (1989). The tails of ubiquitin precursors are ribosomal proteins whose fusion to ubiquitin facilitates ribosome biogenesis. *Nature.* **338**, 394-401.

Finley, D., Ciechanover, A. and Varshavsky, A. (1984). Thermolability of ubiquitin-activating enzyme from the mammalian cell cycle mutant ts85. *Cell.* **37**, 43-55.

Finley, D., Ozkaynak, E. and Varshavsky, A. (1987). The yeast polyubiquitin gene is essential for resistance to high temperatures, starvation, and other stresses. *Cell.* **48**, 1035-46.

Fischer, U., Janicke, R. U. and Schulze-Osthoff, K. (2003). Many cuts to ruin: a comprehensive update of caspase substrates. *Cell Death Differ.* **10**, 76-100.

Foley, A. C., Skromne, I. and Stern, C. D. (2000). Reconciling different models of forebrain induction and patterning: a dual role for the hypoblast. *Development.* **127**, 3839-54.

Ford, G. C., Harrison, P. M., Rice, D. W., Smith, J. M., Treffry, A., White, J. L. and Yariv, J. (1984). Ferritin: design and formation of an iron-storage molecule. *Philos Trans R Soc Lond B Biol Sci.* **304**, 551-65.

Forsyth, C. M., Lemongello, D., LaCount, D. J., Friesen, P. D. and Fisher, A. J. (2004). Crystal structure of an invertebrate caspase. *J Biol Chem.* **279**, 7001-8. Epub 2003 Nov 27.

Fraser, A. G., McCarthy, N. J. and Evan, G. I. (1997). drICE is an essential caspase required for apoptotic activity in Drosophila cells. *Embo J.* **16**, 6192-9.

Freitas, C., Rodrigues, S., Charrier, J. B., Teillet, M. A. and Palmeirim, I. (2001). Evidence for medial/lateral specification and positional information within the presomitic mesoderm. *Development.* **128**, 5139-47.

Fujimuro, M., Nishiya, T., Nomura, Y. and Yokosawa, H. (2005). Involvement of polyubiquitin chains via specific chain linkages in stress response in mammalian cells. *Biol Pharm Bull.* **28**, 2315-8.

Fujita, E., Egashira, J., Urase, K., Kuida, K. and Momoi, T. (2001). Caspase-9 processing by caspase-3 via a feedback amplification loop in vivo. *Cell Death Differ.* **8**, 335-44.

Fukuda, K. and Kikuchi, Y. (2005). Endoderm development in vertebrates: fate mapping, induction and regional specification. *Dev Growth Differ.* **47**, 343-55.

Gallera, J. (1970). Difference de la reactivite a l'inducteur neurogene entre l'ectoblaste de l'aire opaque et celui de l'aire pellucide chez le poulet.
[Difference in reactivity to the neurogenic inductor between the ectoblast of the area opaca and that of the area pellucida in chickens]. *Experientia.* **26**, 1353-4.

Gallera, J. and Nicolet, G. (1969). [The inductive capacity of the presumptive endoblast located in the young primitive streak of the chick embryo]. *J Embryol Exp Morphol.* **21**, 105-18.

Gallois, P., Makishima, T., Hecht, V., Despres, B., Laudie, M., Nishimoto, T. and Cooke, R. (1997). An Arabidopsis thaliana cDNA complementing a hamster apoptosis suppressor mutant. *Plant J.* **11**, 1325-31.

Garcia-Martinez, V., Darnell, D. K., Lopez-Sanchez, C., Sosic, D., Olson, E. N. and Schoenwolf, G. C. (1997). State of commitment of prospective neural plate and prospective mesoderm in late gastrula/early neurula stages of avian embryos. *Dev Biol.* **181**, 102-15.

Garcia-Martinez, V., Macias, D., Ganan, Y., Garcia-Lobo, J. M., Francia, M. V., Fernandez-Teran, M. A. and Hurle, J. M. (1993). Internucleosomal DNA fragmentation and programmed cell death (apoptosis) in the interdigital tissue of the embryonic chick leg bud. *J Cell Sci.* **106**, 201-8.

Gavel, Y. and von Heijne, G. (1990). Sequence differences between glycosylated and non-glycosylated Asn-X-Thr/Ser acceptor sites: implications for protein engineering. *Protein Eng.* **3**, 433-42.

Gavilanes, J. G., Gonzalez de Buitrago, G., Perez-Castells, R. and Rodriguez, R. (1982). Isolation, characterization, and amino acid sequence of a ubiquitin-like protein from insect eggs. *J Biol Chem.* **257**, 10267-70.

Gavrieli, Y., Sherman, Y. and Ben-Sasson, S. A. (1992). Identification of programmed cell death in situ via specific labeling of nuclear DNA fragmentation. *J Cell Biol* **119**, 493-501.

Gilbert, S. (2006). Developmental Biology. Sunderland: SINAUER ASSOCIATES, INC., Publishers.

Glickman, M. H. and Ciechanover, A. (2002). The ubiquitin-proteasome proteolytic pathway: destruction for the sake of construction. *Physiol Rev.* **82**, 373-428.

Glucksmann, A. (1951). Cell deaths in normal vertebrate ontogeny. *Biol. Rev* **26**, 59-86.

Godsave, S. F. and Slack, J. M. (1989). Clonal analysis of mesoderm induction in Xenopus laevis. *Dev Biol.* **134**, 486-90.

Goldknopf, I. L. and Busch, H. (1975). Remarkable similarities of peptide fingerprints of histone 2A and nonhistone chromosomal protein A24. *Biochem Biophys Res Commun.* **65**, 951-60.

Goldknopf, I. L. and Busch, H. (1977). Isopeptide linkage between nonhistone and histone 2A polypeptides of chromosomal conjugate-protein A24. *Proc Natl Acad Sci U S A.* **74**, 864-8.

Goldstein, G., Scheid, M., Hammerling, U., Schlesinger, D. H., Niall, H. D. and Boyse, E. A. (1975). Isolation of a polypeptide that has lymphocyte-differentiating properties and is probably represented universally in living cells. *Proc Natl Acad Sci U S A.* **72**, 11-5.

Graham, A., Francis-West, P., Brickell, P. and Lumsden, A. (1994). The signalling molecule BMP4 mediates apoptosis in the rhombencephalic neural crest. *Nature.* **372**, 684-6.

Graham, A., Heyman, I. and Lumsden, A. (1993). Even-numbered rhombomeres control the apoptotic elimination of neural crest cells from odd-numbered rhombomeres in the chick hindbrain. *Development.* **119**, 233-45.

Graham, A., Koentges, G. and Lumsden, A. (1996). Neural crest apoptosis and the establishment of craniofacial pattern: an honorable death. *Mol Cell Neurosci.* **8**, 76-83.

Gräper, L. (1929). Die Primitiventwicklung des Hünchens nach stereokinematographischen Untersuchungen, kontrolliert durch vitale Farbmarkierung und verglichen mit der Entwicklung anderer Wirbeltiere. *Arch. EntwMech. Org* **116**, 382-429.

Grapin, A. and Constam, D. B. (2004). Endoderm Development. Cold Spring Harbor, New York Cold Spring Harbor Labolatory Press.
Gray, P. W., Glaister, D., Chen, E., Goeddel, D. V. and Pennica, D. (1986). Two interleukin 1 genes in the mouse: cloning and expression of the cDNA for murine interleukin 1 beta. *J Immunol.* **137**, 3644-8.
Grunz, H. and Tacke, L. (1989). Neural differentiation of Xenopus laevis ectoderm takes place after disaggregation and delayed reaggregation without inducer. *Cell Differ Dev.* **28**, 211-7.
Guan, J. L., Machamer, C. E. and Rose, J. K. (1985). Glycosylation allows cell-surface transport of an anchored secretory protein. *Cell.* **42**, 489-96.
Gurdon, J. B. (1987). Embryonic induction--molecular prospects. *Development.* **99**, 285-306.
Ha, Y., Theil, E. C. and Allewell, N. M. (1997). Preliminary analysis of amphibian red cell M ferritin in a novel tetragonal unit cell. *Acta Crystallogr D Biol Crystallogr.* **53**, 513-23.
Haas, A. L., Baboshina, O., Williams, B. and Schwartz, L. M. (1995). Coordinated induction of the ubiquitin conjugation pathway accompanies the developmentally programmed death of insect skeletal muscle. *J Biol Chem.* **270**, 9407-12.
Haas, A. L., Warms, J. V., Hershko, A. and Rose, I. A. (1982). Ubiquitin-activating enzyme. Mechanism and role in protein-ubiquitin conjugation. *J Biol Chem.* **257**, 2543-8.
Haglund, K. and Dikic, I. (2005). Ubiquitylation and cell signaling. *Embo J.* **24**, 3353-9. Epub 2005 Sep 8.
Hamburger, A. E., West, A. P., Jr., Hamburger, Z. A., Hamburger, P. and Bjorkman, P. J. (2005). Crystal structure of a secreted insect ferritin reveals a symmetrical arrangement of heavy and light chains. *J Mol Biol.* **349**, 558-69. Epub 2005 Apr 12.
Hamburger, V. and Hamilton, H. L. (1951). A series of normal stages in the development of the chick embryo. *J. Morphology* **88**, 49-92.
Hardy, K. (1999). Apoptosis in the human embryo. *Rev Reprod.* **4**, 125-34.
Harrell, C. M., McKenzie, A. R., Patino, M. M., Walden, W. E. and Theil, E. C. (1991). Ferritin mRNA: interactions of iron regulatory element with translational regulator protein P-90 and the effect on base-paired flanking regions. *Proc Natl Acad Sci U S A.* **88**, 4166-70.
Harrison, H. and Adams, P. C. (2002). Hemochromatosis. Common genes, uncommon illness? *Can Fam Physician.* **48**, 1326-33.
Harrison, P. M. and Arosio, P. (1996). The ferritins: molecular properties, iron storage function and cellular regulation. *Biochim Biophys Acta.* **1275**, 161-203.
Harrison, P. M., Hempstead, P. D., Artymiuk, P. J. and Andrews, S. C. (1998). Structure-function relationships in the ferritins. *Met Ions Biol Syst.* **35**, 435-77.
Hasan, M. R., Koikawa, S., Kotani, S., Miyamoto, S. and Nakagawa, H. (2006). Ferritin forms dynamic oligomers to associate with microtubules in vivo: implication for the role of microtubules in iron metabolism. *Exp Cell Res.* **312**, 1950-60. Epub 2006 Apr 17.
Hatada, Y. and Stern, C. D. (1994). A fate map of the epiblast of the early chick embryo. *Development.* **120**, 2879-89.
Hatakeyama, S., Yada, M., Matsumoto, M., Ishida, N. and Nakayama, K. I. (2001). U box proteins as a new family of ubiquitin-protein ligases. *J Biol Chem.* **276**, 33111-20. Epub 2001 Jul 2.

Hatfield, P. M. and Vierstra, R. D. (1992). Multiple forms of ubiquitin-activating enzyme E1 from wheat. Identification of an essential cysteine by in vitro mutagenesis. *J Biol Chem.* **267**, 14799-803.
Hatsugai, N., Kuroyanagi, M., Yamada, K., Meshi, T., Tsuda, S., Kondo, M., Nishimura, M. and Hara-Nishimura, I. (2004). A plant vacuolar protease, VPE, mediates virus-induced hypersensitive cell death. *Science.* **305**, 855-8.
Hatta, K. and Takahashi, Y. (1996). Secondary axis induction by heterospecific organizers in zebrafish. *Dev Dyn.* **205**, 183-95.
Hauptmann, P., Riel, C., Kunz-Schughart, L. A., Frohlich, K. U., Madeo, F. and Lehle, L. (2006). Defects in N-glycosylation induce apoptosis in yeast. *Mol Microbiol.* **59**, 765-78.
Hawley, S. H., Wunnenberg-Stapleton, K., Hashimoto, C., Laurent, M. N., Watabe, T., Blumberg, B. W. and Cho, K. W. (1995). Disruption of BMP signals in embryonic Xenopus ectoderm leads to direct neural induction. *Genes Dev.* **9**, 2923-35.
Helenius, A. (1994). How N-linked oligosaccharides affect glycoprotein folding in the endoplasmic reticulum. *Mol Biol Cell.* **5**, 253-65.
Hemmati-Brivanlou, A., Kelly, O. G. and Melton, D. A. (1994). Follistatin, an antagonist of activin, is expressed in the Spemann organizer and displays direct neuralizing activity. *Cell.* **77**, 283-95.
Hemmati-Brivanlou, A. and Melton, D. (1997). Vertebrate neural induction. *Annu Rev Neurosci.* **20**, 43-60.
Hemmati-Brivanlou, A. and Melton, D. A. (1992). A truncated activin receptor inhibits mesoderm induction and formation of axial structures in Xenopus embryos. *Nature.* **359**, 609-14.
Hemmati-Brivanlou, A. and Melton, D. A. (1994). Inhibition of activin receptor signaling promotes neuralization in Xenopus. *Cell.* **77**, 273-81.
Hengartner, M. O., Ellis, R. E. and Horvitz, H. R. (1992). Caenorhabditis elegans gene ced-9 protects cells from programmed cell death. *Nature.* **356**, 494-9.
Hengartner, M. O. and Horvitz, H. R. (1994). The ins and outs of programmed cell death during C. elegans development. *Philos Trans R Soc Lond B Biol Sci.* **345**, 243-6.
Henkart, P. A. (1996). ICE family proteases: mediators of all apoptotic cell death? *Immunity.* **4**, 195-201.
Hensey, C. and Gautier, J. (1997). A developmental timer that regulates apoptosis at the onset of gastrulation. *Mech Dev* **69**, 183-95.
Hensey, C. and Gautier, J. (1998). Programmed cell death during Xenopus development: a spatio-temporal analysis. *Dev Biol* **203**, 36-48.
Hentze, M. W. and Kuhn, L. C. (1996). Molecular control of vertebrate iron metabolism: mRNA-based regulatory circuits operated by iron, nitric oxide, and oxidative stress. *Proc Natl Acad Sci U S A.* **93**, 8175-82.
Herbst, C. (1901). Formative Reize in der tierischen Ontogenese.: Georgi, Leipzig.
Herscovics, A. and Orlean, P. (1993). Glycoprotein biosynthesis in yeast. *Faseb J.* **7**, 540-50.
Hershko, A. (1983). Ubiquitin: roles in protein modification and breakdown. *Cell.* **34**, 11-2.
Hershko, A. and Ciechanover, A. (1998). The ubiquitin system. *Annu Rev Biochem.* **67**, 425-79.
Hershko, A., Ciechanover, A. and Rose, I. A. (1981). Identification of the active amino acid residue of the polypeptide of ATP-dependent protein breakdown. *J Biol Chem.* **256**, 1525-8.

Hershko, A., Heller, H., Elias, S. and Ciechanover, A. (1983). Components of ubiquitin-protein ligase system. Resolution, affinity purification, and role in protein breakdown. *J Biol Chem.* **258**, 8206-14.
Hicke, L. (2001). Protein regulation by monoubiquitin. *Nat Rev Mol Cell Biol.* **2**, 195-201.
Hirata, M. and Hall, B. K. (2000). Temporospatial patterns of apoptosis in chick embryos during the morphogenetic period of development. *Int J Dev Biol.* **44**, 757-68.
Hitchcock, A. L., Auld, K., Gygi, S. P. and Silver, P. A. (2003). A subset of membrane-associated proteins is ubiquitinated in response to mutations in the endoplasmic reticulum degradation machinery. *Proc Natl Acad Sci U S A.* **100**, 12735-40. Epub 2003 Oct 13.
Hochstrasser, M. (2000). Biochemistry. All in the ubiquitin family. *Science.* **289**, 563-4.
Homma, S., Yaginuma, H. and Oppenheim, R. W. (1994). Programmed cell death during the earliest stages of spinal cord development in the chick embryo: a possible means of early phenotypic selection. *J Comp Neurol.* **345**, 377-95.
Hong, N. A., Cado, D., Mitchell, J., Ortiz, B. D., Hsieh, S. N. and Winoto, A. (1997). A targeted mutation at the T-cell receptor alpha/delta locus impairs T-cell development and reveals the presence of the nearby antiapoptosis gene Dad1. *Mol Cell Biol.* **17**, 2151-7.
Hong, N. A., Flannery, M., Hsieh, S. N., Cado, D., Pedersen, R. and Winoto, A. (2000). Mice lacking Dad1, the defender against apoptotic death-1, express abnormal N-linked glycoproteins and undergo increased embryonic apoptosis. *Dev Biol.* **220**, 76-84.
Hong, N. A., Kabra, N. H., Hsieh, S. N., Cado, D. and Winoto, A. (1999). In vivo overexpression of Dad1, the defender against apoptotic death-1, enhances T cell proliferation but does not protect against apoptosis. *J Immunol.* **163**, 1888-93.
Hoppe, T. (2005). Multiubiquitylation by E4 enzymes: 'one size' doesn't fit all. *Trends Biochem Sci.* **30**, 183-7.
Horiuchi, H., Furusawa, S. and Matsuda, H. (2006). Maintenance of chicken embryonic stem cells in vitro. *Methods Mol Biol.* **329**, 17-34.
Horrocks, P. and Newbold, C. I. (2000). Intraerythrocytic polyubiquitin expression in Plasmodium falciparum is subjected to developmental and heat-shock control. *Mol Biochem Parasitol.* **105**, 115-25.
Hsu, D. R., Economides, A. N., Wang, X., Eimon, P. M. and Harland, R. M. (1998). The Xenopus dorsalizing factor Gremlin identifies a novel family of secreted proteins that antagonize BMP activities. *Mol Cell.* **1**, 673-83.
Hu, Y., Benedict, M. A., Ding, L. and Nunez, G. (1999). Role of cytochrome c and dATP/ATP hydrolysis in Apaf-1-mediated caspase-9 activation and apoptosis. *Embo J.* **18**, 3586-95.
Huang, T. T. and D'Andrea, A. D. (2006). Regulation of DNA repair by ubiquitylation. *Nat Rev Mol Cell Biol.* **7**, 323-34.
Hunt, L. T. and Dayhoff, M. O. (1977). Amino-terminal sequence identity of ubiquitin and the nonhistone component of nuclear protein A24. *Biochem Biophys Res Commun.* **74**, 650-5.
Hurle, J. M., Ros, M. A., Garcia-Martinez, V., Macias, D. and Ganan, Y. (1995). Cell death in the embryonic developing limb. *Scanning Microsc.* **9**, 519-33; discussion 533-4.

Ikegami, R., Hunter, P. and Yager, T. D. (1999). Developmental activation of the capability to undergo checkpoint-induced apoptosis in the early zebrafish embryo. *Dev Biol.* **209**, 409-33.
Iwai, K., Drake, S. K., Wehr, N. B., Weissman, A. M., LaVaute, T., Minato, N., Klausner, R. D., Levine, R. L. and Rouault, T. A. (1998). Iron-dependent oxidation, ubiquitination, and degradation of iron regulatory protein 2: implications for degradation of oxidized proteins. *Proc Natl Acad Sci U S A* **95**, 4924-8.
Izpisua-Belmonte, J. C., De Robertis, E. M., Storey, K. G. and Stern, C. D. (1993). The homeobox gene goosecoid and the origin of organizer cells in the early chick blastoderm. *Cell.* **74**, 645-59.
Jacobson, M. D., Weil, M. and Raff, M. C. (1997). Programmed cell death in animal development. *Cell* **88**, 347-54.
James, R. G., Kamei, C. N., Wang, Q., Jiang, R. and Schultheiss, T. M. (2006). Odd-skipped related 1 is required for development of the metanephric kidney and regulates formation and differentiation of kidney precursor cells. *Development.* **133**, 2995-3004. Epub 2006 Jun 21.
James, R. G. and Schultheiss, T. M. (2005). Bmp signaling promotes intermediate mesoderm gene expression in a dose-dependent, cell-autonomous and translation-dependent manner. *Dev Biol.* **288**, 113-25. Epub 2005 Oct 21.
Janicke, R. U., Ng, P., Sprengart, M. L. and Porter, A. G. (1998a). Caspase-3 is required for alpha-fodrin cleavage but dispensable for cleavage of other death substrates in apoptosis. *J Biol Chem.* **273**, 15540-5.
Janicke, R. U., Sprengart, M. L., Wati, M. R. and Porter, A. G. (1998b). Caspase-3 is required for DNA fragmentation and morphological changes associated with apoptosis. *J Biol Chem.* **273**, 9357-60.
Jeffs, P., Jaques, K. and Osmond, M. (1992). Cell death in cranial neural crest development. *Anat Embryol (Berl).* **185**, 583-8.
Jeffs, P. and Osmond, M. (1992). A segmented pattern of cell death during development of the chick embryo. *Anat Embryol (Berl).* **185**, 589-98.
Johnson, A. L. and Bridgham, J. T. (2000). Caspase-3 and -6 expression and enzyme activity in hen granulosa cells. *Biol Reprod.* **62**, 589-98.
Jones, C. M., Lyons, K. M., Lapan, P. M., Wright, C. V. and Hogan, B. L. (1992). DVR-4 (bone morphogenetic protein-4) as a posterior-ventralizing factor in Xenopus mesoderm induction. *Development.* **115**, 639-47.
Joubin, K. and Stern, C. D. (1999). Molecular interactions continuously define the organizer during the cell movements of gastrulation. *Cell.* **98**, 559-71.
Jurisicova, A. and Acton, B. M. (2004). Deadly decisions: the role of genes regulating programmed cell death in human preimplantation embryo development. *Reproduction.* **128**, 281-91.
Kaplan, H. A., Welply, J. K. and Lennarz, W. J. (1987). Oligosaccharyl transferase: the central enzyme in the pathway of glycoprotein assembly. *Biochim Biophys Acta.* **906**, 161-73.
Kelleher, D. J. and Gilmore, R. (1997). DAD1, the defender against apoptotic cell death, is a subunit of the mammalian oligosaccharyltransferase. *Proc Natl Acad Sci U S A.* **94**, 4994-9.
Kerr, J. F., Wyllie, A. H. and Currie, A. R. (1972). Apoptosis: a basic biological phenomenon with wide-ranging implications in tissue kinetics. *Br J Cancer.* **26**, 239-57.
Kerscher, O., Felberbaum, R. and Hochstrasser, M. (2006). Modification of Proteins by Ubiquitin and Ubiquitin-Like Proteins. *Annu Rev Cell Dev Biol* **5**, 5.

Khokha, M. K., Hsu, D., Brunet, L. J., Dionne, M. S. and Harland, R. M. (2003). Gremlin is the BMP antagonist required for maintenance of Shh and Fgf signals during limb patterning. *Nat Genet.* **34**, 303-7.
Khokha, M. K., Yeh, J., Grammer, T. C. and Harland, R. M. (2005). Depletion of Three BMP Antagonists from Spemann's Organizer Leads to a Catastrophic Loss of Dorsal Structures. *Dev Cell* **8**, 401-11.
Kim, H. Y., Klausner, R. D. and Rouault, T. A. (1995). Translational repressor activity is equivalent and is quantitatively predicted by in vitro RNA binding for two iron-responsive element-binding proteins, IRP1 and IRP2. *J Biol Chem.* **270**, 4983-6.
Kim, S. R., Lee, K. S., Yoon, H. J., Park, N. S., Lee, S. M., Kim, I., Seo, S. J., Sohn, H. D. and Jin, B. R. (2004a). Molecular cloning, expression and characterization of cDNAs encoding the ferritin subunits from the beetle, Apriona germari. *Comp Biochem Physiol B Biochem Mol Biol.* **138**, 423-33.
Kim, Y. I., Cho, J. H., Yoo, O. J. and Ahnn, J. (2004b). Transcriptional regulation and life-span modulation of cytosolic aconitase and ferritin genes in C.elegans. *J Mol Biol.* **342**, 421-33.
Kimura, W., Yasugi, S., Stern, C. D. and Fukuda, K. (2006). Fate and plasticity of the endoderm in the early chick embryo. *Dev Biol.* **289**, 283-95. Epub 2005 Dec 9.
Kintner, C. R. and Dodd, J. (1991). Hensen's node induces neural tissue in Xenopus ectoderm. Implications for the action of the organizer in neural induction. *Development.* **113**, 1495-505.
Klausner, R. D., Rouault, T. A. and Harford, J. B. (1993). Regulating the fate of mRNA: the control of cellular iron metabolism. *Cell.* **72**, 19-28.
Knezevic, V., De Santo, R. and Mackem, S. (1998). Continuing organizer function during chick tail development. *Development.* **125**, 1791-801.
Knoetgen, H., Teichmann, U., Wittler, L., Viebahn, C. and Kessel, M. (2000). Anterior neural induction by nodes from rabbits and mice. *Dev Biol.* **225**, 370-80.
Kochav, S., Ginsburg, M. and Eyal-Giladi, H. (1980). From cleavage to primitive streak formation: a complementary normal table and a new look at the first stages of the development of the chick. II. Microscopic anatomy and cell population dynamics. *Dev Biol.* **79**, 296-308.
Kornfeld, R. and Kornfeld, S. (1985). Assembly of asparagine-linked oligosaccharides. *Annu Rev Biochem.* **54**, 631-64.
Kos, R., Tucker, R. P., Hall, R., Duong, T. D. and Erickson, C. A. (2003). Methods for introducing morpholinos into the chicken embryo. *Dev Dyn.* **226**, 470-7.
Kroemer, G., El-Deiry, W. S., Golstein, P., Peter, M. E., Vaux, D., Vandenabeele, P., Zhivotovsky, B., Blagosklonny, M. V., Malorni, W., Knight, R. A. et al. (2005). Classification of cell death: recommendations of the Nomenclature Committee on Cell Death. *Cell Death Differ.* **12**, 1463-7.
Kroetz, M. B. (2005). SUMO: a ubiquitin-like protein modifier. *Yale J Biol Med.* **78**, 197-201.
Kugawa, F. and Aoki, M. (2004). Expression of the polyubiquitin gene early in the buprenorphine hydrochloride-induced apoptosis of NG108-15 cells. *DNA Seq* **15**, 237-45.
Kuhlbrodt, K., Mouysset, J. and Hoppe, T. (2005). Orchestra for assembly and fate of polyubiquitin chains. *Essays Biochem.* **41**, 1-14.
Kuida, K. (2000). Caspase-9. *Int J Biochem Cell Biol.* **32**, 121-4.
Kuida, K., Haydar, T. F., Kuan, C. Y., Gu, Y., Taya, C., Karasuyama, H., Su, M. S., Rakic, P. and Flavell, R. A. (1998). Reduced apoptosis and cytochrome c-mediated caspase activation in mice lacking caspase 9. *Cell.* **94**, 325-37.

Kuida, K., Zheng, T. S., Na, S., Kuan, C., Yang, D., Karasuyama, H., Rakic, P. and Flavell, R. A. (1996). Decreased apoptosis in the brain and premature lethality in CPP32-deficient mice. *Nature.* **384**, 368-72.
Kyte, J. and Doolittle, R. F. (1982). A simple method for displaying the hydropathic character of a protein. *J Mol Biol.* **157**, 105-32.
Lakhani, S. A., Masud, A., Kuida, K., Porter, G. A., Jr., Booth, C. J., Mehal, W. Z., Inayat, I. and Flavell, R. A. (2006). Caspases 3 and 7: key mediators of mitochondrial events of apoptosis. *Science.* **311**, 847-51.
Lamb, T. M., Knecht, A. K., Smith, W. C., Stachel, S. E., Economides, A. N., Stahl, N., Yancopolous, G. D. and Harland, R. M. (1993). Neural induction by the secreted polypeptide noggin. *Science.* **262**, 713-8.
LaVaute, T., Smith, S., Cooperman, S., Iwai, K., Land, W., Meyron-Holtz, E., Drake, S. K., Miller, G., Abu-Asab, M., Tsokos, M. et al. (2001). Targeted deletion of the gene encoding iron regulatory protein-2 causes misregulation of iron metabolism and neurodegenerative disease in mice. *Nat Genet* **27**, 209-14.
Lawson, A., Schoenwolf, G. C., England, M. A., Addai, F. K. and Ahima, R. S. (1999). Programmed cell death and the morphogenesis of the hindbrain roof plate in the chick embryo. *Anat Embryol (Berl).* **200**, 509-19.
Lawson, D. M., Artymiuk, P. J., Yewdall, S. J., Smith, J. M., Livingstone, J. C., Treffry, A., Luzzago, A., Levi, S., Arosio, P., Cesareni, G. et al. (1991). Solving the structure of human H ferritin by genetically engineering intermolecular crystal contacts. *Nature.* **349**, 541-4.
Lawson, D. M., Treffry, A., Artymiuk, P. J., Harrison, P. M., Yewdall, S. J., Luzzago, A., Cesareni, G., Levi, S. and Arosio, P. (1989). Identification of the ferroxidase centre in ferritin. *FEBS Lett.* **254**, 207-10.
Lazar, G. A., Desjarlais, J. R. and Handel, T. M. (1997). De novo design of the hydrophobic core of ubiquitin. *Protein Sci.* **6**, 1167-78.
Le Douarin, N. (1969). [Details of the interphase nucleus in Japanese quail (Coturnix coturnix japonica)]. *Bull Biol Fr Belg.* **103**, 435-52.
Le Douarin, N. M. and Teillet, M. A. (1973). The migration of neural crest cells to the wall of the digestive tract in avian embryo. *J Embryol Exp Morphol.* **30**, 31-48.
Le Gall, J. Y., Jouanolle, A. M., Mosser, J. and David, V. (2005). [Human iron metabolism]. *Bull Acad Natl Med.* **189**, 1635-47; discussion 1647.
Lenkinski, R. E., Chen, D. M., Glickson, J. D. and Goldstein, G. (1977). Nuclear magnetic resonance studies of the denaturation of ubiquitin. *Biochim Biophys Acta.* **494**, 126-30.
Levi, S. and Arosio, P. (2004). Mitochondrial ferritin. *Int J Biochem Cell Biol.* **36**, 1887-9.
Levi, S., Corsi, B., Bosisio, M., Invernizzi, R., Volz, A., Sanford, D., Arosio, P. and Drysdale, J. (2001). A human mitochondrial ferritin encoded by an intronless gene. *J Biol Chem.* **276**, 24437-40. Epub 2001 Apr 25.
Levi, S., Luzzago, A., Franceschinelli, F., Santambrogio, P., Cesareni, G. and Arosio, P. (1989a). Mutational analysis of the channel and loop sequences of human ferritin H-chain. *Biochem J.* **264**, 381-8.
Levi, S., Salfeld, J., Franceschinelli, F., Cozzi, A., Dorner, M. H. and Arosio, P. (1989b). Expression and structural and functional properties of human ferritin L-chain from Escherichia coli. *Biochemistry.* **28**, 5179-84.
Levi, S., Yewdall, S. J., Harrison, P. M., Santambrogio, P., Cozzi, A., Rovida, E., Albertini, A. and Arosio, P. (1992). Evidence of H- and L-chains have co-operative roles in the iron-uptake mechanism of human ferritin. *Biochem J.* **288**, 591-6.

Levin, M., Johnson, R. L., Stern, C. D., Kuehn, M. and Tabin, C. (1995). A molecular pathway determining left-right asymmetry in chick embryogenesis. *Cell.* **82**, 803-14.
Levinger, L. and Varshavsky, A. (1982). Selective arrangement of ubiquitinated and D1 protein-containing nucleosomes within the Drosophila genome. *Cell.* **28**, 375-85.
Levy, R. R., Cordonier, H., Czyba, J. C. and Guerin, J. F. (2001). Apoptosis in preimplantation mammalian embryo and genetics. *Ital J Anat Embryol.* **106**, 101-8.
Lewis, W. H. (1907). Transplantation of the lips of the blastopore in Rana pipiens. *Am J Anat* **7**, 137-141.
Li, P., Nijhawan, D., Budihardjo, I., Srinivasula, S. M., Ahmad, M., Alnemri, E. S. and Wang, X. (1997). Cytochrome c and dATP-dependent formation of Apaf-1/caspase-9 complex initiates an apoptotic protease cascade. *Cell.* **91**, 479-89.
Lin, T. Y., Wang, S. M., Fu, W. M., Chen, Y. H. and Yin, H. S. (1999). Toxicity of tunicamycin to cultured brain neurons: ultrastructure of the degenerating neurons. *J Cell Biochem.* **74**, 638-47.
Linask, K. K., Knudsen, K. A. and Gui, Y. H. (1997). N-cadherin-catenin interaction: necessary component of cardiac cell compartmentalization during early vertebrate heart development. *Dev Biol.* **185**, 148-64.
Linden, R., Martins, R. A. and Silveira, M. S. (2005). Control of programmed cell death by neurotransmitters and neuropeptides in the developing mammalian retina. *Prog Retin Eye Res.* **24**, 457-91. Epub 2004 Dec 15.
Lindquist, S. and Craig, E. A. (1988). The heat-shock proteins. *Annu Rev Genet.* **22**, 631-77.
Linker, C. and Stern, C. D. (2004). Neural induction requires BMP inhibition only as a late step, and involves signals other than FGF and Wnt antagonists. *Development.* **131**, 5671-81.
Linsenmayer, T. F., Cai, C. X., Millholland, J. M., Beazley, K. E. and Fitch, J. M. (2005). Nuclear ferritin in corneal epithelial cells: tissue-specific nuclear transport and protection from UV-damage. *Prog Retin Eye Res.* **24**, 139-59. Epub 2004 Nov 11.
Lints, T. J., Parsons, L. M., Hartley, L., Lyons, I. and Harvey, R. P. (1993). Nkx-2.5: a novel murine homeobox gene expressed in early heart progenitor cells and their myogenic descendants. *Development.* **119**, 419-31.
Liu, Y. C., Penninger, J. and Karin, M. (2005). Immunity by ubiquitylation: a reversible process of modification. *Nat Rev Immunol.* **5**, 941-52.
Livingstone, C. D. and Barton, G. J. (1993). Protein sequence alignments: a strategy for the hierarchical analysis of residue conservation. *Comput Appl Biosci.* **9**, 745-56.
Lopez-Sanchez, C., Garcia-Martinez, V. and Schoenwolf, G. C. (2001). Localization of cells of the prospective neural plate, heart and somites within the primitive streak and epiblast of avian embryos at intermediate primitive-streak stages. *Cells Tissues Organs.* **169**, 334-46.
Lumsden, A., Sprawson, N. and Graham, A. (1991). Segmental origin and migration of neural crest cells in the hindbrain region of the chick embryo. *Development.* **113**, 1281-91.
Lund, P. K., Moats-Staats, B. M., Simmons, J. G., Hoyt, E., D'Ercole, A. J., Martin, F. and Van Wyk, J. J. (1985). Nucleotide sequence analysis of a cDNA encoding human ubiquitin reveals that ubiquitin is synthesized as a precursor. *J Biol Chem.* **260**, 7609-13.
Macias, D., Ganan, Y., Ros, M. A. and Hurle, J. M. (1996). In vivo inhibition of programmed cell death by local administration of FGF-2 and FGF-4 in the interdigital areas of the embryonic chick leg bud. *Anat Embryol (Berl).* **193**, 533-41.

Madeo, F., Herker, E., Maldener, C., Wissing, S., Lachelt, S., Herlan, M., Fehr, M., Lauber, K., Sigrist, S. J., Wesselborg, S. et al. (2002). A caspase-related protease regulates apoptosis in yeast. *Mol Cell.* **9**, 911-7.

Makishima, T., Nakashima, T., Nagata-Kuno, K., Fukushima, K., Iida, H., Sakaguchi, M., Ikehara, Y., Komiyama, S. and Nishimoto, T. (1997). The highly conserved DAD1 protein involved in apoptosis is required for N-linked glycosylation. *Genes Cells.* **2**, 129-41.

Makishima, T., Yoshimi, M., Komiyama, S., Hara, N. and Nishimoto, T. (2000). A subunit of the mammalian oligosaccharyltransferase, DAD1, interacts with Mcl-1, one of the bcl-2 protein family. *J Biochem (Tokyo).* **128**, 399-405.

Marchant, L., Linker, C., Ruiz, P., Guerrero, N. and Mayor, R. (1998). The inductive properties of mesoderm suggest that the neural crest cells are specified by a BMP gradient. *Dev Biol.* **198**, 319-29.

Matsui, S. I., Seon, B. K. and Sandberg, A. A. (1979). Disappearance of a structural chromatin protein A24 in mitosis: implications for molecular basis of chromatin condensation. *Proc Natl Acad Sci U S A.* **76**, 6386-90.

McLarren, K. W., Litsiou, A. and Streit, A. (2003). DLX5 positions the neural crest and preplacode region at the border of the neural plate. *Dev Biol* **259**, 34-47.

Merino, R., Ganan, Y., Macias, D., Economides, A. N., Sampath, K. T. and Hurle, J. M. (1998). Morphogenesis of digits in the avian limb is controlled by FGFs, TGFbetas, and noggin through BMP signaling. *Dev Biol.* **200**, 35-45.

Merino, R., Ganan, Y., Macias, D., Rodriguez-Leon, J. and Hurle, J. M. (1999). Bone morphogenetic proteins regulate interdigital cell death in the avian embryo. *Ann N Y Acad Sci.* **887**, 120-32.

Metzstein, M. M., Stanfield, G. M. and Horvitz, H. R. (1998). Genetics of programmed cell death in C. elegans: past, present and future. *Trends Genet.* **14**, 410-6.

Mezquita, J., Chiva, M., Vidal, S. and Mezquita, C. (1982). Effect of high mobility group nonhistone proteins HMG-20 (ubiquitin) and HMG-17 on histone deacetylase activity assayed in vitro. *Nucleic Acids Res.* **10**, 1781-97.

Mezquita, J., Lopez-Ibor, B., Pau, M. and Mezquita, C. (1993). Intron and intronless transcription of the chicken polyubiquitin gene UbII. *FEBS Lett.* **319**, 244-8.

Mezquita, J., Oliva, R. and Mezquita, C. (1987). New ubiquitin mRNA expressed during chicken spermiogenesis. *Nucleic Acids Res.* **15**, 9604.

Mezquita, J., Pau, M. and Mezquita, C. (1988). cDNA encoding a chicken ubiquitin-fusion protein identical to the corresponding human protein. *Nucleic Acids Res.* **16**, 11838.

Mezquita, J., Pau, M. and Mezquita, C. (1997). Characterization and expression of two chicken cDNAs encoding ubiquitin fused to ribosomal proteins of 52 and 80 amino acids. *Gene.* **195**, 313-9.

Miller, S. A. and Briglin, A. (1996). Apoptosis removes chick embryo tail gut and remnant of the primitive streak. *Dev Dyn.* **206**, 212-8.

Missirlis, F., Holmberg, S., Georgieva, T., Dunkov, B. C., Rouault, T. A. and Law, J. H. (2006). Characterization of mitochondrial ferritin in Drosophila. *Proc Natl Acad Sci U S A.* **103**, 5893-8. Epub 2006 Mar 29.

Mita, K., Ichimura, S. and Nenoi, M. (1991). Essential factors determining codon usage in ubiquitin genes. *J Mol Evol.* **33**, 216-25.

Miyake, H., Hara, I., Arakawa, S. and Kamidono, S. (2000). Stress protein GRP78 prevents apoptosis induced by calcium ionophore, ionomycin, but not by glycosylation inhibitor, tunicamycin, in human prostate cancer cells. *J Cell Biochem.* **77**, 396-408.

Mizoguchi, H., Kudo, D., Shimizu, Y., Hirota, K., Kawai, S. and Hino, A. (2000). Distribution of apoptosis-like cells in sea urchin early embryogenesis. *Zygote.* **8**, S76.
Mizoguchi, T., Izawa, T., Kuroiwa, A. and Kikuchi, Y. (2006). Fgf signaling negatively regulates Nodal-dependent endoderm induction in zebrafish. *Dev Biol.* **300**, 612-22. Epub 2006 Sep 9.
Mladenka, P., Hrdina, R., Hubl, M. and Simunek, T. (2005). The fate of iron in the organism and its regulatory pathways. *Acta Medica (Hradec Kralove).* **48**, 127-35.
Mogi, K., Toyoizumi, R. and Takeuchi, S. (2000). Correlation between the expression of the HNK-1 epitope and cellular invasiveness in prestreak epiblast cells of chick embryos. *Int J Dev Biol.* **44**, 811-4.
Mohammadi, M., McMahon, G., Sun, L., Tang, C., Hirth, P., Yeh, B. K., Hubbard, S. R. and Schlessinger, J. (1997). Structures of the tyrosine kinase domain of fibroblast growth factor receptor in complex with inhibitors. *Science.* **276**, 955-60.
Montero, J. A., Ganan, Y., Macias, D., Rodriguez-Leon, J., Sanz-Ezquerro, J. J., Merino, R., Chimal-Monroy, J., Nieto, M. A. and Hurle, J. M. (2001). Role of FGFs in the control of programmed cell death during limb development. *Development.* **128**, 2075-84.
Mori, H., Kondo, J. and Ihara, Y. (1987). Ubiquitin is a component of paired helical filaments in Alzheimer's disease. *Science.* **235**, 1641-4.
Munro, S. and Pelham, H. (1985). What turns on heat shock genes? *Nature.* **317**, 477-8.
Muramatsu, T., Mizutani, Y., Ohmori, Y. and Okumura, J. (1997). Comparison of three nonviral transfection methods for foreign gene expression in early chicken embryos in ovo. *Biochem Biophys Res Commun.* **230**, 376-80.
Nakashima, T., Sekiguchi, T., Kuraoka, A., Fukushima, K., Shibata, Y., Komiyama, S. and Nishimoto, T. (1993). Molecular cloning of a human cDNA encoding a novel protein, DAD1, whose defect causes apoptotic cell death in hamster BHK21 cells. *Mol Cell Biol.* **13**, 6367-74.
Nakayama, K. I. and Nakayama, K. (2006). Ubiquitin ligases: cell-cycle control and cancer. *Nat Rev Cancer.* **6**, 369-81.
Negron, J. F. and Lockshin, R. A. (2004). Activation of apoptosis and caspase-3 in zebrafish early gastrulae. *Dev Dyn.* **231**, 161-70.
Neidhardt, F. C., VanBogelen, R. A. and Vaughn, V. (1984). The genetics and regulation of heat-shock proteins. *Annu Rev Genet.* **18**, 295-329.
New, D. A. T. (1955). A new technique for the cultivation of chick embryo in vitro. *J.Embryology and Experimental Morphology* **3**, 326-331.
Nicolet, G. (1965). [Autoradiographic study of the fate of cells invaginating through Hensen's node in the chick embryo at the definitive streak stage]. *Acta Embryol Morphol Exp.* **8**, 213-20.
Nicolet, G. (1970). [An autoradiographic study of the presumptive fate of the primitive streak in chick embryos]. *J Embryol Exp Morphol.* **23**, 70-108.
Nie, G., Chen, G., Sheftel, A. D., Pantopoulos, K. and Ponka, P. (2006). In vivo tumor growth is inhibited by cytosolic iron deprivation caused by the expression of mitochondrial ferritin. *Blood* **6**, 6.
Nikonov, A. V., Snapp, E., Lippincott-Schwartz, J. and Kreibich, G. (2002). Active translocon complexes labeled with GFP-Dad1 diffuse slowly as large polysome arrays in the endoplasmic reticulum. *J Cell Biol.* **158**, 497-506. Epub 2002 Aug 5.
Nishii, K., Tsuzuki, T., Kumai, M., Takeda, N., Koga, H., Aizawa, S., Nishimoto, T. and Shibata, Y. (1999). Abnormalities of developmental cell death in Dad1-deficient mice. *Genes Cells.* **4**, 243-52.

Oppenheim, R. W. (2001). Viktor Hamburger (1900-2001). Journey of a neuroembryologist to the end of the millennium and beyond. *Neuron.* **31**, 179-90.
Oppenheimer, J. M. (1936). Transplantation experiments on developing teleosts (Fundulus and Perca). *J. Exp. Zool* **72**, 409-437.
Osley, M. A. (2004). H2B ubiquitylation: the end is in sight. *Biochim Biophys Acta.* **1677**, 74-8.
Otto, A., Schmidt, C. and Patel, K. (2006). Pax3 and Pax7 expression and regulation in the avian embryo. *Anat Embryol* **28**, 28.
Ozkaynak, E., Finley, D., Solomon, M. J. and Varshavsky, A. (1987). The yeast ubiquitin genes: a family of natural gene fusions. *Embo J.* **6**, 1429-39.
Ozkaynak, E., Finley, D. and Varshavsky, A. (1984). The yeast ubiquitin gene: head-to-tail repeats encoding a polyubiquitin precursor protein. *Nature.* **312**, 663-6.
Pain, B., Clark, M. E., Shen, M., Nakazawa, H., Sakurai, M., Samarut, J. and Etches, R. J. (1996). Long-term in vitro culture and characterisation of avian embryonic stem cells with multiple morphogenetic potentialities. *Development.* **122**, 2339-48.
Pan, G., Humke, E. W. and Dixit, V. M. (1998). Activation of caspases triggered by cytochrome c in vitro. *FEBS Lett.* **426**, 151-4.
Pannett, C. A. and Compton, A. (1924). The cultivation of tissues in saline embryonic juice *Lancet.*
Pantopoulos, K. (2004). Iron metabolism and the IRE/IRP regulatory system: an update. *Ann N Y Acad Sci.* **1012**, 1-13.
Pearce, J. J., Penny, G. and Rossant, J. (1999). A mouse cerberus/Dan-related gene family. *Dev Biol.* **209**, 98-110.
Pera, E., Stein, S. and Kessel, M. (1999). Ectodermal patterning in the avian embryo: epidermis versus neural plate. *Development.* **126**, 63-73.
Percy, M. E., Bauer, S. J., Rainey, S., McLachlan, D. R., Dhar, M. S. and Joshi, J. G. (1995). Localization of a new ferritin heavy chain sequence present in human brain mRNA to chromosome 11. *Genome.* **38**, 450-7.
Perez-Sala, D. and Mollinedo, F. (1995). Inhibition of N-linked glycosylation induces early apoptosis in human promyelocytic HL-60 cells. *J Cell Physiol.* **163**, 523-31.
Peter, K. (1938). Untersuchungen über die Entwicklung des Dotterentoderms. 1. Die Entwicklung des Entoderms beim Hühnchen. *Z. mikr. Anat. Forsch* **43**, 362-415.
Petitte, J. N., Liu, G. and Yang, Z. (2004). Avian pluripotent stem cells. *Mech Dev.* **121**, 1159-68.
Pexieder, T. (1975). Cell death in the morphogenesis and teratogenesis of the heart. *Adv Anat Embryol Cell Biol.* **51**, 3-99.
Pfeffer, P. L., De Robertis, E. M. and Izpisua-Belmonte, J. C. (1997). Crescent, a novel chick gene encoding a Frizzled-like cysteine-rich domain, is expressed in anterior regions during early embryogenesis. *Int J Dev Biol.* **41**, 449-58.
Philpott, C. C., Klausner, R. D. and Rouault, T. A. (1994). The bifunctional iron-responsive element binding protein/cytosolic aconitase: the role of active-site residues in ligand binding and regulation. *Proc Natl Acad Sci U S A.* **91**, 7321-5.
Picard, V., Renaudie, F., Porcher, C., Hentze, M. W., Grandchamp, B. and Beaumont, C. (1996). Overexpression of the ferritin H subunit in cultured erythroid cells changes the intracellular iron distribution. *Blood.* **87**, 2057-64.
Piccolo, S., Sasai, Y., Lu, B. and De Robertis, E. M. (1996). Dorsoventral patterning in Xenopus: inhibition of ventral signals by direct binding of chordin to BMP-4. *Cell.* **86**, 589-98.
Pickart, C. M. (2001). Ubiquitin enters the new millennium. *Mol Cell.* **8**, 499-504.

Poelmann, R. E. and Gittenberger-de Groot, A. C. (2005). Apoptosis as an instrument in cardiovascular development. *Birth Defects Res C Embryo Today.* **75**, 305-13.
Ponka, P., Beaumont, C. and Richardson, D. R. (1998). Function and regulation of transferrin and ferritin. *Semin Hematol* **35**, 35-54.
Pop, C., Timmer, J., Sperandio, S. and Salvesen, G. S. (2006). The apoptosome activates caspase-9 by dimerization. *Mol Cell.* **22**, 269-75.
Postigo, A. A., Depp, J. L., Taylor, J. J. and Kroll, K. L. (2003). Regulation of Smad signaling through a differential recruitment of coactivators and corepressors by ZEB proteins. *Embo J.* **22**, 2453-62.
Poulain, M. and Lepage, T. (2002). Mezzo, a paired-like homeobox protein is an immediate target of Nodal signalling and regulates endoderm specification in zebrafish. *Development.* **129**, 4901-14.
Psychoyos, D. and Stern, C. D. (1996). Fates and migratory routes of primitive streak cells in the chick embryo. *Development.* **122**, 1523-34.
Quaresima, B., Tiano, M. T., Porcellini, A., D'Agostino, P., Faniello, M. C., Bevilacqua, M. A., Cimino, F. and Costanzo, F. (1994). PCR analysis of the H ferritin multigene family reveals the existence of two classes of processed pseudogenes. *PCR Methods Appl.* **4**, 85-8.
Quintana, C., Cowley, J. M. and Marhic, C. (2004). Electron nanodiffraction and high-resolution electron microscopy studies of the structure and composition of physiological and pathological ferritin. *J Struct Biol.* **147**, 166-78.
Reversade, B. and De Robertis, E. M. (2005). Regulation of ADMP and BMP2/4/7 at opposite embryonic poles generates a self-regulating morphogenetic field. *Cell.* **123**, 1147-60.
Rex, M., Orme, A., Uwanogho, D., Tointon, K., Wigmore, P. M., Sharpe, P. T. and Scotting, P. J. (1997). Dynamic expression of chicken Sox2 and Sox3 genes in ectoderm induced to form neural tissue. *Dev Dyn* **209**, 323-32.
Ribar, B., Prakash, L. and Prakash, S. (2006). Requirement of ELC1 for RNA polymerase II polyubiquitylation and degradation in response to DNA damage in Saccharomyces cerevisiae. *Mol Cell Biol.* **26**, 3999-4005.
Riederer, M. A. and Hinnen, A. (1991). Removal of N-glycosylation sites of the yeast acid phosphatase severely affects protein folding. *J Bacteriol.* **173**, 3539-46.
Riedl, S. J. and Shi, Y. (2004). Molecular mechanisms of caspase regulation during apoptosis. *Nat Rev Mol Cell Biol.* **5**, 897-907.
Ritossa, F. (1962). A new puffing pattern induced by temperature shock and DNP in Drosophila. *Experientia.* **18**, 571-573.
Robzyk, K., Recht, J. and Osley, M. A. (2000). Rad6-dependent ubiquitination of histone H2B in yeast. *Science.* **287**, 501-4.
Rocamora, N. and Agell, N. (1990). Methylation of chick UbI and UbII polyubiquitin genes and their differential expression during spermatogenesis. *Biochem J.* **267**, 821-9.
Rodriguez, J. and Lazebnik, Y. (1999). Caspase-9 and APAF-1 form an active holoenzyme. *Genes Dev.* **13**, 3179-84.
Rojo, E., Martin, R., Carter, C., Zouhar, J., Pan, S., Plotnikova, J., Jin, H., Paneque, M., Sanchez-Serrano, J. J., Baker, B. et al. (2004). VPEgamma exhibits a caspase-like activity that contributes to defense against pathogens. *Curr Biol.* **14**, 1897-906.
Rosenquist, G. C. (1966). A radioautographic study of labeled grafts in the chick blastoderm: Development from primitive-streak stages to stage 12 *Carnegie Inst. Wash. Contrib. Embryol.* **38**, 31-110.

Rosenquist, G. C. (1972). Endoderm movements in the chick embryo between the early short streak and head process stages. *J Exp Zool.* **180**, 95-103.
Saiki, R. K., Gelfand, D. H., Stoffel, S., Scharf, S. J., Higuchi, R., Horn, G. T., Mullis, K. B. and Erlich, H. A. (1988). Primer-directed enzymatic amplification of DNA with a thermostable DNA polymerase. *Science.* **239**, 487-91.
Saint-Jeannet, J. P., Huang, S. and Duprat, A. M. (1990). Modulation of neural commitment by changes in target cell contacts in Pleurodeles waltl. *Dev Biol.* **141**, 93-103.
Saleh, A., Srinivasula, S. M., Acharya, S., Fishel, R. and Alnemri, E. S. (1999). Cytochrome c and dATP-mediated oligomerization of Apaf-1 is a prerequisite for procaspase-9 activation. *J Biol Chem.* **274**, 17941-5.
Salghetti, S. E., Caudy, A. A., Chenoweth, J. G. and Tansey, W. P. (2001). Regulation of transcriptional activation domain function by ubiquitin. *Science.* **293**, 1651-3. Epub 2001 Jul 19.
Salvesen, G., Lloyd, C. and Farley, D. (1987). cDNA encoding a human homolog of yeast ubiquitin 1. *Nucleic Acids Res.* **15**, 5485.
Sambrook, J., Fritsch, E. F. and Maniatis, T. (1989). Molecular Cloning, a laboratory manual, 2nd edition, CSH.
Samejima, K., Svingen, P. A., Basi, G. S., Kottke, T., Mesner, P. W., Jr., Stewart, L., Durrieu, F., Poirier, G. G., Alnemri, E. S., Champoux, J. J. et al. (1999). Caspase-mediated cleavage of DNA topoisomerase I at unconventional sites during apoptosis. *J Biol Chem.* **274**, 4335-40.
Sanders, E. J., Khare, M. K., Ooi, V. C. and Bellairs, R. (1986). An experimental and morphological analysis of the tail bud mesenchyme of the chick embryo. *Anat Embryol (Berl).* **174**, 179-85.
Sanders, E. J., Torkkeli, P. H. and French, A. S. (1997). Patterns of cell death during gastrulation in chick and mouse embryos. *Anat Embryol (Berl)* **195**, 147-54.
Sang, H. (2004). Prospects for transgenesis in the chick. *Mech Dev.* **121**, 1179-86.
Sanjay, A., Fu, J. and Kreibich, G. (1998). DAD1 is required for the function and the structural integrity of the oligosaccharyltransferase complex. *J Biol Chem.* **273**, 26094-9.
Santamaria, R., Bevilacqua, M. A., Maffettone, C., Irace, C., Iovine, B. and Colonna, A. (2006). Induction of H-ferritin synthesis by oxalomalate is regulated at both the transcriptional and post-transcriptional levels. *Biochim Biophys Acta* **7**, 7.
Sasai, Y., Lu, B., Steinbeisser, H. and De Robertis, E. M. (1995). Regulation of neural induction by the Chd and Bmp-4 antagonistic patterning signals in Xenopus. *Nature.* **377**, 757.
Sasai, Y., Lu, B., Steinbeisser, H., Geissert, D., Gont, L. K. and De Robertis, E. M. (1994). Xenopus chordin: a novel dorsalizing factor activated by organizer-specific homeobox genes. *Cell.* **79**, 779-90.
Sato, S. M. and Sargent, T. D. (1989). Development of neural inducing capacity in dissociated Xenopus embryos. *Dev Biol.* **134**, 263-6.
Savare, J., Bonneaud, N. and Girard, F. (2005). SUMO represses transcriptional activity of the Drosophila SoxNeuro and human Sox3 central nervous system-specific transcription factors. *Mol Biol Cell.* **16**, 2660-9. Epub 2005 Mar 23.
Sawada, K. and Aoyama, H. (1999). Fate maps of the primitive streak in chick and quail embryo: ingression timing of progenitor cells of each rostro-caudal axial level of somites. *Int J Dev Biol.* **43**, 809-15.
Schiedlmeier, B. and Schmitt, R. (1994). Repetitious structure and transcription control of a polyubiquitin gene in Volvox carteri. *Curr Genet.* **25**, 169-77.

Schlesinger, M. J., Asburner, M. and Tissieres, A. (1982). Heat shock from bacteria to man. *Cold Spring Harbor Laboratory* **Cold Spring Harbor**.
Schoenwolf, G. C. (1981). Morphogenetic processes involved in the remodeling of the tail region of the chick embryo. *Anat Embryol (Berl).* **162**, 183-97.
Schoenwolf, G. C. (1982). On the morphogenesis of the early rudiments of the developing central nervous system. *Scan Electron Microsc.*, 289-308.
Schoenwolf, G. C. (1992). Morphological and mapping studies of the paranodal and postnodal levels of the neural plate during chick neurulation. *Anat Rec.* **233**, 281-90.
Schoenwolf, G. C., Garcia-Martinez, V. and Diaz, M. S. (1992). Mesoderm movement and fate during amphibian gastrulation and neurulation *Dev. Dynam* **193**, 235-248.
Schulte-Merker, S., Lee, K. J., McMahon, A. P. and Hammerschmidt, M. (1997). The zebrafish organizer requires chordino. *Nature.* **387**, 862-3.
Schultheiss, T. M., Xydas, S. and Lassar, A. B. (1995). Induction of avian cardiac myogenesis by anterior endoderm. *Development.* **121**, 4203-14.
Schwartz, L. M., Myer, A., Kosz, L., Engelstein, M. and Maier, C. (1990). Activation of polyubiquitin gene expression during developmentally programmed cell death. *Neuron.* **5**, 411-9.
Seleiro, E. A., Connolly, D. J. and Cooke, J. (1996). Early developmental expression and experimental axis determination by the chicken Vg1 gene. *Curr Biol.* **6**, 1476-86.
Selleck, M. A. and Stern, C. D. (1991). Fate mapping and cell lineage analysis of Hensen's node in the chick embryo. *Development.* **112**, 615-26.
Selleck, M. A. and Stern, C. D. (1992). Evidence for stem cells in the mesoderm of Hensen's node and their role in embryonic pattern formation.: New York: Plenum Press.
Shah, S. B., Skromne, I., Hume, C. R., Kessler, D. S., Lee, K. J., Stern, C. D. and Dodd, J. (1997). Misexpression of chick Vg1 in the marginal zone induces primitive streak formation. *Development.* **124**, 5127-38.
Sharp, P. M. and Li, W. H. (1987). Ubiquitin genes as a paradigm of concerted evolution of tandem repeats. *J Mol Evol.* **25**, 58-64.
Sheng, G., dos Reis, M. and Stern, C. D. (2003). Churchill, a zinc finger transcriptional activator, regulates the transition between gastrulation and neurulation. *Cell.* **115**, 603-13.
Sheng, G. and Stern, C. D. (1999). Gata2 and Gata3: novel markers for early embryonic polarity and for non-neural ectoderm in the chick embryo. *Mech Dev* **87**, 213-6.
Shi, Y. (2002). Apoptosome: the cellular engine for the activation of caspase-9. *Structure.* **10**, 285-8.
Shi, Y. (2004). Caspase activation: revisiting the induced proximity model. *Cell.* **117**, 855-8.
Silberstein, S., Collins, P. G., Kelleher, D. J. and Gilmore, R. (1995). The essential OST2 gene encodes the 16-kD subunit of the yeast oligosaccharyltransferase, a highly conserved protein expressed in diverse eukaryotic organisms. *J Cell Biol.* **131**, 371-83.
Silberstein, S. and Gilmore, R. (1996). Biochemistry, molecular biology, and genetics of the oligosaccharyltransferase. *Faseb J.* **10**, 849-58.
Silver, J. and Hughes, A. F. (1973). The role of cell death during morphogenesis of the mammalian eye. *J Morphol.* **140**, 159-70.
Skromne, I. and Stern, C. D. (2001). Interactions between Wnt and Vg1 signalling pathways initiate primitive streak formation in the chick embryo. *Development.* **128**, 2915-27.

Skromne, I. and Stern, C. D. (2002). A hierarchy of gene expression accompanying induction of the primitive streak by Vg1 in the chick embryo. *Mech Dev.* **114**, 115-8.
Slee, E. A., Harte, M. T., Kluck, R. M., Wolf, B. B., Casiano, C. A., Newmeyer, D. D., Wang, H. G., Reed, J. C., Nicholson, D. W., Alnemri, E. S. et al. (1999). Ordering the cytochrome c-initiated caspase cascade: hierarchical activation of caspases-2, -3, -6, -7, -8, and -10 in a caspase-9-dependent manner. *J Cell Biol.* **144**, 281-92.
Smith, S. R., Cooperman, S., Lavaute, T., Tresser, N., Ghosh, M., Meyron-Holtz, E., Land, W., Ollivierre, H., Jortner, B., Switzer, R., 3rd et al. (2004). Severity of neurodegeneration correlates with compromise of iron metabolism in mice with iron regulatory protein deficiencies. *Ann N Y Acad Sci* **1012**, 65-83.
Smith, S. R., Ghosh, M. C., Ollivierre-Wilson, H., Hang Tong, W. and Rouault, T. A. (2006). Complete loss of iron regulatory proteins 1 and 2 prevents viability of murine zygotes beyond the blastocyst stage of embryonic development. *Blood Cells Mol Dis* **7**, 7.
Smith, W. C. and Harland, R. M. (1992). Expression cloning of noggin, a new dorsalizing factor localized to the Spemann organizer in Xenopus embryos. *Cell.* **70**, 829-40.
Smith, W. C., Knecht, A. K., Wu, M. and Harland, R. M. (1993). Secreted noggin protein mimics the Spemann organizer in dorsalizing Xenopus mesoderm. *Nature.* **361**, 547-9.
Song, Z., McCall, K. and Steller, H. (1997). DCP-1, a Drosophila cell death protease essential for development. *Science.* **275**, 536-40.
Spemann, H. (1901). Uber Korrelation in der Entwicklung des Auges. *Verh Anat Ges.* **15**, 61-79.
Spemann, H. and Mangold, H. (1924). Über Induktion von Embryonalanlagen durch Implantation artfremder Organisatoren. *Wilh. Roux' Arch. EntwMech. Organ.* **100**, 599-638.
Spratt, N. T., Jr. and Haas, H. (1960). Integrative mechanisms in development of early chick blastoderm I. Regulated potentiality of separate parts. *J Exp Zool.* **145**, 97-138.
Srinivasula, S. M., Ahmad, M., Fernandes-Alnemri, T. and Alnemri, E. S. (1998). Autoactivation of procaspase-9 by Apaf-1-mediated oligomerization. *Mol Cell.* **1**, 949-57.
Stainier, D. Y. (2002). A glimpse into the molecular entrails of endoderm formation. *Genes Dev.* **16**, 893-907.
Staub, O. and Rotin, D. (2006). Role of ubiquitylation in cellular membrane transport. *Physiol Rev.* **86**, 669-707.
Steffek, A. J., Mujwid, D. K. and Johnston, M. C. (1979). Scanning electron microscopy (SEM) of cranial neural crest migration in chick embryos. *Birth Defects Orig Artic Ser.* **15**, 11-21.
Stern, C. D. (1990). The marginal zone and its contribution to the hypoblast and primitive streak of the chick embryo. *Development.* **109**, 667-82.
Stern, C. D. (1998). Detection of multiple gene products simultaneously by in situ hybridization and immunohistochemistry in whole mounts of avian embryos. *Curr Top Dev Biol* **36**, 223-43.
Stern, C. D. (1999). Grafting Hensen's node. *Methods Mol Biol* **97**, 245-53.
Stern, C. D. (2004a). Gastrulation in chick. Cold Spring Harbor, New York Cold Spring Harbor Labolatory Press.

Stern, C. D. (2004b). Neural Induction. Cold Spring Harbor, New York: Cold Spring Harbor Labolatory Press.
Stern, C. D. (2004c). The chick embryo--past, present and future as a model system in developmental biology. *Mech Dev.* **121**, 1011-3.
Stern, C. D. (2005a). Neural induction: old problem, new findings, yet more questions. *Development* **132**, 2007-2021.
Stern, C. D. (2005b). The chick; a great model system becomes even greater. *Dev Cell.* **8**, 9-17.
Stern, C. D. and Canning, D. R. (1988). Gastrulation in birds: a model system for the study of animal morphogenesis. *Experientia.* **44**, 651-7.
Stern, C. D. and Canning, D. R. (1990). Origin of cells giving rise to mesoderm and endoderm in chick embryo. *Nature.* **343**, 273-5.
Stern, C. D. and Ireland, G. W. (1981). An integrated experimental study of endoderm formation in avian embryos. *Anat Embryol (Berl)* **163**, 245-63.
Stevens, P. W., Dodgson, J. B. and Engel, J. D. (1987). Structure and expression of the chicken ferritin H-subunit gene. *Mol Cell Biol.* **7**, 1751-8.
Storey, K. G., Crossley, J. M., De Robertis, E. M., Norris, W. E. and Stern, C. D. (1992). Neural induction and regionalisation in the chick embryo. *Development.* **114**, 729-41.
Streit, A., Berliner, A. J., Papanayotou, C., Sirulnik, A. and Stern, C. D. (2000). Initiation of neural induction by FGF signalling before gastrulation. *Nature.* **406**, 74-8.
Streit, A., Lee, K. J., Woo, I., Roberts, C., Jessell, T. M. and Stern, C. D. (1998). Chordin regulates primitive streak development and the stability of induced neural cells, but is not sufficient for neural induction in the chick embryo. *Development.* **125**, 507-19.
Streit, A., Sockanathan, S., Perez, L., Rex, M., Scotting, P. J., Sharpe, P. T., Lovell-Badge, R. and Stern, C. D. (1997). Preventing the loss of competence for neural induction: HGF/SF, L5 and Sox-2. *Development* **124**, 1191-202.
Streit, A. and Stern, C. D. (1999a). Establishment and maintenance of the border of the neural plate in the chick: involvement of FGF and BMP activity. *Mech Dev* **82**, 51-66.
Streit, A. and Stern, C. D. (1999b). Mesoderm patterning and somite formation during node regression: differential effects of chordin and noggin. *Mech Dev.* **85**, 85-96.
Streit, A. and Stern, C. D. (2001). Combined whole-mount in situ hybridization and immunohistochemistry in avian embryos. *Methods.* **23**, 339-44.
Sugimoto, A., Hozak, R. R., Nakashima, T., Nishimoto, T. and Rothman, J. H. (1995). dad-1, an endogenous programmed cell death suppressor in Caenorhabditis elegans and vertebrates. *Embo J* **14**, 4434-41.
Sun, L. and Chen, Z. J. (2004). The novel functions of ubiquitination in signaling. *Curr Opin Cell Biol.* **16**, 119-26.
Surguladze, N., Patton, S., Cozzi, A., Fried, M. G. and Connor, J. R. (2005). Characterization of nuclear ferritin and mechanism of translocation. *Biochem J.* **388**, 731-40.
Suzuki, A., Chang, C., Yingling, J. M., Wang, X. F. and Hemmati-Brivanlou, A. (1997a). Smad5 induces ventral fates in Xenopus embryo. *Dev Biol.* **184**, 402-5.
Suzuki, A., Ueno, N. and Hemmati-Brivanlou, A. (1997b). Xenopus msx1 mediates epidermal induction and neural inhibition by BMP4. *Development.* **124**, 3037-44.
Suzuki, H. R., Padanilam, B. J., Vitale, E., Ramirez, F. and Solursh, M. (1991). Repeating developmental expression of G-Hox 7, a novel homeobox-containing gene in the chicken. *Dev Biol.* **148**, 375-88.

Tanner, W. and Lehle, L. (1987). Protein glycosylation in yeast. *Biochim Biophys Acta.* **906**, 81-99.
Telford, J. L., Macchia, G., Massone, A., Carinci, V., Palla, E. and Melli, M. (1986). The murine interleukin 1 beta gene: structure and evolution. *Nucleic Acids Res.* **14**, 9955-63.
Theil, E. C. (1987). Ferritin: structure, gene regulation, and cellular function in animals, plants, and microorganisms. *Annu Rev Biochem.* **56**, 289-315.
Theil, E. C. (1990). Ferritin mRNA translation, structure, and gene transcription during development of animals and plants. *Enzyme.* **44**, 68-82.
Theil, E. C. (2003). Ferritin: at the crossroads of iron and oxygen metabolism. *J Nutr.* **133**, 1549S-53S.
Thompson, J. D., Higgins, D. G. and Gibson, T. J. (1994). CLUSTAL W: improving the sensitivity of progressive multiple sequence alignment through sequence weighting, position-specific gap penalties and weight matrix choice. *Nucleic Acids Res.* **22**, 4673-80.
Thomson, A. M., Rogers, J. T. and Leedman, P. J. (1999). Iron-regulatory proteins, iron-responsive elements and ferritin mRNA translation. *Int J Biochem Cell Biol* **31**, 1139-52.
Thornberry, N. A., Rano, T. A., Peterson, E. P., Rasper, D. M., Timkey, T., Garcia-Calvo, M., Houtzager, V. M., Nordstrom, P. A., Roy, S., Vaillancourt, J. P. et al. (1997). A combinatorial approach defines specificities of members of the caspase family and granzyme B. Functional relationships established for key mediators of apoptosis. *J Biol Chem.* **272**, 17907-11.
Thorne, A. W., Sautiere, P., Briand, G. and Crane-Robinson, C. (1987). The structure of ubiquitinated histone H2B. *Embo J.* **6**, 1005-10.
Tirosh-Finkel, L., Elhanany, H., Rinon, A. and Tzahor, E. (2006). Mesoderm progenitor cells of common origin contribute to the head musculature and the cardiac outflow tract. *Development.* **133**, 1943-53. Epub 2006 Apr 19.
Tonegawa, A., Funayama, N., Ueno, N. and Takahashi, Y. (1997). Mesodermal subdivision along the mediolateral axis in chicken controlled by different concentrations of BMP-4. *Development.* **124**, 1975-84.
Torti, F. M. and Torti, S. V. (2002). Regulation of ferritin genes and protein. *Blood.* **99**, 3505-16.
Tur-Kaspa, R., Teicher, L., Levine, B. J., Skoultchi, A. I. and Shafritz, D. A. (1986). Use of electroporation to introduce biologically active foreign genes into primary rat hepatocytes. *Mol Cell Biol.* **6**, 716-8.
Uehara, M. and Ueshima, T. (1988). Studies of neural tube development in the chicken embryo tail. *Anat Embryol (Berl).* **179**, 149-55.
Ulrich, H. D. (2003). Protein-protein interactions within an E2-RING finger complex. Implications for ubiquitin-dependent DNA damage repair. *J Biol Chem.* **278**, 7051-8. Epub 2002 Dec 19.
Urbe, S. (2005). Ubiquitin and endocytic protein sorting. *Essays Biochem.* **41**, 81-98.
Uwanogho, D., Rex, M., Cartwright, E. J., Pearl, G., Healy, C., Scotting, P. J. and Sharpe, P. T. (1995). Embryonic expression of the chicken Sox2, Sox3 and Sox11 genes suggests an interactive role in neuronal development. *Mech Dev* **49**, 23-36.
Vakaet, L. (1970). Cinephotomicrographic investigations of gastrulation in the chick blastoderm. *Arch Biol (Liege).* **81**, 387-426.
Vakaet, L. (1984). The initiation of gastrula ingression in the chick blastoderm. *Am. Zool* **24**, 555-562.

van de Lavoir, M. C., Mather-Love, C., Leighton, P., Diamond, J. H., Heyer, B. S., Roberts, R., Zhu, L., Winters-Digiacinto, P., Kerchner, A., Gessaro, T. et al. (2006). High-grade transgenic somatic chimeras from chicken embryonic stem cells. *Mech Dev.* **123**, 31-41. Epub 2005 Dec 1.

van der Mark, F., Bienfait, F. and van den Ende, H. (1983a). Variable amounts of translatable ferritin mRNA in bean leaves with various iron contents. *Biochem Biophys Res Commun.* **115**, 463-9.

van der Mark, F., van den Briel, W. and Huisman, H. G. (1983b). Phytoferritin is synthesized in vitro as a high-molecular-weight precursor. Studies on the synthesis and the uptake in vitro of the precursors of ferritin and ferredoxin by intact chloroplasts. *Biochem J.* **214**, 943-50.

Varshavsky, A. (1996). The N-end rule: functions, mysteries, uses. *Proc Natl Acad Sci U S A.* **93**, 12142-9.

Vaux, D. L. (1993). Toward an understanding of the molecular mechanisms of physiological cell death. *Proc Natl Acad Sci U S A.* **90**, 786-9.

Vaux, D. L. and Korsmeyer, S. J. (1999). Cell death in development. *Cell.* **96**, 245-54.

Vecino, E., Hernandez, M. and Garcia, M. (2004). Cell death in the developing vertebrate retina. *Int J Dev Biol.* **48**, 965-74.

Viebahn, C. (2004). Gastrulation in the Rabbit. Cold Spring Harbor, New York: Cold Spring Harbor Labolatory Press.

Waddington, C. H. (1932). Experiments on the development of chick and duck embryos cultivated in vitro. *Phil. Trans. Roy. Soc. Lond* **221**, 179-230.

Waddington, C. H. (1933). Induction by coagulated organisers in the chick embryo. *Nature (London)* **131**, 275.

Waddington, C. H. (1934). Experiments on Embryonic Induction: III. A Note on Inductions by Chick Primitive Streak Transplanted to the Rabbit Embryo *J Exp Biol* **11**, 224-227.

Waddington, C. H. (1936). Organizers in Mammalian Development. *Nature* **138**, 125.

Waddington, C. H. (1937). Experiments on determination in the rabbit embryo. *Arch Biol (Liege).* **48**, 273-290.

Wagner, D. S. and Mullins, M. C. (2002). Modulation of BMP activity in dorsal-ventral pattern formation by the chordin and ogon antagonists. *Dev Biol.* **245**, 109-23.

Wakamatsu, Y., Mochii, M., Vogel, K. S. and Weston, J. A. (1998). Avian neural crest-derived neurogenic precursors undergo apoptosis on the lateral migration pathway. *Development.* **125**, 4205-13.

Walker, B. K., Lei, H. and Krag, S. S. (1998). A functional link between N-linked glycosylation and apoptosis in Chinese hamster ovary cells. *Biochem Biophys Res Commun.* **250**, 264-70.

Wallis, J. W., Aerts, J., Groenen, M. A., Crooijmans, R. P., Layman, D., Graves, T. A., Scheer, D. E., Kremitzki, C., Fedele, M. J., Mudd, N. K. et al. (2004). A physical map of the chicken genome. *Nature.* **432**, 761-4.

Watson, D. C., Levy, W. B. and Dixon, G. H. (1978). Free ubiquitin is a non-histone protein of trout testis chromatin. *Nature.* **276**, 196-8.

Wei, Y. and Mikawa, T. (2000). Formation of the avian primitive streak from spatially restricted blastoderm: evidence for polarized cell division in the elongating streak. *Development.* **127**, 87-96.

Wetzel, N. C. (1929). *Jour. Bact.* **18**, 117.

Wiborg, O., Pedersen, M. S., Wind, A., Berglund, L. E., Marcker, K. A. and Vuust, J. (1985). The human ubiquitin multigene family: some genes contain multiple directly repeated ubiquitin coding sequences. *Embo J.* **4**, 755-9.

Wijsman, J. H., Jonker, R. R., Keijzer, R., van de Velde, C. J., Cornelisse, C. J. and van Dierendonck, J. H. (1993). A new method to detect apoptosis in paraffin sections: in situ end-labeling of fragmented DNA. *J Histochem Cytochem* **41**, 7-12.
Wilkinson Iv, J., Di, X., Schonig, K., Buss, J. L., Kock, N. D., Cline, J. M., Saunders, T. L., Bujard, H., Torti, S. V. and Torti, F. M. (2006). Tissue-specific expression of ferritin H regulates cellular iron homeostasis in vivo. *Biochem J* **1**, 1.
Wilkinson, K. D., Cox, M. J., O'Connor, L. B. and Shapira, R. (1986). Structure and activities of a variant ubiquitin sequence from bakers' yeast. *Biochemistry.* **25**, 4999-5004.
Wilkinson, K. D., Urban, M. K. and Haas, A. L. (1980). Ubiquitin is the ATP-dependent proteolysis factor I of rabbit reticulocytes. *J Biol Chem.* **255**, 7529-32.
Wilson, P. A. and Hemmati-Brivanlou, A. (1995). Induction of epidermis and inhibition of neural fate by Bmp-4. *Nature.* **376**, 331-3.
Wilson, P. A., Lagna, G., Suzuki, A. and Hemmati-Brivanlou, A. (1997). Concentration-dependent patterning of the Xenopus ectoderm by BMP4 and its signal transducer Smad1. *Development.* **124**, 3177-84.
Winther, J. R., Stevens, T. H. and Kielland-Brandt, M. C. (1991). Yeast carboxypeptidase Y requires glycosylation for efficient intracellular transport, but not for vacuolar sorting, in vivo stability, or activity. *Eur J Biochem.* **197**, 681-9.
Woltering, E. J., van der Bent, A. and Hoeberichts, F. A. (2002). Do plant caspases exist? *Plant Physiol.* **130**, 1764-9.
Woo, M., Hakem, R., Soengas, M. S., Duncan, G. S., Shahinian, A., Kagi, D., Hakem, A., McCurrach, M., Khoo, W., Kaufman, S. A. et al. (1998). Essential contribution of caspase 3/CPP32 to apoptosis and its associated nuclear changes. *Genes Dev.* **12**, 806-19.
Wu, K. J., Polack, A. and Dalla-Favera, R. (1999). Coordinated regulation of iron-controlling genes, H-ferritin and IRP2, by c-MYC. *Science.* **283**, 676-9.
Xu, R. H., Kim, J., Taira, M., Zhan, S., Sredni, D. and Kung, H. F. (1995). A dominant negative bone morphogenetic protein 4 receptor causes neuralization in Xenopus ectoderm. *Biochem Biophys Res Commun.* **212**, 212-9.
Xue, D. and Horvitz, H. R. (1997). Caenorhabditis elegans CED-9 protein is a bifunctional cell-death inhibitor. *Nature.* **390**, 305-8.
Yabe, T., Shimizu, T., Muraoka, O., Bae, Y. K., Hirata, T., Nojima, H., Kawakami, A., Hirano, T. and Hibi, M. (2003). Ogon/Secreted Frizzled functions as a negative feedback regulator of Bmp signaling. *Development.* **130**, 2705-16.
Yabu, T., Kishi, S., Okazaki, T. and Yamashita, M. (2001a). Characterization of zebrafish caspase-3 and induction of apoptosis through ceramide generation in fish fathead minnow tailbud cells and zebrafish embryo. *Biochem J.* **360**, 39-47.
Yabu, T., Todoriki, S. and Yamashita, M. (2001b). Stress-induced apoptosis by heat shock, UV and gamma-ray irradiation in zebrafish embryos detected by increased caspase activity and whole-mount TUNEL staining. *Fisheries Science* **67**, 333-340.
Yan, Q., Liu, J. P. and Li, D. W. (2006). Apoptosis in lens development and pathology. *Differentiation.* **74**, 195-211.
Yang, D. C., Jiang, X., Elliott, R. L. and Head, J. F. (2002). Antisense ferritin oligonucleotides inhibit growth and induce apoptosis in human breast carcinoma cells. *Anticancer Res* **22**, 1513-24.

Yang, H. J., Wang, K. C., Chi, J. G., Lee, M. S., Lee, Y. J., Kim, S. K. and Cho, B. K. (2003). Neural differentiation of caudal cell mass (secondary neurulation) in chick embryos: Hamburger and Hamilton Stages 16-45. *Brain Res Dev Brain Res.* **142**, 31-6.
Yang, L., Zhang, H., Hu, G., Wang, H., Abate-Shen, C. and Shen, M. M. (1998). An early phase of embryonic Dlx5 expression defines the rostral boundary of the neural plate. *J Neurosci.* **18**, 8322-30.
Yatskievych, T. A., Pascoe, S. and Antin, P. B. (1999). Expression of the homebox gene Hex during early stages of chick embryo development. *Mech Dev.* **80**, 107-9.
Yeo, W. and Gautier, J. (2003). A role for programmed cell death during early neurogenesis in xenopus. *Dev Biol.* **260**, 31-45.
Yeo, W. and Gautier, J. (2004). Early neural cell death: dying to become neurons. *Dev Biol.* **274**, 233-44.
Yokouchi, Y., Sakiyama, J., Kameda, T., Iba, H., Suzuki, A., Ueno, N. and Kuroiwa, A. (1996). BMP-2/-4 mediate programmed cell death in chicken limb buds. *Development.* **122**, 3725-34.
Yoshimi, M., Sekiguchi, T., Hara, N. and Nishimoto, T. (2000). Inhibition of N-linked glycosylation causes apoptosis in hamster BHK21 cells. *Biochem Biophys Res Commun.* **276**, 965-9.
Yoshioka, H., Ishimaru, Y., Sugiyama, N., Tsunekawa, N., Noce, T., Kasahara, M. and Morohashi, K. (2005). Mesonephric FGF signaling is associated with the development of sexually indifferent gonadal primordium in chick embryos. *Dev Biol.* **280**, 150-61.
Yost, H. J. and Lindquist, S. (1991). Heat shock proteins affect RNA processing during the heat shock response of Saccharomyces cerevisiae. *Mol Cell Biol.* **11**, 1062-8.
Young, F. M., Illingworth, P. J. and Fraser, H. M. (1998). Ubiquitin and apoptosis in the corpus luteum of the marmoset monkey (Callithrix jacchus). *J Reprod Fertil.* **114**, 163-8.
Young, R. W. (1984). Cell death during differentiation of the retina in the mouse. *J Comp Neurol.* **229**, 362-73.
Yuan, J., Shaham, S., Ledoux, S., Ellis, H. M. and Horvitz, H. R. (1993). The C. elegans cell death gene ced-3 encodes a protein similar to mammalian interleukin-1 beta-converting enzyme. *Cell.* **75**, 641-52.
Yuan, J. Y. and Horvitz, H. R. (1990). The Caenorhabditis elegans genes ced-3 and ced-4 act cell autonomously to cause programmed cell death. *Dev Biol.* **138**, 33-41.
Zaffran, S. and Frasch, M. (2002). Early signals in cardiac development. *Circ Res.* **91**, 457-69.
Zahringer, J., Konijn, A. M., Baliga, B. S. and Munro, H. N. (1975). Mechanism of iron induction of ferritin synthesis. *Biochem Biophys Res Commun.* **65**, 583-90.
Zancani, M., Peresson, C., Biroccio, A., Federici, G., Urbani, A., Murgia, I., Soave, C., Micali, F., Vianello, A. and Macri, F. (2004). Evidence for the presence of ferritin in plant mitochondria. *Eur J Biochem.* **271**, 3657-64.
Zhao, G., Bou-Abdallah, F., Arosio, P., Levi, S., Janus-Chandler, C. and Chasteen, N. D. (2003). Multiple pathways for mineral core formation in mammalian apoferritin. The role of hydrogen peroxide. *Biochemistry.* **42**, 3142-50.
Zheng, H., Bhavsar, D., Dugast, I., Zappone, E. and Drysdale, J. (1997). Conserved mutations in human ferritin H pseudogenes: a second functional sequence or an evolutionary quirk? *Biochim Biophys Acta.* **1351**, 150-6.
Zheng, H. D., Bhavsar, D. and Drysdale, J. (1995). An unusual human ferritin H sequence from chromosome 4. *DNA Seq.* **5**, 173-5.
Zhivotovsky, B. (2003). Caspases: the enzymes of death. *Essays Biochem.* **39**, 25-40.

Zhu, L., Belo, J. A., De Robertis, E. M. and Stern, C. D. (1999). Goosecoid regulates the neural inducing strength of the mouse node. *Dev Biol.* **216**, 276-81.
Zimmerman, L. B., De Jesus-Escobar, J. M. and Harland, R. M. (1996). The Spemann organizer signal noggin binds and inactivates bone morphogenetic protein 4. *Cell.* **86**, 599-606.
Zou, H., Li, Y., Liu, X. and Wang, X. (1999). An APAF-1.cytochrome c multimeric complex is a functional apoptosome that activates procaspase-9. *J Biol Chem.* **274**, 11549-56.
Zuzarte-Luis, V. and Hurle, J. M. (2005). Programmed cell death in the embryonic vertebrate limb. *Semin Cell Dev Biol.* **16**, 261-9. Epub 2005 Jan 16.